University of Nottingham
UK | CHINA | MALAYSIA

THE EFFECT OF CIGARETTE SMOKE EXTRACT AND E-CIGARETTE VAPE EXTRACT ON EXTRACELLULAR VESICLE PRODUCTION BY HUMAN IMMUNE CELLS

Nancy Ester Gomez, BSc, MSc.

Thesis submitted to the University of Nottingham for the degree of Doctor of Philosophy

School of Life Sciences

Table of Contents

DEDICATION i

ACKNOWLEDGEMENTS ii

ABBREVIATIONS iii

Abstract vi

Publications viii

COVID-19 Impact Statement xii

1.0 Introduction 2

1.1. Chronic Obstructive Pulmonary Disease (COPD) 2

1.1.1. Definition of COPD 3

1.1.2. Diagnosis of COPD 3

1.1.3. Treatment of COPD 4

1.1.4. Risk factors of COPD 5

1.1.5. Exacerbation of COPD 9

1.2. Pathogenesis of COPD 9

1.2.1. Chronic bronchitis 12

1.2.2. Emphysema 13

1.2.3. Small airway disease 13

1.2.4. Systemic effects of COPD 14

1.3. Cigarette smoke 15

1.3.1. Tobacco Toxicology 15

1.4. Immune response on exposure to cigarette smoke 16

1.4.1. Inflammation in the lungs 17

1.4.2. Epithelial cells 19

1.4.3. Macrophages 21

1.4.4. Dendritic cells 23

1.4.5. Natural Killer Cells 25

1.4.6. Natural Killer (NK) T cells 27

1.4.7. Neutrophils 28

1.4.8. Eosinophils 30

1.4.9. T lymphocytes 31

1.4.10. B lymphocytes and antibodies 33

1.5. E-cigarettes 35

1.5.1. Toxicology of e-cigarette constituents 37

1.6. Immune response on exposure to e-cigarette vape 38

1.6.1. Inflammation in the lungs 39

1.6.2. Epithelial cells 40

1.6.3. Macrophages 41

1.6.4. Dendritic cells 42

1.6.5. Natural killer cells 42

1.6.6. Neutrophils....43
1.6.7. Eosinophils....44
1.6.8. T lymphocytes....45
1.6.9. B lymphocytes and antibodies....45
1.6.10. Cytokines....45
1.6.11. Systemic response....46
1.7. Extracellular Vesicles (EVs)....47
1.7.1. EV subtypes....47
1.7.2. Biogenesis and release of exosomes....49
1.7.3. Biogenesis and release of microvesicles....50
1.7.4. Tetraspanins associated with EVs....51
1.7.5. Cargo of EVs....53
1.8. EVs and cigarette smoking....54
1.8.1. EVs in pathophysiology....55
1.8.2. Endothelial cell-derived EVs....55
1.8.3. Epithelial cell-derived EVs....58
1.8.4. Monocyte/Macrophage-derived EVs....60
1.8.5. Neutrophil-derived EVs....62
1.8.6. T lymphocyte-derived EVs....63
1.8.7. Platelet-derived EVs....63
1.8.8. EVs derived from other cell types....64
1.8.9. DNA in EVs....64
1.8.10. RNA in EVs....65
1.8.11. Proteins in EVs....66
1.8.12. EVs as biomarkers....68
1.9. EVs and e-cigarette smoking....71
1.9.1. Endothelial cell-derived EV....71
1.9.2. Epithelial cell-derived EVs....72
1.9.3. Platelet-derived EVs....73
1.9.4. EVs derived from other cell types....74
1.9.5. DNA in EVs....75
1.9.6. RNA in EVs....75
1.9.7. Proteins in EVs....76
1.9.8. EVs as biomarkers....78
1.10. Study Aims....80
1.11. Hypothesis....80
2.0. Methods....82
2.1. Processing of blood samples and Peripheral Blood Mononuclear Cell (PBMC) Isolation. 82
2.2. T cell Activation....84
2.3. Cigarette Smoke Extraction....85
2.4. E-cigarette vapour extraction....86
2.5. Cell Viability (Annexin V and Propidium Iodide (PI) staining)....88
2.6. Flow cytometric analysis of activated T cells....88
2.7. Controls set for EV analysis....90

2.8. Calcein AM staining for EVs 91
2.9. Tetraspanin staining of EVs 91
2.10. EV Isolation by size exclusion chromatography (SEC) 91
2.11. Nano-flow cytometry (nFCM) analysis 92
2.12. Transmission electron microscopy (TEM) 93
2.13. Nanoparticle tracking analysis (NTA) 93
2.14. Introduction of EVs to activated T-cells 94
2.15. ImageStreamX Small Particles Acquisition and Analysis 94
2.16. Protein measurements 95
2.17. Macsplex surface protein profiling 95
2.18. Extracellular Staining of PBMCs 96
2.19. Flow Cytometry for cell analysis 97
2.20. High-Dimensional Analysis of Flow Cytometry Data 98
2.21. Protein Digestion 98
2.22. Data analysis 100

3.0. Optimising methods for analysis of EVs 102
3.1. Introduction 102
3.1.1. Current technology and guidelines for EV studies 102
3.1.2. Aim 105
3.2. Methods 105
3.2.1. Processing of blood samples and Peripheral Blood Mononuclear Cell (PBMC) Isolation. 105
3.2.2. T cell Activation 105
3.2.3. Cell Viability (Annexin V and Propidium Iodide (PI) staining) 105
3.2.4. Flow cytometric analysis 106
3.2.5. Controls set for EV analysis 106
3.2.6. Calcein AM staining of EVs 106
3.2.7. Tetraspanin staining of EVs 106
3.2.8. EV isolation by Size Exclusion Chromatography 106
3.2.9. Nano-flow cytometry (nFCM) analysis 107
3.2.10. Transmission electron microscopy (TEM) 107
3.2.11. Nanoparticle Tracking Analysis (NTA) 107
3.2.12. Protein digestion 107
3.2.13. Introduction of EVs to activated T-cells 107
3.2.14. ImageStreamX (ISX) Small Particles Acquisition and Analysis 107
3.2.15. Protein measurements 108
3.2.16. Macsplex surface protein profiling 108
3.2.17. Data analysis 108
3.3. Results 108
3.3.1. Demographics 108
3.3.2. T cell activation 109
3.3.3. Serum-free media 114
3.3.4. Imaging flow cytometry (IFC) 116
3.3.5. Calcein concentration 117
3.3.6. Detergent control 120
3.3.7. Controls for study of EVs 122
3.3.8. Analysis of PBMC-derived EVs by nano-flow cytometry (nFCM) 124

3.3.9. Analysis of PBMC-derived EVs by conventional transmission electron microscopy (TEM) and nanoparticle tracking analysis (NTA) 127
3.3.10. Proteomic analysis of PBMC-derived EVs 129
3.3.11. Characterisation of tetraspanin content of EVs 137
3.3.12. Protein measurement of isolated EVs 141
3.3.13. Surface protein profiling by multiplexed bead assay 142
3.3.14. Internalisation of EVs 144
3.4. Discussion 147

4.0. EVs produced by CSE- and ECVE-exposed PBMCs 155
4.1. Introduction 155
4.1.1. EVs produced by cells exposed to cigarette smoke ..... **Error! Bookmark not defined.**
4.1.2. EVs produced by cells exposed to e-cigarette vapour ... **Error! Bookmark not defined.**
4.1.3. Aim 155
4.2. Methods 157
4.2.1. Processing of blood samples and Peripheral Blood Mononuclear Cell (PBMC) Isolation. 157
4.2.2. Cigarette smoke extract 157
4.2.3. E-cigarette vape extract 157
4.2.4. Controls set for EV analysis 157
4.2.5. Calcein AM staining of EVs 158
4.2.6. Tetraspanin staining of EVs 158
4.2.7. EV isolation by Size Exclusion Chromatography 158
4.2.8. ImageStreamX Small Particles Acquisition and Analysis 158
4.2.9. Protein measurements 158
4.2.10. Macsplex surface protein profiling 159
4.2.11. Data analysis 159
4.3. Results 161
4.3.1. Cigarette smoke extract 161
4.3.2. EV production at 24 and 48 hours following CS exposure 162
4.3.3. Cigarette Smoke on EV Production by PBMCs at 32 hours 167
4.3.4. Production of EVs from PBMCs exposed to CSE and ECVE 173
4.3.5. Tetraspanin profile of EVs from PBMCs exposed to CSE and ECVE 174
4.3.5. Membrane profile of EVs exposed to CSE and ECVE 177
4.4. Discussion 180

5.0. Effect of CSE and ECVE on PBMCs 189
5.1. Introduction 189
5.2. Methods 191
5.2.1. Processing of blood samples and Peripheral Blood Mononuclear Cell (PBMC) Isolation. 191
5.2.2. Conditioned smoke extract 191
5.2.3. E-cigarette vape extract 191
5.2.4. Extracellular Staining 191
5.2.5. Flow Cytometry 192
5.2.6. High Dimensional Analysis of Flow Cytometry Data 193
5.2.7. Data analysis 193
5.3. Results 195
5.3.1. Viability of PBMCs 195

5.3.2. PBMC phenotype profiling....196
5.3.2. Clustering analysis....211
5.4. Discussion....230
6.0 Discussion....234
References:....240

DEDICATION

This thesis is dedicated to my husband, Nick, who has been a constant source of support and encouragement throughout this journey. Thank you for being with me every step of the way.

I also dedicate this thesis to my parents, Gladys and Guillermo, for their sacrifice and encouragement in my studies. They have been my source of inspiration, support, and guidance. They taught me to be unique, determined, to believe in myself, and to always persevere. To my mom and dad, this is for you.

ACKNOWLEDGEMENTS

First, I would like to thank my supervisors, Professor Lucy Fairclough, Dr David Onion and Dr Victoria James, who have given me continuous support over the past four years. Without their support, understanding, encouragement and faith, this would not have been possible.

I also wish to thank my family for their continuous support, love and encouragement. Their words of encouragement gave me continuous strength to face up to the challenges throughout my life. I would like to thank my friends for their encouragement, for bringing me laughter and joy, and for being on this journey with me.

I would also like to thank my colleagues in the department of Immunology.

Finally, I wish to thank the University of Nottingham Vice Chancellor Scholarship program who provided funding for this project.

ABBREVIATIONS

AADT	alpha-1 antitrypsin deficient
AARDC1	arrestin domain-containing protein 1
AAT	alpha-1 antitrypsin
AMs	alveolar macrophages
APC	antigen presenting cell
ApoBDs	apoptotic bodies
ARF6	ADP-ribosylation factor 6
BAL	bronchoalveolar lavage
COPD	chronic obstructive pulmonary disease
CS	cigarette smoke
CXCL	chemokine (C-X-C motif) ligand
CSE	cigarette smoke extract
DCs	dendritic cells
ECVE	e-cigarette vapour extract
ENDS	electronic nicotine delivery systems
ERK	extracellular signal-regulated kinase
ESCRTs	endosomal sorting complexes required for transport
EVs	extracellular vesicles
EVALI	e-cigarette or vaping product use-associated lung injury
FEV_1	forced expiratory volume in 1 second
FVC	forced vital capacity
GM-CSF	granulocyte-macrophage colony-stimulating factor
GOLD	global initiative for chronic obstructive lung disease
GWAS	genome-wide association studies
hBD-2	human β-defensin-2
HBECs	human bronchial epithelial cells

HLA	human leukocyte antigen
HSP	heat shock protein
ICS	inhaled corticosteroids
IFC	imaging flow cytometry
IFN	interferon
IL	interleukin
ILVs	intraluminal vesicles
IPA	ingenuity pathway analysis
ISEV	International Society for Extracellular Vesicles
LABAs	long acting β-2 agonists
LMIC	low- and middle-income countries
LPS	lipopolysaccharides
LT	leukotriene
MCP	monocyte chemoattractant protein
MHC	major histocompatibility complex
MIFlowCyt-EV	Minimum Information about a FC experiment standard in an EV-FC-specific reporting framework
MIP	macrophage inflammatory protein
MISEV	minimal information for studies of extracellular vesicles
MLCK	myosin light chain kinase
MMPs	matrix metalloproteinases
MT1MMP	membrane-type 1 matrix metalloproteinase
MVB	multivesicular bodies
NE	neutrophil elastase
NETs	neutrophil extracellular traps
nFCM	nanoparticle flow cytometry
NFκB	nuclear factor κB
NK	natural killer

NKT	natural killer T cell
NTA	nanoparticle tracking analysis
PBMCs	peripheral blood mononuclear cells
PG	propylene glycol
PS	phosphatidylserine
ROS	reactive oxygen species
SAD	small airway disease
SEC	size exclusion chromatography
sEVs	small EVs
TCR	T cell receptor
TEM	transmission electron microscopy
TEMs	tetraspanin-enriched microdomains
TGF	transforming growth factor
TGN	trans-Golgi network
TNF	tumour necrosis factor
TSG101	tumour susceptibility gene 101
VAMP3	vesicle associated membrane protein 3
VG	vegetable glycerine
WHO	World Health Organization

Abstract

Background:

Chronic Obstructive Pulmonary Disease (COPD) is a common inflammatory airway disease, affecting the airways, lung parenchyma and vasculature, and is characterized by irreversible airflow limitation. Cigarette smoking is a significant risk factor associated with various diseases, including COPD, cardiovascular disease and cancers. E-cigarettes are promoted as a safer alternative to cigarettes and are being used as substitutes to quit cigarette smoking to reduce risk to health. Extracellular vesicles (EVs) are important intercellular communication mediators released by cells into the extracellular environment, with the capacity to transfer biological signals and information between cells and as such, influence the recipient cell function. Both cigarette smoke and e-cigarettes have been linked to increased release of EVs from a number of cellular sources. Therefore, the aim of this thesis was to investigate the effect of cigarette smoke extract (CSE) and e-cigarette vapour extract (ECVE) on the production of EVs by cells of the immune system.

Methods:

Peripheral blood mononuclear cells (PBMCs) from healthy individuals were exposed to CSE and ECVE. EVs produced by PBMCs were observed using various techniques, including transmission electron microscopy (TEM), nanoparticle tracking analysis (NTA), nanoparticle flow cytometry (nFCM), imaging flow cytometry (IFC) and flow cytometry. Membrane profile of EVs, focusing on tetraspanins and cell specific markers, was also investigated. PBMC phenotypes were analysed by spectral flow cytometry.

Results:

In this study, a protocol was optimised to analyse immune cell-derived EVs, focusing on high-throughput flow-based methods, including IFC that incorporates a novel gating

strategy (using the spot count feature) and a rapid staining protocol that allows for quantification of EVs in culture and following isolation. CSE or ECVE did not significantly alter the number of EVs produced by PBMCs. However, the tetraspanin profile of EVs did change between conditions, particularly the expression of CD9 and CD63. There were also significant differences in the membrane profile of EVs between treatment and control, specifically of CD40, CD41b, CD42a, CD69 and CD31. Finally, spectral flow cytometry analysis showed that CSE and ECVE do influence some cell populations. Clustering analysis identified 15 clusters present but showed no significant differences between the clusters

Conclusion:

Overall, this study has outlined a method to study extracellular vesicles derived from immune cells in an inflammatory disease model. Although the number of EVs did not significantly change, the results of this study suggest that CSE and ECVE may modify EV profiles in humans, and exposure to these components can result in changes within the cells producing EVs, consequently affecting EV formation.

Publications

1. **Gomez N**, James V, Onion D, Fairclough LC. Extracellular vesicles and chronic obstructive pulmonary disease (COPD): a systematic review. Respiratory research. 2022 Apr 5;23(1):82.

2. **Gomez NE**, James V, Arkill KP, Nizamudeen ZA, Onion D, Fairclough LC. PBMC-derived extracellular vesicles in a smoking-related inflammatory disease model. European Journal of Immunology. 2023 Mar 16:2250143.

3. Gumber L, **Gomez N**, Hopkins G, Tucis D, Bartlett L, Ayling K, Vedhara K, Steers G, Chakravorty M, Rutter M, Jackson H, Tighe P, Ferraro A, Power S, Pradère MJ, Onion D, Lanyon PC, Pearce FA, Fairclough L. Humoral and cellular immunity in patients with rare autoimmune rheumatic diseases following SARS-CoV-2 vaccination. Rheumatology. 2022 Oct 1;62(6):2294-303.

4. Gumber L, Jackson H, **Gomez N**, Hopkins G, Tucis D, Chakravorty M, Tighe P, Grainge M, Rutter M, Ferraro A, Power S, Pradère MJ, Lanyon PC, Pearce FA, Fairclough L, 2023. Antibody response to four doses of SARS-CoV-2 vaccine in rare autoimmune rheumatic diseases: an observational study. Rheumatology Advances in Practice, p.rkad097.

5. Hopkins G, **Gomez N**, Tucis D, Bartlett L, Steers G, Burns E, Brown M, Harvey-Cowlishaw T, Lauder S, Scurr M, Capitani L, Burnell S, Rees T, Smart K, Somerville M, Gallimore A, Perera M, Potts M, Metaxaki M, Krishna B, Jackson H, Tighe P, Onion D, Godkin A, Wills M and Fairclough L. Decreased Humoral and T Cell Responses to Asymptomatic SARS-CoV-2 Infection in Education (The ACE Cohort). (*In Preparation*).

6. Jackson H, Hopkins G, **Gomez N**, Tucis D, Bartlett L, Steers G, Tighe P, Onion D, Wills M, Godkin A, Fairclough L. Cross-reactive antibody responses in young adults following asymptomatic and symptomatic SARS-CoV-2 infection and vaccination. (*In Preparation*).

Conference Presentations

1. **Gomez N**, James V, Onion D, Fairclough LC. Optimising methods to analyse extracellular vesicles using ISX. Presentation. Imaging Flow Cytometry Workshop / The Midlands Innovation Flow Cytometry Group · 10 June, 2021

2. **Gomez N**, James V, Onion D, Fairclough LC. The effect of cigarette smoke and e-cigarette vape exposure on the production of extracellular vesicles by immune cells. Presentation. UKEV Virtual Forum 2021 / UK Society for Extracellular Vesicles · 14 December, 2021

3. **Gomez N**, James V, Onion D, Fairclough LC. The effect of cigarette smoke and e-cigarette vape exposure on the production of extracellular vesicles by immune cells. Presentation. Midlands Innovation Flow Cytometry Meeting. 25 April, 2022.

4. **Gomez NE**, James V, Onion D, Fairclough LC. The effect of cigarette smoke and e-cigarette vapour on the production of extracellular vesicles by immune cells. Presentation. Midlands EV Network Launch. 21 September 2023.

5. **Gomez N**, Hopkins G, Tucis D, Bartlett L, Browne W, Granata S, Jackson H, Onion D, Fairclough LC. The Fairclough Lab Research. Poster, Session Chair. BSI Midlands Immunology Annual Symposium, 13 May, 2022.

6. **Gomez NE**, James V, Arkill KP, Nizamudeen ZA, Onion D, Fairclough LC. Comprehensive analysis of cigarette smoke induced extracellular vesicles from peripheral blood mononuclear cells. Poster. UKEV Forum 2022 / UK Society for Extracellular Vesicles · 02 December, 2022.

7. **Gomez NE**, James V, Arkill KP, Nizamudeen ZA, Onion D, Fairclough LC. Comprehensive analysis of cigarette smoke induced extracellular vesicles from peripheral blood mononuclear cells. Poster. British Society for Immunology Congress 2022· 06 December, 2022.

COVID-19 Impact Statement

During the COVID-19 pandemic, the university closed all the labs for 6 months (March – September 2020). This resulted in the inability to conduct any research in the lab and with restrictions when then labs finally opened. This work depended on having volunteers donate blood, which was limited by government guidelines during this time. Additionally, I volunteered to conduct research in Virology at QMC, and I also worked on two COVID-19 projects led by my PhD supervisor, Prof Lucy Fairclough, during my PhD. Due to the work during the pandemic, I was awarded the Vice-Chancellor's Team medal along with other members of the lab in December 2022.

Introduction

1.0 Introduction

1.1. Chronic Obstructive Pulmonary Disease (COPD)

Chronic Obstructive Pulmonary Disease (COPD) is a common inflammatory airway disease, affecting the airways, lung parenchyma and vasculature, and is characterized by irreversible airflow limitation. According to the World Health Organisation (WHO), COPD is the third leading cause of death worldwide, causing over 3 million deaths in 2019 [1]. It is estimated that over 70% of COPD cases in high-income countries and 30-40% of COPD cases in low- and middle-income countries (LMIC) can be linked to tobacco smoking [1]. In the UK, COPD is the second most common lung disease with approximately 1.2 million people diagnosed [2]. COPD is also diagnosed in non-smokers, where other environmental exposures lead to disease [3]. Other risk factors include chronic exposure to biomass smoke, household indoor smoke and outdoor air pollution. Biomass fuel smoke has been identified as an independent risk factor leading to the development of COPD, particularly in low- and middle-income countries highly dependent on the use of biomass fuels [4]. COPD is also influenced by genetic factors, with gene associate studies identifying hundreds of genetic variants that affect risk for COPD, decreased lung function and other COPD-related traits [5, 6].

Symptoms of COPD are commonly chronic cough, excessive mucus production, air trapping, dynamic hyperinflation and shortness of breath upon physical exertion [4, 7, 8]. Indeed, COPD exhibits symptoms beyond the lung, with systemic inflammation, and is often associated with other diseases, such as cardiovascular diseases and metabolic syndrome [9]. COPD comprises two diseases; emphysema and chronic bronchitis which leads to damage of the small airways and long-term inflammation.

1.1.1. Definition of COPD

The working definition of COPD has been defined in the 2017 update of the Global Initiative for Obstructive Lung Disease (GOLD) guidelines as "a common, preventable and treatable disease that is characterised by persistent respiratory symptoms and airflow limitation due to airway and/or alveolar abnormalities, usually caused by significant exposure to noxious particles or gases" [10]. COPD is a preventable disease with existing primary, secondary and tertiary prevention strategies. These range from primary strategies including smoking cessation and adequate treatment of asthma, to secondary strategies which include early detection of disease and subsequent modification of risk factor exposure, to tertiary strategies including prevention of complications in patients with established disease [11]. COPD is also a treatable disorder, whereby clinical trials are continuing to assess optimum combinations of pharmacological and non-pharmacological therapies that result in improvement of health status and reduction of hospital admission and mortality associated with COPD [12]. Severity of disease and response to intervention varies between individuals with similar smoking and exposure history; therefore, interventions are tailored to the individual, recognising the various phenotypes in COPD. In addition, COPD is an irreversible disease, whereby obstruction does not revert in response to bronchodilators, anti-inflammatory treatment or spontaneously [11].

1.1.2. Diagnosis of COPD

Although there is an increased awareness and focus on COPD, there is still widespread under-recognition and under-diagnosis of the disease. According to the Global Initiative for Chronic Obstructive Lung Disease (GOLD), the current diagnosis of COPD is based on three features including spirometry, observation of symptoms and significant exposure to toxic stimuli [13].

GOLD pragmatically uses a fixed forced expiratory volume in 1 second/forced vital capacity (FEV_1/FVC ratio) of 0.70 as the threshold for defining COPD and, based on post-bronchodilator FEV_1 values, has classified COPD into four categories, from stage 1 to

stage 4 COPD (Table 1.1) [14, 15]. Additionally, there is a recent recommendation for repeat spirometry for patients with an initial FEV1/FVC ratio in the range of 0.6-0.8 in order to account for day-to-day biological variability and to increase the specificity of the diagnosis. Furthermore, observed symptoms of COPD during diagnosis include dyspnoea, chronic cough, sputum production or wheezing, and significant exposure to toxic or noxious stimuli including a history of smoking cigarettes, measured by pack-years, or other environmental exposure [13].

Table 1.1. Spirometric classification of COPD severity based on post-bronchodilator FEV_1 values.

Stage	**FEV_1/FVC**	**Predicted FEV_1**
I (mild)	<0.70	>0.80
II (moderate)	<0.70	0.50≤ FEV_1 <0.80
III (severe)	<0.70	0.30≤ FEV_1 <0.50
IV (most severe)	<0.70	0.30 < FEV_1

1.1.3. Treatment of COPD

The therapeutic approach to COPD has improved over the last two decades, however, treatment remains heavily dependent on the use of bronchodilators and corticosteroids. Initial advice given to patients with COPD is to quit smoking to prevent further damage to the lungs and airways [16] and to maintain an active lifestyle and receive influenza/pneumococcal vaccination [17]. Secondhand smoking is also known to damage lung function so limitation of exposure to involuntary smoke is also recommended. Bronchodilators are the first and main treatment given to patients with COPD, even when there is limited reversibility of airflow obstruction [18]. Bronchodilators work by relaxing and widening airways, making breathing easier. Current available bronchodilators include β-agonists, which increase cyclic adenosine monophosphate within many cells, therefore promoting airway smooth-muscle relaxation [16, 18]. Short-acting β-2 agonists are given to patients with mild intermittent

symptoms and include salbutamol and terbutaline [16]. Long-acting β-2 agonists (LABAs) prevent nocturnal bronchospasms, increase exercise endurance and improve quality of life; they include salmeterol, formoterol and indacaterol [16]. Theophylline, a methylxanthine agent, is another bronchodilator that acts by increasing cAMP and respiratory smooth muscle relaxation. Although not commonly used, theophylline has modest effects on lung function in moderate to severe COPD [17].

Anticholinergics or muscarinic antagonists, which act by blocking muscarinic receptors that are known to be effective in COPD, are a second type of bronchodilator. They decrease hyperinflation and improve dyspnea, decrease exacerbation and improve health-related quality of life. Anticholinergics include short-acting ipratropium bromide and long-acting tiotropium [16].

Furthermore, in patients with moderate to severe COPD and exacerbation, inhaled corticosteroids (ICS) are recommended combined with a LABA to improve lung function and reduce exacerbation [17]. Another anti-inflammatory therapy for COPD is phosphodiesterase-4 inhibitors such as roflumilast, which inhibit the breakdown of cAMP and may the reduce the risk of exacerbations [17]. Antibiotics including azithromycin which may also reduce risk of exacerbations in patients prone to exacerbations are also recommended. Mucolytics, such as carbocysteine and N-acetylcysteine, and antioxidants have been used to reduce exacerbations and to help improve the health status of patients not receiving ICS [17].

1.1.4. Risk factors of COPD

The risk of COPD is associated with interactions between genetic factors and various environmental exposures that may also be affected by comorbidities. One of the major risk factors associated with COPD is cigarette smoking; however, this association is highly affected by genes as not all smokers develop COPD [11]. Cigarette smokers are exposed to more than 7,000 constituents in both its gaseous and particulate phases, including nicotine, carcinogens, toxins and oxidants [19]. Cigarette smoking has a stimulating effect on the respiratory tract and long-term smoking can damage the

structure of the air duct walls and the septum of the alveolar wall and cause interstitial fibrosis. Additionally, cigarette smoking causes increased secretions from the mucus glands and causes obstructive bronchiolitis, further aggravating the progression of lung tissue lesions [20]. Exposure to cigarette smoking also drives increased production of cytokines and/or chemokines that result in the recruitment of neutrophils, macrophages and dendritic cells, resulting in inflammation. This leads to the production of large amounts of reactive oxygen species (ROS) and innate and adaptive immune responses [19, 20]. Accumulating data have demonstrated a dose-dependent association between cigarette smoking and COPD, where increasing mean pack years of smoking results in worsening airway obstruction [19, 21]. Smoking during pregnancy can also negatively affect foetal lung growth, resulting in the development of lung diseases [11]. Indeed, exposure to tobacco in utero and early life presents a significant risk factor for the development of COPD in adulthood [19].

Water pipe smoking or hookah used to consume tobacco produces greater quantities of by-products such as carbon monoxide, nicotine, carcinogens and heavy metals, than cigarettes. One session of water pipe smoking is comparable to 2-10 cigarettes and the pulmonary consequences mirror those associated with cigarette smoking, including a decline in lung function and increased risk for COPD and lung cancer [22, 23].

Furthermore, pollution and/or occupational exposure contribute to approximately 15-20% of the population burden of COPD [24]. Indeed, chronic exposure to biomass smoke, ambient air pollution and opportunistic exposure to fumes and dust are associated with an increased risk of developing chronic bronchitis and COPD [4]. A main concern with the use of biomass fuel are the inefficient stoves for combustion which generates toxic gases, including carbon monoxide and nitrogen oxides, and suspended particulate matter that contains volatile organic compounds including methane, aldehydes, benzene and its derivatives and polycyclic aromatic hydrocarbons [4]. Moreover, air pollution is a mixture of particulate matter and gaseous components such as ozone, volatile organic compounds, carbon monoxide and nitrogen oxides.

Particulate matter is the main constituent of indoor and outdoor air pollution and can be inhaled deep into the lungs and has been associated with oxidative stress and inflammation-induced damage of the respiratory system [4]. As such, particulate matter contributes significantly to the development of COPD and indeed, the exacerbation of COPD.

Genetic factors are also important determinants of COPD. The most well-established genetic factor associated with COPD is a deficiency of the serine protease α1 antitrypsin (AAT), found in 1-3% of patients with COPD, and when combined with smoking or other environmental exposures, increases the risk of emphysema [6, 11, 25]. AAT is encoded by the SERPINA1 gene and is the major plasma protease inhibitor of leukocyte elastase, which is located in the granules of neutrophils. Homozygosity for the SERPINA1*Z allele is the most common cause of severe AAT deficiency and results from a single base pair change in the coding sequence of the SERPINA1 gene, leading to a single amino acid substitution; therefore, causing AAT polymers to form in the hepatocytes that synthesize most AAT [6, 25]. This polymerisation and retention of polymers in the endoplasmic reticulum of hepatocytes causes a decrease in the amount of plasma AAT available to protect the lung against elastolytic damage. The imbalance between the AAT protective screen and the neutrophil elastase burden leads to unchecked proteolytic activity and consequently, to emphysema [25]. Severe AAT deficiency can also be caused by heterozygosity of one Z allele and one null allele, which leads to the absence of AAT production [6]. Furthermore, the application of genome-wide association studies (GWAS) has led to the discovery of other genetic variants associated with COPD susceptibility (Table 1.2.) [26].

Table 1.2. COPD risk genes identified through the application of genome-wide association studies (GWAS) and proteins associated with genes [26].

COPD Risk gene	Protein affected
SERPINA1	serine protease α1 antitrypsin (AAT)
CHRNA3	nicotinic acetylcholine receptor
CHRNA5	nicotinic acetylcholine receptor
IREB2	iron-responsive element binding protein-2
HHIP	Hedgehog interacting protein
FAM13A	family with sequence similarity member 13A
AGER	Receptor for Advanced Glycation-End products (RAGE)
IL27	IL27

Electronic cigarettes (E-cigarettes), handheld nicotine-delivery devices, have been adopted as a perceived safer alternative due to their ability to deliver nicotine in a manner simulating conventional cigarettes but without exposure to burned tobacco plant material [27]. However, research has shown that e-cigarette use was associated with an increased prevalence of chronic bronchitis and COPD exacerbations and has demonstrated a more rapid decline in lung function in e-cigarette users, even after adjusting for increased tobacco smoking associated with e-cigarettes [27]. Additionally, the use of flavour additives, such as benzaldehyde which is common in cherry-flavour liquid, is of concern, as they may cause increased airway irritation [27, 28]. Some flavours contain diacetyl, which has been linked to bronchiolitis obliterans or "popcorn workers lung" [27]. Vaping of e-cigarettes produces vaporised nicotine and solvent decomposition products, along with flavouring additives, that induce oxidative stress and inflammation. This in turn triggers cellular responses including reduced respiratory immune cell function, impaired epithelial barrier function, increased DNA damage and increased activation of metalloproteinases (MMPs), among others, that may ultimately lead to airway remodelling, mucus hypersecretion, and fibrosis, resulting in the development of COPD [19].

1.1.5. Exacerbation of COPD

Exacerbations of COPD cause detrimental effects on patients, including significant morbidity and mortality, and thus are important to prevent [29]. During exacerbation of COPD, there is increased airway and systemic inflammation, and symptoms such as breathlessness and sputum production worsen and can lead to hospitalization [30]. Exacerbations of COPD are considered to be caused by complex interactions between the host, bacteria, viruses, and environmental exposures, which increase the inflammatory burden in the lower airways. In exacerbations, there is increased numbers of inflammatory cells, particularly neutrophils, cytokines, chemokines and proteases in the airways, with increased concentrations of particular cytokines and C-reactive protein in the blood [31].

Currently, the exacerbation of COPD is a contentious area to define, despite the fact that these periods present a significant burden on COPD patients. A broad definition of COPD exacerbation is the worsening of the patient's condition, although this may be inaccurate due to no established clinical markers, signs or symptoms that can identify an exacerbation of the condition [32]. COPD exacerbations are defined clinically as periods of increasing respiratory symptoms including cough, increased sputum volume and purulence, wheezing, increased dyspnoea and/or systemic distress, and where there is a need for antibiotics [29]. COPD exacerbation is mainly common in patients with advanced COPD and has also been associated with viral or bacterial infections [33].

1.2. Pathogenesis of COPD

Pathogenesis of COPD involves inflammation, an imbalance between proteases and antiproteases and an imbalance between oxidants and antioxidants in the lungs. There are two subtypes of COPD, namely chronic bronchitis and emphysema. It has been suggested that various immune cells and a variety of cellular and molecular pathways are involved in inflammation and play critical roles in COPD pathogenesis. Both innate and adaptive immune cells are involved, with an increase of inflammatory cells in the

airways of COPD patients when compared to non-smokers or smokers who have not developed the disease [34].

In patients with COPD, chronic inflammation is present in the lower respiratory tract and is characterized by an accumulation of macrophages in the bronchioles and alveoli, neutrophils in the airway lumen and within pulmonary tissue, and B cells and CD8 + T cells in the small airways [34, 35]. Additionally, mast cells are also in increased levels in the airway wall, with mast cell mediators present in the Broncho-alveolar lavage (BAL) fluid of COPD patients. Eosinophils are also present in the airway wall and found in induced sputum, suggesting that both cell types play a role [34]. Epithelial and mesenchymal cells, both structural cells of the lungs, have been identified as producers of inflammatory mediators that are involved in the pathogenesis of COPD [34]. Lung inflammation is COPD is maintained by a number of factors including viral infections, which increase release of mediators and adhesion molecules, and recurrent viral and bacterial infections, which cause a chronic inflammatory state [36, 37]. Bacterial and viral infections also commonly cause COPD exacerbations and disease severity, as they facilitate secondary inflammation [36].

Oxidative burden is increased in COPD. Both the gas and tar phase of CS deliver large amounts of free radicals including carbon-, nitrogen-, and oxygen-centred radical species. CS and reactive oxygen and nitrogen species released from inflammatory cells are the main sources of oxidants, creating an imbalance of oxidants and antioxidants and leading to oxidative stress [38]. Various makers of oxidative stress are increased in stable COPD. Furthermore, during disease exacerbation, these markers are further increased. Effects of oxidative stress include inactivation of antiproteases, stimulation of mucus production and amplification of inflammation through augmentation of transcription factor activation, such as nuclear factor κB (NFκB), which in turn results in gene expression of pro-inflammatory mediators [38].

Furthermore, there is increased production of proteases and inactivation or reduced production of antiproteases, resulting in an imbalance. CS and inflammation result in oxidative stress which then further stimulates several inflammatory cells to release a

combination of proteases and inactivated antiproteases [34]. Neutrophils produce some of the main proteases involved, including serine protease elastase, cathepsin G, and protease 3. Other proteases, including cysteine proteases and cathepsins E, A, L and S are produced by macrophages. Metalloproteases MMP-8, MMP-9, and MMP-12 are also produced. The main antiproteases involved in emphysema include α_1 antitrypsin, secretory leucoprotease inhibitors and tissue inhibitors of metalloproteases. A study by Gadek et al showed a nearly twofold decrease in the functional activity of α_1 antitrypsin in the lungs of cigarette smokers compared to non-smoking individuals [39].

Initially, an enhanced or abnormal inflammation beyond the normal protective inflammatory response in the lungs is focused in the peripheral airways and lung parenchyma and persists even when exposure to the irritant ceases. Smoking impairs repair responses thus resulting in structural changes in the airways, including airway epithelial cell metaplasia and mucus hyperplasia from tissue destruction [34, 35]. Mucus hyperplasia leads to mucus hypersecretion, resulting in a chronic productive cough that is characteristic of chronic bronchitis [40]. Smoking can also cause abnormal repair, causing peribronchiolar fibrosis, and the damage also includes alveolar wall destruction, which is characteristic of emphysema and leads to air trapping [7]. The hallmark features of COPD pathogenesis are featured in Figure 1.1.

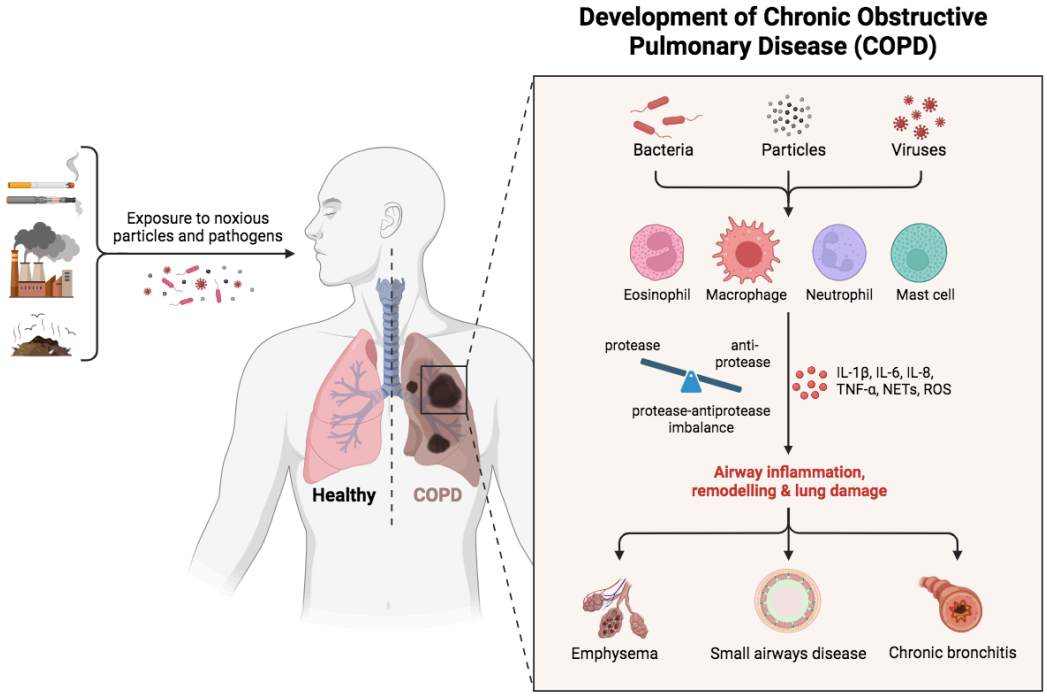

Figure 1.1. Schematic representation of the pathogenesis of COPD. Exposure to cigarette smoke, other noxious particles and pathogens results in activation of immune cells (e.g. neutrophils, macrophages, eosinophils), which drives production inflammatory mediators, such as cytokines, chemokines, proteases, and ROS. The activated cells also release proteases such as serine protease elastase and MMP-9. Together, these leads to chronic inflammation, airway remodelling and lung damage, resulting in emphysema, small airway disease and chronic bronchitis.

1.2.1. Chronic bronchitis

It is estimated that chronic bronchitis is exhibited by two-thirds of patients with COPD [41]. Chronic bronchitis is defined as chronic productive cough with sputum production for 3 months a year for 2 consecutive years [42, 43]. Chronic bronchitis is associated with several clinical consequences which include accelerated decline of lung function, increased risk of exacerbations, reduced health-related quality of life and worse overall mortality [42, 44]. Chronic bronchitis occurs when the innate immune system responds to toxic particles and gases associated with inhaled cigarette smoke, leading to inflammation in the epithelium and in the mucus-producing glands. Excessive mucus is caused by overproduction and hypersecretion by goblet cells and reduced elimination of mucus due to poor ciliary function, distal airway occlusion and ineffective cough [44]. As

a result, chronic bronchitis is characterized by mucus hypersecretion, reduced mucociliary clearance and increased permeability of the airspace epithelial barrier [34]. Symptoms of chronic bronchitis include chronic cough and sputum production [34, 41, 45].

1.2.2. Emphysema

Pulmonary emphysema is defined as the enlargement of the distal airspaces, beyond the terminal bronchioles, as a result of the destruction of the alveolar walls [34, 35, 45]. Exposure to cigarette smoke results in abnormal wound healing and the prevention of repair of lung injury. Exposure also kills endothelial cells and endothelial cell precursors and inhibits epithelial cell proliferation [35]. Consequently, there is enlargement of the distal airspaces beyond the terminal bronchioles and reduction of maximal expiratory airflow, as the elastic recoil force that drives air out of the lungs is decreased [34].

1.2.3. Small airway disease

Small airway disease (SAD) is recognized as a key pathological feature of COPD. The small airways are less than 2mm in diameter, and there is a significant increase in small airway resistance in COPD patients compared to controls [34, 46]. SAD is characterised by airway remodelling, mucus plugging and immune cell infiltration [47]. Injury caused by environmental exposures or infection induces the wound healing process which increases airway wall thickness, thus decreasing the airway lumen. Cigarette smoking results in a reduction of cilia length in the small airways, which leads to decreased mucociliary clearance [47]. This reduction in clearance, along with mucus hypersecretion secretion, narrows and then closes the lumen of the smaller conducting airways [48]. Mucus plugging can also lead to infection, as the mucous can harbour pathogenic microorganisms that promote inflammation and tissue destruction. Immune cell infiltration also occurs whereby there is increased recruitment of neutrophils, macrophages, B cells and T cells to the small airways, with CD8+ T cells suggested to be

the predominant inflammatory cells that contribute to small airway obstruction and tissue damage [47, 49, 50].

1.2.4. Systemic effects of COPD

Presently, COPD is considered a complex and multifactorial disease, causing effects beyond the lung, with systemic manifestations and comorbidities, including cardiovascular disease, osteoporosis and diabetes [51]. The most commonly recognised systemic manifestations of COPD include the presence of concomitant cardiovascular compromise, skeletal muscle wasting, cachexia (loss of fat-free mass), pulmonary hypertension, osteoporosis, anaemia, increased gastroesophageal reflux, and clinical depression and anxiety [51].

Cigarette Smoke (CS) may result in systemic inflammation; however, the degree of systemic inflammation is even greater in COPD patients. Indeed, patients with COPD, in particular those with severe disease or exacerbations, show increased evidence of systemic inflammation, measured as increased circulating cytokines, chemokines, and acute phase proteins, or as abnormalities in circulating cells [51-53]. Increased markers of systemic inflammation in COPD are cytokines, including IL-6, IL-8, IL-1β, TNF-α and adipokines, acute phase proteins, including C-reactive protein (CRP), fibrinogen, serum amyloid A and surfactant D, and circulating cells, including monocytes, neutrophils and lymphocytes [51, 53].

The depletion of muscle mass and function is another recognised feature of COPD, often accompanied by cachexia [54]. It is thought that during conditions such as COPD, the muscles and skin preferentially lose proteins, whereas visceral organs lose little or no proteins. Muscle fibre type shifts from type I to type II have been observed in COPD, which results in reduction of muscle strength and thus reduced exercise capacity and decreased quality of life [55].

1.3. Cigarette smoke

Cigarette smoke (CS) is a significant risk factor associated with various diseases, including COPD, cardiovascular disease and cancers. Exposure to CS is the most significant risk factor associated with COPD [56]. According to the World Health Organisation, tobacco use kills over 7 million people each year worldwide, including from second-hand smoke exposure [57]. CS is an aerosol that consist of solid and liquid droplets in a gaseous phase and contains over 4500 different substances with various toxic, mutagenic and carcinogenic effects, resulting in health risks associated with smoking [58, 59]. Inhaled particulate matter from CS is usually deposited in the respiratory tract depending on the size, whereby larger particulates are deposited in the upper airways and smaller particulates are deposited in the alveoli. CS causes oxidative stress which activates epithelial cells, alveolar macrophages, neutrophils and T lymphocytes, resulting in low-grade inflammation and recruitment of inflammatory cells to the airways. CS also increases the virulence of pathogens, resulting in an increased risk of pulmonary infections [59].

1.3.1. Tobacco Toxicology

Substances found in CS include nicotine, tar, ammonia, carbon monoxide, carbon dioxide, formaldehyde, acrolein, acetone, polyaromatic aromatic hydrocarbons, hydroxyquinone, nitrogen oxides and cadmium. Indeed, specific metals have been detected in tobacco and tobacco smoke which reach the lungs after repeated inhalations of CS [60, 61]. Metals of particular interest in CS are cadmium, lead, nickel, arsenic, beryllium, aluminium and cobalt, as they are classified as carcinogens by the International Agency for Research on Cancer [60, 61]. Toxic elements cadmium, mercury, nickel, lead, manganese and arsenic also result in the production of ROS, leading to oxidative stress [60]. Additionally, some of these metals take a long time to be cleared from the lungs, particularly cadmium which is known to have a biological half-life of 13 to 24 years and chromium with an undetermined half-life.

Other harmful components of CS include compounds that may occur in the particulate or gaseous phase of the smoke and include about 5,000 compounds. The leading harmful components are found to be nicotine, aromatic amines, phenols, tobacco-specific nitrosamines, polycyclic aromatic hydrocarbons, carbon monoxide, nitrogen oxides, aldehydes and ketones carbonyl compounds, hydrogen cyanide and ammonia [62]. CS is known to also contain traces of microbial cell components, including bacterial lipopolysaccharide (LPS) [63, 64]. Therefore, due to its thousands of cytotoxic, mutagenic, carcinogenic and antigenic chemicals, CS activates epithelial cells of the lungs and in turn cells of the immune system, inducing the release of chemokines and inflammatory mediators, thus promoting chronic inflammation in the airways [63].

1.4. Immune response on exposure to cigarette smoke

CS affects both the innate and adaptive (cell-mediated and humoral) immune responses. CS is associated with both the release and the inhibition of pro-inflammatory and anti-inflammatory mediators, where a number of pulmonary and systemic cytokines are involved in the chronic inflammation observed in smokers. Continuous exposure to CS and other inhaled irritants stimulates the structural and inflammatory cells present in the respiratory tract. With continuous exposure to CS, there is activation of the airway epithelial cells which reduces the length and motility of cilia responsible for mucus removal [65]. This may lead to the accumulation of inflammatory pathogens and debris in the respiratory tract [64]. Consequently, in response to the toxic particles found in CS and the debris, there is activation of macrophages, dendritic cells and airway epithelial cells that release mediators that recruit and activate CD8+ T-lymphocytes and neutrophils [66]. In addition, CS is known to stimulate apoptosis in the epithelial cells of the alveoli, and chronic exposure to CS leads to excessive epithelial cell death. Thus, there is loss of the alveolar and small airway integrity that in turn, reduces lung function [64].

1.4.1. Inflammation in the lungs

Disease pathogenesis of COPD is associated with an excessive CS-induced inflammatory response of the airways and the lungs. Patients with COPD have a characteristic pattern of inflammation with elevated numbers of neutrophils in the airway lumen and increased numbers of macrophages, T lymphocytes and B lymphocytes [67, 68]. Here, the inflammatory response involves both the innate and adaptive immune response. Indeed, a similar pattern of inflammation and mediator expression has been observed in smokers without airflow limitation [67].

CS and other inhaled irritants activate airway epithelial cells and macrophages, where they release a variety of chemotactic mediators that drive influx of circulating neutrophils, monocytes and lymphocytes into the lung and produce inflammatory mediators, including tumour necrosis factor (TNF)-α, interleukin (IL)-1β, IL-6, IL-8 and granulocyte-macrophage colony-stimulating factor (GM-CSF) [67, 69, 70]. The recruitment of inflammatory cells into the lung and their constant presence following exposure to CS results in a risk of tissue damage due to the release of chemotactic and toxic mediators such as proteolytic enzymes and ROS [71]. Indeed, ROS activates NF-κB, which switches on a number of inflammatory genes leading to an increased inflammatory response [67]. CS also drives increased release of chemokine (C-X-C motif) ligand 1 (CXCL1), CXCL8, CCL2, and leukotriene (LT) B_4, chemoattractants that induce chemotaxis of neutrophils and monocytes [72]. Additionally, CS increases secretion of elastolytic enzymes, including matrix metalloproteinases (MMPs) -2, -9 and -12 from macrophages, suggesting that elastolytic activity is increased by exposure to CS [67]. Studies involving murine models have also demonstrated lung inflammation due to exposure to CS. Perez-Rial et al [73] observed that exposure to whole-body CS in a single day induced lung inflammation in mice. The study showed increased levels of monocytes in BAL and an increase in MMP-1 and TNF-α protein levels in the lung tissue, indicating an increase of proinflammatory monocytes associated with major tissue damage due to acute lung inflammation [73]. John et al [74] observed in mice exposed to CS for three days a strong acute inflammatory response in the lung, where BAL

demonstrated neutrophil influx and increased cytokine secretion (keratinocyte chemoattractant (KC), TNF-a, macrophage inflammatory protein (MIP)-2, MIP-1a, monocyte chemoattractant protein (MCP)-1). The study also observed proinflammatory gene expression (KC, MIP-2, MMP12), and upregulated GM-CSF production in lung tissue [74].

Finally, CS also has suppressive effects on host defences against pathogens, compromising both innate and adaptive immune mechanisms. Indeed, CS exposure in humans has been shown to be associated with an increased risk of influenza infections and increased risk of severe symptoms [75, 76], triggering an exaggerated inflammatory response compared to healthy individuals and exacerbation of symptoms. Viral infections exacerbate inflammation through increased production of proinflammatory cytokines, including IL-6, TNF-α and IL-8, which contribute to airway narrowing and obstruction and tissue damage [77]. Viral infections also promote airway remodelling in COPD patients, which further contribute to airflow limitation and respiratory symptoms [78]. Lastly, oxidative stress in the lungs of COPD patients is promoted during viral infections, leading to increased production of ROS and oxidative damage to lung tissue, exacerbating inflammation and contributing to disease progression [79]. Together, these mechanisms contribute to progression of COPD and exacerbation of symptoms experienced in COPD patients following viral infections.

Therefore, CS results in a number of effects (Figure 1.1.), including activation of epithelial cells and alveolar macrophages, an influx of inflammatory immune cells, the release of proinflammatory mediators and decreased defence against pathogens, all of which drive inflammation in the lung.

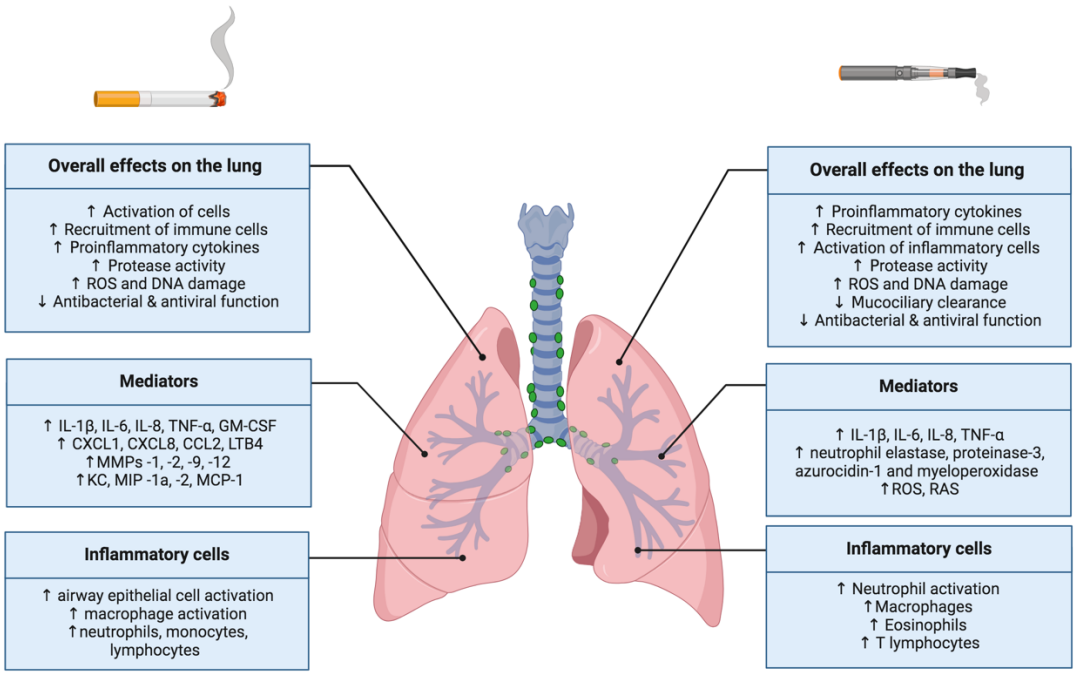

Figure 1.2. Overview of the inflammatory effect of cigarette smoking and e-cigarette vaping on the lung. Both cigarette smoking and e-cigarette vaping result in increased activation of epithelial cells and macrophages, increased activation and infiltration of inflammatory cells, increased cytokines and chemokines production, increased protease activity, increased ROS and DNA damage, and reduced antibacterial and antiviral activity by cells in the lung, all which drive inflammation in the lung.

1.4.2. Epithelial cells

Airway epithelial cells line the surface of the respiratory tract and function as the lungs' primary line of defence against environmental insults such as pathogens, inspired noxious particles and allergens [70]. The airway epithelium is comprised of specialised epithelial cell types including ciliated, mucous, goblet, Clara and basal cells in the bronchial epithelium, and type I and type II cells in the alveolar epithelium [70, 80]. The cells in the epithelium are joined by tight and adherent junctions, forming the apical junctional complex, thus forming a relatively impermeable barrier [70]. Additionally, this physical barrier is maintained by a mucociliary barrier composed of cilia, a periciliary fluid layer and a mucus layer, where mucociliary clearance results from the organized ciliary movements to remove pollutants and inhaled particles from the distal airway

toward the pharynx [81]. Usually, upon injury, airway epithelial cells initiate a rapid wound repair process where the cells produce innate immune mediators to enhance host defences at the wounded area [82]. However, this repair process may be modified directly through CS exposure or indirectly by CS-induced inflammation, thereby promoting epithelial remodelling and persistent airway inflammation [82]. Indeed, CS induces changes in the airway epithelial layer, resulting in goblet cell hyperplasia, modified cilia length, decreased ciliogenesis, decreased ciliary beat frequency and epithelial barrier dysfunction [70, 83].

CS causes oxidative damage in alveolar epithelial cells, as it enhances intracellular ROS levels with depletion of glutathione, resulting in cell growth arrest, cell detachment and enhanced epithelial permeability [84-88]. The oxidative damage in alveolar epithelial cells caused by CS ultimately results in cell death, by either apoptosis or necrosis, depending on the magnitude of CS exposure [87, 89]. Alveolar epithelial cell death triggers the initiation of epithelial repair processes. However, exposure to CS inhibits the ability of epithelial cells to migrate, attach to the extracellular matrix and heal wounds [87, 90]. Additionally, the augmentation of alveolar epithelial cell death can contribute to the pathogenesis of pulmonary emphysema, a lung disease associated with CS. Indeed, increased levels of apoptosis in epithelial and endothelial cells have been previously observed in the alveolar walls of smokers with pulmonary emphysema [91, 92].

Furthermore, CS has been shown to increase the release of proinflammatory cytokines, IL-6 and IL-8, by human bronchial epithelial cells (HBECs) in a concentration-dependent manner, possibly contributing to airway inflammation in smokers [88, 93, 94]. CS has also been shown to cause cytotoxic effects on bronchial epithelial cells, as a time-dependent reduction in cell viability was observed in BEAS-2B (lung epithelial cell line) cells following exposure to CS *in vitro* [95]. CS inhibits the ability of HBECs to participate in the repair process, due to CS inhibiting HBEC proliferation and chemotaxis [90]. CS also inhibits the ability of these cells to remodel extracellular matrix [90]. Therefore, CS enhances lung injury by causing epithelial cell death and inhibiting the epithelial repair

processes, contributing to the architectural and functional disruption that results in lung diseases associated with cigarette smoking.

Exposure to CS also compromises the host defence function of the airway epithelium, as study has shown that smokers with pneumonia had significantly lower levels of endogenous antibiotic peptide human β-defensin-2 (hBD-2) in their mucosal secretions [88, 96]. Epithelial cells are known to be the main cellular source of hBD-2 in the lung, with defensins having a role in pulmonary host defence [97]. A study by Pace et al also observed reduced expression of hBD-2 in the central airways of smokers, with expression of hBD-2 positively correlating with lung function in COPD [98]. In addition to reduced barrier integrity and expression of tight junction, these effects lead to a defect in host defence and disruption of the epithelial barrier. Thus, CS causes airway epithelial barrier dysfunction that may contribute to the pathogenesis of chronic lung diseases, including COPD.

1.4.3. Macrophages

Macrophages are key effector cells of the innate immune system that carry out various functions involved in host defence and immunity against pathogens [99]. Macrophages have a wide array of cell surface receptors, intracellular mediators and essential secretory molecules required for the recognition, engulfment and destruction of invading pathogens and for the regulation of other immune cell types [100].

Macrophages are classified based on their function, into two phenotypes: inflammation-promoting M1-polarised macrophages (classically activated) and anti-inflammatory M2-polarised macrophages (alternatively activated) [101, 102]. They can change their phenotype depending on the local environment and are known to form two distinct polarised phenotypes *in vitro* after cytokine exposure in monocyte-derived macrophages [59]. In vivo, however, macrophage activation has been described as a continuum, as it has been noted that many of the M1/M2 markers are co-expressed on the same macrophages [102]. For example, CD206 is ubiquitously expressed by all pulmonary macrophages [103]. Indeed, study has shown that macrophages exposed to

a combination of LPS, interferon (IFN)-γ, IL-4, and IL-13 develop a mixed activation state with cells expressing both M1 marker CD86 and M2 marker CD206, instead of polarising to discrete phenotypes [102].

M1 macrophages are involved in the destruction of intracellular pathogens and produce proinflammatory cytokines, producing a T helper 1(Th-1) cell environment [104]. M1 are characterised by their expression of HLA-DR, CD14, CD86 and CD38 [59, 102]. M2 macrophages are involved in downregulating inflammation and tissue repair, thus producing a Th-2 cell environment, and are characterised by their expression of CD36, CD206 and CD163 [59].

Macrophages are abundantly present in the lung microenvironment, where they are known as alveolar macrophages (AM), the resident mononuclear phagocytes of the lungs that play an important role in the immune response that occurs in the lungs [105]. AMs induce regulatory effect through non-specific immune-defence mechanisms, including phagocytosis, production of inflammatory mediators, such as ROS, and production of inflammatory cytokines like IL-1, IL-2, IL-4, IL-6, IL-8, TNF- α and IFN-γ [59]. AMs also regulate and resolve inflammation through the expression of anti-inflammatory mediators and via efferocytosis [59].

Early responses to inhaled toxins such as CS result in the recruitment of macrophages and neutrophils to the lungs through the increased production of IL-8 [59]. CS increases levels of alveolar macrophages in the lungs of smokers and COPD patients, where they particularly accumulate in the alveoli, bronchioli and small airways [106]. Macrophages phagocytise irritants and produce MCP-1 in addition to IL-8, which induces further neutrophil influx into the airways [99, 107, 108]. Indeed, increased levels of MCP-1 have been observed in sputum samples of COPD patients [72]. CS also reduces phenotypic markers of M1 phenotype and/or increases markers of M2 phenotype, which has been implicated in dysregulated inflammation [59, 109]. Furthermore, CS significantly reduces the phagocytic function of macrophages, reducing its ability to clear the inflammatory cells and debris from the lungs [59, 105, 110]. The interaction between CS and AMs results in modification to the extracellular matrix proteins which significantly

downregulates their ability to phagocytose apoptotic neutrophils [110]. Expression of TLR2 surface markers is reduced in AMs from smokers compared to non-smokers and, upon LPS stimulation, levels of messenger RNA (mRNA) and protein expression did not increase, suggestive of a decreased antimicrobial response present in CS [59, 111]. CS exposure also reduces expression of TLR4 in monocyte-derived macrophages, with increased intracellular ROS and reduced antioxidant glutathione, implicated in oxidative stress and lung inflammation and observed in the pathogenesis of emphysema [59, 112].

CS also results in modification to the proteolytic enzymes (proteinases) released by AMs. Expression of matrix metalloproteinase (MMP)-12 is increased in smokers compared to non-smokers [113]. MMP-12 degrades elastin and contributes to emphysema [59, 114]. Additionally, MMP-12 may increase expression of placenta growth factor (PGF) by increasing early-growth response protein 1 (EGR-1) level through activation of protease-activated receptor 1 (PAR-1) [115], which results in bronchial epithelial cell apoptosis and further drives emphysema [59, 114, 115]. AMs, in response to CS, also produced increased levels of elastolytic cysteine proteinases and cathepsin S, both having the capacity to cause significant lung damage [59].

Overall, CS has a number of effects on AMs, including changes in phenotype, the ability to phagocytose and kill bacteria, ROS production, efferocytosis, and proteinase release. This results in acute and chronic inflammation with further inflammatory cell recruitment, which in turn results in lung destruction and remodelling with increased susceptibility to pulmonary infection and development of CS-induced lung diseases [59]. Many of the changes persist even after smoking cessation, and further understanding of the mechanisms of CS on AMs and other lung populations is necessary to reduce the risk of further lung injury.

1.4.4. Dendritic cells

Dendritic cells (DC) are professional antigen-presenting cells (APCs) that link the innate immune response and adaptive immune response through direct cell-to-cell interactions

and/or cytokine production [116, 117]. This type of antigen presenting cells is the most proficient inducer of the primary and secondary immune response as they recognize, process and present the antigen to naïve lymphocytes [117, 118]. Subtypes of DCs are characterised by surface markers and function and arise from bone marrow precursors that colonise peripheral tissue through the blood or the lymphatic system [119]. Subtypes of DCs are separated into type 1 and type 2 classical/conventional DCs (cDC1 and cDC2, respectively) and plasmacytoid DCs (pDCs) [120]. Human cDC1s are generally found in the mucosa and vascular wall, and they express CD141 and CLEC9A, and can also express the C-type lectin receptor langerin [120, 121]. They are functionally distinct from other DC subsets due to their ability to elicit Th1 responses and uniquely cross-present apoptotic cell-associated antigens [120]. cDC2s are CD1c+ and in the lung, are major producers of proinflammatory chemokines, thus responsible for recruiting inflammatory cells. They can activate Th2 and Th17 responses [121]. pDCs are distributed throughout the lungs, airways, parenchyma and alveolar septa, and are essential during antiviral responses due to their ability to produce type I IFNs [120]. Pulmonary DCs exist as immature APCs, efficient in antigen uptake. However, during DC maturation, their antigen uptake ability declines as the antigen presenting ability is enhanced. In antigen presentation, MHC II molecules are the first classical signal of this process, along with co-stimulatory molecules, including CD86 and CD40 [119]. Upon antigen capture, immature DCs are activated, causing them to mature and migrate to lymphoid organs, where they display the antigen-derived peptides on their MHC molecules and induce activation and proliferation of the antigen-specific lymphocytes [118].

Active cigarette smoking significantly affects the number, distribution and differentiation of DCs [70, 122]. Indeed, CS exposure leads to decreased numbers of bronchial mucosal DCs in COPD and asthma patients [123, 124]. Furthermore, CS exposure impairs the maturation and function of DCs, where DCs exposed to CS display diminished T cell stimulatory capacity [125], have reduced cell surface expression of MHC II and costimulatory molecules CD80 and CD86, and have a decreased capacity to

induce production of IL-2 by T cells [70]. This is also accompanied by the suppression of chemokine receptor expression and the induction of co-stimulatory receptors [126]. Givi et al [119] demonstrated that short-term (24 hours) CS extract stimulation of DCs influenced the maturation status of newly differentiated and immature DCs towards more mature cells as revealed by the upregulation of MHC II, CD83, CD40, reduction of antigen-uptake capacity and enhanced secretion of pro-inflammatory (IL-12, IL-6, TNF-α) cytokines [119]. The study also demonstrated that long-term CS extract exposure suppressed the development of functional DCs, revealed by their reduced CD11c/MHC II, CD83, CD86 and CD40 expression, reduced production of cytokines, and reduced ability to stimulate T cells [119]. As CS significantly impairs DCs' ability to stimulate T cells, DCs also have a decreased capacity to induce T cell proliferation and Th1 differentiation, on the other hand, increasing DC-dependent Th2 differentiation [118, 127, 128]. Indeed, Alkhattabi et al also showed that CS extract treatment of human monocyte-derived DCs (moDCs) reduced the expression of pro-inflammatory signalling molecules [129]. Overall, CS modulates DC-mediated responses, where it affects both the function and maturation of DCs. Indeed, the suppressive effects of CS on the function and maturation of DCs may result in an impaired immune response to infection.

1.4.5. Natural Killer Cells

Natural Killer (NK) cells are large granular lymphocytes that secrete perforin, granzyme, TNF-α and IFN-γ, similar to cytotoxic lymphocytes, however, they do not express a T cell receptor and are part of the innate immune response [130]. CS has been shown to be linked to a decrease in the number and proportion of circulating NK cells, which continues many years after smoking cessation [131]. Furthermore, CS exposure both suppresses and stimulates NK cell activity. Current smokers have been found to have reduced activity of NK cells compared to non-smokers and former smokers [132], however, these changes are reversible as NK cell activity is restored to levels of non-smokers after 6 weeks of smoking cessation [70, 133, 134]. The level of NK cell activity in

current smokers has been observed to decrease with increases in the number of cigarettes smoked, even after adjusting for age and sex [132]. Additionally, NK cells from long-term smokers have a decreased intracellular IL-6 concentration, a cytokine that recruits CD4+ cells, suggesting that long-term smoking may affect immune responses at the systemic level with NK cells being involved [135]. Along with reduced cytotoxic activity, a study has also demonstrated that CS has negative effects on the production of inflammatory cytokines from NK cells. Indeed, CS has been reported to inhibit TNF-α and IFN-γ from NK cells from non-smokers in vitro [136] and also suppresses the induction of IL-15 and IL-15 mediated NK cell functions in human peripheral blood mononuclear cells (PBMCs) [137]. CS, however, may also exert a stimulatory effect on NK cells. Increased accumulation of activated CD69+ NK cells in parenchymal and mucosal locations in the airway was observed after acute CS exposure [138]. CS exposure also results in increased epithelial-derived IL-33 levels, which in turn increases IL-33 receptor ST2 expression on macrophages and NK cells, significantly contributing to the increase of type I pro-inflammatory responses in the lungs during infection [139]. Indeed, acute smoking has been associated with systemic activation of NK cells, whereas activation of pulmonary NK cells has been shown to be dependent on coincidence of COPD, irrespective of current smoking status [140]. A previous study by Urbanowicz et al showed an increased proportion of NK cells in the induced sputum of COPD subjects compared to healthy smokers and non-smokers, and that NK cells in COPD subjects also had increased cytotoxic activity, as shown by their expression of perforin and granzyme B, compared to smokers and healthy non-smokers [141]. Wang et al showed that in peripheral blood, current smokers, regardless of disease state, had the highest proportion of activated NK cells compared with ex-smokers with COPD and healthy non-smokers, with NK cell activation positively correlating with the number of cigarettes smoked [140].

1.4.6. Natural Killer (NK) T cells

NKT cells are described as innate-like lymphocytes that share features of both innate and adaptive immune cells [142]. They are a subset of T cells that co-express αβ-T-cell receptor and NK1.1, and are reactive to the MHC class–I-like molecule CD1d [143]. Unlike, conventional T cells, NKT cells recognize lipid antigens in a CD1d-dependent or independent manner [143, 144]. They express T cell membrane proteins, including CD3, and NK cell markers, including CD56, CD61 and inhibitory NK receptors [142]. NKT cells are present in extremely low numbers in the peripheral blood but are more commonly found among T lymphocytes in the liver and bone marrow, in the thymus and spleen and are in higher frequency in pancreatic and mesenteric lymph nodes [142] When activated, NKT cells readily secrete cytokines including IL-4 and IFN-γ [142], and cause targeted cell death through their use of the perforin/granzyme granule exocytosis pathway [145].

A previous study by Urbanowicz et al has shown that relative numbers of peripheral blood NKT-like (CD56+CD3+) cells are reduced in COPD subjects and that these cells have a defective effector function, due to reduced expression of perforin and granzyme B [145]. Ubranowicz et al further demonstrated an increased proportion of NK and NKT-like cells in the induced sputum of COPD subjects, with significantly more cytotoxic effector function than smokers and healthy non-smokers [146]. Furthermore, Hogan et al [147] observed a significant reduction of circulating invariant NKT (iNKT) cells in the peripheral blood of healthy smokers compared to age-matched non-smokers. Indeed, the study also observed that CS extract exposure in-vitro resulted in a significant alteration in iNKT cell function, with a significant defect in cytokine production and cytotoxic ability, and inhibition of CD107 [147]. Pichavant et al [148] showed, in a mouse model, that exposure to CS resulted in the accumulation of activated iNKT cells in the lungs and that smoking-related oxidative damage may be mediated through iNKT cells. Strom et al [149] demonstrated that proportions of NK, iNKT and NKT-like cells in the BAL fluid increased with pack-years. The study also showed that current smoking was associated with a marked increase in iNKT and NKT-like cells but not in NK cells [149].

Wang et al [140] also observed that smokers with or without COPD had higher proportions of activated CD8 T lymphocytes, NKT-like cells and NK cells in their peripheral blood compared with healthy non-smokers and ex-smokers with COPD. Together, these studies show that CS alters the numbers and activation of NKT cells, which may drive the pathogenesis of COPD.

1.4.7. Neutrophils

Neutrophils are the most abundant leukocyte in human blood, making up 70% of all circulating white blood cells, and are involved in the front-line defence of the immune system and produce a number of reactive oxygen metabolites, inflammatory cytokines, lipid mediators, tissue-damaging enzymes, and antibacterial peptides [150, 151]. They are produced in the bone marrow from hematopoietic stem cells and are then released and remain in circulation until recruited to tissues where they carry out several specialised functions, including phagocytosis, degranulation, oxidative burst and release of neutrophil extracellular traps (NETs) [152]. Neutrophils are able to migrate very quickly from peripheral blood into peripheral tissue, due to infection or tissue damage [153]. Indeed, neutrophil migration is influenced by chemoattractants, particularly IL-8, produced by the host during inflammation and pathogen-derived factors [153]. Neutrophils have a key role in controlling and eliminating lung infections by their release of ROS and proteases at the site of infection.

Airway neutrophilia is a hallmark feature of patients with chronic inflammatory lung diseases, including COPD, and is associated with disease development [151, 154]. Neutrophils and their products are considered key mediators of the inflammatory changes that occur in the airways of patients with COPD. Indeed, neutrophils have been shown to cause a number of pathological features associated with COPD, including emphysema [150, 154]. Inhalation of noxious agents and any acute exacerbations stimulate airway epithelial cells and macrophages to release the NF-κB and p38 MAPK-dependent release of neutrophil chemotactic mediators, thus promoting neutrophil mobilisation, recruitment and activation within the airways [155]. Neutrophils are

stimulated by the inhalation of toxic particles, including CS, to secrete proteases that cause tissue destruction and release mediators that promote airway inflammation. The resulting degranulation of neutrophils results in accumulation of serine proteases, myeloperoxidase (MPO) and matrix metalloproteinase (MMP)-8 and MMP-9, which trigger proteolytic degradation of the airway extracellular matrix; thus, driving emphysematous disease [155-157]. The enzymatic breakdown of the extracellular matrix results in further release of neutrophil chemoattractant proline-glycine-proline (PGP) within the airways, and together with CS, maintain a cycle of CXC motif chemokine receptor 2 (CXCR2)-mediated neutrophilic chemotaxis and the resulting clinical disease [155, 158].

Many studies have shown that neutrophils play a major role in airway inflammation that is central to the pathophysiology of COPD which contributes to tissue damage and destruction. Patients with COPD all have airway neutrophilia, regardless of their clinical phenotype (chronic bronchitis, emphysema or even eosinophilic COPD), disease severity, and rate of decline or age of onset [159-161]. Studies have shown that neutrophil counts are related to airway obstruction, decline in FEV_1, reduction in gas transfer and development of emphysema [154, 160, 162]. Thus, blood neutrophil count may be a useful indicator of risk of exacerbations and mortality in COPD, as peripheral neutrophil counts reflect systemic inflammation that is linked to disease severity and co-morbidities in COPD [154, 160, 163]. Furthermore, CS is a potent inducer of neutrophilic inflammation. Exposure to CS leads to necrosis of bronchial epithelial cells, the release of DAMPS and the production of pro-inflammatory cytokine, resulting in the induction of neutrophilic airway inflammation [164]. Increased numbers of neutrophils in BALF have been observed after exposure to CS [70, 164, 165]; and CS has also been shown to modify activation of neutrophils and chemotaxis, possibly impairing immune responses observed in smokers [166].

1.4.8. Eosinophils

Although neutrophilic inflammation is a predominant characteristic of COPD, approximately 20—40% of patients demonstrate an eosinophilic phenotype [167]. Indeed, eosinophils have recently been recognised to be involved in the inflammatory response of COPD. Eosinophils are inflammatory leukocytes that, under normal conditions, are inactive and low in count, making up 1-4% of the total white blood count. Differentiation into a mature eosinophil is stimulated by IL-5, which also plays a role in the survival, trafficking, activation and effector functions of eosinophils along with IL-3 and granulocyte/macrophage-colony-stimulating factor (GM-CSF) [168]. Upon exposure to inflammatory cues, eosinophils are activated and recruited to the lungs, where secretion of a variety of mediators including chemokines, cytokines and cytotoxic granular products contribute to inflammation [167, 168]. Migration of these cells to the lungs is triggered by specific chemotactic factors including CCL5 (RANTES), CCL7 (MCP3), CCL11 (eotaxin 1), CCL13 (MCP-4), CCL15, CCL24 and CCL6. Once in the lungs, eosinophils release proinflammatory mediators including basic proteins (major basic protein, eosinophil cationic protein, eosinophil peroxidase, and eosinophil-derived neurotoxin), cytokines (IL2, IL3, IL4, IL5, IL10, IL12, IL13, IL16, IL25), chemokines (CCL5, CCL11, CCL13) and growth factors (tumour necrosis factor (TNF), transforming growth factor (TGF)α/β) that contribute to persistent inflammation and tissue damage [168]. Previous study has shown that active smoking in stable COPD patients significantly increased the accumulation of eosinophils in distal airspaces of the lungs [169]. Elevated levels of eosinophils and eosinophil-associated proinflammatory factors have been detected in the airways and blood of patients with COPD, suggesting that eosinophils play an active role in inflammatory processes [168, 170, 171]. Furthermore, upon migration of eosinophils to the lungs, eosinophil-derived proinflammatory mediators drive persistent inflammation which in turn contributes to exacerbations [168, 172]. Indeed, increasing evidence suggests a link between increased concentrations of eosinophil and exacerbation of COPD, as studies have reported increased eosinophil

counts associated with an increased exacerbation risk [171, 173, 174] and others have observed increased eosinophil counts during exacerbations [168, 175, 176].

1.4.9. T lymphocytes

T lymphocytes (T cells) are a major subset of immune cells that mediate the adaptive immune response [177]. Naïve T cells are activated and differentiate upon antigen recognition to generate effector T cells, and some memory and regulatory T cells. There are two major classes of T cells that have different effector functions. These two classes are distinguished by the expression of the cell-surface proteins, CD4 and CD8, and the two types differ in the class of MHC molecule they recognize. The classes of MHC molecules are MHC class I and MHC class II, which differ in their structure and expression pattern on tissues of the body. CD4 binds to MHC II molecule and acts as a co-receptor for T cell receptors that recognize class II MHC:peptide ligands. CD8 binds to the MHC class I molecule and binds simultaneously to the same class I MHC:peptide complex being recognized by a T cell receptor, therefore acting as a co-receptor and enhancing T cell response. Cytotoxic CD8 T cells can induce apoptosis in target cells. Helper CD4 T cells are crucial for defence against both extracellular and intracellular pathogens, as they help to stimulate B cells and activate macrophages.

T lymphocytes of particular interest in COPD are the CD8+ T cells, as they have been shown to be present in elevated levels in the lungs of patients with COPD and produce cytokines that may contribute to emphysema [178]. Indeed, studies have revealed that smokers have increased levels of CD8+ T cells in the lungs compared to non-smokers [105]. A study by Forsslund et al [179] observed an increased percentage of CD8+ T cells in BAL of smokers with or without COPD compared to non-smokers, whereas for CD4+ T cells, there was a decreased frequency in BAL but increased frequency in the blood of smokers compared to non-smokers. Wang et al [140]showed an increased proportion of activated CD8 T cells in the peripheral blood of current smokers compared with ex-smokers with COPD and healthy non-smokers; also demonstrating that CD8 T cell activation is positively correlated with the number of cigarette smoked [140].

CD8+ cells are activated by DCs via antigen presentation on the MHC-I complex, and once activated, these cells identify target cells, releasing perforin and granzyme that disrupt the cell membrane and induce apoptosis of the target cell [180]. CS modifies T cell responses, resulting in increased susceptibility of cigarette smokers to respiratory tract infections. Once present in the lungs, these T cells can carry out their effector functions and do so partly by producing Th1 cytokines, particularly IFN-γ and IFN-inducible protein (IP)-10 [118, 181]. Overexpression of IFN-γ results in apoptosis, inflammation and emphysema [178]. In addition, IP-10 facilitates the production of the enzyme elastase which contributes to the fragmentation of elastin and pulmonary injury [177]. However, CS can also significantly suppress cytokine production, leading to a modified immune response by these cells [105]. In addition, the main effector function of CD8+ T cells is the ability to cause the apoptosis of target cells via an increased perforin expression and cytotoxic activity, which may also play a role in the damage of lung tissue of patients with emphysema [178, 181].

A second adaptive immune cell affected by CS is the CD4+ T helper cells, a study has shown that smoking alters the frequency of these cells in the BAL and the blood [179]. Indeed, increased numbers of activated (CD69+) naïve and effector CD4+ T cells have been observed in BAL in smokers compared to non-smokers, where this effect was particularly significant in smokers with COPD [179]. Another study has shown that chronic exposure to CS significantly elevated the numbers of Th1 and Th17 cells and also resulted in an increased expression of Th1-type cytokine IFN-γ and Th17-type IL-17A, causing pulmonary inflammation as a result of chronic CS exposure [177]. CD4+ T helper cells are activated by DC via the presentation of the antigen-derived peptide on an MHC-II complex [118]. DCs, along with the secretion of IL-2, initiate and shift the response to a persistent Th1-type chronic inflammation. In addition, Th2-type cells synthesise and release cytokines, particularly IL-4, that enhance mucus hypersecretion normally seen as an early response to CS and resulting in chronic bronchitis [118].

1.4.10. B lymphocytes and antibodies

B lymphocytes (B cells) are another major subset of immune cells that mediate the adaptive immune response, specifically the humoral immune response which is characterised by the production of antibodies. B cells are distinguished from T cells by the structure of the antigen receptor they express, the B-cell receptor (BCR). The BCR is formed by the same genes that encode antibodies, a class of proteins also called immunoglobulins (Ig). After an antigen binds directly to a BCR, the B cell will proliferate and differentiate into a plasma cell, which is the effector form of B lymphocytes. Plasma cells secrete antibodies that have the same antigen specificity as the surface BCR, therefore targeting the antigen that activates the B cells. Additionally, B cells are equally critical to cellular immunity, as they participate in T cell activation via antigen presentation, co-stimulation and cytokine production, and affect antimicrobial defences and tissue inflammation [182]. They also serve as regulatory cells that modulate both cell-mediated and humoral responses.

An increase in the number of small airways containing B cells and lymphoid follicles has been observed in patients with GOLD stage III-IV COPD compared to stage 0-II [183]. Elevated numbers of B cells in the mucosa of large airways of COPD patients compared to controls have also been noted [184]. Indeed, CS has been associated with an increase in the percentage of CD19+ B cells and an increase in the percentage of activated B cells (CD19+, HLA-DR bright cells) found in PBMCs from smokers when compared to non-smokers [185]. Additionally, previous studies have shown that CS results in a higher prevalence of class-switched memory B cells in peripheral blood [186] and memory IgG+ B cells in the lung [187]. CS has also been shown to modulate the levels of antibodies. Ferson et al [133] observed that smokers had lower IgG and IgA Immunoglobulin levels in their sera compared to non-smokers. Andersen et al [188] also show decreased serum IgG and IgA levels in smokers compared to non-smokers, and a study by Gerrard et al [189] showed significantly lower IgG and IgM levels in the serum of smokers compared to non-smokers. Indeed, other studies have also shown decreased levels of most immunoglobulin classes in smokers [190-192], except for IgE, which has been found to

be elevated in smokers [193, 194], resulting in an increased risk of development of atopic diseases and asthma [195].

Despite the decrease in immunoglobulin levels, CS is associated with increased levels of autoantibodies, including anti-nuclear rheumatoid factors [196-198]. Autoimmune antibody responses previously described include elastin-specific autoimmune responses in smokers with emphysema [199, 200], autoantibodies to epithelial cell antigens in patients with COPD[200] and endothelial cell-targeted antibodies in a rat model of autoimmune emphysema [201].

1.5. E-cigarettes

E-cigarettes are handheld battery-operated devices containing a cartridge that when activated generates vapour or aerosols without combustion [202, 203]. They are considered an alternative to traditional cigarettes and as such are used as a substitute to quit cigarette smoking as a way of reducing risk to health [203, 204]. The e-liquid solution used in e-cigarettes is made up of a mixture of propylene glycol (PG) (glycerine mixed with ethylene glycol is also used), vegetable glycerol, nicotine and flavouring agents [203, 205, 206]. Typically, an e-cigarette is made up of a mouthpiece, a cartridge, a heating element also known as the atomizer and a battery, and e-cigarettes can be disposable or rechargeable (Figure 2) [203, 206]. E-liquid solution is added to the cartridge of the device and then supplied to the atomizer. So, when the e-cigarette is activated, a small metal coil in the atomizer heats up and the solution is aerosolised into a vapour that is then inhaled by the user [207]. The design of e-cigarettes has evolved since their introduction. Currently, there are four generations of e-cigarettes (Table 1.2): the cig-a-like (first generation), pens/laser pointer (second generation), mods (third generation), and pods (fourth generation) [208, 209].

The use of e-cigarettes has been promoted as a safe alternative to cigarettes, and thus its use has expanded quickly, particularly among adolescents. However, an increasing amount of evidence suggests that e-cigarettes are a source of toxic chemical exposure with carcinogenic properties, and that the ultrafine particles delivered by e-cigarettes may contribute to pulmonary and systemic inflammatory processes and increase the risk of respiratory and cardiovascular diseases [206, 207]. Indeed, many smokers who intend to quit cigarette smoking by using e-cigarettes end up as dual users, where there may be higher levels of exposure to harmful chemicals compared to those who only smoke cigarettes [210].

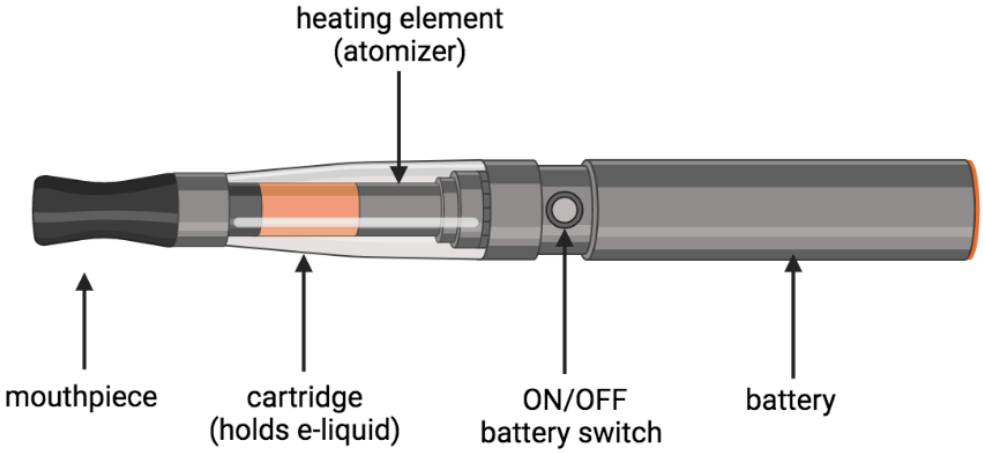

Figure 1.3. Structure of an electronic cigarette.

Table 1.3. General characteristics of four generations of electronic cigarettes.

Generation	Term	Features
First generation	Cig-a-like	Classic style; 3-piece EC: separate batter, atomizer and fluid reservoir
Second generation	Pens/laser pointer	Clearomizers; removable atomizing unit and larger transparent fluid reservoir
Third generation	Mods	Modified (Mods) atomizers; can come in tank form
Fourth generation	Pods	Atomizing units based on new technology

1.5.1. Toxicology of e-cigarette constituents

E-cigarettes generally contain components including propylene glycol (PG) and glycerol mixed with concentrated flavours and varying percentages of nicotine [203]. PG is a clear, colourless, viscous liquid at room temperature, typically used by chemical, food and pharmaceutical industries as a humectant to absorb extra water and maintain moisture in products including medicines, cosmetics and foods [211, 212]. It is also used as a solvent for food colours and flavours, paints, plastics, intravenous drugs and oral preparation of medicines. PG is generally recognized as a safe food additive [212]. Glycerol is an oily, hygroscopic liquid, typically derived from naturally occurring fats and oils (as vegetable glycerin). It is used in food products, oral care products, personal care products, pharmaceutical products and natural supplements [212, 213]. Most e-liquids contain a mixture of 30-50% glycerol and the balance as PG and both chemicals are considered safe. However, evidence has shown that PG can lead to unfavourable effects, as it alters physiological processes [214], results in acute toxicity [215] and dermal, ocular and airway irritation [211, 213, 216]. Furthermore, when heated, PG and glycerol form thermal degradation products, including acetone, acetaldehyde, formaldehyde, methylglyoxal, propionaldehyde and acrolein [211]. Aldehydes, including carcinogens like formaldehyde, acetaldehyde and acrolein, have been found in emissions from all generations of e-cigarettes [211, 217, 218].

Furthermore, e-cigarettes use e-liquids which are composed of numerous chemicals used to flavour them [211]. Over 7,000 unique e-liquid flavours have become available to e-cigarette users [219], where many of the flavourings are considered safe for ingestion but this does not reflect their ability to induce inhalation toxicity [211, 219]. Over 140 unique flavouring compounds have been detected across 28 e-liquids [220], and over 150 chemicals found in 277 refill fluids, with most containing flavours over 1 mg/mL in concentration [221]. Some studies have detected common flavourants in concentrations greater than those required to elicit cytotoxicity [211, 222, 223]. Indeed, a study by Bahl et al [224] observed the toxicity of 36 different e-liquids and 29 different flavours on human embryonic stem cells, mouse neural stem cells and human

pulmonary fibroblasts using a metabolic activity assay. Their findings showed that e-liquids with menthol and caramel flavours had a significant cytotoxic effect on pulmonary fibroblast and e-liquids with cinnamon flavour were most cytotoxic in all cell lines [224]. Further in-vitro studies have observed that cinnamon-flavoured e-liquids result in high cytotoxicity [225, 226] and a more enhanced pro-inflammatory response [227, 228].

Another component added to e-liquids is nicotine, a highly addictive chemical obtained from tobacco leaves. The concentration of nicotine in e-liquids ranges from 0 to 20 mg/mL, depending on the manufacturer, however, some commercial e-liquids have concentrations up to 54 mg/mL [212]. E-cigarettes also contain traces of cadmium, lead, nickel, xylene, methylbenzaldehyde and silica, among other toxic compounds, including toxic metals [206]. Indeed, the heating element within an e-cigarette is considered the largest source of toxic metal exposure, as metals transfer into the e-liquid and aerosols and are therefore inhaled by e-cigarette users [229]. Metals often detected in e-cigarettes include chromium, nickel, selenium and aluminium, whereas iron and lead have only been found in some products [230, 231].

1.6. Immune response on exposure to e-cigarette vape

With the increasing concern of the use of e-cigarettes, studies have been attempting to elucidate the acute and long-term effects of e-cigarettes. Indeed, emerging evidence suggests that e-cigarette use affects both innate and adaptive immunity [232]. Some studies have shown that primary human bronchial epithelial cells exposed to e-liquid solution resulted in significant decrease in cell viability and increased oxidative stress when compared to air-exposed cells [205]. In addition, nicotine was found to reduce ciliary beat frequency, which may affect mucociliary clearance. E-cigarettes, however, are known to affect various aspects of the human body [203].

1.6.1. Inflammation in the lungs

The health effects of exposure to e-cigarettes, particularly chronic exposure, are uncertain. E-cigarettes, however, emit volatile carbonyls, ROS, furans and metals, some of which are known to be toxic to the lungs. As e-cigarette use is rapidly growing among non-smokers, including youth and young adults, there has been an epidemic of hospitalisations and deaths of e-cigarette users due to acute lung injury, termed as e-cigarette or vaping use-associated lung injury (EVALI) [233].

The use of e-cigarettes results in a number of adverse effects that may lead to inflammation in the lungs (Figure 1.2.). Exposure to e-cigarettes stimulates epithelial cells and immune cells in the upper airway and lung to secrete proinflammatory cytokines including IL-1 β, IL-6, IL-8 and TNF- α [234-236]. Indeed, IL-6 and IL-8 are indicators of an ongoing inflammatory response in epithelial cells and monocytes, and IL-8 is a potent neutrophil attractant [233]. E-cigarette exposure also activates neutrophils, leading to degranulation of stored mediators and enzymes, oxidative bursts and release of NETs, which results in a significant increase of neutrophil elastase, proteinase 3, azurocidin-1 and myeloperoxidase [237]. Increased protease activity from exposure to e-cigarette vapour can damage the lung basement membrane and extracellular matrix, leading to emphysema [233]. The main cells found to be recruited to the lungs during exposure to e-cigarette aerosols include macrophages, neutrophils, eosinophils and T cells [235, 238-240]. E-cigarette exposure also drives increased production of reactive aldehyde species and ROS, which induce apoptosis, mitochondria dysfunction and protein inactivation, and induce cellular damage, respectively [233, 241-243]. Indeed, these highly reactive species can drive lung pathogenesis [244]. The increased generation of ROS due to e-cigarette exposure further induces inflammatory responses, as observed in both human epithelial cells and murine models [228]. E-cigarette exposure also compromises mucociliary clearance by reducing the ciliary beat frequency in both in vitro and in vivo models [245, 246]. E-cigarette vapour exposure also inhibits the antibacterial function of epithelial cells, macrophages and neutrophils [236, 247, 248]. This establishes a favourable environment for pathogenic bacterial

colonization and growth, resulting in chronic inflammation [233]. Exposure to e-cigarette vapour results in excessive production of ROS, inflammatory cytokines and chemokines that may induce an inflammatory state in alveolar macrophages within the lung, which is partly dependent on nicotine [233]. Furthermore, airway epithelial cells from e-cigarette users were found to have decreased expression of Toll-like receptor 3, suggestive of impaired viral immunity resulting from e-cigarette use [249, 250]. Indeed, infection of e-cigarette-exposed mice with influenza leads to increased lung inflammation and injury [250]. The inability to control the viral infection may lead to excessive lung inflammation in response to viral infection[250].

Overall, e-cigarette use results in increased cytokines and chemokines, increased infiltration and activity of inflammatory cells, increased ROS, and DNA damage. It also causes impaired mucociliary clearance and reduced antibacterial activity and antiviral by many cells in the lung, which may result in chronic inflammation in the lung.

1.6.2. Epithelial cells

Studies have investigated the physiological implications of e-cigarette use on airway epithelial cells. A recent study has suggested that acute e-cigarette exposure leads to mucociliary dysfunction *in vivo*, comparable to exposure to cigarette smoke extract [245]. Impaired mucociliary action has also been observed in the nasal mucosa [251] and in bronchial epithelial cells *in vitro* [246]. Crotty Alexander et al [236]showed that primary human bronchial epithelial cells cultured to air-liquid interface displayed reduced airway barrier function when exposed to EC vapour for 15 minutes daily. Furthermore, e-cigarette vape exposure of HBECs causes reduced cell viability and oxidative stress [252]. Indeed, genes related to apoptosis, xenobiotic stress and oxidative stress have been shown to be upregulated in HBECs exposed to e-cigarette vapour [253]. E-cigarette vapour also downregulated the expression of genes associated with the assembly and movement of cilia, suggestive of a reduction of ciliated cells in airway epithelium and impaired mucociliary clearance [253]. Additionally, e-cigarette vapour containing balsamic flavouring or nicotine was found to trigger morphological

changes, elevated LDH release and reduced viability in human cell lines derived from lung epithelium (A549) [254]. The study further showed that the influence of flavour was greater than that of nicotine and that the e-cigarette vapour humectants alone did not produce these effects [254]. E-cigarette vape extract has also been found to significantly elevate LDH release from bronchial epithelial cells in healthy and COPD patients, also inducing the production of cytokines such as IL-6 and IL-8 [255]. Indeed, BECs from the COPD patients showed lower IL-6, CXCL10 and CCL5 production after poly I:C stimulation when compared to the healthy donors [255], which may result in reduced antiviral activity in bronchial epithelium and increased susceptibility to infection. Overall, e-cigarette vapour exposure results in a number of implications on airway epithelial cells including impaired mucociliary clearance, reduced airway barrier functions, reduced cell viability and oxidative stress, increased LDH release and production of IL-6 and IL-8, and reduced antiviral activity. As mucociliary clearance is the initial host defence mechanism within the lung and essential in the clearance of foreign particles or the airways [256], damages or changes of this mechanism impair pulmonary function, thus increasing the risk of infection.

1.6.3. Macrophages

Exposure to e-cigarette vapour leads to modifications of macrophage function, including reduced phagocytic action, suggestive of impaired defence ability [257]. A study has shown that sputum samples obtained from healthy participants demonstrated impaired bacterial phagocytosis by AMs following exposure to e-cigarette extract *in vitro* [234]. Ween et al [258] also demonstrated significantly reduced macrophage phagocytosis of non-typeable *Haemophilus influenzae* following exposure to apple-flavoured e-liquids and nicotine. Indeed, transcriptome analysis of AMs from patients who inhaled 10 puffs from an e-cigarette showed that there were changes in expression of over 60 RNAs, some of which were involved in inflammation and immunity, where these changes may result in impaired host defence [259]. This can be noted in a study where mice exposed to e-cigarette vapour were found to have significantly reduced pulmonary clearance

after intranasal infection with *S. pneumoniae*, which was in part due to impaired AM phagocytic function [250]. On exposure to e-cigarette vape condensate, macrophages demonstrate dose-dependent cytotoxicity, inducing apoptosis with nicotine-dependent and -independent responses, amplified by the vaping process [234]. Additionally, macrophages increase the production of proinflammatory cytokines, such as IL-6, IL-8, and TNF-α, when exposed to e-cigarette aerosol extract, driving inflammation [232, 234]. AMs have also been shown to enhance the production of ROS, chemokines and metalloproteinases [234]. Overall, e-cigarette vaping causes disturbances in AM function, including impaired phagocytic function, increased cytotoxicity and increased production of ROS and proinflammatory mediators. These disturbances could in turn increase the risk of infection and enhance susceptibility to COPD.

1.6.4. Dendritic cells

Although studies have shown that e-cigarettes have a number of effects on various cells of the immune system, including epithelial and endothelial cells, fibroblasts, macrophages and neutrophils, studies on the effect of e-cigarettes on human DCs are limited [203]. A study by Chen et al observed that DCs exposed to e-cigarette vape extract had enhanced proinflammatory cytokine IL-6 production and upregulated expression of 29 signalling molecules and other cytoplasmic proteins [260]. The study also showed that e-cigarette vape extract exposure inhibited surface expression of HLA-DR and CD86 in LPS-matured DCs, where both molecules are involved in DC-T cell interaction [260]. Furthermore, immunophenotyping of lung immune cells from mice exposed to e-cigarette aerosols showed increased number of DCs, along with CD4+ T cells and CD19+ B cells [261]. E-cigarette exposure to DCs does modulate their function and activity, and more studies need to be done to fully elucidate these effects.

1.6.5. Natural killer cells

Studies have indicated that cigarette smoking is associated with reduced circulating NK cells and reduced NK cell-mediated killing of cancer cells in vitro. However, studies on

the effect of e-cigarettes on NK cells are limited. Clapp et al [262] evaluated the effects of flavoured e-liquids and cinnamaldehyde flavouring on NK cell function. This study showed that exposure of NK cells to cinnamon-flavoured e-liquids suppressed NK cell cytotoxicity function, as measured by the ability to kill leukaemia target cells [262]. As can be noted, the study here observed e-liquid prior to vaping, however, the effects of exposure to e-cigarette vapour or aerosol need to be elucidated.

1.6.6. Neutrophils

One of the most common responses to e-cigarette exposure is neutrophilic-driven inflammation. Neutrophils are recruited when epithelial cells secrete IL-17, and this is aided by the expression of epithelial intercellular adhesion molecule (ICAM)-1, which neutrophils bind to through CD11b and CD18 [263]. Recent studies have evaluated this neutrophil response to e-cigarette vape exposure. A study by Corriden et al [248] observed a 4.2-fold reduction of neutrophilic chemotaxis towards components of bacterial cell walls. Neutrophils also exhibited a 48% reduction in the production of ROS, an important component of neutrophil extracellular traps, and as such, NET production was reduced by 3.5-fold, suggestive of an extensive reduction in neutrophil efficiency [248]. Additionally, the study showed, in a physiological mouse model, that e-cigarette vapour inhalation resulted in reduced neutrophil migration in infected spaces and a higher burden of *Pseudomonas* [248]. Clapp et al [262] observed a dose-dependent suppression of neutrophil, macrophage and NK cell cytotoxic function on exposure to the e-cigarette flavouring compound, cinnamaldehyde. This study also showed that flavoured e-liquids induced a significant increase in neutrophil IL-8 secretion and affected NET formation [262]. Neutrophils exposed to e-cigarette vapour extract show increased expression of CD11b and CD66b and increased release of NE, MMP-9 and CXCL8 [264]. Indeed, neutrophilic enzymes associated with chronic lung disease, including NE, MMP-9 and myeloperoxidase, have been observed in increased levels in sputum obtained from both CS and e-cigarette users [237]. Sputum from e-cigarette users also uniquely exhibited a significant increase in neutrophil granulocyte-related and

NET-related proteins, although neutrophil count change was not significant [237]. Together, the studies suggest that exposure to e-cigarettes affects neutrophilic response in the lungs.

1.6.7. Eosinophils

Acute eosinophilic pneumonia (AEP) is an eosinophilic lung disease characterised by an acute onset febrile respiratory illness with BAL eosinophilia, with cigarette smoking being a major risk factor [265, 266]. In AEP, a strong inflammatory stimulus recruits macrophages and neutrophils to lung tissue, inducing the production of proinflammatory cytokines such as IL-5, IL-6, IL-7 and TNF, which may then cause eosinophil-rich exudate within the alveoli [266]. Cigarette smoking is considered a major risk factor [266]. More recently, e-cigarette has been included as a risk factor [265], as recent studies have demonstrated that the mechanism of inflammation and cytokine stimulation in e-cigarette users is similar to that of cigarette smokers [228, 267]. Thota et al [268] previously reported a case where a 20-year-old healthy man developed AEP after smoking an e-cigarette, with BAL demonstrating abundant macrophages, eosinophils and scattered benign respiratory epithelial cells [268]. In this case, the right upper lobe cell count yielded 74% eosinophils, with >25% eosinophils in BAL being one of the defining factors of AEP [268]. Arter et al [266] also reported AEP in a previously healthy 18-year-old female with a two-month history of e-cigarette smoking, where 26% eosinophils were found in the BAL. As there were no other traditional exposures to AEP, e-cigarettes were considered the most likely causative agent [266]. Furthermore, Suhling et al [269] reported three cases in Germany of acute pulmonary illness, where BAL findings for all three patients indicated eosinophilic inflammation. AEP and pulmonary eosinophilia commonly progress to respiratory failure requiring invasive mechanical ventilation and intensive care. A review of the reported cases of AEP associated with e-cigarette vaping found the median age to be 20 with 42% being 18 years old or younger [265]. Data concerning e-cigarette and AEP are obtained mainly

from case reports, as studies investigating the effect of e-cigarettes on eosinophils are limited.

1.6.8. T lymphocytes

As has been previously noted, the understanding of respiratory health risks of e-cigarette vapour inhalation is poorly investigated. Indeed, research observing the effect of e-cigarettes on T cells is limited. A study by Szafran et al showed that mice exposed to e-cigarette aerosol had increased number of DCs, CD4+ T cells and CD19+ B cells in the lung, suggestive of ongoing inflammation [261]. Furthermore, Wang et al observed that sub-chronic e-cigarette exposure with nicotine in a murine model increased inflammatory influx of macrophages and T lymphocytes and increased proinflammatory cytokines in BALF [239].

1.6.9. B lymphocytes and antibodies

There are currently no known studies investigating the effect of e-cigarette vape on B lymphocytes and their antibody production.

1.6.10. Cytokines

Exposure to e-cigarette vapour has been shows to increase free radicals in the airways [234, 270], leading to modifications in proinflammatory cytokines in the lung tissue [271]. Suryadinata et al [271] showed that alveolar macrophages from male rats exposed to e-cigarette vapour had increased levels of IL-8 and decreased levels of IL-10, suggesting an inflammatory reaction in the lung tissue. Scott et al [234] also observed that macrophage culture exposed to e-cigarette vapour extract significantly increased release of IL-6, TNF-α, CXCL-8, monocyte chemoattractant protein 1 and MMP-9. Furthermore, Han et al [272] observed that e-cigarette exposure significantly increased the production of multiple proinflammatory cytokines, including M-CSF, IL-1rα, IL-10, and TGF-β in BAL fluid of mice bearing COPD-like pulmonary abnormality. Overall,

increase in proinflammatory cytokines due to e-cigarette use leads to inflammation in the lungs.

1.6.11. Systemic response

Exposure to e-cigarette vapour leads to activation of multiple inflammatory responses. Chatterjee et al [273] showed that smoking-naïve healthy subjects had increased serum levels of ROS and ICAM-1 following e-cigarette challenge which returned to baseline levels after 6 hours, suggesting that acute e-cigarette aerosol inhalation leads to a transient increase in oxidative stress and inflammation. Jackson et al [274] showed that e-cigarette users had a significant increase in plasma IgE levels compared to nonusers. Furthermore, a study by Singh et al [275] observed that e-cigarette users had significant increase in inflammation markers and decrease in pro-resolving lipid mediators in plasma and endothelial dysfunction. Plasma levels of IL-1β, IL-6, IL-8, IL-13, IFN-γ, MMP-9, and intercellular cell adhesion molecule-1 (ICAM-1) were significantly higher in e-cigarette users compared to nonusers, whereas pro-resolving lipid mediators, resolvin D_1 and resolvin D_2 were significantly decreased [275]. Singh et al [275] also observed significant increase in growth factor (endothelial growth factor, vascular endothelial growth factor, β-nerve growth factor, platelet-derived growth factor-AA, stem cell factor, hepatocyte growth factor and placental growth factor) levels in plasma of e-cigarette users compared to nonusers.

1.7. Extracellular Vesicles (EVs)

Extracellular vesicles (EVs) are important intercellular communication mediators released by cells into the extracellular environment [276, 277]. EVs have the capacity to transfer biological signals and information between cells and as such, influence the recipient cell function [278]. These signals are transmitted by various biomolecules including protein, lipids, nucleic acids and sugars in phospholipid-enclosed vesicles that provide protection and allow for delivery to sites distant from the origin [278]. Various physiological and pathological functions of both cells involved may be influenced, and as such the importance of pathophysiological roles for EVs is being explored as these vesicles can also be a danger to their own microenvironment [276, 278, 279]. EVs are derived from most cell types and have been isolated from biological fluids like saliva, urine, nasal and BAL fluid, amniotic fluid, breast milk, plasma, serum and seminal fluid [278].

1.7.1. EV subtypes

Heterogeneity of EVs has been determined. Firstly, based on their biogenesis, EVs are distinguished into two basic types, exosomes and ectosomes. Exosomes have an endosomal origin and are generated in multivesicular bodies (MVBs) in the form of intraluminal vesicles (ILVs), and that once formed, the MVB can fuse with the plasma membrane to release its contents as exosomes [280, 281]. Exosomes are often also distinguished from other EV classes by their small size, generally smaller than 200 nm [278, 282]. Exosomes contain signalling molecules such as microRNA (miRNA), mRNA, soluble proteins and others, and contain ribosomal RNA or fragments of them [283]. They transfer information to their extracellular environment through endocytosis or by direct fusion with the plasma membrane of the target cells [284]. Exosomes also contain specific membrane proteins such as tetraspanins, flotillin, tumor susceptibility gene 101 (TSG101), Alix and heat shock proteins. Tetraspanins CD63, CD81, and CD9 and heat shock protein (Hsp70) are present in exosomes and as such are sometimes used as exosomal markers [285]. Apart from their role as communicating agents, exosomes are

also engaged in immune responses and are involved in several biological activities [286]. The other route of biogenesis is through the release of plasma membrane-derived EVs, known as ectosomes, which include microvesicles (MVs) [281]. Ectosomes can be as small as exosomes or up to several μm in size [287]. They contain various proteins and lipids that are like those in the membranes of their cell of origin and are also known to be enriched in phosphatidylserine (PS) which allows them to be quantified or identified by FACS analysis after staining with annexin V [288, 289]. Ectosomes, such as MVs, may also contain some proteins and mRNA derived from the cytoplasm during membrane blebbing and can seize infectious particles such as viruses or intact organelles from the cytoplasm [288]. Apoptotic bodies (ApoBDs) are the largest of the EVs with a diameter of 1-5 μm and are generated from cells undergoing apoptosis [290]. They share the same surface markers as the cells that they originate from. ApoBDs may contain DNA, microRNAs, proteins and lipids and so, can facilitate cell-to-cell communication [291]. Other EVs include oncosomes, released by transformed cells with exaggerated membrane plasticity, migrasomes trailing behind migrating cells, and exophers, exomeres, and elongated particles which have been revealed by recent discoveries [287, 292, 293].

Furthermore, the EVs found to be most abundant in biological fluids are small EVs, ranging in diameter of 50-150 nm [281]. Medium-sized EVs are less abundant and range in size from about 200-800 nm. The least abundant population of EVs are large EVs which have a diameter above 1 μm and include apoptotic bodies, migrasomes, large oncosomes and migrasomes [281].

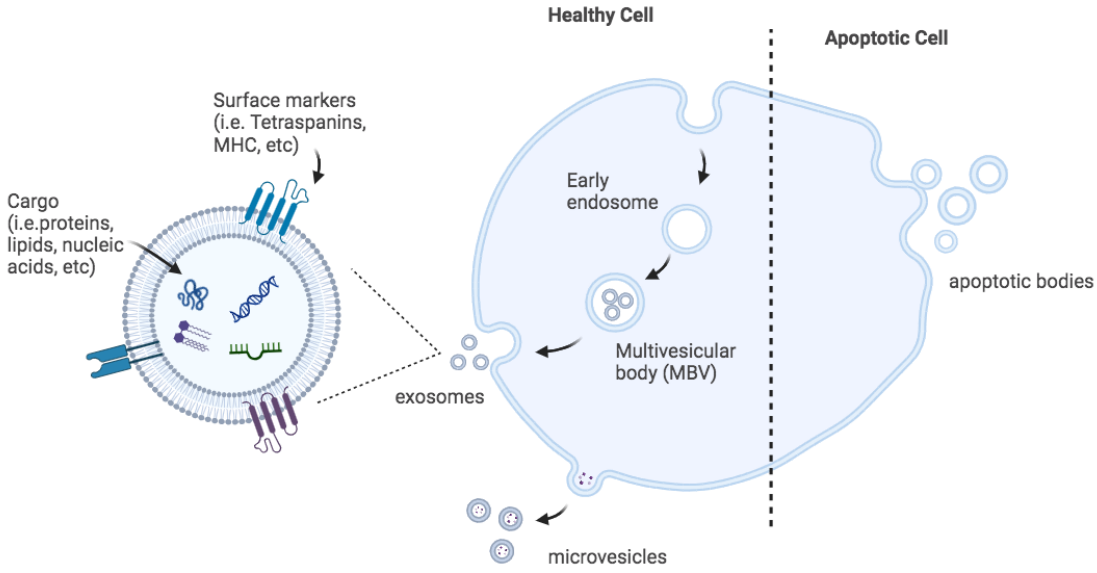

Figure 1.4. Extracellular vesicles (EVs). EVs are derived from most cell types and have different mechanism of intracellular origins. EVs are release by cells either by direct budding from the plasma membrane or by fusion of multivesicular bodies (MVBs) with the plasma membrane. They carry biological signals which include biomolecules such as protein, lipids, nucleic acids and sugars.

1.7.2. Biogenesis and release of exosomes

The generation of exosomes occurs in three steps; biogenesis, transport and release. Exosomes are derived from an endosomal system, where early endosomes undergo inward budding of the plasma membrane or, in some cases, are formed from a trans-Golgi network (TGN) [294]. Early endosomes mature into late endosomes and fuse to form intraluminal vesicles (ILVs) inside multivesicular bodies (MVBs) [294, 295]. ILV formation involves two distinct processes, including reorganisation of the endosome membrane such that it becomes highly enriched in tetraspanins, particularly in tetraspanins CD9 and CD63, and recruitment of the endosomal sorting complexes required for transport (ESCRTs) to the site of ILV formation. The ESCRT machinery is a cytoplasmic multi-subunit system important for membrane remodelling, which enables the budding of vesicles and sorting of cargo in MVBs. There are four core ESCRT complexes, namely ESCRT-0, -I, -II, and –III, plus several accessory proteins including

Vps4 [296, 297]. MVBs are then transported to the plasma membrane via the cytoskeletal and microtubule network [295, 296].
After MVBs are formed, they can either be transported to lysosomes where their contents are degraded after membrane fusion or the MVBs fuse with the plasma membrane and release the ILVs into the extracellular milieu in the form of exosomes [298].

1.7.3. Biogenesis and release of microvesicles

The biogenesis of microvesicles is less defined compared to exosomes, although different mechanisms have been found to be responsible for the shedding of microvesicles. Microvesicles are considered ubiquitous vesicles that are formed through the outward budding and fission of the plasma membrane and result from the dynamic interplay between phospholipid redistribution and cytoskeletal protein contraction [299]. The combination of several factors results in the formation of microvesicles, for example redistribution of phospholipids, including the repositioning of phosphatidylserine to the outer leaflet, and contraction of the actin-myosin machinery [295]. Initially, ADP-ribosylation factor 6 (ARF6) triggers a cascade, activating phospholipase D (PLD). This is followed by the recruitment of extracellular signal-regulated kinase (ERK) to the plasma membrane, which phosphorylates and activates the myosin light chain kinase (MLCK) that then triggers the release of the microvesicles [295, 300]. These MVs are specifically loaded with ARF6, MHC-I, β1-integrin, VAMP3 and MT1MMP [300]. Furthermore, the ESCRT machinery has been described as another mechanism involved in the synthesis of microvesicles. Recruitment of ESCRT-I subunit TSG101 and vacuolar protein sorting 4 (VPS4) to the plasma membrane via binding to adaptor protein arrestin domain-containing protein 1 (AARDC1) promotes the release of MVs containing TSG101, AARDC1 and other cellular proteins [295, 299, 301, 302]. External factors can also induce the release of MVs, including an influx of calcium which redistributes phospholipids to increase the release of MVs [303, 304], and hypoxia-

promoting MV release following expression of Ras-related protein RAB22A via hypoxia-inducible factors [305].

1.7.4. Tetraspanins associated with EVs

EVs are highly enriched in tetraspanins that are membrane-spanning proteins with a conserved structure that function primarily as membrane protein organizers. They belong to a large family of proteins that span the membrane four times and form small and large extracellular loops, one inner loop and N-terminal and C-terminal ends located inside the cytoplasm [306]. As transmembrane proteins, tetraspanins have the ability to form clusters and interact with a wide variety of transmembrane and cytosolic signalling proteins, therefore organising membrane microdomains or 'tetraspanin-enriched microdomains' (TEMs) [307]. Tetraspanins are known to have a broad tissue distribution and as stated above, CD9, CD81, CD63 and CD82 are particularly enriched in the membrane of exosomes [307, 308]. However, tetraspanin expression has also been detected on cell surfaces, therefore, tetraspanins may also be found on plasma membrane-derived vesicles including microvesicles, which directly bud from the membrane [308].

Tetraspanins are able to interact with a number of membrane receptor and signalling molecules, forming specialised TEMs that may function in EV biogenesis, EV cargo selection, binding and uptake of EVs by target cells, and antigen presentation by EVs in the context of an immune response [307]. Tetraspanins are crucial players in exosome biogenesis and secretion, particularly in the ESCRT-independent pathways [308, 309]. Tetraspanins are able to modulate membranes by affecting their curvatures, directly predetermining their participation in EV formation [308, 310]. Umeda et al [310] described the reversed cone-like molecular shape of CD9 which generates membrane curvature in crystalline lipid layers, suggesting clustering of tetraspanin molecules could modulate membrane curvature thereby enabling exosome budding [310]. Clustering could also facilitate the subsequent interaction of C-terminal regions of tetraspanins, that being the cytoplasmic tail, with cytoskeletal

actin that may be involved in EV fission from the parent cell membrane [308]. Chairoungdua et al [311] observed that exosome secretion was defective in bone marrow DCs from CD9 knockout mice compared to their wild-type counterparts. Furthermore, tetraspanins regulate the sorting of proteins, and possibly RNA, to EVs. Metalloproteinases are a set of molecules targeted to EVs by insertion into TEMs, where they are selectively associated with tetraspanins [307]. For example, CD10 metalloproteinase, which is involved in B cell maturation and migration to the blood circulation, selectively associates with tetraspanin CD9, as study has shown that knockdown of CD9 expression promoted a two-fold decrease in the amount of endogenous CD10 released with EVs [306]. Furthermore, in the immune system, sorting of MHC-I and MHC-II to EVs may be dependent on their recruitment to TEMs. B-, T- and dendritic-cell-derived EVs are enriched in tetraspanins CD9, CD63, CD81, CD82 and in MHC-I and MHC-II molecules [307]. Buschow et al demonstrated that MHC-II sorts together with CD9 to luminal vesicles that are subsequently secreted as exosomes and that this pathway exists in immature DCs and is upregulated when iDCs cognately interact with antigen-specific CD4+ T cells [312].

The process of EV targeting and uptake by recipient cells has not been fully elucidated, however, molecules found in TEMs of EVs and recipient cells, particularly tetraspanins, integrins and other adhesion proteins, are involved in the process of binding, fusion and targeting of EVs and selective uptake of EVs by recipient cells [308]. Rana et al [313] demonstrated that selective exosome uptake by cells and tissues is dependent on the tetraspanin web composition. Another study has shown the involvement of tetraspanins CD9 and CD81, together with integrin $\alpha_v\beta_3$, in the targeting and uptake of exosomes by DCs [314].

Although tetraspanins are currently applied mostly as markers of EVs as recommended by ISEV, research has pointed out their significant role in EV biogenesis, cargo selection and uptake. Further research is necessary to fully elucidate the functional role of tetraspanins in the various aspects of EV biology.

1.7.5. Cargo of EVs

EVs contain a rich and varied range of cargo that includes proteins, metabolites, lipids and nucleic acids, which can be taken up by other cells[315, 316]. EVs derive their cargo from the contents of the cells that produce them. Indeed, characterising the cargo of EVs is of significant interest due to their possible use as potential biomarkers of disease or to understand their functional effects[316].

Nucleic acids of EVs include a variety of biotypes that represent a selected portion of the RNA content of the source cell, such as small non-coding RNA (including microRNA (miRNA, mi-R)), fragmented and intact mRNA, ribosomal RNA (rRNA) and long non-coding RNA (lncRNA) [316, 317]. RNAs enclosed in EVs reflect the type and physiological/pathological state of their source cells but can also differ significantly in the type of RNA and relative concentration of particular RNA sequences from the RNA content found in the cytoplasm of the donor cells [295, 316]. Indeed, RNA contained in EVs can impact the functional properties of cells that uptake them[316]. Next-generation sequencing studies have provided detailed knowledge about the presence of various species of RNAs in small EVs and have suggested that particular groups of RNAs in EVs may be dependent on the source of EVs, although the actual contribution of individual RNA fractions in EVs needs further study[318]. Once taken up by recipient cells, RNAs enclosed in EVs need to enter the cytoplasm where they need to escape degradation by the endosomal pathway in order to elicit a functional response [316].

One subtype of RNA that is of interest in EV studies is miRNAs, which are small non-coding RNAs composed of 21-25 nucleotides that function in the regulation of gene expression [317, 319]. EVs have the ability to export miRNA outside cells and affect gene expression in distant cells, thereby inducing phenotypic changes. Indeed, EVs containing miRNAs have been shown to be involved in the mechanism of COPD [320]. Studies have reported EVs containing significantly increased levels of miRNAs in COPD patients compared to healthy controls and from cells after exposure to cigarette smoke [321, 322]. One particular miRNA identified is miR-21, which drives excessive autophagy in COPD when upregulated [323]. Additionally, uptake of miR-21 by macrophages results in

the polarisation of the macrophages into M2 phenotype that has been found to negatively correlate with the lung function of mouse COPD models [324].
Furthermore, over 10,000 unique proteins have been identified in EVs from human cells, tissues and bodily fluids [315]. Proteomic studies done on EV cargo have demonstrated that EV cargo is dependent on cell type of origin, physiological or pathological conditions and the type of EVs [325]. Additionally, cytoplasmic proteins are the most abundant in EVs isolated from biological fluids (47%) and cell culture media (43%), whereas membrane proteins represent 28% and 34% of proteins in EVs isolated from biological fluids and cell culture media, respectively[326]. Nuclear and mitochondrial proteins are found in lower amounts in EVs. Proteomics studies have also revealed "specific" exosomal markers, including tetraspanins, binding protein Alix, and ESCRTs, although these proteins have also been identified in both MVs and apoptotic bodies[327-329]. Exosome- and MV-associated proteins have been analysed by the Ingenuity Pathway Analysis (IPA) platform, identifying the main biological functions of these proteins, including cellular movement, cell-to-cell signalling, tissue development, cancer and viral infections[325].
Lipids are fundamental molecular components of EVs, however, research regarding the lipid composition and function in EVs is limited. Studies have demonstrated an enrichment from cells to exosomes of 2 to 3 times for cholesterol, sphingomyelin, glycosphingolipids and phosphatidylserine [330-332]. EVs also mediate the exchange of lipids between various cells. Particularly, small EVs (sEVs) have a bilayer membrane which surrounds cytosolic material, thus able to transport lipids using a distinct mechanism. Furthermore, immune cell-derived sEVs have been demonstrated to have a phospholipid composition distinct of that found in their parent cells [333].

1.8. EVs and cigarette smoking

Cigarette smoke (CS) has profound effects on the release of EVs by various cell types. On exposure to CS, mononuclear cells release EVs which induce production of IL-8,

monocyte chemoattractant protein-1 and upregulation of CD54 on bronchial epithelial cells [334]. Additionally, CS enhances the release of exosomes by airway epithelial cells [335] and the EVs derived from CSE-treated airway epithelial cells have been found to be enriched in the COPD-associated protein cysteine-rich angiogenic protein 61 (CCN1), which in turn contributes to the release of vascular endothelial growth factor and IL-8 [336]. Smoke-exposed bronchial epithelial cells release EVs that induce differentiation of lung fibroblasts into myofibroblasts, suggestive of EVs contributing to fibrotic development [337].

1.8.1. EVs in pathophysiology

The role of EVs in COPD has become an area of increased interest as EVs have key cell-to-cell communication roles in cellular responses and are involved in the physiological role and pathology of various diseases, including pulmonary diseases [33]. Studies have shown that respiratory cells and immune cells release EVs which can be found in the BAL fluid and can also exit into circulation [338, 339]. EVs originating from the airways have the potential to initiate and propagate inflammation in lung and systemic inflammatory conditions, both of which are associated with COPD. It is to be noted that cigarette smoke, a key factor of COPD, may lead to increased release of proinflammatory EVs [338].

1.8.2. Endothelial cell-derived EVs

CS causes stress and damage to the endothelial layer and induces the release of EVs from endothelial cells, therefore it is important to note the relationship of these EVs on the development of lung damage. Research studies [340-347] have noted an elevation in CD31+/CD42b- or CD31+CD62E+ endothelial microparticles (EMPs) in their investigations of endothelial EV (EEVs) levels in COPD (Table 1.3.). The increased levels of CD31+/42b- EMPs suggested that there was active endothelial apoptosis and endothelial damage. Furthermore, Strulovici-Barel [341] noted that upon smoking cessation, healthy smokers had a significant decrease in total EMP levels after 12

months, compared to healthy smokers who continued to smoke. However, for COPD patients, the EMP levels had no significant change for patients who quit smoking compared to those who continued to smoke. Garcia-Lucio et al [343] observed a significantly elevated EMP level for COPD patients and healthy smokers when compared to healthy non-smokers, noting also a reduced number of progenitor cells (PCs) for the COPD patients, reflecting an imbalance between endothelial damage and a reduced repair capacity. Liu et al [345] observed, in an animal model of COPD, that the elevated levels of CD31+/42b- EMPs increased with an increased time of CS exposure. Nieri et al [346] observed a direct relationship between endothelial EVs and IL-6, suggesting there is release of endothelial EVs upon an inflammatory stimulus. Mobarezz et al showed significantly increased levels of endothelial cell-derived (CD62E+) and platelet-derived (CD41+) EVs in healthy occasional smokers after 30 puffs of e-cigarette vapour in 30 minutes, suggestive of underlying vascular changes [348]. Furthermore, Serban et al [349] observed that acute exposure to soluble components of CS stimulated the release of endothelial EVs with distinct miRNA cargo which affected the clearance of apoptotic cells by specialised macrophages. It has been suggested that deficient efferocytosis of apoptotic cells contributes to sustained inflammation in COPD [350]. As can be noted, increases in circulating endothelial-derived EVs observed in CS exposure were associated with markers of endothelial dysfunction.

Table 1.4. Summary of studies on the endothelial cell-derived extracellular vesicles. [1]

Endothelial cells				
Author, Year [Ref]	**Title**	**Aim**	**Type**	**Conclusion**
Takahashi *et al*., 2013 [340]	Differences in the released endothelial microparticle subtypes between pulmonary microvascular endothelial cells and aortic endothelial cells *in vitro*	Evaluate the effects of common stimuli involved in COPD on endothelial microparticles (EMPs) released. Investigate whether increased circulating EMP subtypes reflect the degree and site of endothelial injury in COPD patients	*in vitro*	H_2O_2 and cigarette smoke extract (CSE) induced apoptosis, resulting in the release of PECAM EMPs from pulmonary ECs and MCAM EMPs from both pulmonary and aortic EC types. TNF-a stimulation resulted in EC activation, resulting in the upregulation of E-selectin, a mechanism that occurs during COPD exacerbation. Thus, EMP subtypes reflect differences among stimuli and site of injury in COPD mechanism.
Strulovici-Barel *et al.,* 2016 [341]	Persistence of Circulating Endothelial Microparticles in COPD Despite Smoking Cessation	Investigate whether elevated levels of circulating apoptotic EMPs persists in COPD smokers following smoking cessation, reflecting continuous lung endothelial injury that persists even after the stress of smoking is removed	*ex vivo* human	Total pulmonary capillary EMP levels were highest in healthy smokers, followed by COPD smokers, when compared to non-smokers, with 48% of healthy smokers and 45% of COPD smokers showing increased levels of apoptotic EMPs. This suggests active pulmonary capillary apoptosis ongoing in both healthy and COPD smokers that persisted even after they stopped smoking following their baseline assessment.
Thomashow *et al*., 2013 [342]	Endothelial microparticles in mild chronic obstructive pulmonary disease and emphysema	Examine the relationships of circulating levels of EMPs with COPD.	*ex vivo* human	CD31+ EMPs were elevated in COPD and were positively related to percent emphysema. Additionally, CD62E+ EMPs were elevated in severe COPD and with hyperinflation. These cellular markers may implicate endothelial apoptosis in the pathogenesis of COPD and emphysema.
Garcia-Lucio *et al.,* 2018 [343]	Imbalance between endothelial damage and repair capacity in chronic obstructive pulmonary disease	Investigate whether COPD patients have an imbalance between EMPs to PCs (progenitor cells) compared to non-smokers and current smokers. Evaluate the effect of cigarette smoke on these circulating markers.	*ex vivo* human	COPD patients presented a significantly disturbed ratio of elevated circulating apoptotic EMP levels with reduced bone marrow-derived PC numbers, reflecting an imbalance between endothelial damage and reduced repair capacity.
Barak *et al*., 2017 [344]	Disturbed blood flow worsens endothelial dysfunction in moderate-severe chronic obstructive pulmonary disease	To test whether oscillatory shear stress further exacerbates endothelial dysfunction in patients with moderate-severe COPD and to observe any potential link between	*in vivo / ex vivo* human	In moderate-severe COPD patients, acutely disturbed blood flow further deteriorates endothelial dysfunction that is compounded with increases in circulating MPs indicative of endothelial apoptosis (CD31+/CD41b-), and is of greater consequence

[1] EMPs = endothelial microparticles; PECAM = CD31(+)/CD41(-) microparticles; EC = endothelial cells; MCAM = CD146(+) microparticles.

		chronic hypoxemia and EMPs in COPD.		given the already impaired vasculature of this population.
Liu *et al*., 2014 [345]	Circulating endothelial microparticles involved in lung function decline in a rat exposed in cigarette smoke maybe from apoptotic pulmonary capillary endothelial cells	Investigate if the number of EMPs is elevated in rats exposed in cigarette smoke, and whether the elevated EMPs are derived from pulmonary capillaries	*in vivo* mice	Exposure of rats to CS resulted in high levels of circulating CD42b/CD31+ EMPs (cEMPs), which increased with an increase in time of exposure. High levels of CD42b/CD31+ cEMPs reflected the decline of small airway function indirectly in early COPD and would be useful for evaluating the degree of COPD progression.
Nieri *et al*., 2021 [346]	Circulating Extracellular Vesicles Are Associated with Disease Severity and Interleukin-6 Levels in COPD: A Pilot Study	Analyse endothelial-(E) and monocyte-derived (M) EV levels in COPD patients grouped according to the 2011 GOLD classification and analyse the relationship between EV and plasmatic markers of inflammation.	*ex vivo* human	Circulating endothelial- and monocyte-derived extracellular vesicles increase along with COPD severity. The relationship among EEV and IL-6 suggests a biological link between inflammation and endothelial activation/damage.
Lascano *et al.*, 2021 [347]	Association of Systemic Endothelial-Derived and Platelet-Derived Microparticles With Clinical Outcomes in Chronic Obstructive Pulmonary Disease	Analyse whether eMPs and pMPs are associated with COPD status and/or severity.	*ex vivo* human	Most MPs measured do not correlate significantly with COPD status, COPD severity, or exacerbations in our cohort. The apoptotic eMP 62E+/eMP 31+ ratio may be a useful marker of early endothelium apoptosis and early recognition of the disease process. Platelet activation assessed by pMP 41+31+ increases with disease severity and may be an important feature for stage 4 COPD patients.

1.8.3. Epithelial cell-derived EVs

Airway epithelial cells are a major cell population that when exposed to cigarette smoke release EVs with distinct cargo that can modulate activity of recipient cells [351]. Studies have observed that CS triggers and affects the release of EVs from epithelial cells [335, 336, 352-356] (Table 1.4.). Moon et al [336] observed that airway epithelial cells exposed to CSE released EV containing full-length CCN1, which induced the secretion of cytokines IL-8 and VEGF in cells that did not have direct contact with CSE; thus, promoting lung inflammation. Feller et al [352] also observed that EVs in serum from COPD patients who continued to smoke contained inflammation inducer and PPAR gamma inhibitor Wnt5a and proinflammatory cytokines IL-8 and IL-6. Song et al [355]

showed that injured alveolar epithelial type II (AEC-II) cells treated with CSE secreted EVs that affected the biological characteristics of mesenchymal stem cells and contained significantly dysregulated exosomal lncRNAs. Xia et al [356] showed that human bronchial epithelial cells exposed to CSE released EVs containing miR-93 that when taken up by macrophages, increased levels of MMP-9 and MMP-12, inducing elastin degradation. Overall, CS exposure leads to increased EVs from airway epithelial cells with distinct cargo that can modulate the activity of recipient cells.

Table 1.5. Summary of studies on epithelial cell-derived EVs.

Epithelial cells				
Author, Year [Ref]	**Title**	**Aim**	**Type**	**Conclusion**
Benedikter *et al.,* 2017 [335]	Cigarette smoke extract induced exosome release is mediated by depletion of exofacial thiols and can be inhibited by thiol-antioxidant	Investigate whether oxidative components of CSE are responsible for EV release and whether this could be prevented using the thiol antioxidants N-acetyl-L-cysteine (NAC) or glutathione (GSH)	*in vitro*	CSE exposure enhances the exosome release by airway epithelial cells (AEC) and this is mediated by thiol-reactive compounds like carbonyl acrolein, which may act by depleting extracellular free thiols.
Moon *et al*., 2014 [336]	CCN1 secretion and cleavage regulate the lung epithelial cell functions after cigarette smoke	Investigate whether CCN1 is a potentially crucial factor for the pathogenesis of CS-induced emphysema	*in vitro* *in vivo mice*	CS enhanced the release of exosomes containing full-length CCN1 (flCCN1) from lung epithelial cells. Exosome-mediated secretion of flCCN1 triggers inflammatory responses by mediating IL-8 release to distant portions of the lungs and subsequent neutrophil recruitment. Additionally, cleaved CCN1 (cCCN1) were generated from exosome-enriched CCN1 via secreted plasmin and promoted emphysematous changes.
Feller *et al.,* 2018 [352]	Cigarette smoke-induced pulmonary inflammation becomes systemic by circulating extracellular vesicles containing Wnt5a and inflammatory cytokines	Demonstrate a potential mechanism for the systemic nature of COPD	*in vitro ex vivo* human *in vivo* mice	CS triggers release of EVs carrying pro-inflammatory cytokines and inflammation inducer Wnt5a, in turn triggering systemic inflammation and thus making COPD a complex disease that is hard to control.
Zou *et al*., 2021 [353]	Release and Actions of Inflammatory Exosomes in Pulmonary Emphysema: Potential	Investigate if exosome-mediated release of NLRP3 inflammasome products instigates the inflammatory response in the lung during emphysema.	*in vivo* mice	NLRP3 inflammasome activation and associated inflammatory exosome release are critically implicated in the development of inflammation during PPE-induced emphysema.

	Therapeutic Target of Acupuncture			
Wang *et al.*, 2021 [354]	Cigarette smoke extract-treated airway epithelial cells-derived exosomes promote M1 macrophage polarization in chronic obstructive pulmonary disease	Investigate whether the exosomes derived from CSE-treated AECs regulate macrophage polarization and subsequently affect the progression of COPD by modulating TREM-1 expression	*in vitro*	Exosomes derived from CSE-treated AECs aggravate CS-induced lung inflammation and tissue injury in mice, which is associated with the promotion of M1 macrophage polarization by these exosomes through upregulation of TREM-1 expression.
Song *et al.*, 2021 [355]	Exosomal lncRNA TCONS_00064356 derived from injured alveolar epithelial type II cells affects the biological characteristics of mesenchymal stem cells	Investigate whether injured alveolar cells communicate with MSCs via secretion of exosomes and investigate the role of exosomal lncRNAs derived from injured alveolar cells to identify novel therapeutic targets for COPD	*in vitro*	Injured AEC-II cells can affect the biological characteristics of MSCs via secretion of exosomes and the dysregulated exosomal lncRNAs that may be involved in this process were screened out.
Xia *et al.*, 2022 [356]	The aberrant cross-talk of epithelium–macrophages via METTL3-regulated extracellular vesicle miR-93 in smoking-induced emphysema	Assess the role of EV miR-93 in bronchial epithelium exposed to cigarette smoke and the cross-talk between these cells and macrophages in smoking-induced emphysema	*in vitro*	CS exposure induces elevation of METTL3-promoted miR-93 maturation, and miR-93 is transferred from bronchial epithelial cells into macrophages by EVs. In macrophages, miR-93 activates the JNK pathway by targeting DUSP2, which increases the levels of MMP9 and MMP12, inducing elastin degradation. Therefore, CS induces emphysema by a mechanism in which METTL3-mediated EV miR-93 via m6A is involved in aberrant cross-talk of lung epithelial cells and macrophages.

1.8.4. Monocyte/Macrophage-derived EVs

Studies have also observed the effect of CS on the production of EVs from monocytes and macrophages (Table 1.5.). Nieri et al [346] observed an increase in monocyte-derived EVs with COPD severity. As previously mentioned, CS actively promotes EV-dependent proinflammatory signalling. Indeed, Chen et al [357] observed that macrophages exposed to CS released EV containing the proinflammatory alarmin high-mobility group box 1 (HMGB1), a nuclear protein that serves as a “danger signal” and cytokine that mediates sterile inflammation. CS alters alveolar macrophage packaging of SOC3 into secreted MVs, where SOC3, once taken up by epithelial cells, functions in the

control of inflammatory and immune response [358]. Furthermore, exposure to CS inhibits internalisation of these alveolar macrophage-derived EVs by target cells, leading to a more proinflammatory effect [359].

Table 1.5. Summary of studies on macrophage-derived EVs.

Monocytes/Macrophages				
Author, Year [Ref]	**Title**	**Aim**	**Type**	**Conclusion**
Nieri *et al*., 2021 [346]	Circulating Extracellular Vesicles Are Associated with Disease Severity and Interleukin-6 Levels in COPD: A Pilot Study	Analyse endothelial-(E) and monocyte-derived (M) EV levels in COPD patients grouped according to the 2011 GOLD classification and analyse the relationship between EV and plasmatic markers of inflammation.	*ex vivo* human	Circulating endothelial- and monocyte-derived extracellular vesicles increase along with COPD severity. The relationship among EEV and IL-6 suggests a biological link between inflammation and endothelial activation/damage.
Chen *et al*., 2016 [357]	Translocation of Endogenous Danger Signal HMGB1 From Nucleus to Membrane Microvesicles in Macrophages	Establish a cell-culture model to explore the effects of tobacco smoke extract (TSE) exposure on the redistribution and release of nuclear HMGB1 from macrophages, into the extracellular milieu in both soluble and microvesicle-associated form.	*in vitro*	Inhibition of CRM1 interfered with the translocation of HMGB1 induced by TSE from the nucleus to the cytoplasm, and the subsequent release from the cell membrane onto TSE-MVs.
Bourdonnay *et al*., 2015 [358]	Transcellular delivery of vesicular SOCS proteins from macrophages to epithelial cells blunts inflammatory signaling	Investigate the ability of products secreted by AMs to attenuate JAK-STAT signaling in AECs.	*in vitro* *in vivo mice*	AMs secrete SOCS1 and SOCS3 proteins in vesicles that can be taken up by AECs to mediate inhibition of cytokine-induced STAT activation
Schneider *et al*., 2017 [359]	Mechanisms and modulation of microvesicle uptake in a model of alveolar cell communication	Investigate mechanisms involved in EV update in a model of pulmonary alveolar cell-cell communication.	*in vitro*	MV internalization occurs via a pathway more consistent with fluid-phase than receptor-dependent endocytosis and is subject to bidirectional modulation by relevant pathologic perturbations.

1.8.5. Neutrophil-derived EVs

Genschemer et al [360] observed EVs from neutrophils and carried out *in vitro* studies using cell lines and *in vivo* mice and *ex vivo* human studies (Table 1.6). The study concluded that exosomes released from neutrophils carried neutrophil elastase (NE) and were found to bind to the extracellular matrix (ECM), leading to emphysema. Margaroli et al [361] also studied neutrophil-derived EVs, where EV-bound NE functioned in mediating emphysema.

Table 1.6. Summary of studies on neutrophil-derived EVs.

Neutrophils				
Author, Year [Ref]	**Title**	**Aim**	**Type**	**Conclusion**
Genschemer *et al.,*2019 [360]	Activated PMN exosomes: pathogenic entities causing matrix destruction and disease in the lung	Investigate whether neutrophil elastase (NE) exists in exosomal form and whether such exosomes might bypass a1AT and contribute to inflammatory lung disease	*in vitro* *ex vivo* human *in vivo* mice	NE exists in an active, substrate-accessible form when associated with exosomes from activated PMN (polymorphonuclear leukocytes, i.e. neutrophils) and is resistant to a1AT. Activated PMN exosomes bind ECM via MAC-1 and degrade ECM via NE. CD66b+/NE+ PMN exosomes cause emphysema when administered to mice and when residing in COPD patients.
Margaroli *et al.*, 2016 [361]	A novel in vivo model for extracellular vesicle-induced emphysema	Develop a mouse-to-mouse EV-transfer model to expand on neutrophil-derived EVs and further explore discrete disease-related mechanisms	*in vivo* mice	This study highlights a rapid, novel neutrophil driven mechanism of emphysema mediated by mouse neutrophil derived EV-bound NE. EVs from in vivo LPS activated mouse neutrophils induced COPD-like disease in naive recipients through an alpha-1 antitrypsin resistant, NE-dependent mechanism.

1.8.6. T lymphocyte-derived EVs

Qiu et al [362] observed that T lymphocyte microparticles (TLMPs) were significantly upregulated in COPD patients compared to healthy volunteers and further noted that CD4+ and CD8+ TLMPs reduced cell viability and induced production of inflammatory cytokines (Table 1.7.). Studies investigating the effect of CS on T cell production of EVs are currently limited.

Table 1.7. Summary of studies on T lymphocyte-derived EVs.

T-lymphocytes				
Author, Year [Ref]	**Title**	**Aim**	**Type**	**Conclusion**
Qiu *et al.*, 2020 [362]	Increased airway T lymphocyte microparticles in chronic obstructive pulmonary disease induces airway epithelial injury	Examine T lymphocyte microparticles (TLMP) subpopulations in BALF of patients with COPD and and explore the effects of MPs derived from different T cell subpopulations on airway epithelium	*ex vivo* human	The numbers of MPs derived from T lymphocytes in BALF were significantly upregulated in COPD patients compared with healthy volunteers. Isolated CD4+ and CD8+ TLMPs reduced cell viability and induced significant production of inflammatory cytokines including IL-6, MCP-1, MCP-2, MMP-9 and TNF-α in HBEs, while the levels of anti-inflammatory cytokine IL-10 were decreased. TLMPs in the airways may lead to airway epithelial injury and inflammation and serve essential roles in the pathophysiology of COPD.

1.8.7. Platelet-derived EVs

Platelet EVs are known to have pro-inflammatory properties, as they contain and transport bioactive molecules such as CCL5 and CXCL4 to sites of inflammation on the vessel wall, resulting in the recruitment of monocytes [363]. Platelet EVs can also influence behaviour and differentiation states of cells including monocytes and smooth muscle cells [364, 365]. They are also known to promote thrombosis on atherosclerotic plaques [366]. Studies investigating platelet-derived EVs following exposure to CS are currently limited.

1.8.8. EVs derived from other cell types

Production of EVs from other cell types has also been investigated (Table 1.8.). Russell et al [367] observed increased EVs from dendritic cells exposed to CSE compared to control, and that the CSE-EVs had significantly lower expression of CD81 and significant upregulation of HLA-ABC, CD31, and CD45 on their membrane compared to control EVs. Zou et al [353] noted significantly increased levels of IL-1B-containing exosomes in the bronchoalveolar lavage from mice with emphysema but did not specify the cells the exosomes were derived from.

Table 1.8. Summary of studies on EVs derived from other cell types.

Other cell types				
Author, Year [Ref]	**Title**	**Aim**	**Type**	**Conclusion**
Russell *et al.,* 2022 [367]	Cigarette smoke-induced extracellular vesicles from dendritic cells alter T-cell activation and HIV replication	Understand the role of cigarette smoke extract (CSE) on dendritic cell-derived EVs and their capacity to activate and differentiate T-cells	*in vitro*	CSE exposure alters EV production from dendritic cells, and these CSE-EVs can push T-cell differentiation towards Th17 and Th1 lineages.
Zou *et al*., 2021 [353]	Release and Actions of Inflammatory Exosomes in Pulmonary Emphysema: Potential Therapeutic Target of Acupuncture	Investigate if exosome-mediated release of NLRP3 inflammasome products instigates the inflammatory response in the lung during emphysema.	*in vivo* mice	NLRP3 inflammasome activation and associated inflammatory exosome release are critically implicated in the development of inflammation during PPE-induced emphysema.

1.8.9. DNA in EVs

EVs carry various biomolecules and of particular interest are nucleic acids including mRNAs, miRNAs and non-coding RNAs and DNA sequences. One study investigated whether EVs containing mitochondrial DNA (mtDNA) are released upon CS exposure (Table 1.9.). Giordano et al [368] showed that bronchial epithelial cells exposed to CS released EVs containing mtDNA. Research investigating DNA in EVs following CS exposure is limited.

Table 1.9. Summary of studies on EVs containing DNA.

Other cell types				
Author, Year [Ref]	**Title**	**Aim**	**Type**	**Conclusion**
Giordano *et al.,* 2022 [368]	Extracellular Release of Mitochondrial DNA: Triggered by Cigarette Smoke and Detected in COPD	Elucidate whether mtDNA is released upon CS exposure and is detected in the plasma of former smokers affected by COPD as a possible consequence of airway damage	*in vitro*	Exposure to a sublethal dose of CSE decreased mitochondrial membrane potential, increased oxidative stress, dysregulated mitochondrial dynamics, and triggered mtDNA release in EVs. This study associates markers of mitochondrial stress, inflammation, and senescence with mtDNA release induced by CSE exposure.

1.8.10. RNA in EVs

Some EVs have the ability to export miRNA outside cells and affect gene expression in distant cells, thereby inducing phenotypic changes [276, 369]. Studies [321, 322, 337, 349] have observed that CS caused changes in the miRNA levels in EVs (Table 1.10.). Furthermore, these studies [321, 322] observed that CS modified the levels of miR-21 carried by EVs. He et al [321] noted that CS reduced levels of miR-21 in EVs derived from BEAS-2B cells but that EVs obtained from the serum of COPD patients carried significantly higher levels of miR-21. Xu et al [322] concluded that CS exposure increased miR-21 levels in exosomes from human bronchial epithelial cells (HBECs). Fujita et al [337] noted that EVs from HBECs treated with CS had distinct and varying levels of 8 miRNAs, which had either increased levels or decreased levels when compared to the non-treated group. Together, the studies suggest that the CS-induced changes in miRNA cargo of EVs result in myofibroblast differentiation [322, 337], inference of efferocytosis [349] or polarization of macrophages to M2 [321], which are all characteristic of the pathogenesis in COPD.

Table 1.10. Summary of studies on EVs containing RNA.

microRNA				
Author, Year [Ref]	**Title**	**Aim**	**Type**	**Conclusion**
He *et al*., 2019 [321]	Bronchial epithelial cells extracellular vesicles ameliorate epithelial-mesenchymal transition in COPD pathogenesis by alleviating M2 macrophage polarization	Investigate whether EVs could influence the occurrence of inflammatory lung disease (in particular COPD) through contained microRNAs	*in vitro* *ex vivo* human *in vivo* mice	EVs found in the serum contained significantly higher levels of miR-21 in COPD patients than healthy people. CS was found to reduce levels of miR-21 in EVs of BEAS-2B cells at 1%, 3% and 5% when compared to 0%. Macrophages were then found to uptake these EVs, resulting in polarization into M2 phenotype which negatively correlated with lung function of mouse COPD models.
Xu *et al*., 2018 [322]	Exosomal microRNA-21 derived from bronchial epithelial cells is involved in aberrant epithelium-fibroblast cross-talk in COPD induced by cigarette smoking	Evaluate the expression of miR-21 in exosomes derived from bronchial epithelial cells exposed to CSE and investigate the mechanism for exosomal miR-21 in airway remodeling	*in vitro* *ex vivo* human *in vivo* mice	CS exposure induces increases of miR-21 levels transferred by exosomes from human bronchial epithelial (HBE) cells into bronchial fibroblast cells, promoting myofibroblast differentiation by increases of HIF-1a transcriptional activity.
Fujita *et al.,* 2015 [337]	Suppression of autophagy by extracellular vesicles promotes myofibrobasts differentiation in COPD pathogenesis	Investigate an EV-mediated intercellular communication mechanism between primary human bronchial epithelial cells (HBECs) and lung fibroblasts (LFs)	*in vitro*	CSE-induced HBEC derived EVs had modified components, 8 miRNAs including miR-210, when compared to non-treated HBEC-derived EVs. HBEC-derived EV miR-210 caused significant increase in collagen type I and a-SMA expression in lung fibroblasts (LFs) which are characteristic of myofibroblast differentiation via EVs.
Serban *et al*., 2016 [349]	Structural and functional characterization of endothelial microparticles released by cigarette smoke	Investigate the role of signallingolf pathways typically involved in endothelial apoptosis in EMPs release and the role of CS-induced EMPs and their impact on specialized phagocytes	*in vitro* *ex vivo* human *in vivo / ex vivo* mice	CS, via aSMase, releases circulating EMPs with distinct microRNA cargo. CS-induced apoptotic and exosomal EMPs carry ceramides and specific miRNAs in circulation and result in interference of efferocytosis.

1.8.11. Proteins in EVs

Three studies have investigated proteins in EVs after exposure to CS (Table 1.11.). Sundar et al [370] identified novel proteins including CD5 antigen-like (CD5L), fibronectin (FN1), clusterin (CLU), gelsolin (GSN), hyaluronan-binding protein (HABP2), apolipoprotein D (APOD) and ECM-glycoprotein gene (EFEMP1) differentially enriched in plasma-derived EVs from smokers and patients with COPD compared to nonsmokers.

These proteins are known to be involved in the regulation of immune response, in blood coagulation and complement activation, and play a key role in various lung diseases [370]. Additionally, Benedikter et al observed that 24 proteins of the pathway haemostasis, including tissue factor, were significantly upregulated in CSE-induced airway epithelial EVs. Benedikter et al [371] also showed an enhanced procoagulant effect of CSE-induced EVs *in vitro*, dependent on EV-associated TF, suggesting CS-induced EVs may contribute to increased cardiovascular and respiratory risk observed in smokers [371]. Wang et al [372] demonstrated that CS had a great influence on exosomal protein expression in EVs from human bronchial epithelial cells (HBEs) compared to e-cigarette vapour and control. Wang et al [372] further showed that differential expressed exosomal proteins in CS-EVs were significantly enriched in pathways in cancer. Research investigating proteins in EVs following CS exposure is currently limited.

Table 1.11. Summary of studies on EVs containing proteins.

microRNA				
Author, Year [Ref]	**Title**	**Aim**	**Type**	**Conclusion**
Sundar *et al*., 2019 [370]	Proteomic Analysis of Plasma-Derived Extracellular Vesicles in Smokers and Patients with Chronic Obstructive Pulmonary Disease	Characterise plasma-derived EVs in smokers and patients with COPD using mass spectrometry	*ex vivo* human	Several common EV markers enriched in the data set were compared with top 100 plasma-derived EV markers from databases. Using a pairwise comparison, several novel proteins such as CD5L, FN1, CLU, GSN, HABP2, APOD, and EFEMP1 differentially enriched in smokers and patients with COPD compared to nonsmokers were identified.
Benedikter *et al*., 2019 [371]	Proteomic analysis reveals procoagulant properties of cigarette smoke-induced extracellular vesicles	Characterize the proteomic composition of basal and CSE-induced airway epithelial EVs	*in vitro*	Proteomic analysis allowed for prediction of procoagulant properties of CSE-EVs which were confirmed in vitro. Cigarette smoke-induced EVs may contribute to the increased cardiovascular and respiratory risk observed in smokers.
Wang et al., 2023 [372]	Exosome proteomics study of the effects of traditional cigarettes and electronic cigarettes on human bronchial epithelial cells	Evaluate the cytotoxicities of e-Cig and t-Cig condensate solutions (e-CigCS and t-CigCS) on human bronchial epithelial cells (16HBE cells) in vitro	*in vitro*	t-Cig condensate solution markedly inhibited the viability of 16HBE cells in a dose-dependent manner, while e-Cig condensate did not, even with its nicotine concentration reaching 100 μg/mL.

1.8.12. EVs as biomarkers

According to the Global Initiative for Chronic Obstructive Lung Disease (GOLD), the current diagnosis of COPD is based on three features including spirometry, observation of symptoms and significant exposure to toxic stimuli [13]. The use of EVs as biomarkers for COPD has been investigated [373-384], where studies have observed changes in EV levels and changes in the cargo of EVs (Table 1.12.). Studies [373, 375, 377, 379, 381] noted elevated levels of EVs in COPD patients, observing specific microparticles. Lacedonia et al [373] observed significantly elevated levels of CD31+ MPs in the sputum of COPD patients that negatively correlated with forced expiratory volume in 1 second (FEV1). Takahashi et al [375] showed that elevated levels of CD62E+ MPs in plasma of COPD patients had significant negative correlations with FEV1 changes. Furthermore, Jung et al [377] identified a series of plasma EVs (CD45, CD28, CTLA4, TNF-R-II, and CD16) highly expressed in patients with COPD. Gordon et al [374] noted elevated levels of EMPs with apoptotic characteristics in smokers with reduced DL_{CO}, indicative of early lung destruction. Soni et al [379] noted that BALF neutrophil MVs significantly correlated with clinically relevant disease severity indexes. Bazzan et al [381] observed increased levels of EVs from alveolar macrophages in BAL of smokers with COPD compared to smokers without COPD and nonsmokers, which correlated with the pack-years and disease severity according to FEV1. Luccheti et al [380] observed that EVs are detectable in exhaled breathe condensate (EBC) and sputum of COPD patients, however, the cell source of these EVs was not identified.

Studies have also observed miRNA and protein profiles in EVs. Sundar et al [376] and Kaur et al [384] observed distinct miRNA profiles in EVs of COPD patients when compared to smokers and/or non-smokers. Indeed, Carpi et al [382] noted that miR-206, miR-133a-5p and miR-133a-3p levels can discriminate between COPD patients. Shen et al [383] observed that expression levels of three exosomal miRNAs were negatively associated with FEV1. Koba et al [378] observed that expression of fibulin-3 correlated with lung function and emphysema. Together these studies indicate that EVs

can lead to the development of more accurate biomarkers to diagnose COPD and monitor disease progression.

Table 1.12. Summary of studies on EVs as biomarkers.

Biomarkers				
Author, Year [Ref]	**Title**	**Aim**	**Type**	**Conclusion**
Lacedonia *et al.,* 2016 [373]	Microparticles in sputum of COPD patients: a potential biomarker of the disease?	Investigate the presence and source of sputum MPs in COPD patients and to correlate the number and source of MPs to the clinical picture	*ex vivo* human	CD31-MPs, CD66b-MPs, and CD235ab-MPs were upregulated in all COPD patients. High levels of CD31-MPs in COPD sputum negatively correlated with FEV1% and could be a new noninvasive method to monitor disease course.
Gordon *et al*., 2011 [374]	Circulating endothelial microparticles as a measure of early lung destruction in cigarette smokers	Evaluate whether plasma EMP levels are elevated in smokers with early lung destruction as assessed by normal spirometry but reduced diffusing capacity of the lung for carbon monoxide (DL_{CO})	*ex vivo* human	Plasma EMPs with apoptotic characteristics are elevated in smokers with normal spirometry but reduced DL_{CO}.
Takahashi *et al*., 2014 [375]	Annual FEV1 changes and numbers of circulating endothelial microparticles in patients with COPD: a prospective study	Examine the relationship between EMP number and changes in forced expiratory volume in 1s (FEV1) in patients with COPD	*ex vivo* human	High E-selectin (CD62E+) EMP level under a stable condition predicted rapid FEV1 decline after a year in patients with COPD. E-selectin EMP number under a stable condition could be a good biomarker to predict the prognosis of patients with COPD.
Sundar *et al*., 2019 [376]	Small RNA-sequence analysis of plasma-derived extracellular vesicle miRNAs in smokers and patients with chronic obstructive pulmonary disease as circulating biomarkers	Investigate whether smoking and progression of chronic lung disease (i.e. COPD) can alter the composition and packaging of proteins, mRNA and ncRNAs in EVs/exosomes.	*ex vivo* human *in vitro*	RNA-seq analysis carried out on EVs from plasma samples of human subjects showed significant miRNAs up- or down-regulated in smokers vs. COPD and non-smokers vs. COPD pairwise comparisons.
Jung *et al*., 2020 [377]	Surface Proteome of Plasma Extracellular Vesicles as Biomarkers for Pneumonia and Acute Exacerbation of Chronic Obstructive Pulmonary Disease	Identify surface proteins of plasma small EVs (ssEVs) as biomarkers for diagnosis and differentiation of AECOPD to CAP (Community Acquired Pneumonia)	*ex vivo* human	There was a significantly higher expression in plasma sEVs (CD45, CD28, CTLA4, TNF-R-II, and CD16) from patients with AECOPD when compared to CAP patients, allowing for discrimination between the two.
Koba *et al.*, 2021[378]	Proteomics of serum extracellular vesicles identifies a novel COPD biomarker, fibulin-3 from elastic fibres	Assess serum EVs to find novel biomarkers for personalised medicine in COPD using the latest proteomic strategies	*ex vivo* human *in vivo* mice	This study identified novel biomarkers for COPD using next-generation proteomics of serum extracellular vesicles. Notably, the expression of fibulin-3 is

				correlated with lung function and emphysema.
Soni *et al*., 2021 [379]	Intra-alveolar neutrophil-derived microvesicles are associated with disease severity in COPD	Evaluate the profiles of intra-alveolar (within BALF) and circulating (within plasma) MVs in COPD patients, characterizing a variety of MV subtype populations	*ex vivo* human	This study identified a variety of MV subtype populations within the BALF and plasma of COPD patients with a spectrum of disease severity. In this heterogeneous patient cohort ranging from mild to very severe COPD, BALF PMN (i.e., neutrophil) MVs strongly correlate with the BODE index as well as multiple other markers of COPD severity: worsening dyspnea score, degree of airway obstruction and hyperinflation, lung parenchymal damage, and exercise tolerance.
Lucchetti *et al*., 2021 [380]	Detection and characterisation of extracellular vesicles in exhaled breath condensate and sputum of COPD and severe asthma patients	Investigate whether extracellular vesicles are present and detectable in exhaled breathe condensate (EBC) and to perform a preliminary comparison of their concentrations in COPD and healthy control subjects	*ex vivo* human	Extracellular vesicles are detectable in EBC and sputum and measurement of EBC mEV concentrations might be more informative in COPD patients.
Bazzan *et al*., 2021 [381]	Microvesicles in bronchoalveolar lavage as a potential biomarker of COPD	investigate the presence and source of MVs in bronchoalveolar lavage (BAL) of smokers with and without COPD compared with nonsmoking controls	*ex vivo* human	MVs obtained directly from the lung BAL show that, in response to smoking and to the development of COPD, measurable inflammatory signals in alveolar macrophages can be quantified and that their numbers are related to the pack-years and the decrease in lung function.
Carpi *et al*., 2020 [382]	Expression Analysis of Muscle-Specific miRNAs in Plasma-Derived Extracellular Vesicles from Patients with Chronic Obstructive Pulmonary Disease	Analyse the expression profiles of EV-derived myo-miRNAs (specifically miR-206, miR-133a-5p, and miR-133a-3p) in plasma samples collected from patients with COPD	*ex vivo* human	Myo-miRNA are present in EV in the plasma of COPD patients and their expression (miR-206, miR-133a-5p, and miR-133a-3p) can discriminate between COPD patients.
Shen *et al*., 2021[383]	A novel diagnostic signature based on three circulating exosomal mircoRNAs for chronic obstructive pulmonary disease	Evaluate differentially expressed exo-miRNAs in the plasma of patients with COPD and healthy individuals for their potential diagnostic value in COPD	*ex vivo* human	The expression levels of three exo-miRNAs (miR-23a, miR-221 and miR-574) were found to be negatively associated with the forced expiratory volume in the 1st second/forced vital capacity. The three circulating exosomal miRNAs may serve as novel circulating biomarkers for the diagnosis of COPD.

Kaur *et al*., 2021 [384]	Distinct Exosomal miRNA Profiles from BALF and Lung Tissue of COPD and IPF Patients	Compare the miRNA population in the BALF and lung-tissue-derived exosomes from healthy non-smokers, healthy smokers, and patients with COPD in several independent cohorts to identify potential biomarkers to determine the extent of any pulmonary damage at an early stage.	*ex vivo* human	Next generation sequencing results identified three differentially expressed miRNAs in the BALF and one in the lung-derived exosomes from COPD patients, compared to healthy non-smokers. Of these, miR-122-5p was three- or five-fold downregulated among the lung-tissue-derived exosomes of COPD patients compared to healthy non-smokers and smokers, respectively. The identified lung-specific miRNAs associated with COPD can serve as potential biomarkers or therapeutic targets.

1.9. EVs and e-cigarette smoking

The chemicals found in e-cigarettes have been linked to lung disease and cardiovascular disease [385]. Indeed, recent studies have shown that the adverse health effects resulting from e-cigarette use may be mediated in part by circulating EVs [386, 387]. Inhalation of e-cigarette vapour stimulates the release of EVs from a number of cellular sources, including the vasculature, blood cells, cells of the immune system and pulmonary epithelium. As such, EVs may function in activation of cellular responses promoting inflammation and may act as biomarkers.

1.9.1. Endothelial cell-derived EV

One acute adverse physiological change in humans linked to e-cigarettes is vascular changes. An emerging biomarker for endothelial dysfunction is endothelial cell-derived EVs, which are critical in vascular injury, angiogenesis and thrombosis [348, 388]. Research studies have observed that e-cigarette use is associated with increased levels of endothelial cell-derived EVs [348, 389] (Table 1.13.). Antoniewicz et al [389] showed significant increase in the levels of E-selectin positive (CD62e+) EVs following exposure to e-cigarette vapour. Mobarrez et al [348] observed increased levels of circulating endothelial cell- and platelet-derived EVs in healthy occasional smokers following exposure to nicotine-containing e-cigarette vapour, suggesting underlying vascular

changes. The study also noted that e-cigarette vapour without nicotine caused an increase in platelet-derived EVs but no significant changes were observed in levels of endothelial cell-derived EVs, suggesting nicotine as a component in the vapour may have a more compelling effect on EV formation [348]. Taken together, these two studies indicate possible vascular changes after short e-cigarette inhalation; therefore, further studies investigating the effect of e-cigarettes are critical.

Table 1.13. Summary of studies on the endothelial cell-derived EVs.

Endothelial cells				
Author, Year [Ref]	**Title**	**Aim**	**Type**	**Conclusion**
Antoniewicz *et al.*, 2016 [389]	Electronic cigarettes increase endothelial progenitor cells in the blood of healthy volunteers	Measure endothelial progenitor cells (EPCs) and microvesicles (MVs) in healthy young volunteers following short-term exposure to inhalation of e-cigarette vapor (ECV) to determine vascular changes	*ex vivo* human	Vaping exposure caused an increase in EPCs in the blood of the same magnitude as previously demonstrated following conventional cigarette smoking. CD62E expressing EC derived EVs increased slightly, but other EVs remained unaffected.
Mobarrez *et al.*, 2020 [348]	Electronic cigarettes containing nicotine increase endothelial and platelet derived extracellular vesicles in healthy volunteers	Investigate whether e-cigarettes with and without nicotine cause different vascular responses	*ex vivo* human	Brief inhalation of e-cigarette vapor containing nicotine caused an increase in levels of circulating EVs of platelet and endothelial origin, which may signify underlying vascular changes.

1.9.2. Epithelial cell-derived EVs

One study has investigated epithelial cell-derived EVs following exposure to e-cigarette vapour (Table 1.14.). Wang et al [372] exposed 16-HBE cells to cigarette smoke, tobacco-flavoured e-cigarette and menthol-flavoured e-cigarette condensate solution and observed a total of 431 differential expressed exosomal proteins (DEEPs) in test groups compared to control. Indeed, the study noted that 205 DEEPs and 125 DEEPs were dysregulated in the tobacco-flavoured and menthol-flavoured e-cigarette groups, respectively. Furthermore, EVs from the e-cigarette groups were found to have 7 DEEPs to pathways associated with cancer, although this was less than the cigarette smoke group [372].

Table 1.14. Summary of studies on the epithelial cell-derived EVs.

Epithelial cells				
Author, Year [Ref]	**Title**	**Aim**	**Type**	**Conclusion**
Wang et al., 2023 [372]	Exosome proteomics study of the effects of traditional cigarettes and electronic cigarettes on human bronchial epithelial cells	Evaluate the cytotoxicities of e-Cig and t-Cig condensate solutions (e-CigCS and t-CigCS) on human bronchial epithelial cells (16HBE cells) in vitro	*in vitro*	t-Cig condensate solution markedly inhibited the viability of 16HBE cells in a dose-dependent manner, while e-Cig condensate did not, even with its nicotine concentration reaching 100 μg/mL.

1.9.3. Platelet-derived EVs

Studies have also assessed EVs derived from platelets exposed to e-cigarette vapour (Table 1.15.). Kerr et al [387] demonstrated that the number of platelet microparticles increased following e-cigarette exposure in 20 healthy male smokers. Furthermore, Mobarrez et al [348] observed increased levels of circulating platelet-derived EVs, carrying platelet markers CD62P and CD154, in healthy smokers following exposure to nicotine-containing e-cigarette vapour, suggesting platelet activation. Additionally, this study noted that this increase was also observed following exposure to e-cigarette vapour without nicotine [348].

Table 1.15. Summary of studies on platelet cell-derived EVs.

Endothelial cells				
Author, Year [Ref]	**Title**	**Aim**	**Type**	**Conclusion**
Kerr *et al*., 2019 [387]	Acute effects of electronic and tobacco cigarettes on vascular and respiratory function in healthy volunteers: a cross-over study	Assess the acute effects of nicotine-containing electronic cigarettes versus tobacco smoking on vascular and respiratory function and circulating microparticles, particularly platelet microparticles and endothelial microparticles	*ex vivo* human	Acute exposure to tobacco smoking as well as electronic cigarettes influences vascular and respiratory function. Where tobacco smoking significantly increased microparticle formation, indicative of possible endothelial injury, electronic cigarettes use induced vasoreactivity and decreased peak expiratory flow.
Mobarrez *et al*., 2020 [348]	Electronic cigarettes containing nicotine increase endothelial and platelet derived extracellular vesicles in healthy volunteers	Investigate whether e-cigarettes with and without nicotine cause different vascular responses	*ex vivo* human	Brief inhalation of e-cigarette vapor containing nicotine caused an increase in levels of circulating EVs of platelet and endothelial origin, which may signify underlying vascular changes.

1.9.4. EVs derived from other cell types

The effect of e-cigarettes has also been investigated in other cell types (Table 1.16.). Molony et al [390] observed that bladder cancer-derived EVs exposed to e-cigarette liquid were able to promote oxidative stress, inflammatory signalling and DNA damage in recipient non-malignant urothelial cells, increasing their risk of subsequent carcinogenesis. Indeed, the study noted that menthol e-liquid-induced bladder cancer EVs significantly increased rates of malignant urothelial cell transformations, compared to unflavoured e-liquid and CS [390]. Furthermore, Mills et al [391] observed elevated levels of circulating plasma EVs in e-cigarette vapour- and CS-exposed rats, compared with air-exposed control animals; however, this study did not specify the cell types EVs were derived from.

Table 1.16. Summary of studies on EVs derived from other cell types.

Other cell types				
Author, Year [Ref]	**Title**	**Aim**	**Type**	**Conclusion**
Molony *et al*., 2023 [390]	E-liquid exposure induces bladder cancer cells to release extracellular vesicles that promote non-malignant urothelial cell transformation	Analyze the characteristics of EVs released by BC cells exposed to cigarette smoke extract or different E-liquids, with a specific focus on the ability of these EVs to promote the malignant transformation of recipient urothelial cells consistent with a potential field cancerization effect	*in vitro*	Smoking- and E-cigarette-related BCEVs were able to promote oxidative stress, inflammatory signaling, and DNA damage in recipient SV-HUC urothelial cells.
Mills *et al*., 2022 [391]	Short-term effects of electronic cigarettes on cerebrovascular function: A time course study	Evaluate a single episode of cigarette versus Ecig exposure on middle cerebral artery (MCA) reactivity and determined how long after the exposure MCA responses took to return to normal	*in vivo* rats	Acute MCA dysfunction is associated with exposure to e-cigs and cigarettes and persists for ≤ 3 days after single exposure. The data shows that MCA dysfunction correlates with increases in circulating EV concentration.

1.9.5. DNA in EVs

There are currently no known studies investigating DNA in EVs from cells exposed to e-cigarette vapour.

1.9.6. RNA in EVs

Studies have also investigated EVs after exposure to e-cigarette vapour (Table 1.17.). A study by Singh et al [392] noted that 17 miRNAs were differentially altered in plasma EVs from e-cigarette users compared to non-smokers, where 4 miRNAs were downregulated and 13 miRNAs were upregulated in e-cigarette users. The study noted that the downregulated miRNAs are associated with cancer and cardiovascular complications and upregulated miRNAs function in human NK cell function, epithelial-mesenchymal transition and suppression of cell migration and invasion of cancer [392]. Singh et al also showed significant changes in 7 tRNAs in plasma EVs from e-cigarette users compared to non-smokers. Analysis in the study showed significant increase in 6 tRNAs ($tRNA^{Val}$, $tRNA^{Glu}$, $tRNA^{Asp}$, $tRNA^{Gly}$, $tRNA^{Arg}$ and $tRNA^{His}$) and a decrease in $tRNA^{Cys}$

[392]. tRNAs function in tumour development and are associated with the pathological characteristics of lung adenocarcinoma and cancer-specific survival [393]. Furthermore, Kaur et al [394] observed changes in expression of 13 long non-coding RNAs (lncRNA) gene loci among e-cigarette users compared to non-smokers. In particular, a four-fold increase was observed in the TC0800007080.hg.1 gene locus that encodes Bcl2 interacting protein 3 like-protein (BNIP3L), which is known to promote airway epithelial cell injury on exposure to CS [395]. Indeed, increased expression of BNIP3L is associated with aggravated mitophagy, a hallmark of pulmonary diseases such as COPD [396].

Table 1.17. Summary of studies on EVs containing RNA.

Other cell types				
Author, Year [Ref]	**Title**	**Aim**	**Type**	**Conclusion**
Singh *et al*., 2020 [392]	Exosomal microRNAs are novel circulating biomarkers in cigarette, waterpipe smokers, E-cigarette users and dual smokers	Identify, characterise and compare the plasma-derived exosomal microRNAs in E-cig users (E-Cig), waterpipe smokers (WPS), dual smokers (DS) and cigarette smokers (CS) with normal/non-smokers (NS)	*ex vivo* human	Plasma exosomes of cigarette smokers, waterpipe smokers, e-cig users and dual smokers have common differential expression of microRNAs which may serve to distinguish smoking and vaping subjects from NS.
Kaur *et al*., 2020 [394]	Differential plasma exosomal long non-coding RNAs expression profiles and their emerging role in E-cigarette users, cigarette, waterpipe, and dual smokers	Characterise the long non-coding RNA (lncRNA) content of the plasma-derived exosomes from a representative population of these tobacco product users to help identify novel biomarkers, which may be relevant to the associated pulmonary pathologies, such as COPD, asthma, and IPF	*ex vivo* human	Alterations in a distinct set of lncRNAs among subjects exposed to E-cig vapor, cigarette smoke, waterpipe smoke and dual smoke with some overlaps were observed. Gene enrichment analyses of the differentially expressed lncRNAs demonstrated enrichment in the lncRNAs involved in crucial biological processes including steroid metabolism, cell differentiation and proliferation.

1.9.7. Proteins in EVs

Studies have investigated protein content in EVs after exposure to e-cigarette vapour (Table 1.18.). Been et al [397] showed that mice who had chronic, low-level mango-flavoured e-cigarette aerosol exposure resulted in significant differences in protein cargo of EVs between male and female mice, where male mice exhibited a greater

number of distinct proteins compared to female mice. Additionally, Been et al [397] showed that there was protein enrichment in a number of pathways associated with immune function including neutrophil degranulation, phagosome, and platelet degranulation. Molony et al [390] observed that bladder cancer cells exposed to menthol e-liquid released EVs enriched with phosphoglycerate mutase 1 (PGAM1) compared to CSE-EVs or unflavoured e-liquid EVs. PGAM1 has been identified as a pro-oncogenic protein upregulated in bladder cancer cells, supporting aerobic glycolysis and tumour cell growth [398]. Wang et al also showed that HBEs exposed to e-cigarette condensate solution released EVs containing proteins associated with cancer [372].

Table 1.18. Summary of studies on EVs containing proteins.

Other cell types				
Author, Year [Ref]	**Title**	**Aim**	**Type**	**Conclusion**
Been *et al*., 2023 [397]	Chronic low-level JUUL aerosol exposure causes pulmonary immunologic, transcriptomic, and proteomic changes	Investigate the impact of chronic, low-level JUUL aerosol exposure on multiple lung outcomes	*in vivo* mice	Even low exposure to JUUL aerosols impact pulmonary outcomes at the cellular and molecular levels. Exposure significantly alter transcriptional regulation of important inflammatory genes and alter inflammatory cell populations in the airways. These changes were paralleled by observations of sex-specific differences in proteomic expression in acellular EVs.
Molony *et al*., 2023 [390]	E-liquid exposure induces bladder cancer cells to release extracellular vesicles that promote non-malignant urothelial cell transformation	Analyse the characteristics of EVs released by BC cells exposed to cigarette smoke extract or different E-liquids, with a specific focus on the ability of these EVs to promote the malignant transformation of recipient urothelial cells consistent with a potential field cancerization effect	*in vitro*	Smoking- and E-cigarette-related BCEVs were able to promote oxidative stress, inflammatory signaling, and DNA damage in recipient SV-HUC urothelial cells.
Wang et al., 2023 [372]	Exosome proteomics study of the effects of traditional cigarettes and electronic cigarettes on human bronchial epithelial cells	Evaluate the cytotoxicities of e-Cig and t-Cig condensate solutions (e-CigCS and t-CigCS) on human bronchial epithelial cells (16HBE cells) in vitro	*in vitro*	t-Cig condensate solution markedly inhibited the viability of 16HBE cells in a dose-dependent manner, while e-Cig condensate did not, even with its nicotine concentration reaching 100 μg/mL.

1.9.8. EVs as biomarkers

As EVs can be isolated from various biofluids including plasma, serum, saliva, and urine, they can be used as novel circulation biomarkers of injury and/or disease progression. A study by Singh et al [392] demonstrated that plasma EVs from cigarette smokers, waterpipe smokers, e-cigarette users and dual smokers have common differential expression of miRNAs that may be used to distinguish smoking and vaping subjects from non-smokers (Table 1.19.). The study also noted that miRNA has-let-7a-5p has high sensitivity and specificity to distinguish non-smokers from the rest of users [392]. Kaur et al [394] observed changes in expression of 13 long non-coding RNAs (lncRNA) gene loci among e-cigarette users compared to non-smokers (Table 1.19.). The study identified targets that pointed towards a possible risk of lung injury and/or related pathology amongst these individuals. In particular, an increase of TC0800007080.hg.1 gene locus that encodes BNIP3L, which is associated with aggravated mitophagy, was observed in e-cigarette smokers. These are the only known current studies observing EVs as biomarkers after exposure to e-cigarette vapour. Therefore, further studies are needed to identify and validate EVs as potential biomarkers of e-cigarette toxicity.

Table 1.19. Summary of studies on EVs as biomarkers.

Other cell types				
Author, Year [Ref]	**Title**	**Aim**	**Type**	**Conclusion**
Singh *et al*., 2020 [392]	Exosomal microRNAs are novel circulating biomarkers in cigarette, waterpipe smokers, E-cigarette users and dual smokers	Identify, characterise and compare the plasma-derived exosomal microRNAs in E-cig users (E-Cig), waterpipe smokers (WPS), dual smokers (DS) and cigarette smokers (CS) with normal/non-smokers (NS)	*ex vivo* human	Plasma exosomes of cigarette smokers, waterpipe smokers, e-cig users and dual smokers have common differential expression of microRNAs which may serve to distinguish smoking and vaping subjects from NS.
Kaur *et al*., 2020 [394]	Differential plasma exosomal long non-coding RNAs expression profiles and their emerging role in E-cigarette users, cigarette, waterpipe, and dual smokers	Characterise the long non-coding RNA (lncRNA) content of the plasma-derived exosomes from a representative population of these tobacco product users to help identify novel biomarkers, which may be relevant to the associated	*ex vivo* human	Alterations in a distinct set of lncRNAs among subjects exposed to E-cig vapor, cigarette smoke, waterpipe smoke and dual smoke with some overlaps were observed. Gene enrichment analyses of the differentially expressed lncRNAs demonstrated enrichment in the

		pulmonary pathologies, such as COPD, asthma, and IPF		lncRNAs involved in crucial biological processes including steroid metabolism, cell differentiation and proliferation.

1.10. Study Aims

COPD is an inflammatory disease of the airways that affects millions of people yearly. Cigarette smoke is a main risk factor for COPD and recently, e-cigarette have been introduced as a method to aid in quitting cigarette smoking. However, it is not known whether e-cigarettes lead to the development of COPD. EVs are known to have a role in the pathology of several diseases, including pulmonary disease, due to their function in cell-to-cell communication. Research investigating the effect of cigarette smoke and e-cigarette vapour on the production of extracellular vesicles by cells of the immune system is limited. As a result, this research aimed to explore the early effects of cigarette smoke and e-cigarette vapour, i.e. the production of extracellular vesicles by immune cells, that may lead to COPD. The present work first aimed to optimise and develop techniques to study EVs. Additionally, this study used these optimised techniques to investigate the effect of cigarette smoke extract and e-cigarette vapour extract on the production of extracellular vesicles by cells of the immune system. Finally, this study aimed to examine the effect of cigarette smoke extract and e-cigarette vapour extract on the phenotype of immune cells producing EVs.

1.11. Hypothesis

Cigarette smoke extract and e-cigarette vapour extract will modify production of EVs by immune cells. This study also hypothesised that cigarette smoke extract and e-cigarette vapour extract will modify the phenotype of immune cells producing EVs, which may be reflected in the markers expressed by the cells and the EVs produced.

Materials and Methods

2.0. Methods

2.1. Processing of blood samples and Peripheral Blood Mononuclear Cell (PBMC) Isolation.

Ethical approval was obtained from the Medical School Ethics Committee (FMHS REC ref 121-1706) and individuals consented to the study prior to blood donation. Blood was drawn by venepuncture and collected into heparin tubes (Fisher Scientific, Loughborough, UK) for PBMC isolation. Isolation of PBMCs from fresh whole blood was done by histopaque density gradient centrifugation. Specifically, 20 ml of blood was diluted 2:1 in RPMI 1640 medium (Sigma, Poole, UK). The diluted blood was layered over histopaque 1077 (Sigma, Poole, UK) and centrifuged at 800g for 22 minutes, with the slowest acceleration and the brake off. The resultant mononuclear layer was removed from the surface of the histopaque and washed twice with RPMI 1640 medium, then re-suspended in a known volume. A cell count was performed using a hemocytometer and cell viability was determined using trypan blue staining. PBMCs were resuspended at 1 x 10^6 cells/ml in RPMI 1640 medium containing 10% Fetal Bovine Serum (FBS), Penicillin/Streptomycin solution (10000 U/mL) (Fisher Scientific, Loughborough, UK) and Hepes solution (1M) (Sigma, Poole, UK).

For studies concerning EVs, five different mediums were used to test the optimal medium for EV analysis. According to the Minimal Information for Studies of Extracellular Vesicles 2018 (MISEV2018) guidelines set by the International Society for Extracellular Vesicles (ISEV), the use of FCS results in the presence of EVs, which could affect results in terms of EVs/mL [399]. Table 2.1 shows the five mediums used and their properties.

Table 2.1. Mediums with their source and features described. These were used to identify suitable media for EV experiments.

Media	Source	Features
RPMI 1640 medium + FBS	Sigma (Poole, UK)	RPMI 1640 - Conventional culture media with a broad range of applications for mammalian cells. FBS – Media supplement used in a wide range of cell culture applications, providing many non-defined growth-promoting and survival-enhancing factors to cells in culture. Heat inactivated.
RPMI 1640 medium + exosome depleted FBS (exo-FBS)	Sigma (Poole, UK) & ThermoFisher (Loughborough, UK)	RPMI 1640 - Conventional culture media with a broad range of applications for mammalian cells. Exosome-sized and CD63 vesicles removed in exo-FBS (≥90% of exosomes depleted)
AIM V	ThermoFisher (Loughborough, UK)	Serum-free media for immunological studies
Immunocult-XF	Stem Cell Technologies (Cambridge, UK)	Serum-free and animal-component-free medium
X-Vivo 15	SLS (Nottingham, UK)	Serum-free media for most hematopoietic cell types including dendritic cells, lymphocytes, monocytes, macrophages and granulocytes

2.2. T cell Activation

To set an optimised method for T-cell activation and analysis for optimisation of methods (Chapter 3, section 3.1.3.2.), two concentrations (2 and 5 µg/mL) of α(anti)-human CD3 antibody were tested under two settings (immobilised vs soluble). Different parameters including concentration and soluble or immobilised α-CD3 that were tested can be noted in Table 2.2 α-CD3 was immobilised by coating onto the wells of a 96-well plate for at least 30 minutes at 37 ^{o}C, and the plate was then washed twice using cold sterile PBS, as has been previously done in this lab.

Table 2.2. Parameters used set optimised method for T-cell activation and analysis.

Condition of α-CD3	α-CD3 concentration (µg/mL)	Incubation time for antibodies (minutes)
Immobilised	2	30
	5	30
Soluble	2	30
	5	30

For all other experiments, the following conditions were used. To immobilise α-CD3 on plates for T cell stimulation, 100 µL of α-CD3 (2 µg/ml diluted in sterile PBS (Sigma, Poole, UK)) was added to wells of a 96-well plate (Corning, Flintshire, UK), unstimulated wells received 100 µL of sterile PBS only. The plate was then placed in the incubator for 90 minutes. Once PBMCs were isolated and re-suspended as required, the plate was washed twice with cold sterile PBS. A cell suspension of 200 µL was added to each well at a concentration of 2 x 10^{6} cells/mL. To the stimulated wells, 2 µg/mL α-CD28 was added. The plate was then placed in an incubator (37°C, 5% CO_2) for relevant time courses of 24 hours and 48 hours.

2.3. Cigarette Smoke Extraction

Cigarette Smoke Extract (CSE) was used as an aqueous solution containing many of the chemicals associated with exposure to cigarette smoke. The solution was made fresh on the day of the experiment to be used as quickly as possible. CSE was made in a fume hood, with a 3-way tap set up in the fume hood where one section leads to the cigarette on the stand, the second section to a Universal containing 20 mL phenol-red free RPMI (Sigma, Poole, UK), and the third section to a 50mL syringe (Figure 2.1.). The tap was switched on lighting the cigarette so that the tubing leading to the Universal was OFF, and the 50ml syringe was then drawn out. The tap to the Universal was then switched ON and the 50ml of smoke was bubbled slowly through the medium. This process was repeated until the cigarette was finished. The crude CSE was then filtered using a 0.45 μm pore filter to remove bacteria and/or large particles. The absorbance of CSE at 320 nm was determined by spectrophotometry. Absorbance at 320 nm was done to measure tar content in CSE preparations as has been shown in previous studies [129, 400, 401]. The machine was blanked with fresh phenol-red free medium, and CSE was measured at the following dilutions – 1:1, 1:2, 1:5, 1:10. The dilution required to get an absorbance of 0.15 (100% CSE) was then calculated.

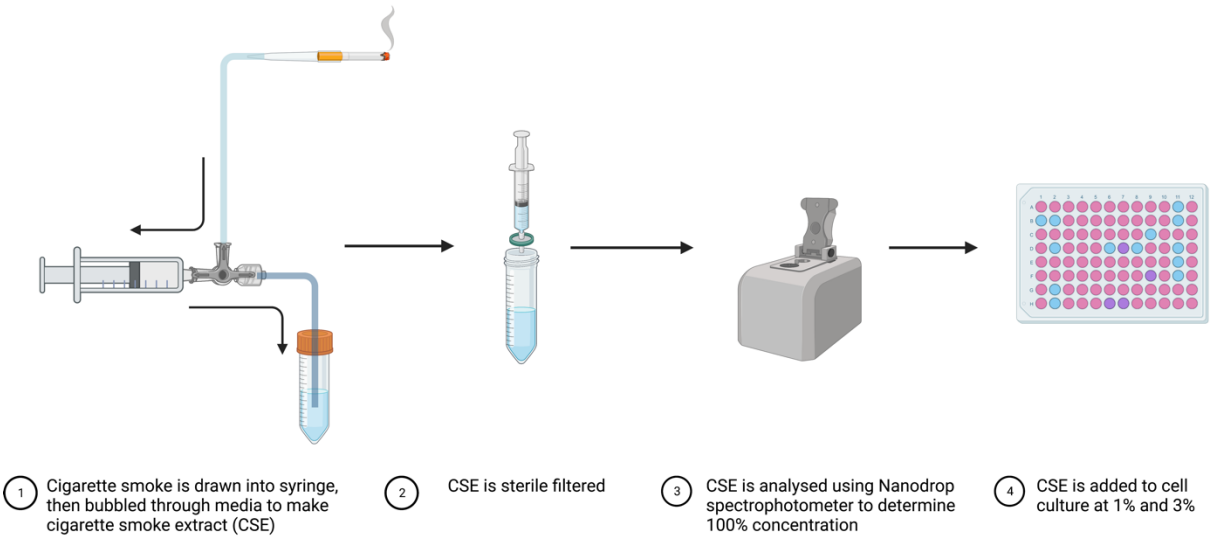

Figure 2.1. *In-vitro* cigarette smoke model. Cigarette smoke extract (CSE) is generated by drawing smoke from one Marlborough Red cigarette through a syringe and bubbling the smoke through phenol red-free culture medium. This is then sterile filtered and analysed on a Nanodrop at 320nm to determine 100% CSE. 1% and 3% CSE are added to isolated PBMCs.

2.4. E-cigarette vapour extraction

E-cigarette solution is an aqueous solution with many of the chemicals associated with exposure to e-cigarettes. Solution for e-cigarettes was made fresh on the day of the experiment and used as quickly as possible. E-liquid containing 50/50 propylene glycol (PG)/vegetable glycerine (VG) with 12mg/mL nicotine was made. The e-cigarette used was a Vapemate device (Vapemate, Brentwood, UK). Once the e-cigarette solution was prepared, 300 µL of it was added to the cartridge of the e-cigarette. The e-cigarette was tested to ensure it was working correctly and then weighed. The mass was recorded. Phenol-red free RPMI (Sigma, Poole, UK) (20 mL) was added to a sterile Universal. Using a 3-way tap and flexible tubing, the e-cigarette, a 60mL syringe and the universal tube containing RPMI were connected (Figure 2.2.). The tap between the e-cigarette and syringe was turned ON. The e-cigarette was then turned on and the vapour was drawn

into the syringe. The tap to the Universal was then switched ON and the entire volume of vapour was bubbled slowly into the RPMI medium. This was left until the vape could no longer be seen in the Universal. This process was repeated with intervals to check the weight of the e-cigarette until the 200mg of e-liquid was vaped. The medium was then filtered with a 0.45µm filter. The resulting extract is considered as 100% E-cigarette vapour extract (ECVE). ECVE was added to cell culture at a final concentration of 1% and 3% ECVE, as has been done in previous study in this lab [260] and similar to nicotine concentrations in (0.5-3%) CSE used in previous studies [129].

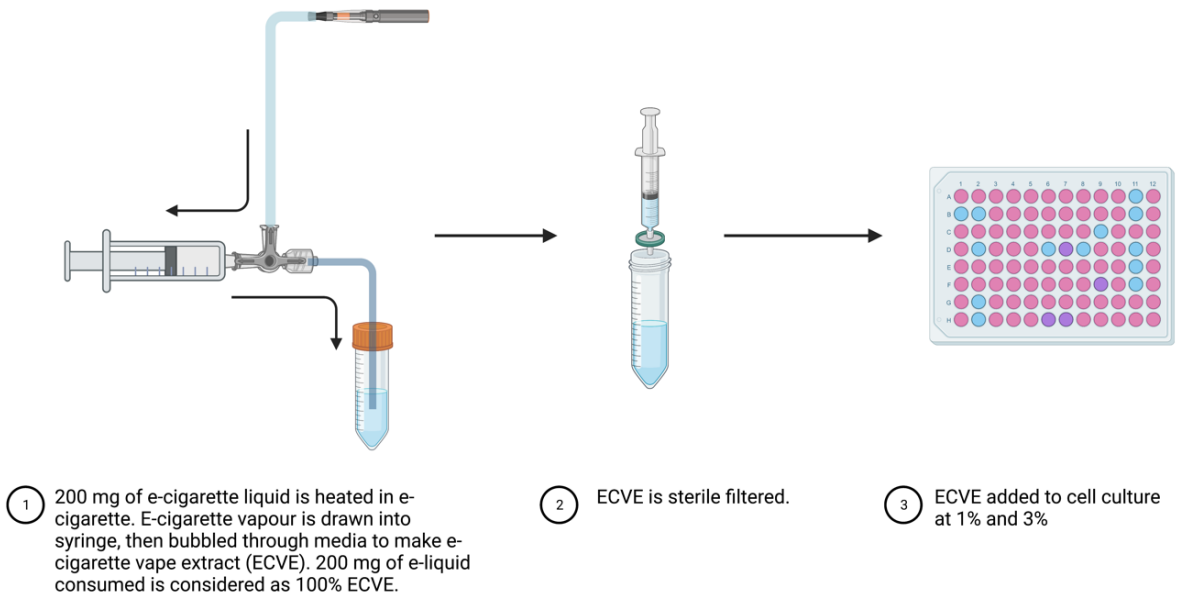

Figure 2.2. In vitro E-cigarette model. E-cigarette vape extract (ECVE) is generated by heating 200mg of e-liquid into a syringe and bubbling through phenol red-free culture medium. This is considered 100% ECVE. It is sterile filtered and 1% and 3% ECVE are added to isolated PBMCs.

2.5. Cell Viability (Annexin V and Propidium Iodide (PI) staining)

Cell viability and apoptosis of PBMCs were tested using annexin V/ PI staining. For this staining, 1x binding buffer was used, made up of 1mL 10x binding buffer in 9mL deionized water and 10^6 cells were stained with Annexin V/PI using the Annexin V-FITC kit (Miltenyi Biotec, Woking, UK), according to manufacturer's instructions. Cells were washed in 1mL of 1x binding buffer and centrifuged at 300xg for 10 minutes. Supernatant was aspirated completely, and cell pellet was resuspended in 100 μL of 1x binding buffer. Annexin V-FITC at a volume of 10μL was added to the cells, and incubated for 15 minutes in the dark at room temperature. The cells were then washed with 1mL 1x binding buffer and centrifuged at 300xg for 10 minutes. Supernatant was aspirated completely, and cell pellet was resuspended in 300 μL of 1x binding buffer. 0.33 μL of propidium iodide (PI) (100 μg/mL) solution was added immediately prior to analysis. This staining was carried out at each relevant time course for tests, i.e. 0 hour, 24 hours, 48 hours. Flow cytometric analysis of cells labelled was performed using BD FACS Canto A (BD Biosciences, Plymouth, UK). A minimum of 20,000 events were acquired. Data were analysed with the use of Kaluza Software (V2.1, Beckman Coulter, High Wycombe, UK).

2.6. Flow cytometric analysis of activated T cells

Harvested PBMCs were stained with antibodies against cell surface markers (Table 3.1). A minimum of 20,000 events were acquired by flow cytometry using BD FACS Canto A (BD Biosciences, Plymouth, UK). Single colours were used to set compensation on the flow cytometer and fluorescence minus one (FMO) controls were used to set quadrants for analysis. Exported data was analysed with the use of Kaluza Software (V2.0 Beckman Coulter, High Wycombe, UK).

Table 3.1.2. Flow cytometry panel for cell surface markers.

Target	Fluorophore	Clone	Product code	Manufacturer	Volume per 100 μL of cells (μL)
CD3	PEVio770	REA613	130-113-140	Miltenyi Biotec	2
CD8	PerCP	BW135/80	130-113-160	Miltenyi Biotec	2
CD56	APC	REA196	130-100-698	Miltenyi Biotec	2
CD25	FITC	4E3	130-113-283	Miltenyi Biotec	2
CD69	PE	REA824	130-112-613	Miltenyi Biotec	2

2.7. Controls set for EV analysis

Following MISEV guidelines and the MIFlowCyt-EV framework for standardized reporting of EV flow cytometry experiments, table 2.4 shows the controls set to enable accurate analysis of EVs [399, 402].

Table 2.4. Assay controls to enable accurate extracellular vesicle analysis and reporting.

Assay controls	**Details**
Buffer only	Medium only – no calcein, no stimulators
Buffer with reagents	Medium only – stimulators added (α-CD3/α-CD28) Calcein added
Unstained controls	No calcein no antibodies
Isotype controls	Isotype controls for α-tetraspanin antibodies Calcein added
Single-stained controls	Calcein only α-human antibodies only (single colours)
Procedural controls	Annexin V/PI staining Fluorescence minus one (FMO) Activation status analysis (α-CD69/α-CD25) Centrifugation of samples
Serial dilutions	Calcein at dilutions of 1:50, 1:100, 1:200, 1:400, 1:800
Detergent-treated EV samples	Tween20 added at 10%, 15% and 20% TritonX-100 added at 0.075% and 0.1%

2.8. Calcein AM staining for EVs

Calcein AM staining for EVs was carried out for EV analysis using imaging flow cytometry (IFC). Previous studies have reported successful labelling of EVs using Calcein AM [403-405], and this method has been used to distinguish between intact EVs and debris. A 1mM stock solution of Calcein AM (Biolegend, London, UK) was prepared by reconstituting in anhydrous DMSO and added to cell suspensions with a final concentration of 0.1µM and incubated for 1 hour (37^{o}C, 5% CO_2).

2.9. Tetraspanin staining of EVs

For staining, α-tetraspanin moAbs for CD9, CD63 and CD81 were added (Table 2.5). Samples were incubated at 37^{o}C for 30 minutes. Equivalent concentrations of the respective isotype controls REA Control Antibody (S) human IgG1, VioBlue (130-113-442) and REA Control Antibody PE human IgG1 (130-113-450) and APC (130-113-434) (Miltenyi Biotec) were added to samples to determine the degree of non-specific binding.

Table 2.5. Flow cytometry panel for tetraspanin markers on EVs.

Target	Fluorophore	Clone	Product code	Manufacturer	Volume per 100 µL of cells (µL)
CD9	VioBlue	REA1071	130-118-809	Miltenyi Biotec	1.0
CD63	PE	REA1055	130-118-077	Miltenyi Biotec	1.0
CD81	APC	REA513	130-119-787	Miltenyi Biotec	1.0

2.10. EV Isolation by size exclusion chromatography (SEC)

4 x 10^6 cells (2 x 10^6 cells/mL) in 2 mL of cell culture medium were cultured for 48 hours in a 24-well plate. Supernatants (2mL) were removed from wells and concentrated to approximately 400–500 µL using a Vivaspin 20, 10 kDa ultrafiltration unit (Sartorius, Epsom, UK) by centrifuge at 3000xg for 10 minutes to pre-clear cell culture supernatant.

EVs were then isolated by size exclusion chromatography using qEV original 35 columns with an automatic fraction collector (AFC) (Izon Science, Lyon, France) that collects EVs ranging from 35 nm to 350 nm. Fractions 1-10 of 1.0 mL were collected and fractions 1-5 were pooled and concentrated using Vivaspin 20 column at 3000xg for 10 minutes. EV fractions (~500 μL) were transferred into 1.5 mL microcentrifuge tubes covered with film to prevent drying and then stored at -80^{o}C.

2.11. Nano-flow cytometry (nFCM) analysis

Nano-flow cytometry analysis was carried out at the NanoFCM Inc laboratory in Nottingham. nFCM is a form of flow cytometry that utilizes instrumentation specifically designed for nano-particle analysis, allowing for thousands of EVs to be characterized per minute both with and without the use of staining techniques. nFCM Is a specialised flow cytometer with small stream size and very slow sample injection rate. The subsequent longer exposure time compare to conventional flow cytometry increases the sensitivity, particularly of the forward and side scatter to allow resolution of very small particles. nFCM is a single particle analysis technique that measures particles aligned in a centre stream by a sheath flow within a micro-channel, where single particle analysis occurs through the measurement of fluorescence signals and scattered light signals in two directions [406]. In nFCM, particle size is estimated by measuring the intensity of forward-scattered (FSC) and side-scattered (SSC) light in the flow of individual particles focused by the sheath flow [406].

nFCM was performed using the Flow NanoAnalyzer U30 (NanoFCM Inc, Nottingham, UK) to determine size and concentration of EV fractions. Prior to data acquisition, three measurements were taken to validate correct alignment of the nFCM instrument, including quality control, size standard and a blank (PBS). A NanoAnalyzer instrument equipped with dual 488/640 lasers was used for simultaneous detection of side scatter (SSC) and fluorescence of individual particles. Single-photon counting avalanche photodiode detections (SPCM APDs) with bandpass filters allowed for collection of light in specific channels (SSC - 488/10; FL1–525/40; FL2–670/30). Gravity fed HPLC-grade

water served as the sheath fluid, sampling pressure by air pump module was 1.0 kPa. Measurements of samples were taken over 1 minute. All samples were diluted to attain a particle count within the optimal range of 2000–12,000/min. Particle concentration and size distribution were calculated using the NanoFCM software (NanoFCM Profession V2.0). The 488/640 lasers were set to 10/50 mW and 10% SSC decay. A single PDF was generated using the nFCM Professional Suite V2.0, providing dot plots, histograms, and statistical data.

2.12. Transmission electron microscopy (TEM)

TEM was carried out at the Biodiscovery Institute at the University of Nottingham with the help of Dr. Zubair Nizamudeen. Isolated EVs were fixed in 3% glutaraldehyde solution in cacodylate buffer for 30 minutes. 10 µL of sample was added to poly-L-Lysine (Sigma-Aldrich, Dorset, UK) (P4707) treated carbon film slot grids (EM resolutions) and left to settle for 15 minutes. Excess sample was removed using blotting paper. Samples were then washed twice with ddH20 (3 minutes each) by placing grids on ddH20 droplets face down on parafilm strip and then stained with 1% uranyl acetate for 5 minutes, excess was removed using blotting paper. TEM was carried out using a Tecnai Biotwin-12 with an accelerating voltage of 100 kV.

2.13. Nanoparticle tracking analysis (NTA)

NTA was carried out at the Biodiscovery Institute at the University of Nottingham with the help of Dr. Zubair Nizamudeen. EVs for NTA analysis were isolated by size exclusion chromatography as stated above. An LM10/14 Nanosight (Nanosight, Malvern Panalytical, Malvern, UK) instrument was used to analyse isolated EVs. Prior to analysis, a 1:10 dilution of 100nm carboxylated polysterene (CPC100; IZON) and a 1:1000 dilution of 200 nm polystyrene (Malvern Panalytical, Malvern, UK) nanoparticles were used to test the sensitivity of the instrument [407]. EV samples were diluted such that less than 200 particles were tracked per image. Automatic settings were applied for the minimum expected particle size, minimum track length, and blur settings. For capture settings,

screen gain was set at 1, and camera level was set at 13 (shutter 1390; gain 372). For analysis settings, screen gain was set at 13, and the detection threshold was set at 3. Five 60 s movies were captured at 30 frames per second for each sample. Data processing and analysis of particle size distribution were performed using NTA Software 3.3 Dev build 3.3.301 (Malvern Panalytical, Malvern, UK).

2.14. Introduction of EVs to activated T-cells

After culturing of activated T cells, isolated EVs from α-CD3/α-CD28-stimulated PBMCs were labelled with calcein were introduced into culture. The cells were then incubated for two time points, 2 hours and 12 hours, at 37°C/5% CO2. For Imaging flow cytometry, the cells were labelled with 2μL of fluorochrome-conjugated antibodies to CD3 per 100 μL of cell culture for 30 minutes at 4°C. The cells were then acquired on the ImageStreamX MK II (Luminex, UK) and analysed using IDEAS software.

2.15. ImageStreamX Small Particles Acquisition and Analysis

Imaging Flow Cytometry (IFC) was performed using ImageStreamX MKII (Luminex, Dartford, UK) with the following laser powers 405 nm (120 mW), 488 nm (200 mW), 561 nm (200 mW), 642 nm (150 mW) and side scatter (SSC) (40 mW). Channels 01 and 09 were set to brightfield (BF) and channel 12 was set to side scatter (SSC). Samples were acquired using the 60X objective with flow speed set to low for a time span of 10 minutes unless the acquisition was complete, using the software INSPIRE. Reference nanobeads (NFPPS-52-4K) (Spherotech, Newcastle, UK) were analysed to display a reference standard. Data analysis was performed using IDEAS software. IDEAS feature 'objects/mL' was utilised to determine the concentration of gated small EVs. A spot count feature was first created (Spot Count_Spot (M09, Ch09, Bright, 1, 1, 1)_4) to exclude any events with a brightfield image. A second spot count feature (M02, Calcein, Bright, 1, 5, 1)_4 was created to include only events with a single calcein 'dot' and to exclude any coincident or clumped EVs.

2.16. Protein measurements

Protein concentrations in isolated EV fractions were measured using a BCA protein assay kit (ThermoFisher, Loughborough, UK) according to manufacturer's instructions. Briefly, the contents of one Albumin Standard (BSA) ampule were diluted into several clean vials, using PBS as the diluent, at final BSA concentrations of 2000, 1500, 1000, 750, 500, 250, 125, 25 and 0 μg/mL. The bicinchoninic acid (BCA) working reagent was prepared by mixing 50 parts of BCA reagent A with 1 part of BCA reagent B (50:1, Reagent A:B) and was then added to standards and unknown sample replicates in a 96-well plate, mixing thoroughly on a plate shaker for 30 seconds. The plate was then incubated at 37^{o}C for 30 minutes. The absorbance was then measured at 560 nm on a GloMax Explorer plate reader (Promega, Southhampton, UK). A standard curve was made by plotting the 560-nm measurement for each BSA versus its concentration in μg/mL and used to determine the protein concentration of each unknown sample.

2.17. Macsplex surface protein profiling

The MACSPlex Exosome Kit (Miltenyi Biotec, Woking, UK) allows for detection of 37 surface markers present on EVs plus two isotypes. These include CD3, CD4, CD19, CD8, human leukocyte antigen (HLA)-DRDPDQ, CD56, CD105, CD2, CD1c, CD25, CD49e, ROR1, CD209, CD9, SSEA4, HLA-ABC, CD63, CD40, CD62P, CD11c, CD81, MCSP1, CD146, CD41b, CD42a, CD24, CD86, CD44, CD326, CD133/1, CD29, CD69, CD142, CD45, CD31, CD20, and CD14, and REA and IgG1. The MACSPlex kit was used according to the manufacturer's instructions for the overnight assay using 1.5 mL tubes. EV concentration was previously determined indirectly by quantifying protein concentration using the BCA protein assay kit. Isolated EVs from each sample diluted to 120 μL using the MACSPlex buffer were added to 1.5 mL tubes. A control tube containing 120 μL MACSPlex buffer was also included. MACSPlex Exosome Capture Beads were resuspended by vortexing for 30 seconds and 15 μL of beads were then added to each tube. Tubes were incubated overnight at room temperature protected from light using an orbital shaker (450 rpm). 500 μL of MACSPlex buffer was added to

each tube. Tubes were then centrifuged at room temperature at 3000xg for 5 minutes. 500 μL of supernatant was carefully aspirated. 5 μL of each MACSPlex Exosome Detection Reagent CD9, CD63 and CD81 was added to each tube and mixed by pipetting up and down. Tubes were incubated for 1 hour at room temperature, protected from light, using an orbital shaker (450 rpm). 500 μL of MACSPlex buffer was then added to each tube and then centrifuged at 3000xg for 5 minutes. 500 μL of supernatant was carefully aspirated, and 500 μL of MACSPlex buffer was then added to each tube. Tubes were incubated for 15 minutes at room temperature and protected from light using an orbital shaker (450 rpm). Tubes were then centrifuged at 3000xg for 5 minutes and 500 μL of supernatant was carefully aspirated. MACSPlex Exosome Capture Beads were resuspended by pipetting up and down.

Samples were analysed using an ID7000 flow cytometer (Sony Biotechnology, Weybridge, UK) in the Flow Cytometry Facility (Queen's Medical Centre) and data were analysed using Kaluza (V2.1, Beckman Coulter, High Wycombe, UK). For analysis, the median fluorescence intensity (MFI) for all 39 capture bead subsets was background corrected by subtracting respective MFI values from matched non-EV buffer or media controls treated like EV-containing samples (buffer/medium + capture beads + antibodies). Data normalization was directed towards CD9/CD63/CD81 APC signal by using the mean of the median signal intensity of the MACSPlex Exosome Capture Beads CD9, CD63, and CD81 as the normalisation factor for each sample. The signal intensity of all beads was divided by the normalisation factor of the respective sample.

2.18. Extracellular Staining of PBMCs

Cells were stained with viability dye and surface markers (Table 2.6.), and incubated in the dark for 30 minutes at 4 °C. Cells were then washed with PBA (PBS, 0.5-1% BSA, 0.1% NaN3 sodium azide*) at 500xg (maximum acceleration and deceleration) for 10 minutes. Cells were fixed with 4% paraformaldehyde and stored at 4 °C.

Table 2.6. Flow cytometry panel for cell surface markers.

Target	Fluorophore	Clone	Product code	Manufacturer	Volume per 100 μL of cells (μL)
Live/Dead	Zombie Aqua		423101	Biolegend	0.3
CD3	PerCP-Cy5.5	OKT3	317336	Biolegend	1
CD4	APC-Fire750	RPA-T4	300560	Biolegend	2
CD8	Alexa Fluor 700	SK1	344724	Biolegend	2
CD56	Brilliant Violet 785	5.1H11	362550	Biolegend	2
CD14	Brilliant Violet 605	63D3	367126	Biolegend	2
CD19	Brilliant Violet 650	SJ25C1	363026	Biolegend	2
CD16	Alexa Fluor 488	3G8	302019	Biolegend	2
CD11c	PE-Cy7	Bu15	337216	Biolegend	2
CD69	PE/ Fire640	FN50	310960	Biolegend	2
CD29	PE	TS2/16	303004	Biolegend	2
HLA-DR	Brilliant Violet 711	L243	307644	Biolegend	2
CD40	Brilliant Violet 421	5C3	334332	Biolegend	2
CD49e	APC	NKI-SAM-1	328012	Biolegend	2

2.19. Flow Cytometry for cell analysis

A minimum of 200,000 lymphocytes were acquired by flow cytometry using an ID7000 spectral cell analyzer (Sony Biotechnology, Weybridge, UK). A spectral matrix was constructed by analysing single colour control samples for all fluorophores before data

was spectrally unmixed using the weighted-least squares method. Exported data was analysed using Kaluza (v2.1 Beckman Coulter, High Wycombe, UK).

2.20. High-Dimensional Analysis of Flow Cytometry Data

Single viable lymphocytes were gated in FlowJo (V10, Becton Dickinson, Plymouth, UK) before equal sampling of 20,000 events from each donor with the DownSample plugin, to provide equal weighting for all donors. The downsampled populations were concatenated in one single file. t-distributed stochastic-neighbour embedding (t-SNE) was performed with opt-SNE learning configuration [408], 1000 iterations, a perplexity of 30, learning rate of 3500, Exact (vantage point tree) KNN and Barnes-Hut gradient algorithm. Next, FlowSOM clustering [409] was performed using 15 meta-clusters and projected on the t-SNE using Cluster Explorer. Identified populations were further explored using the Cluster explorer plugin.

2.21. Protein Digestion

Protein digestion was carried out by Dr. Mandy Peffers at the University of Liverpool. EVs were isolated as previously described. Protein concentration of collected EVs was measured and ideally minimum 10-20 μg starting in minimal volume was used. Isolated EVs were supplemented with 25mM ammonium bicarbonate (Fluka Chemicals Ltd., Gillingham, UK), containing 1% (w/v) RapiGest (Waters, Elstree, Hertfordshire, UK) to a final volume of 160 μL and heated at 80^{o}C for 10 minutes. Diothiothreitol (Sigma-Aldrich, Dorset, UK) was added (60^{o}C, 10 minutes) followed by Iodoacetamide (Sigma-Aldrich, Dorset, UK) (RT, 30 minutes). Any excess iodoacetamide was quenched by adding 9.4 μL diothiothreitol. 10 μL of 0.2 μg/μL trypsin/Lys-C (Promega, Southampton, UK) was added and samples were incubated overnight in the same conditions. Digests were then supplemented with trifluoroacetic acid (TFA, Sigma-Aldrich, Dorset, UK) and incubated for 45 minutes at 37^{o}C in a rotating incubator. Samples were then centrifuged (13,000g, 15 minutes) and supernatants transferred to new lobind tubes. Centrifugation step was repeated and the supernatants were placed into new lobind tubes.

All samples were run in a single batch. 500 ng of each tryptic digest was subjected to liquid chromatography tandem mass spectrometry (LC-MS/MS), using a 2 h gradient. Data-dependent analyses were conducted on a QExactive HF quadrupole-Orbitrap mass spectrometer coupled to a Dionex Ultimate 3000 RSLC nano-liquid chromatograph (Hemel, Hempstead, UK). Sample digests were loaded onto a trapping column (Acclaim PepMap 100 C18, 75 mm _ 2 cm, 3 mm packing material, 100 Å) using a loading buffer of 0.1% (v/v) TFA, 2 % (v/v) acetonitrile in water for 7 min at a flow rate of 12 mL min^{-1}. The trapping column was then set in-line with an analytical column (EASY-Spray PepMap RSLC C18, 75 mm _ 50 cm, 2 mm packing material, 100 Å) and the peptides eluted using a linear gradient of 96.2 % A (0.1 % [v/v] formic acid):3.8 % B (0.1 % [v/v [formic acid in water/acetonitrile [80/20] [v/v]) to 50 % A:50 % B over 90 min at a flow rate of 300 nL min^{-1}, followed by washing at 1% A:99 % B for 5 min and re-equilibration of the column to starting conditions. The column was maintained at 40°C, and the effluent introduced directly into the integrated nano-electrospray ionisation source operating in positive ion mode. The mass spectrometer was operated in data dependent acquisition mode with survey scans between m/z 350e2000 acquired at a mass resolution of 60,000 (FWHM) at m/z 200. The maximum injection time was 100 ms, and the automatic gain control was set to 3e6. The 12 most intense precursor ions with charges states of between 2þ and 5þ were selected for MS/MS with an isolation window of 2 m/z units. The maximum injection time was 100 ms, and the automatic gain control was set to 1e5. Fragmentation of the peptides was by higher-energy collisional dissociation using normalized collision energy of 30%. Dynamic exclusion of mass/charge values to prevent repeated fragmentation of the same peptide was used with an exclusion time of 20 s. For protein identification a local Mascot server (Version 2.6.2), was used against the Unihuman Reviewed database with carbamidomethyl cysteine as a fixed modification and methionine oxidation as a variable modification, peptide mass tolerance of 10 ppm and fragment tolerance of 0.01 Da.

2.22. Data analysis

All statistical analyses were performed using Prism software, version 9.5.0. (GraphPad). All data was analysed for normal distribution using the Kolmogorov-Smirnov test, prior to using a non-parametric or parametric statistical test. Most of the tests used were either One-way ANOVAs or Two-way ANOVAs, followed by Tukey's multiple comparison tests. Significance for tests was defined as $P < 0.05$. The tests used for specific data are detailed throughout the results chapters.

Results

3.0. Optimising methods for analysis of EVs

3.1. Introduction

3.1.1. Current technology and guidelines for EV studies

EVs have been found to be present in all body fluids including blood, urine, breast milk and saliva. EVs are a heterogeneous group of nanoscopic particles with heterogeneity in biogenesis, size and origin and express varying surface markers and a variety of cargo [278, 279, 410]. Their involvement in many physiological and pathological processes make EVs an ideal non-invasive source for biomarkers. Despite the importance of EV biology, EV research faces challenges due to the small size and heterogeneity of EVs. Thus, efforts are being made to refine approaches to isolate and characterise EV populations.

The number of scientific publications investigating the physiological and pathological functions of EVs has increased in the last decade. However, their heterogeneity can lead to issues in obtaining relatively pure preparation and characterisation. The International Society for Extracellular Vesicles (ISEV) has proposed Minimal Information for Studies of Extracellular Vesicles (MISEV) guidelines for the field of EVs [399]. In the guidelines, the ISEV board members detail their recommendations on the "minimal experimental requirements for definition of extracellular vesicles and their function" [399].

One of the challenges in EV research is the use FCS in cell culture medium. MISEV guideline recommend the use of serum-free media, as medium components and supplements are known to either contain EVs or affect EV production and/or composition, respectively [399]. EV-depleted serum has previously been used, however, one study raised doubts concerning the reproducibility of the overall depletion of serum EVs from the EV-depleted serum [411].

Another challenge is the absolute purification or complete isolation of EVs from other entities [399]. Indeed, highly purified EVs are important to associate a function or a biomarker to vesicles compared to other particles. A number of methods have been used to isolate and enrich EVs from biological samples. One of the most commonly used EV isolation and concentration techniques is differential ultracentrifugation; however,

this is associated with some disadvantages, including low yield, damage to vesicles and contamination with non-EV particles and/or proteins [412-414]. Other isolation techniques have been developed including density gradients, precipitation, filtration, size exclusion chromatography and immunoisolation [399, 415]. MISEV 2018 guidelines recommend choosing a separation method based on downstream applications and scientific questions, as there is no single optimal separation method and separation of non-vesicular entities from EVs is not fully achieved by common EV isolation protocols [399].

Additionally, several techniques have been used for the size characterisation, enumeration and phenotyping of EVs. These include transmission electron microscopy (TEM) [407], cryo-TEM [416], confocal microscopy [417], dynamic light scattering (DLS) [418], direct stochastic optical reconstruction microscopy (d-STORM) [419], nanoparticle tracking analysis (NTA) [420], resistive pulse sensing [419] and flow cytometry [418], among others. Indeed, electron microscopy (EM), including TEM, has been used as a standard technique for EV characterisation, whereby high-resolution imaging is used for the acquisition of size and morphology information [419, 421]. A common alternative to EM for characterising EVs is NTA, which depends on the light scattered by particles in Brownian motion. NTA has been shown to accurately analyse the size distribution of monodisperse and polydisperse nanoparticles [422, 423]. This technique also examines concentration and phenotype of EVs. Particle number can also be measured by other light scattering technologies, including flow cytometry. Recently developed techniques combine the advantages of imaging with analysis of large number of events. This includes traditional flow cytometry (FCM), imaging flow cytometry (IFC) and nanoflow cytometry (nFCM). FCM has a higher throughput compared to IFC and nFCM; however, it lacks the resolution to accurately characterise individual EVs, in particular small EVs [424]. IFC, having a lower throughput than FCM but higher than nFCM, captures images of individual cells and particles and enables the discrimination and analysis of single EV due to its ability to detect submicron particles, as demonstrated by previous studies [425-428]. However, IFC is limited in detecting EV populations that are in low

abundance. nFCM has a lower throughput compared to FCM and IFC, however it is designed for small particles and operates at slower flow rates to maintain sensitivity for detecting nanoparticles. It is limited in its sample throughput and multiplexing capabilities, and sample preparation for nFCM analysis can be complex and time-consuming. Currently, MISEV 2018 guidelines provide no recommendation on quantification, however, both the source of EVs and the EV preparation are to be described quantitatively [399].

Furthermore, there exist many subtypes of EVs, of different sizes and cellular origins. Currently, there is no specific marker or universal molecular marker that could characterise each EV subtype specifically; for instance, there is no marker of MVB-derived exosomes compared to other small EVs. MISEV guidelines currently recommend that in protein content-based EV characterisation, at least one protein of categories 1-3 must be analysed to demonstrate the EV nature and the degree of purity of an EV preparation [399]. Proteins in category 1 are transmembrane or GPI-anchored proteins associated to plasma membrane and/or endosomes and include non-tissue specific proteins such as tetraspanins (CD63, CD81, CD82), MHC class I, and tissue specific proteins such as CD9, CD90, CD45 and MHC class II, among others. Category 2 proteins are cytosolic proteins recovered in EVs and include ESCRT-I/II/III, heat shock proteins (HSP A8, HSP84, HSP70), and enzymes such GAPDH, among others. Proteins in category 3 are major components of non-EV co-isolated structures and include lipoproteins and protein/nucleic acid aggregates. Proteins in categories 4 and 5 are required when claiming specific analysis of small EVs and to document functional activities, respectively. Proteins in category 4 include proteins present in the intracellular compartment of eukaryotic secreting cells, excluding the plasma membrane and endosome. Category 5 proteins are soluble extracellular proteins that can associate with EVs by binding to receptors on the EV surface and include cytokines, growth factors, and extracellular matrix. Non-protein components are also commonly used as markers of EVs. This includes dyes that are activated by intracellular components in EVs. For example, Calcein is a cell-permeant non-fluorescent pro-dye that is cleaved by

intravesicular esterase to be converted into a fluorescent analogue that is EV-impermeant, allowing for differentiation of intact EVs from membrane fragments [403]. Additionally, it is necessary to include appropriate negative controls in EV studies, such as dye only and dye plus EV-depleted matrix [399].

3.1.2. Aim

The aim of this chapter was to optimise methodologies to study immune cell-derived EVs following the Minimal Information for Studies of Extracellular Vesicle (MISEV) 2018 guidelines.

3.2. Methods

3.2.1. Processing of blood samples and Peripheral Blood Mononuclear Cell (PBMC) Isolation.

Blood was drawn by venepuncture and collected into heparin tubes for PBMC isolation. Isolation of PBMCs from fresh whole blood was done by histopaque density gradient centrifugation. For studies concerning EVs, five different mediums were used to test optimal medium for EV analysis. Full details of the methodology can be found in chapter 2 section 2.1 and details of reagent used are in table 2.1.

3.2.2. T cell Activation

Human PBMC were stimulated with α-human CD3 (Sigma, Poole, UK) and soluble α-human CD28 antibody (at a final concentration of 2 µg/ml). Full details of methodology can be found in chapter 2, section 2.2.

3.2.3. Cell Viability (Annexin V and Propidium Iodide (PI) staining)

Cell viability and apoptosis of PBMCs was tested using annexin V/PI staining using the Annexin V-FITC kit (Miltenyi Biotec, Woking, UK), according to manufacturer's instructions. Full details of the methodology can be found in chapter 2 section 2.5.

3.2.4. Flow cytometric analysis

Harvested PBMCs were stained with antibodies against cell surface markers. A minimum of 20,000 events were acquired by flow cytometry using BD FACS Canto A (BD Biosciences, Plymouth, UK). Full details of methodology for flow cytometric analysis can be found in chapter 2, section 2.6.

3.2.5. Controls set for EV analysis

Following MISEV guidelines and the MIFlowCyt-EV framework for standardized reporting of EV flow cytometry experiments, controls were set to enable accurate analysis of EVs [399, 402]. Details of the assay controls to enable accurate extracellular vesicles analysis and reporting can be found in Chapter 2, section 2.7, Table 2.4.

3.2.6. Calcein AM staining of EVs

Calcein AM staining for EVs was done to obtain images of the cells and EVs using imaging flow cytometry (IFC). Full details of methodology can be found in chapter 2, section 2.8.

3.2.7. Tetraspanin staining of EVs

For staining, α-tetraspanin moAbs for CD9, CD63 and CD81 were added. Detailed methodology for tetraspanin staining of EVs can be found in chapter 2, section 2.9.

3.2.8. EV isolation by Size Exclusion Chromatography

EV isolation by size exclusion chromatography (SEC) was done using qEV original 35 columns (Izon Science, Lyon, France) and Automatic Fraction Collector (AFC) (Izon Science, Lyon, France) and according to manufacturer's instructions. Detailed methodology can be found in chapter 2, section 2.10.

3.2.9. Nano-flow cytometry (nFCM) analysis

nFCM was performed at the NanoFCM site in Nottingham using the Flow NanoAnalyzer U30 (NanoFCM Inc, Nottingham, UK) to determine size and concentration of EV fractions. Detailed methodology can be found in chapter 2, section 2.11.

3.2.10. Transmission electron microscopy (TEM)

TEM of isolated EVs was carried out at the Biodiscovery Institute at the University of Nottingham. Full details of methodology can be found in chapter 2, section 2.12.

3.2.11. Nanoparticle Tracking Analysis (NTA)

NTA analysis of isolated EVs was carried out at the BioDiscovery Institute at the University of Nottingham using an LM10/14 Nanosight (Nanosight, Malvern Panalytical) instrument. Detailed methodology can be found in chapter 2, 2.13.

3.2.12. Protein digestion

Samples of isolated EVs were sent to the University of Liverpool for proteomic analysis. Detailed methodology can be found in chapter 2, 2.20.

3.2.13. Introduction of EVs to activated T-cells

After culturing of activated T cells, isolated EVs labelled with calcein were introduced into culture. The cells were then incubated for two time points, 2 hours and 12 hours, at 37°C/5% CO2. For Imaging flow cytometry, the cells were labelled with 2μL of fluorochrome-conjugated antibodies to CD3 per 100 μL of cell culture for 30 minutes at 4°C. The cells were then acquired on the ImageStreamX MK II (Luminex, UK) and analysed using IDEAS software.

3.2.14. ImageStreamX (ISX) Small Particles Acquisition and Analysis

Imaging flow cytometry was performed using ImageStreamX (ISX) MK II (Luminex, UK). Details of data acquisition using the ISX can be found in chapter 2, section 2.15. Samples

were acquired for a time span of 10 minutes unless the acquisition was complete, using the software INSPIRE, and exported data was analysed using ISX Data Exploration and Analysis Software (IDEAS).

3.2.15. Protein measurements

Protein concentrations in isolated EV fractions were measured using a BCA protein assay kit (ThermoFisher, Loughborough, UK) according to manufacturer's instructions. Details of methods can be found in chapter 2, section 2.16.

3.2.16. Macsplex surface protein profiling

The MACSPlex Exosome Kit (Miltenyi Biotec, Woking, UK) allows for detection of 37 surface markers present on EVs plus two isotypes. The MACSPlex kit was used according to the manufacturer's instructions for the assay using 1.5 mL tubes. Details of methods can be found in chapter 2, section 2.17.

3.2.17. Data analysis

Data analysis was performed using Prism software, version 8.2.1c (GraphPad, San Diego, USA). Statistically significant differences of sEV concentration for sample vs controls were analysed by ordinary one-way ANOVA, followed by Dunnett's multiple comparisons test (Figure 3.1.10). Statistically significant differences of % focussed single- vs double- vs triple-stained sEVs for each tetraspanins (CD9, CD63, CD81) were analysed by two-way ANOVA, followed by Tukey's multiple comparisons test (Figure 3.1.15.A.).

3.3. Results

3.3.1. Demographics

In total, 21 healthy volunteers (9 females, 12 males) between the ages of 20 – 25 were recruited to this study. Volunteers stated they had no history of smoking cigarettes. The 21 volunteers were used once but not at the same time. Blood was taken from one

volunteer on the day of the start of experiment. Different volunteers were used throughout the assays.

3.3.2. T cell activation

The first aim of this study was to identify a protocol to activate cells efficiently. In immune cells, EVs are released constitutively, however, secretion is enhanced by stimuli, including T cell receptor (TCR) trigger or T cell activation [429, 430]. This experiment was carried out by varying concentrations of α-CD3, either immobilised or soluble. Two concentrations (2 μg/ml vs 5 μg/ml) of α-human CD3 antibody were tested that were either immobilised or soluble. Additionally, incubation times of antibodies for flow cytometry analysis were also varied. Data was collected at time points: 0 hour, 24 hours and 48 hours. To enable measurement of activation, a panel of antibodies was chosen to allow for selection of CD3+ T cell population using flow cytometry, where a minimum of 20,000 events were analysed. Cells were initially selected according to their size (forward scatter FSC) and granularity (side scatter SSC) (**Figure 3.1.1.A.**), followed by selection of singlets (**Figure 3.1.1.B.**). This was then followed by identification of CD3+ T lymphocytes for immobilised αCD3 (**Figure 3.1.1.C.i**). Interestingly, it was not possible to identify the population of interest (i.e. CD3+ T lymphocytes) with soluble α-CD3 as there was little CD3+ population (**Figure 3.1.1.C.ii**). This was possibly due to the TCR being internalised and degraded upon high stimulation [431-433]. CD69 and CD25 staining of CD3+ T lymphocytes was also carried out to identify levels of activation at 0h, and as expected the cells expressed neither activation marker (**Figure 3.1.1.D**). CD3+cells were selected for both immobilised and soluble α-CD3.

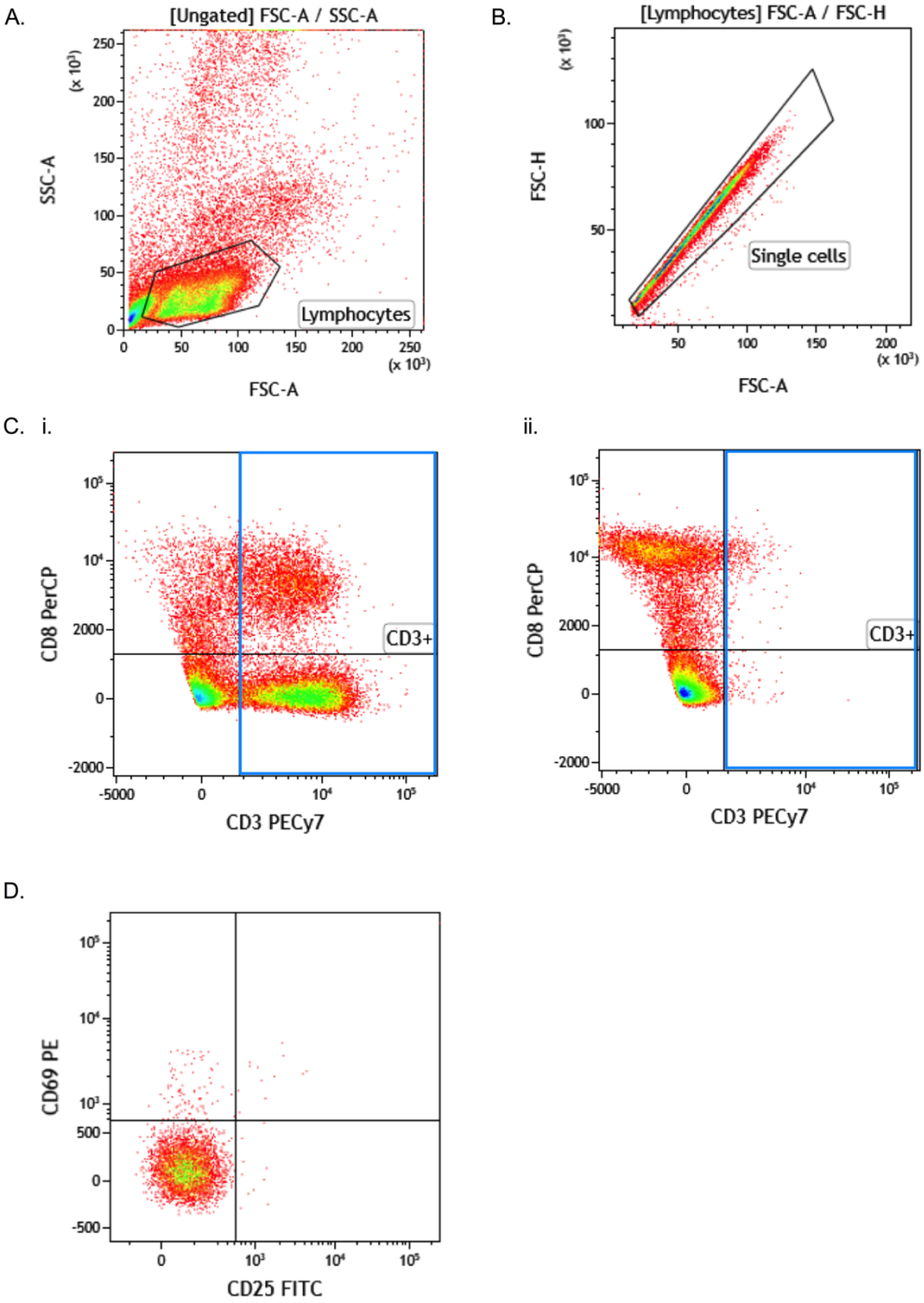

Figure 3.1.1. Representative dot plots gating for cells (n=2). (A) Forward scatter (FSC) vs side scatter (SSC) plot for identification of cells. (B) Selection of singlets. (C) Identification of CD3+ lymphocytes (blue gate) for (i) immobilised α-CD3 and (ii) soluble α-CD3. (D) Representative dot plot for activation of stimulated CD3+ T lymphocytes expressing either CD69 and CD25 (lower quadrant), CD69 alone (upper left quadrant), CD69 and CD25 (upper right quadrant) or CD25 alone (lower right quadrant) at 0 hour.

Analysis of activation levels for CD3+ cells was then carried out using CD69 as an early activation marker against CD25 as a late activation marker. Exemplar dot plots showing the two activation markers for the differing culture times and incubation times are shown in **Figure 3.1.2.**

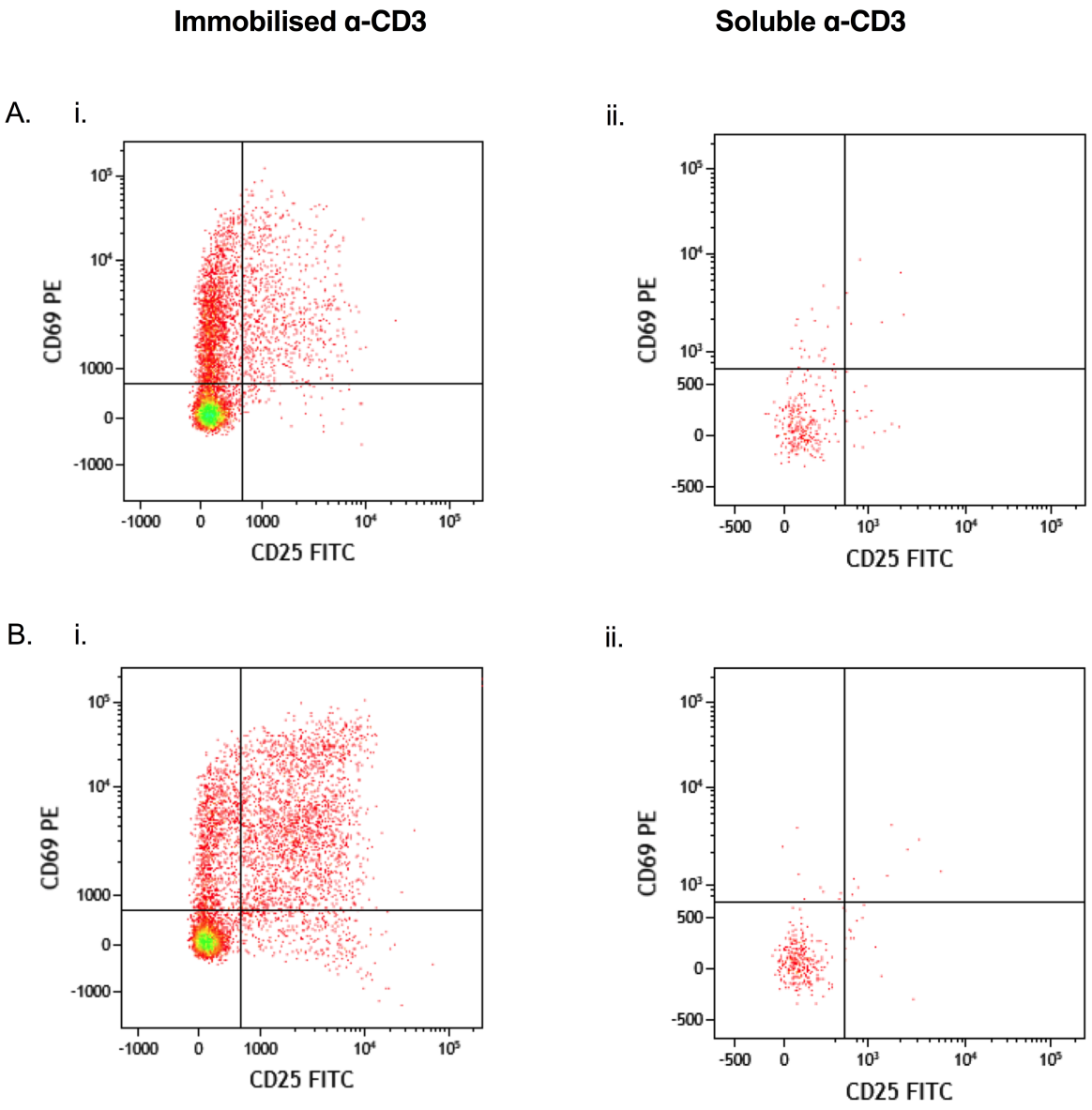

Figure 3.1.2. Activation of CD3+ T lymphocytes ex vivo (n=2). (A) Representative dot plots of activation of CD3+ T lymphocytes (A.i.-ii.) Immobilised vs soluble αCD3 at 24 hours; (B. i-ii) immobilised vs soluble αCD3 at 48 hours.

Gradual change of activation levels from early (CD69+CD25-) to mid (CD69+CD25+) to late (CD69-CD25+) activation can be noted over a 48-hour time period (**Figure 3.1.3.**). The data shows also that there was less activation from soluble α-CD3 at the 48-hour time period (**Figure 3.1.3.**).

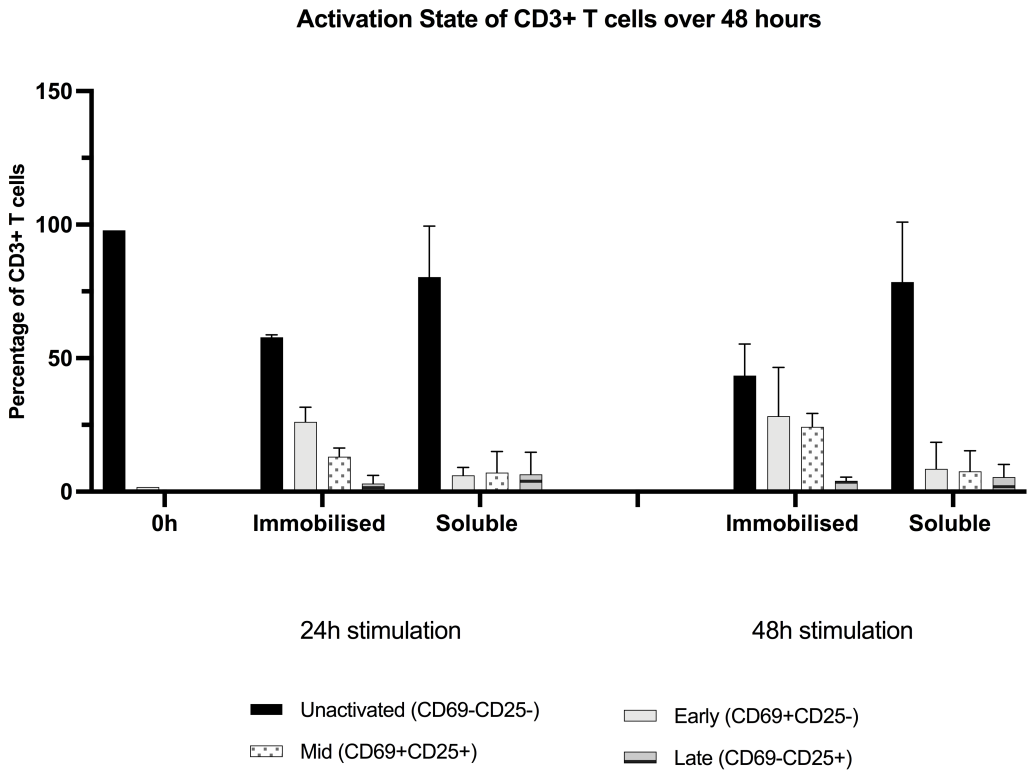

Figure 3.1.3. Activation of CD3+ T lymphocytes from peripheral blood ex vivo (n=2). Activation of CD3+ T lymphocytes in immobilised vs soluble α-CD3 was analysed over a 48-hour period.

As immobilised α-CD3 consistently caused higher levels of activation, two concentrations of immobilised α-CD3 were then tested (**Figure 3.1.4.A.i**.). Results show that there was very little difference in activation between 2μg/mL α-CD3 and 5μg/mL α-CD3 (**Figure 3.1.4.B.**). Therefore, based on the results, immobilised α-CD3 at 2μg/mL was chosen for future experiments to save on costs of buying α-CD3 for activation of cells.

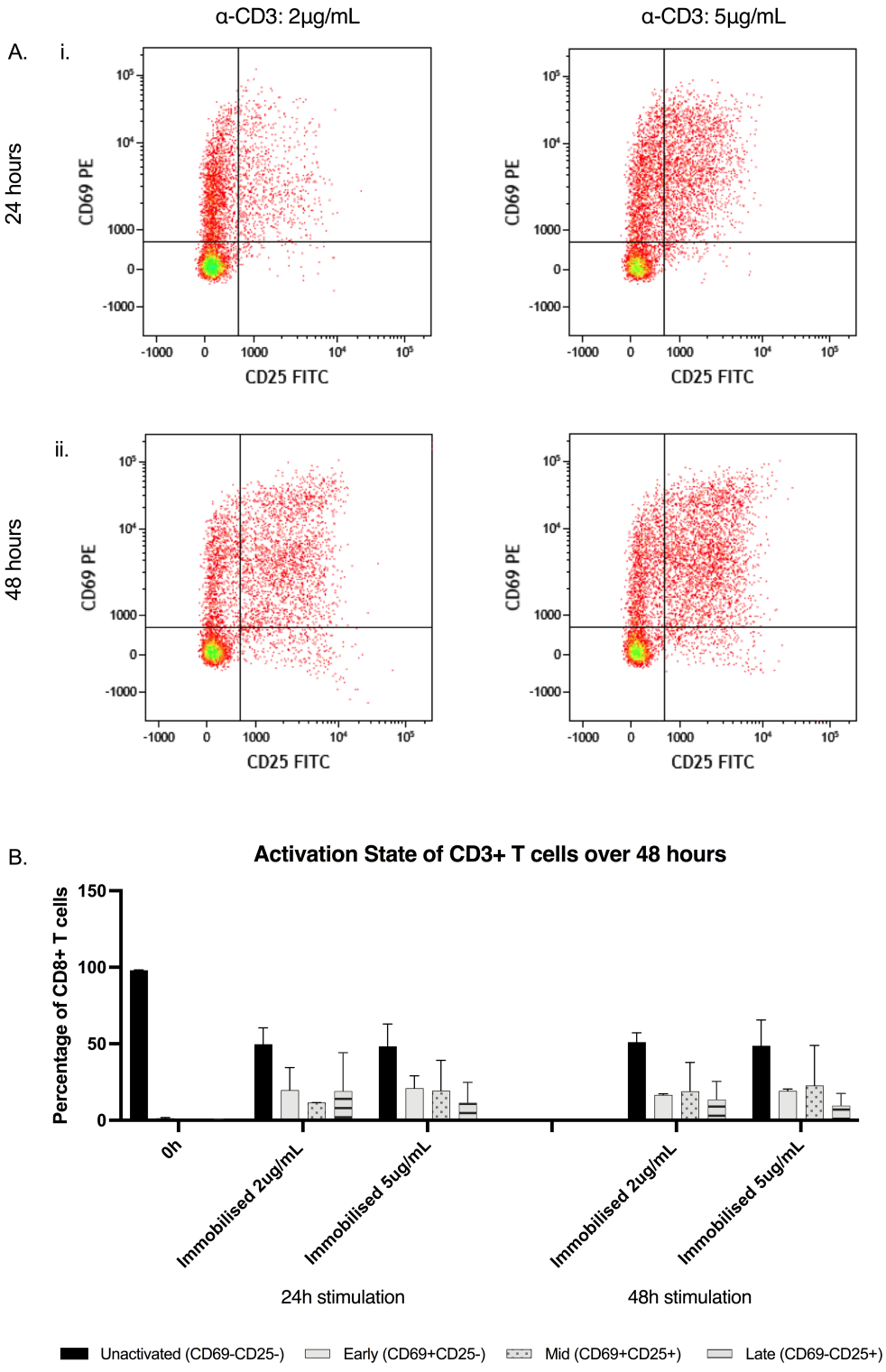

Figure 3.1.4. Activation of CD8+ T lymphocytes ex vivo (n=2). (A) Representative dot plots of activation of CD3+ lymphocytes stimulated with α-CD3 2µg/mL vs 5µg/mL at: (i) 24 hours; (ii) 48 hours. (B) Activation of CD3+ lymphocytes was analysed over a 48-hour period.

3.3.3. Serum-free media

According to MISEV guidelines, as FBS is known to contain EVs, a media without serum was to be used in order to obtain the optimal protocol for culturing cells to produce EVs without the presence of serum EVs. Cells harvested following PBMC isolation into RPMI 1640 were washed twice and re-suspended in 5 different cell culture mediums with a final cell concentration of 2 x 10^6/mL. Of the five mediums tested, three were serum free media, one was with EV-depleted FBS and the last was the medium with FBS (table 2.1.). Cells were then activated with α-CD3/α-CD-28 and cultured for 48 hours. Annexin V/ Propidium Iodide (PI) staining was also carried out at 0 hours and 48 hours for all mediums in order to determine the optimum serum-free or exosome-depleted media for maintaining cell viability.

To determine cell viability, first a dot plot of forward scatter (FCS) vs side scatter (SSC) was created to remove small debris. A second dot plot of Annexin-V vs PI was then created to assess cell viability at 0 hours **(Figure 3.1.5.A)** and after 48 hours in culture (**Figure 3.1.5.B.**). Results show that AIM-V had the highest and most consistent result in terms of viable cells after 48hours (**Figure 3.1.5.C.**). For the other mediums, results showed more variability. Therefore, future experiment would be done with cells harvested into AIM-V media.

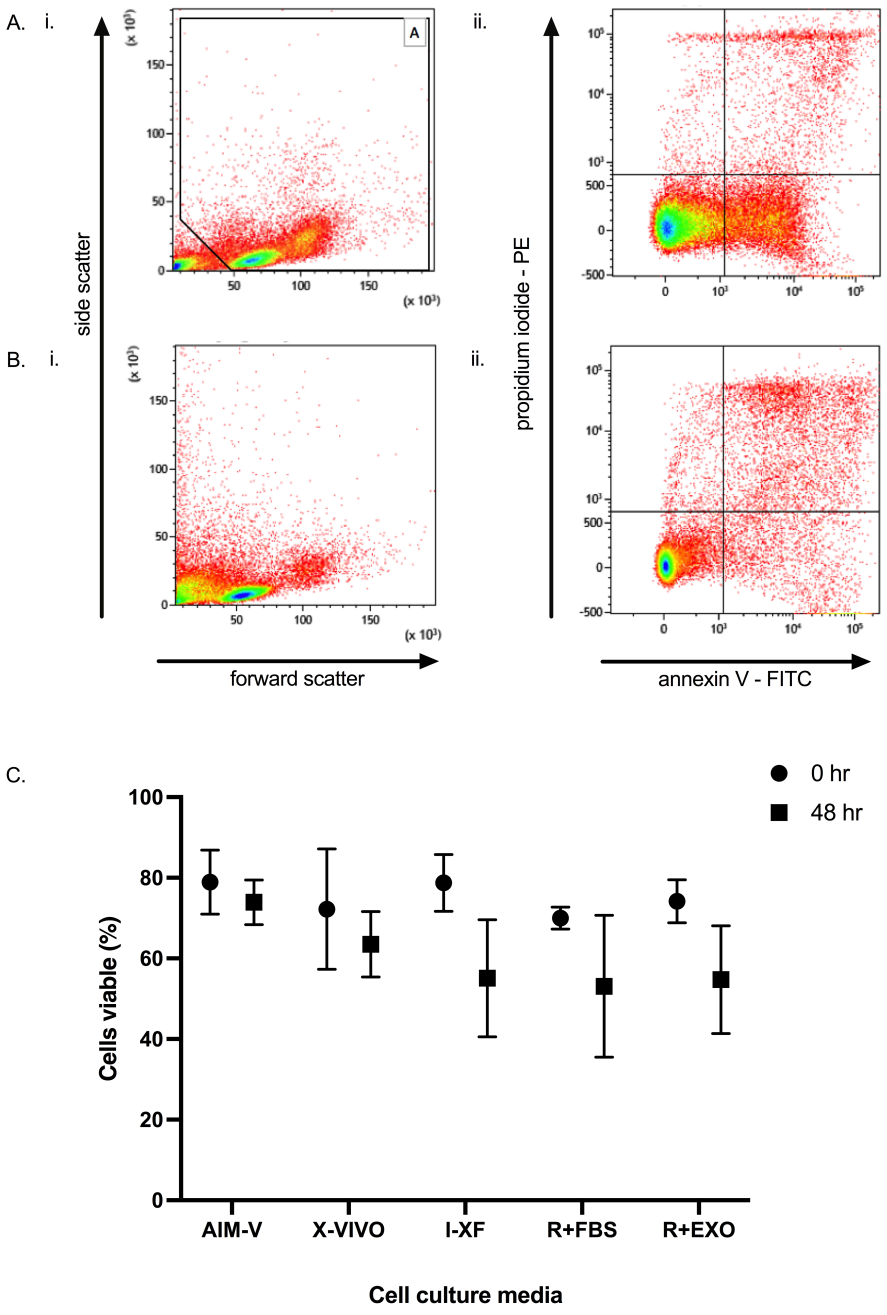

Figure 3.1.5. Annexin V/ Propidium Iodide (PI) analysis of PBMCs in cell culture media (n=3). Representative dot plot of cells in AIM-V media tested with Annexin V (FITC) and PI (PE) at: (A) 0hour and (B) 48hours. (A-B): (i) Initial gate on forward scatter vs side scatter (FCS vs SSC) to remove small debris; (ii) Annexin-V vs PI was plotted to analyse cell viability. (C) Percentage of cell viable based on AnnexinV/PI staining for each media at 0 hours and 48 hours. (I-XF: Immunocult-XF; R+FBS: RPMI 1640 + FBS; R+Exo: RPMI1640 + exosome-depleted FBS).

3.3.4. Imaging flow cytometry (IFC)

Imaging flow cytometry offers high speed single EV detection, enumeration and multiparametric characterisation. The IDEAS program used for EV analysis allows for mask features that can optimise EV analysis. First, fluorescently labelled nanobeads were analysed as reference standards (**Figure 3.1.6.A.i.**), a gate was then set to include all EVs below the 220nm nanobeads and were termed as 'small EVs' (containing exosomes and smaller microvesicles) (**Figure 3.1.6.A.ii.)**. To remove debris and co-incident events, image analysis by 'spot counting' was utilised (**Figure 3.1.6.B.i.)**. This spot count was set at zero, "0", and was done to select for no brightfield images at channel 01 or channel 09 (brightfield) to remove any coincident larger particles. Frames containing only a single calcein 'dot' were selected to remove any coincident or clumped EVs (**Figure 3.1.6.B.ii.**) and thus acts to prove that 'swarming' is not occurring. This was observed as one fluorescent dot in channel 02 (FITC) (**Figure 3.1.6.B.iii.**). Gates were applied to the final plot created that enabled an accurate EV/mL count to be made (**Figure 3.1.6.B.iv.**).

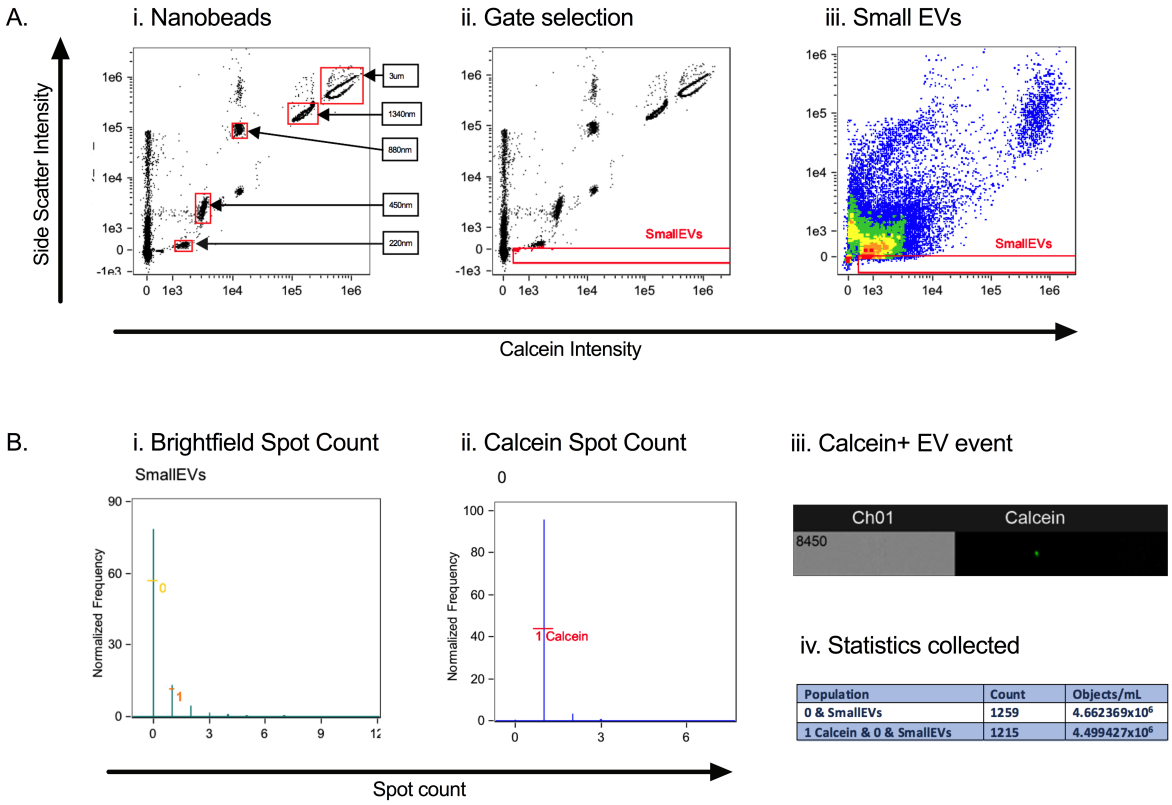

Population	Count	Objects/mL
0 & SmallEVs	1259	4.662369×10^6
1 Calcein & 0 & SmallEVs	1215	4.499427×10^6

Figure 3.1.6. Characterisation of EVs by IFC and calcein dilutions. (A) Setting gates for small EVs analysis with calcein intensity vs side scatter: (i) nanobeads for reference of size with smallest beads at 220nm; (ii) small EVs gate created below 220nm; (iii) small EVs gate copied over to cell culture sample collected for further gating. (B) Collecting events of small EVs: (i) Spot count get set at 0 for brightfield Channel 09; (ii) Spot count for Calcein Channel 02 set at 1 for single small EVs events; (iii) Calcein+ EV with no brightfield image; (iv) Statistics collected from gated EV population.

3.3.5. Calcein concentration

To determine the appropriate concentration of calcein for EV analysis, dilutions of calcein for staining of EVs were tested. To obtain the optimal concentration of calcein for analysis on ImageStreamX (ISX), four dilutions of calcein were initially tested: 1:100, 1:200, 1:400 and 1:800 in two mediums, RPMI+FBS and serum-free AIM-V media. Results show that as the concentration of calcein decreased the number of EVs observed decreased for both media (**Figure 3.1.7.A.**). In addition, calcein at 1:100 had more than triple the EVs/mL than calcein at 1:200. From these results, it was decided

that further dilutions of calcein needed to be investigated, with more concentrated dilutions added to testing.

Additionally, at this point of experiments, 3 other mediums were added to obtain the optimum media for EV experiments as previously described in section 3.1.3.3. A higher concentration of calcein (1:50 dilution) was included to observe the EV count in the five mediums. Results show that higher concentration of calcein, i.e. 1:50, had higher EV count (EVs/mL) for each media (**Figure 3.1.7.B.**). However, in the analysis of Calcein at 1:50 dilution there were more issues with compensation of the files and with spill over of Calcein into adjacent channels. As a result, Calcein 1:100 was selected as the optimum dilution for analysis of EVs using IFC.

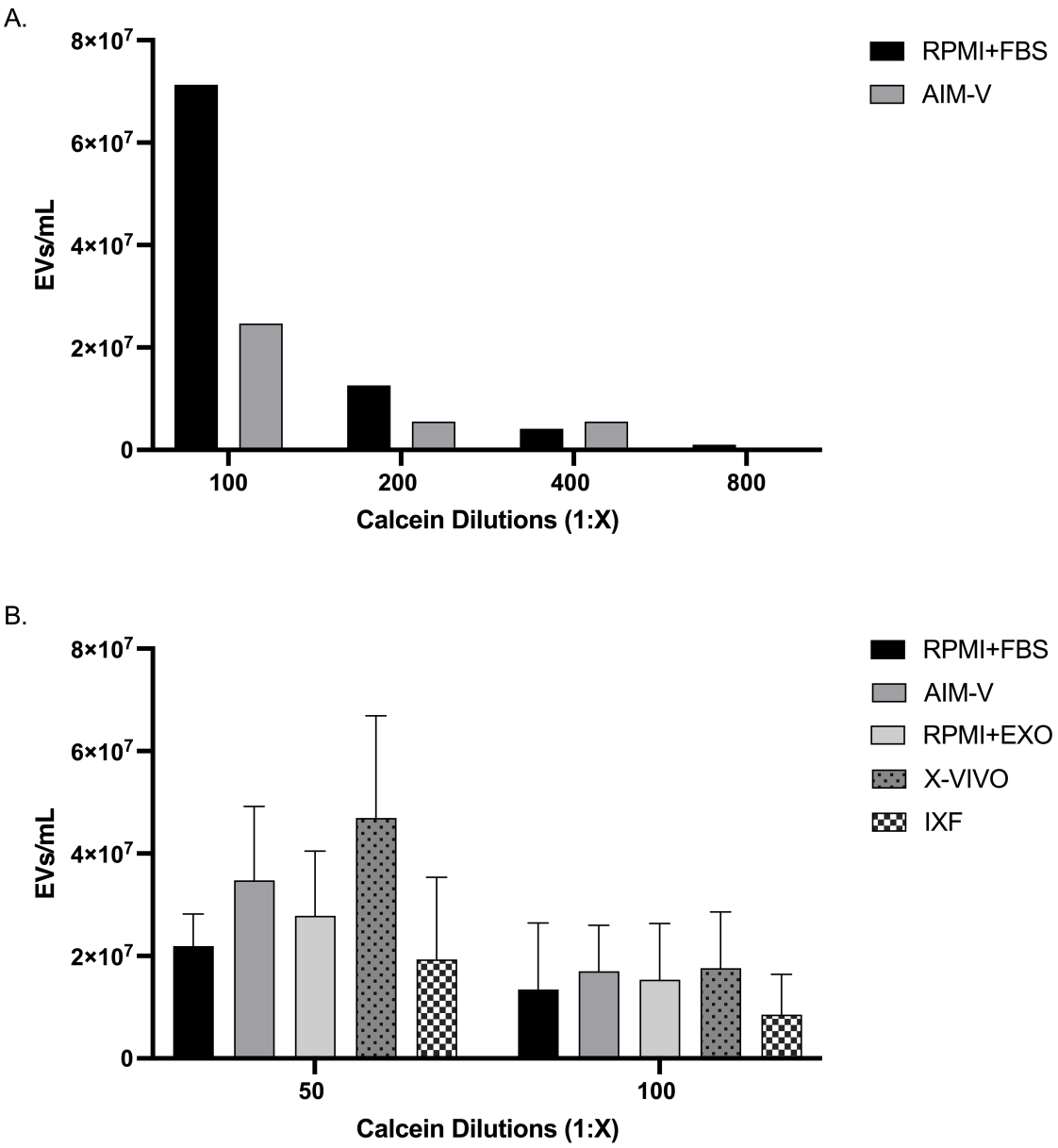

Figure 3.1.7. Calcein concentrations. EV count (EVs/mL) observed for each calcein dilution ranging from (A) 1:100 to 1:800 (n = 1 biological repeat); and (B) 1:50 to 1:100 (n = 3 biological repeats). (R+FBS: RPMI 1640 + FBS; R+Exo: RPMI1640 + exosome-depleted FBS; I-XF: Immunocult-XF).

3.3.6. Detergent control

Detergents are included to determine whether detected events are membrane-enclosed vesicles or other protein complexes. Treatment with detergent will lyse membrane-enclose vesicles, therefore reducing their number and signal. Protein complexes, however, will persist following detergent lysis. Here, two detergents were tested at two final concentrations: Tween20 at 5% and 10%, and TritonX-100 at 0.075% and 0.1%, as recommended by Osteikoetxea et al [434], to investigated various concentrations of detergents to find an optimal detergent concentration for lysing EV subpopulations. This experiment was repeated three times and EVs were gated as previously described (section 3.1.3.4.) to create a final plot and measure EVs in samples with Tween 20 at 5% and 10% (**Figure 3.1.8.A.**) and with Triton-X at 0.075% and 0.1% (**Figure 3.1.8.B.**). Results show that Tween 20 at 10% had the lowest number of EVs/mL, followed by Tween 20 at 5% (**Figure 3.1.8.C.**). Triton-X at both 0.075% and 0.1% had higher counts of EVs/mL and additionally, had higher variation in results. Therefore, future experiments were done using Tween 20 at 10% as the detergent control.

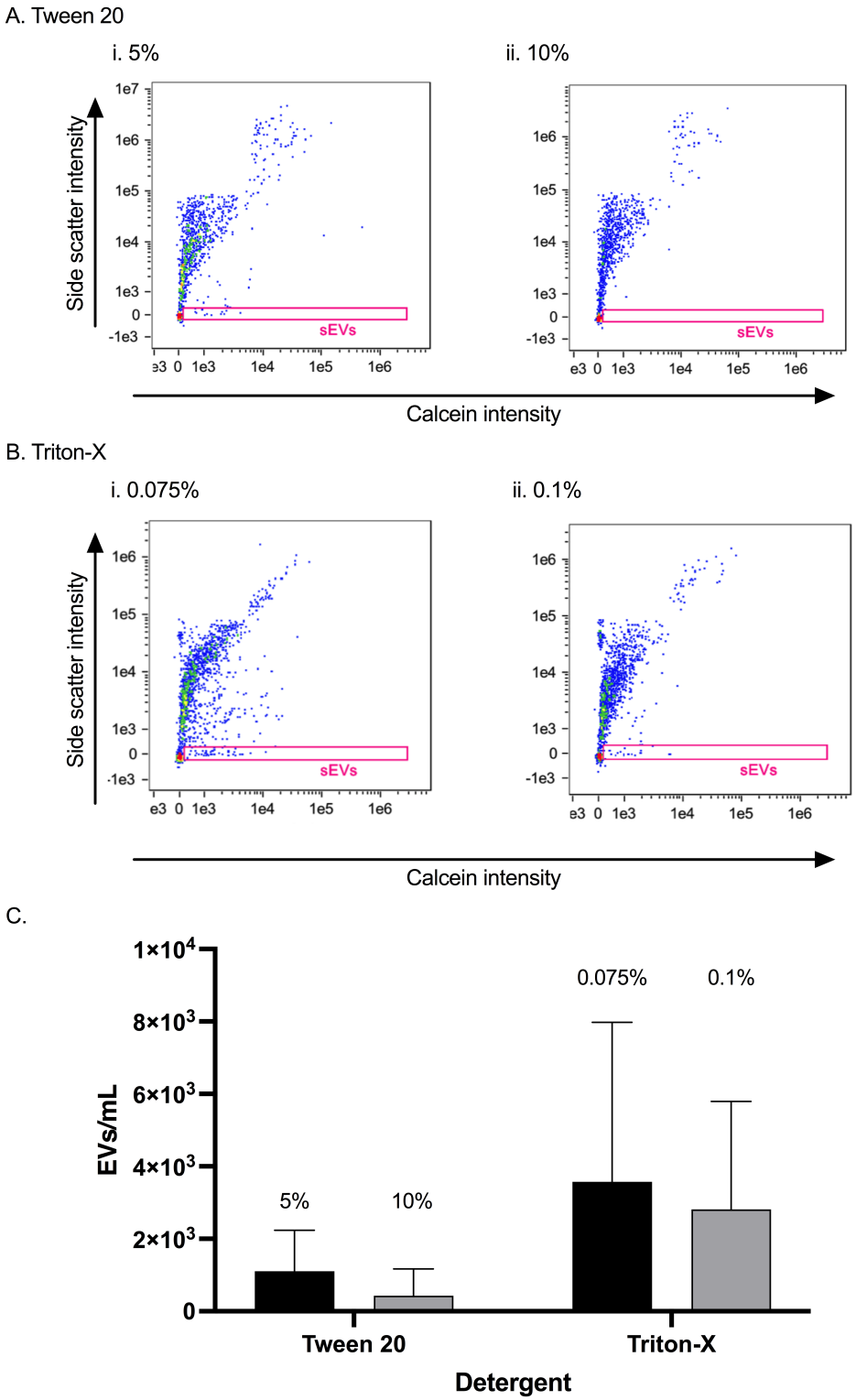

Figure 3.1.8. Detergent control in EV experiments (n=3 biological repeats). Representative images for analysis of detergents: (A) Tween 20 at (i) 5% and (ii) 10%; and (B) Triton-X at (i) 0.075% and (ii) 0.1%. (C) EV count (EVs/mL) for each detergent at each concentration.

3.3.7. Controls for study of EVs

In line with the MISEV 2018 guidelines and the MIFlowCyt-EV framework for standardized reporting of EV flow cytometry experiments, further controls were set for EV experiments. This includes samples stained with calcein or no calcein, a media only control stained with calcein, and the use of a detergent. Therefore, EVs were stained with calcein (**Figure 3.1.9.i.**) or no calcein (**Figure 3.1.9.ii.**), showing EVs were only present in the gate with calcein stained samples. A media only control stained with calcein (**Figure 3.1.9.iii.**) also showed no EVs, and through the addition of 10% Tween-20 detergent to EV samples, it was shown that EV count reduced indicating the material was indeed vesicular in nature (**Figure 3.1.9.iv.**).

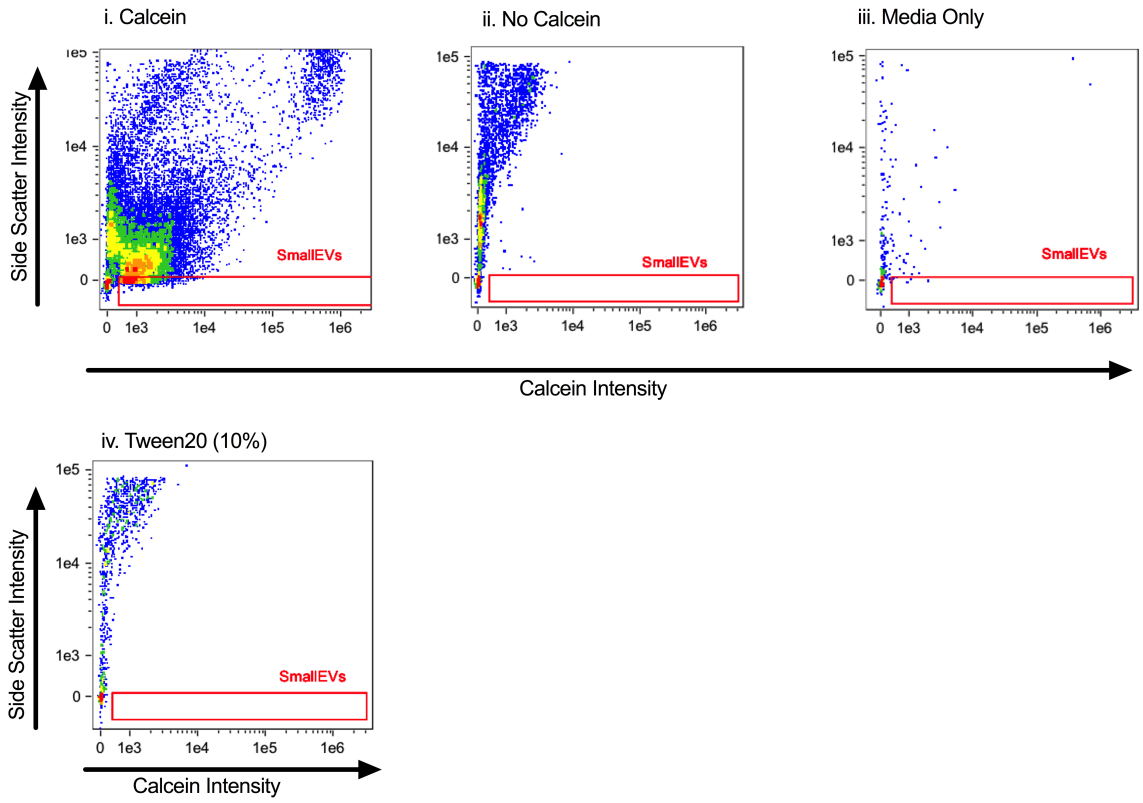

Figure 3.1.9. Controls for EV experiments. Representative images for controls for analysis of EVs: (i) calcein-stained sample; (ii) unstained sample; (iii) calcein-stained AIM-V media only sample; (iv) calcein-stained sample with 10% Tween 20 added (detergent).

The experiments with all controls were repeated 3 times and showed a significant difference in sEVs/mL between the calcein-stained samples and the three controls (**Figure 3.1.10.**) (one-way ANOVA; p = 0.0210). Dunnett's multiple comparison post-hoc analyses showed significant differences between calcein-stained experimental group and no calcein (p = 0.0233), media only (p = 0230) and Tween20 (p = 0.0232) groups.

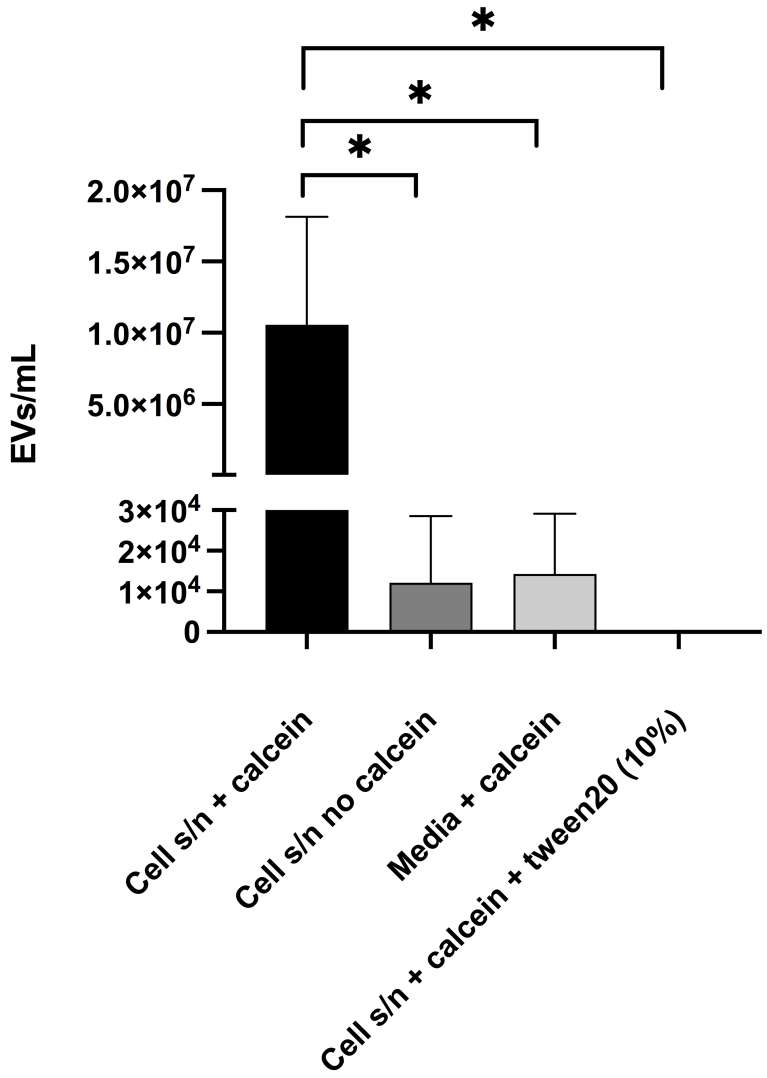

Figure 3.1.10. Controls for EV experiments. Significantly more EVs/mL in the calcein-stained sample compared with unstained sample and calcein-stained media only and detergent added samples (n=3 biological repeats). Data are expressed as mean ± SD. One-way ANOVA, *p<0.05. Dunnett's post-hoc analyses indicated that significantly more particles in calcein-stained experimental compared to no calcein (p = 0.0233), media only (p = 0.0230), Tween20 (p = 0.0232).

3.3.8. Analysis of PBMC-derived EVs by nano-flow cytometry (nFCM)

nFCM was used to analyse fractions obtained from isolation of EVs using SEC. In nFCM, particle size is estimated by measuring the intensity of forward-scattered (FSC) and side-scattered (SSC) light in the flow of individual particles focused by the sheath flow [406]. EVs were isolated from cell supernatant by size exclusion chromatography, where 10 fractions were obtained. Fractions 1-10 were then analysed individually by nFCM to determine fractions that would be pooled for subsequent EV analysis. Size distribution profiles were obtained for each fraction (**Figure 3.1.11.**).

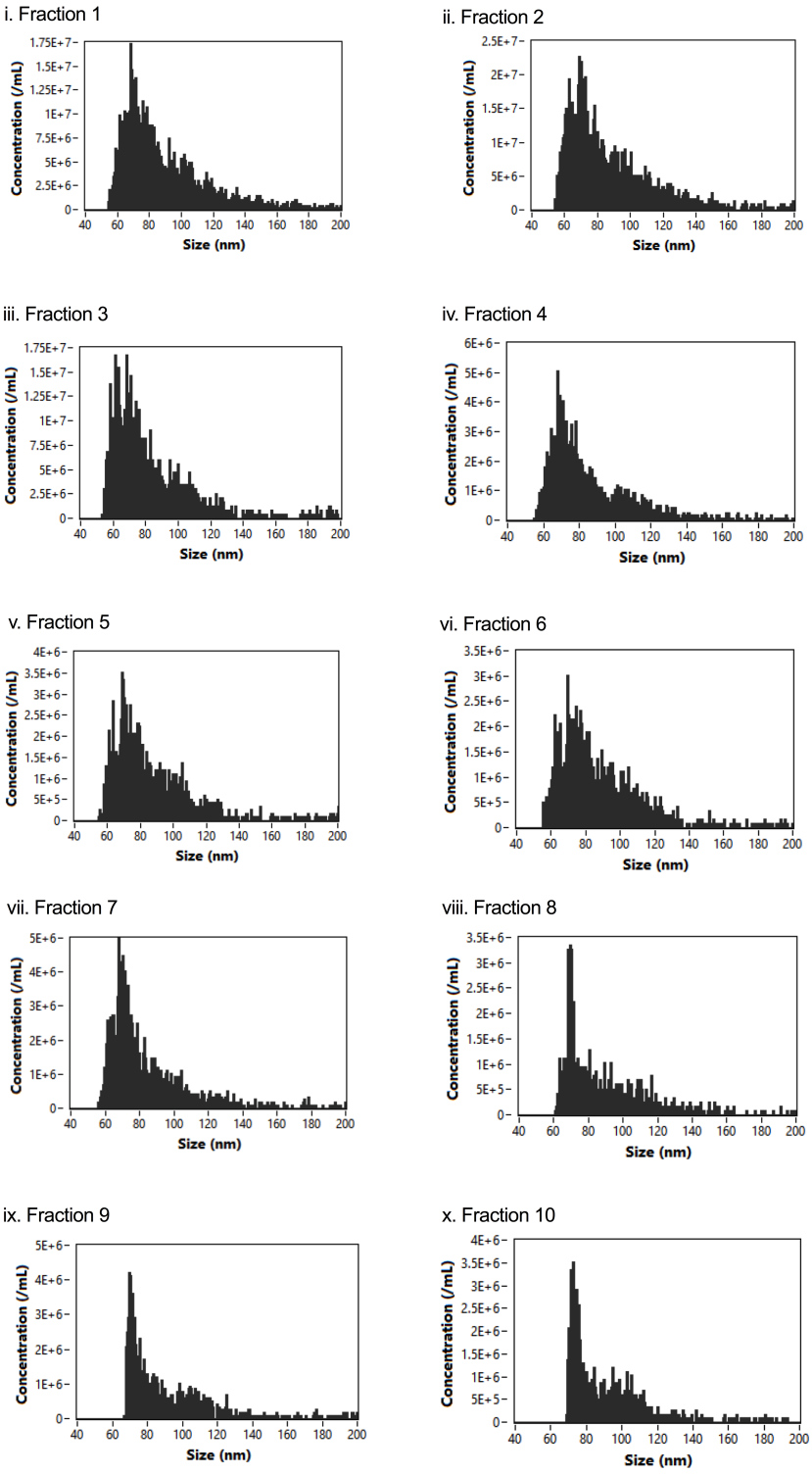

Figure 3.1.11. Analysis of EVs by nFCM. Size distribution profiles for PBMC-derived EVs isolated by SEC. (i-x) Fractions 1-10 were measured by nFCM individually to determine size range and concentration of each fraction. Each histogram is taken from the PDFs generated for the measurements.

In this study, we used the qEV 35nm column which primarily isolates small EVs. According the manufacturer's qEV instructions manual, most EVs should elute in fractions 1-4. nFCM analysis show that mean and median size (nm) of particles all fractions were less than 100nm (**Figure 3.1.12.A.**) and highest concentrations were found in fractions 1-3, with lower concentrations in fractions 4-10 (**Figure 3.1.12.B.**). Fractions 1-5 were selected for subsequent EV analysis to ensure all EVs were included in the study.

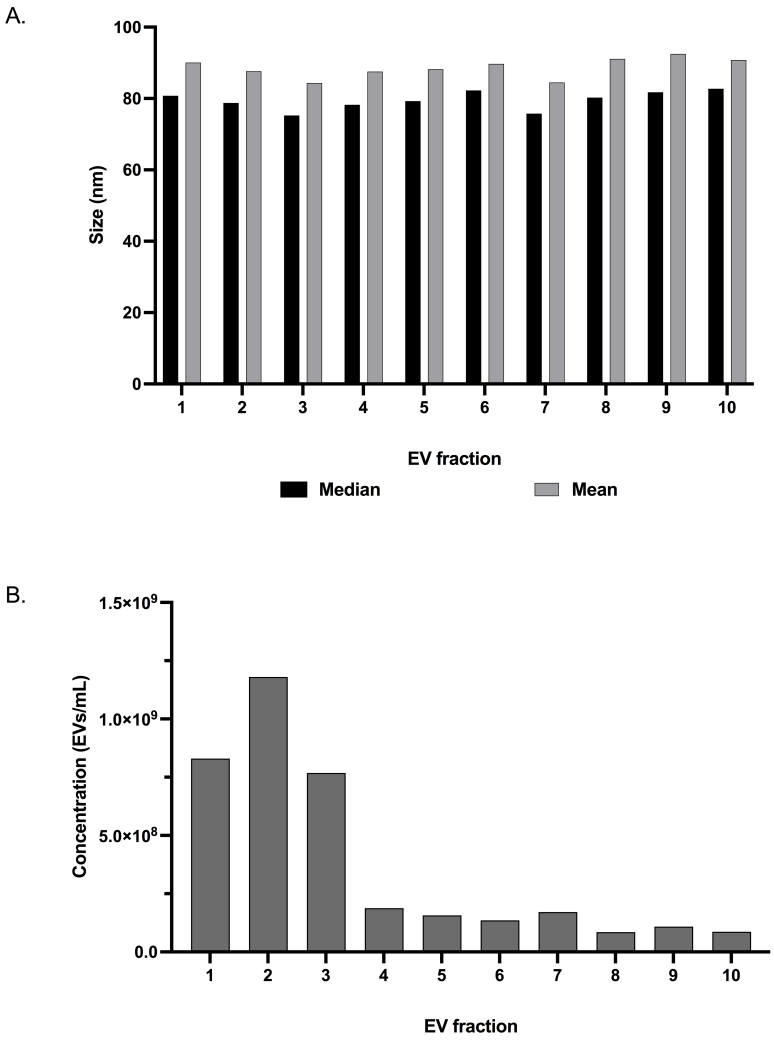

Figure 3.1.12. Analysis of EVs by nFCM. (A) Median and mean size of particles for fractions 1-10. (B) Concentration of particles (EVs/mL) for fractions 1-10. (n = 1 biological repeat)

3.3.9. Analysis of PBMC-derived EVs by conventional transmission electron microscopy (TEM) and nanoparticle tracking analysis (NTA)

To confirm the structure and morphology of EVs released from PBMCs, TEM was performed. Vesicles were isolated from α-CD3/α-CD28 stimulated PBMCs cultured for 48 hours by size exclusion chromatography (SEC) and fractions 1-5 were combined for analysis. Isolated vesicles were then examined by TEM. Calcein-stained vesicles were homogenously spherical, cup-shaped, membrane-enclosed particles consistent with the morphology of EVs (**Figure 3.1.13.A.**). To analyse the size distribution of isolated PBMC-derived EVs, measurements using Nanosight LM10/14 (NTA) was performed. The size distribution obtained by NTA showed that most EVs were under 200 nm in size with a mode of 128 nm (**Figure 3.1.13.B.**).

A.

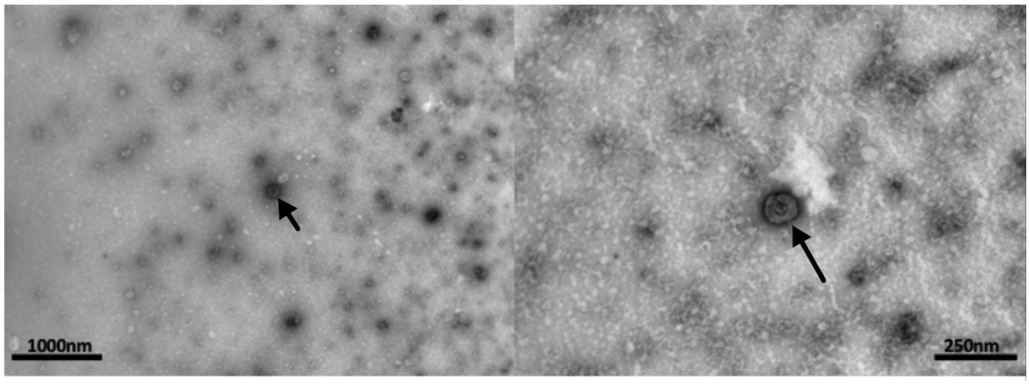

B.

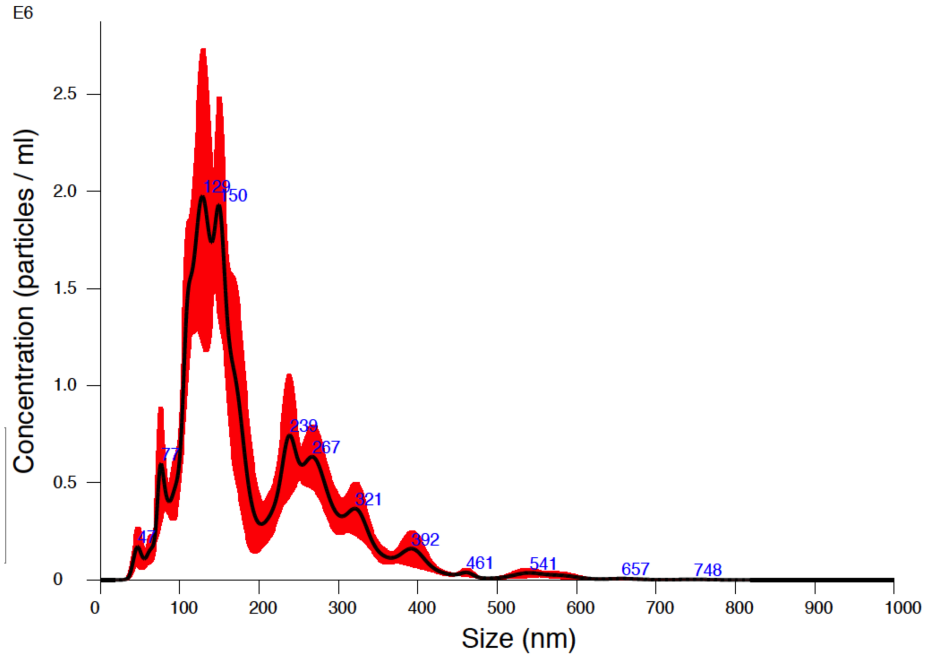

Figure 3.1.13. EV characterisation by TEM, NTA and nFCM. (A) Exemplar transmission electron micrographs of isolated calcien-stained EVs from α-CD3/α-CD28 stimulated PBMCs (11500-63100X). (B) Size distribution of isolated calcien-stained EV population by NTA for 2 biological repeats, 5 technical repeats.

3.3.10. Proteomic analysis of PBMC-derived EVs

To confirm the source of vesicles, proteomic analysis of isolated samples (fractions 1-5) was carried out by mass spectrometry. The unique peptides identified in the isolated EV samples were mapped to the relevant proteins. These data were then integrated to look for protein signatures that have been associated with different vesicle types. Proteins not present in EV samples were listed as not detected. Of the proteins detected, 25 have commonly been reported as associated with EVs [327, 435, 436], 2 proteins usually associated with being part of lysosomes and/or EVs [437], and 1 protein associated with peroxisomes and/or EVs [438], suggesting the isolated EVs did not include intracellular vesicles . Exocarta (www.exocarta.org/ [439]), PeroxisomeDB (www.peroxisomedb.org/ [440]), The Human Lysosome Gene Database (hLGDB) (http://lysosome.unipg.it/ [441]), and Autophagy database (www.tanpaku.org/autophagy/) are databases that were used to search if proteins identified are present in EVs, peroxisomes, lysosomes, and autophagosomes, respectively.

Table 3.1.5. Proteins identified in PBMC-derived EV fractions. The unique peptides identified in the isolated EV samples were mapped to the relevant proteins. These data were then integrated to look for protein signatures that have been associated with different vesicle types. Proteins not present in EV samples were listed as not detected. Of the proteins detected, 25 have commonly been reported as associated with EVs [327, 435, 436], 2 proteins usually associated with being part of lysosomes and/or EVs [437], and 1 protein associated with peroxisomes [438].

Protein	**Unique Peptides Identified**	**Vesicle Type***
ACOX1	Not Detected	Peroxisome
ACOT8	Not Detected	Peroxisome
ATG7	Not Detected	Peroxisome
ATG12	Not Detected	Peroxisome
BAAT	Not Detected	Peroxisome
FOXP2	Not Detected	Peroxisome, EV
FOXP3	Not Detected	Peroxisome
HMGCL	Not Detected	Peroxisome
MAVS	Not Detected	Peroxisome, EV
MUL1	Not Detected	Peroxisome
PEX3	Not Detected	Peroxisome, EV
PEX5	Not Detected	Peroxisome
PEX14	Not Detected	Peroxisome
PEX19	Not Detected	Peroxisome
PEX26	Not Detected	Peroxisome
PMP70	Not Detected	Peroxisome
SLC25A17	Not Detected	Peroxisome
SLC27A2	Not Detected	Peroxisome
ATG5	Not Detected	Lysosome
ATG12	Not Detected	Lysosome
ATG6	Not Detected	Lysosome
CD34	Not Detected	Lysosome

CD68	Not Detected	Lysosome, EV
IGF2R	Not Detected	Lysosome, EV
LAMP1	Not Detected	Lysosome
LC3B	Not Detected	Lysosome
MPO	Not Detected	Lysosome
PAK1	Not Detected	Lysosome
PDGFRB	Not Detected	Lysosome
RAB9A	Not Detected	Lysosome
Ovalbumin	Not Detected	Lysosome
TLR3	Not Detected	Lysosome
TLR7	Not Detected	Lysosome
ULK1	Not Detected	Autophagasomes
ATG5	Not Detected	Autophagasomes
ATG6	Not Detected	Autophagasomes
ATG7	Not Detected	Autophagasomes
ATG9A	Not Detected	Autophagasomes
ATG10	Not Detected	Autophagasomes
ATG12	Not Detected	Autophagasomes
ATG13	Not Detected	Autophagasomes
ATG14	Not Detected	Autophagasomes
AGT16L1	Not Detected	Autophagasomes
LC3A	Not Detected	Autophagasomes
LC3B	Not Detected	Autophagasomes
mTOR	Not Detected	Autophagasomes
NUP62	Not Detected	Autophagasomes
RAB11A	Not Detected	Autophagasomes
WIPI1	Not Detected	Autophagasomes
CD63	Not Detected	Lysosome, EV

DNM1L	RLEEPSLR SSVLESLVGR GVSPEPIHLK LDLMDAGTDAMDVLM GR SSLLDDLLTESEDMAQR TLESVDPLGGLNTIDILTA IR	Peroxisome, EV
LAMP2	SHTALLR IPLNDLFR GILTVDELL AIR	Lysosome, EV
CXCR4	TSAQHALTSVSR	Lysosome, EV
CD9	DVLETFT VK KDVLETF TVK KDVLETF TVK	EV
CD59	FEHCNFNDV TTR LRENELTYYC CK	EV
CD47	IEVSQL LK EGETIIE LK	EV
GNA13	IIHGQDFDQ R	EV
GNA14	LLLLGTGESGK	EV
GNAI1	MFDVGGQR LFDSICNNK TTGIVETHFTFK EIYTHFTCATD TK	EV
GNAI2	MFDVGGQR LFDSICNNK YDEAASYIQSK TTGIVETHFTFK AMGNLQIDFADPSR EIYTHFTCATDTK IAQSDYIPTQQDVLR	EV

	EYQLNDSAAYYLNDLER QLFALSCTAEEQGVLPDDLSG VIR	
GNAI3	MFDVGGQR LFDSICNNK TTGIVETHFTFK EIYTHFTCATDTK ISQSNYIPTQQDV LR	EV
GNAL	LLLLGAGESGK	EV
GNAO1	TTGIVETHFTF K	EV
GNAQ	AHAQLVR VADPAYLPTQQDV LR SLWNDPGIQECYD R	EV
GNAS	IEDYFPEFA R	EV
GNAT3	MFDVGGQR	EV
GNAZ	IAAADYIPTVEDILR	EV
HLA-A	SWTAADMAAQITK WAAVVVPSGEEQR FIAVGYVDDTQFVR THMTHHPISDHEATLR DGEDQTQDTELVETRPAGDGTF QK	EV
HLA-B	WAAVVVPSGEEQR SWTAADTAAQITQ R APWIEQEGPEYWD R THVTHHPISDHEAT LR	EV
HLA-C	AYLEGTCVEWLR SWTAADTAAQITQR THVTHHPLSDHEATLR DGEDQTQDTELVETRPAGDGTF QK	EV
ITGA2	KLAEVGR VAIVVGAPR	EV

	AEYSPCR SCVLPQTK IVLLDVPVR ALSNVEGFER NVGSQTLQTFK VVLCELGNPMK EQNSLDSWGPK LSLNAELQLDR FGSAIAPLGDLDR IYVENDFSWDK AEGGQCPSLLFDLR HDLLVGAPLYMESR TPVGSCFLAQPESGR HDLLVGAPLYMESR ASVQLLVQDSLNPAVK GNSFPASLVVAAEEGER DGYNDIAVAAPYGGPSGR TLGPSQEETGGVFLCPWR TEEAEKTPVGSCFLAQPESGR GEQMASYFGHSVAVTDVNGDGR GAVDIDDNGYPDLIVGAYGANQVAVYR GNSFPASLVVAAEEGEREQNSLDSWGP K LQDPVLVSCDSAPCTVVQCDLQEMAR FGSAIAPLGDLDRDGYNDIAVAAPYGGP SGR	
ITGA4	SQHTTEVVGGAPQHEQIGK	EV
ITGA6	TAHIDVHFLK	EV
ITGA8	LTVYSGPK	EV
ITGAL	GHAVVGAV GAK DWAGGFLD LK	EV
ITGB1	NVLSLTNK IGFGSFVEK GEVFNELVGK SGEPQTFTLK SLGTDLMNEMR FCECDNFNCDR DKLPQPVQPDPVSHCK	EV

	FQGQTCEMCQTCLGVCAE HK	
ITGB2	CHLEDNLYK VTYDSFCSNGVTHR SNEFDYPSVGQLAH K CHPGFEGSACQCER ECIESGPGCTWCQK LLVFATDDGFHFAG DGK GDCDGVQINVPITF QVK	EV
ITGB3	THIALDGR VLEDRPLSDK TTCLPMFGYK WDTANNPLYK FQYYEDSSGK IGDTVSFSIEAK HVLTLTDQVTR GALHDENTCNR YCRDEIESVK CPTCPDACTFK DDLWSIQNLGTK EATSTFTNITYR YCECDDFSCVR NDASHLLVFTTDAK TDTCMSSNGLLCSGR DNCAPESIEFPVSEAR GECLCGQCVCHSSDFGK DAPEGGFDAIMQATVCDEK CECGSCVCIQPGSYGDTCEK DSLIVQVTFDCDCACQAQAEPNSHR CGPGWLGSQCECSEEDYRPSQQDECSPR LAGIVQPNDGQCHVGSDNHYSASTTMDYPSLGL MTEK	EV

** Vesicle type for which protein is commonly found. It should be noted that each protein can be found a number of vesicle types and in other organelles.*

As two samples were provided for proteomic analysis, the proteins identified within each sample were then compared between two samples (sample 15 and sample 16) provided (**Figure 3.1.14.**). In Sample 15, 55 proteins were identified in the screen. In Sample 16, 1,324 proteins were identified. Between the two samples 49 were in common (89% of sample 15 and 3.7% of sample 16). This is likely due to the low number of unique proteins detected in sample 15.

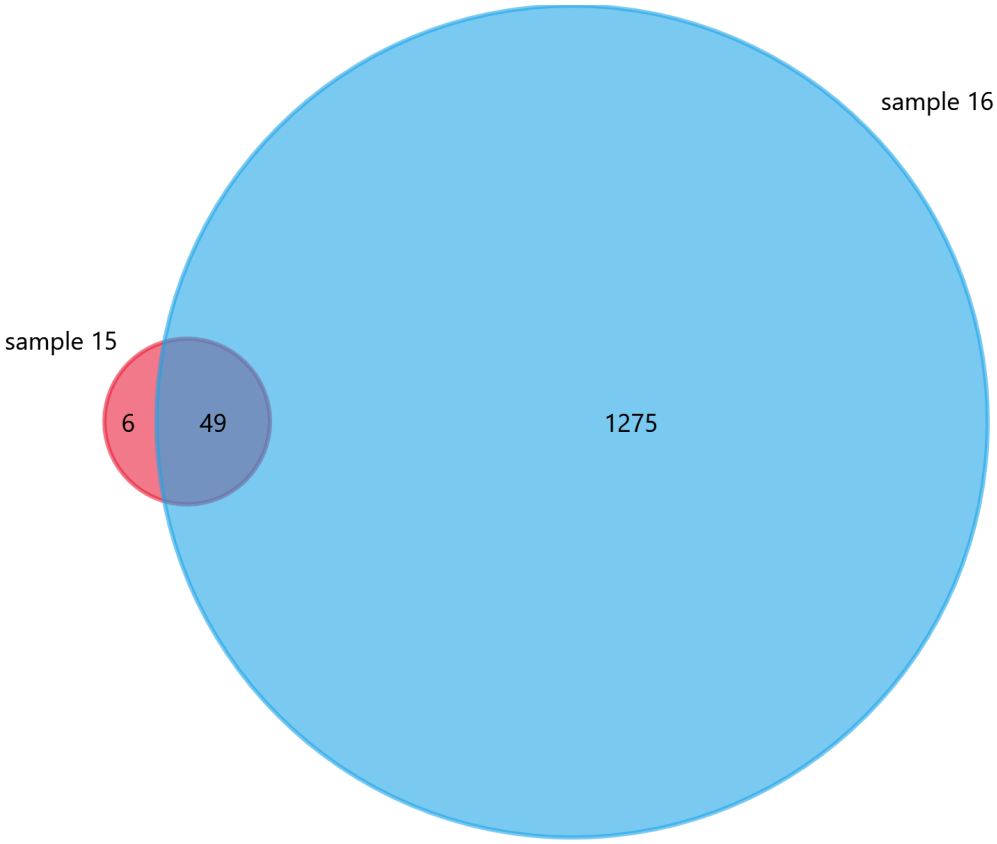

Figure 3.1.14. Comparison of proteins identified within each sample. Fifty-five proteins were identified in sample 15 compared to1,324 proteins in sample 16. Between the two samples 49 proteins were in common (89% of sample 15 and 3.7% of sample 16). (n = 2 technical repeats)

3.3.11. Characterisation of tetraspanin content of EVs

MISEV 2018 guidelines also recommend characterisation of EVs by testing for presence of components associated with EVs [399]. Imaging flow cytometry was used to quantify the amount of EV associated tetraspanins within the calcein labelled PBMC supernatants. EVs were gated as before (**Figure 3.1.15.A.**) and any out of focus events removed (**Figure 3.1.15.B.**) before the application of a sequential set of gates to identify EVs expressing one, two, or three tetraspanins. The gating strategy to identify tetraspanin expression on EVs is shown **Figure 12C-12E**. To set the cut-off for tetraspanin positive EVs, a sample stained only with calcein was analysed and used to set the gate for CD9, CD63, CD81 positivity (**Figure 3.1.15.C.**). Samples stained with calcein and one α-tetraspanin antibody showed the EVs to contain CD9, CD63 or CD81 (**Figure 3.1.15.D. i-iii**). Labelling EVs with multiple antibodies could possibly lead to reduced sensitivity due to steric hindrance around these small vesicles. We therefore tried staining with two or three simultaneous α-tetraspanin antibodies in comparison to the single stained EVs. Two tetraspanins (CD81 and CD9) were then plotted against each other to identify double positive EVs (**Figure 3.1.15.E.**). The gates were set using Fluorescence minus One (FMO) controls used in conventional flow cytometry. The double positive population was then selected and EVs plotted against the final tetraspanin (CD63) to show EVs that were positive for all three tetraspanins **(Figure 3.1.15.F.)**.

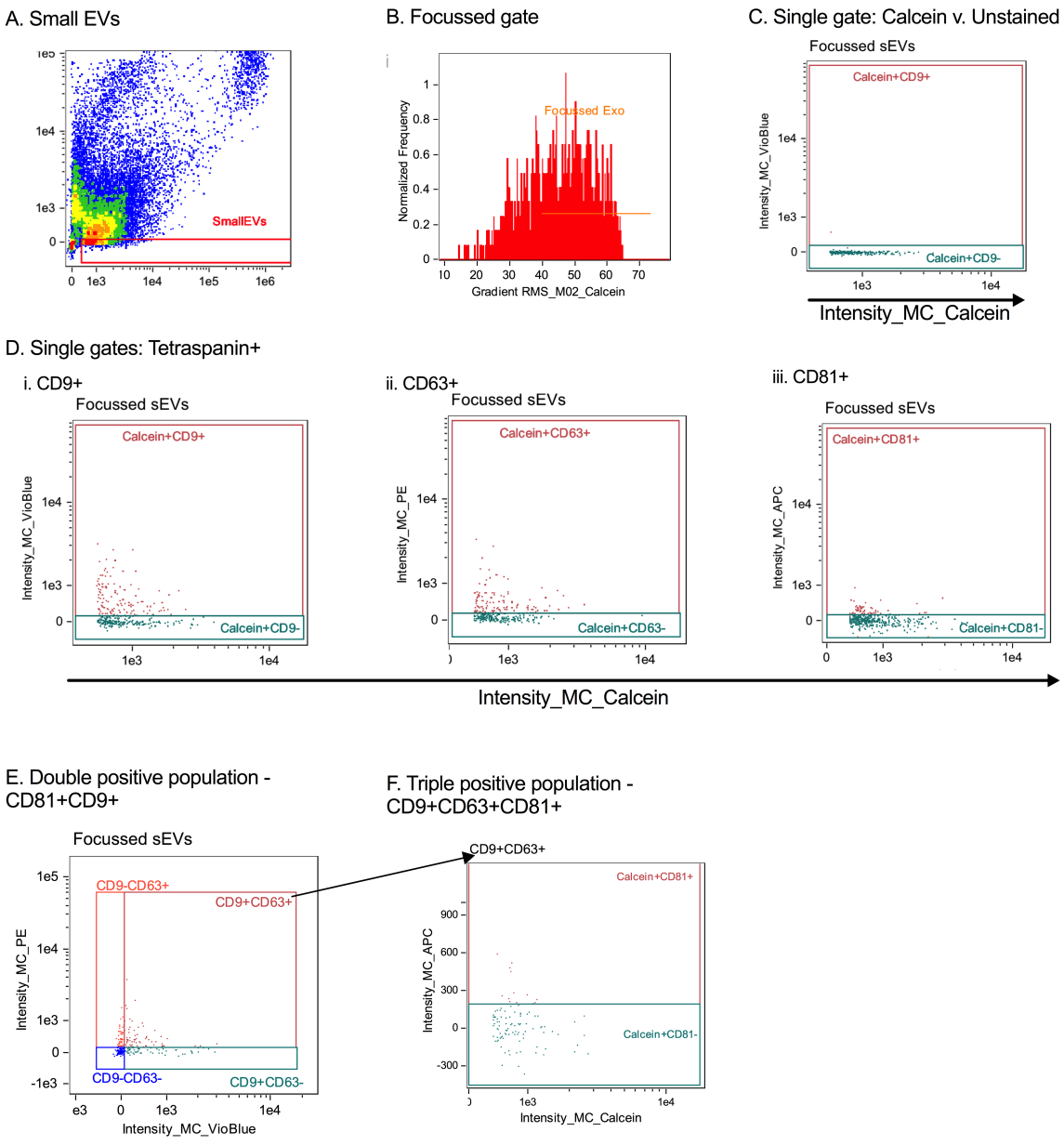

Figure 3.1.15. Tetraspanins CD9, CD63 and CD81 in analysis of small EVs by IFC. (A) Small EV gate for small EVs analysis with Calcein intensity vs side scatter. (B) Focussed check feature was created using gradient RMS for Calcein to remove any artefactual fluorescence when gating tetraspanin data where multiple antibodies were used simultaneously. (C) Representative plot of calcein vs tetraspanins using samples stained with calcein only to create gates for calcein+ tetraspanins+ EVs. (D) Representative plots of calcein+ tetraspanin+ EVs for (i) CD9; (ii) CD63; (iii) CD81. (E) Representative plots for double tetraspanin+ gates created using samples stained with one tetraspanins only (single colours). (F) Double positive population from E selected for plot gating for triple tetraspanins-positive events.

Results showed that single, double or triple staining did not significantly reduce the sensitivity of any of the three markers **(Figure 3.1.16.A.)**. Triple α-tetraspanin staining of the calcein labelled PBMC supernatants revealed that most EVs to contain at least one tetraspanins on their surface (**Figure 3.1.16.B.**).

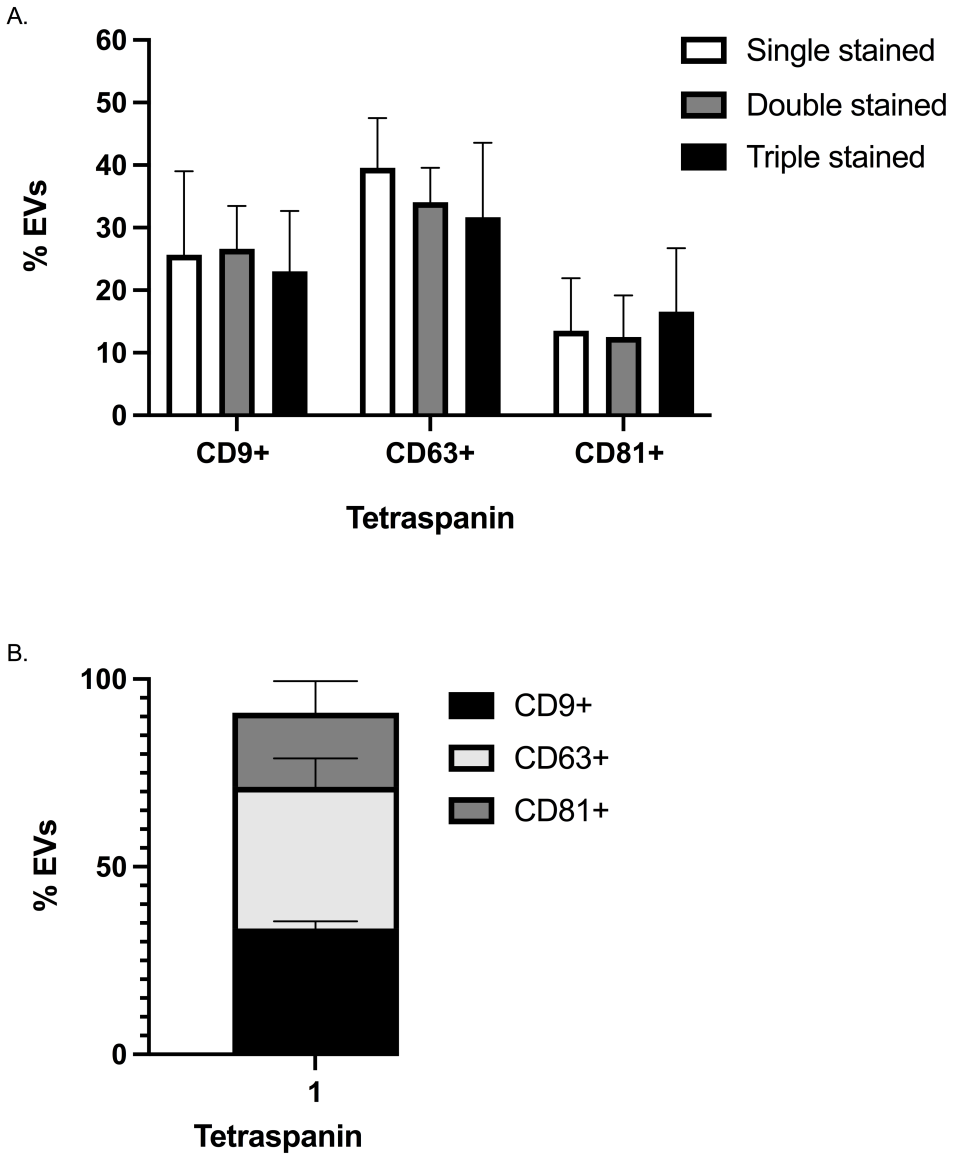

Figure 3.1.16. Tetraspanins CD9, CD63 and CD81 in small EVs (n=5 biological repeats)**.** (A) Graphs showing: no significant differences on the ability to detect CD9, CD63 or CD81 positive EVs with addition of multiple antibodies. (B) Graph showing EVs expressing 1 tetraspanin. Data are expressed as mean ±SD. Two-way ANOVA; Tukey's multiple comparisons post-hoc analyses indicated no significant differences observed.

In addition, we wanted to profile the percentage of EVs expressing one tetraspanin (CD9+ or CD63+ or CD81+), those expressing two tetraspanins (i.e. CD9+CD63+CD81- or CD9+CD63-CD81+ or CD9-CD63+CD81+), and those EVs expressing all three tetraspanins (CD9+CD63+CD81+). Percentage for EVs expressing a single tetraspanin was similar for all three tetraspanins (**Figure 3.1.17.).** Furthermore, for the double tetraspanin-positive EV subpopulations, the highest percentage was observed for CD9+CD63+CD81- EVs. Less than 5% of EVs expressed all three tetraspanins. Results also showed that the lowest percentage of subpopulations of EVs were CD9+CD63-CD81+ EVs and CD9-CD63+CD81+ EVs.

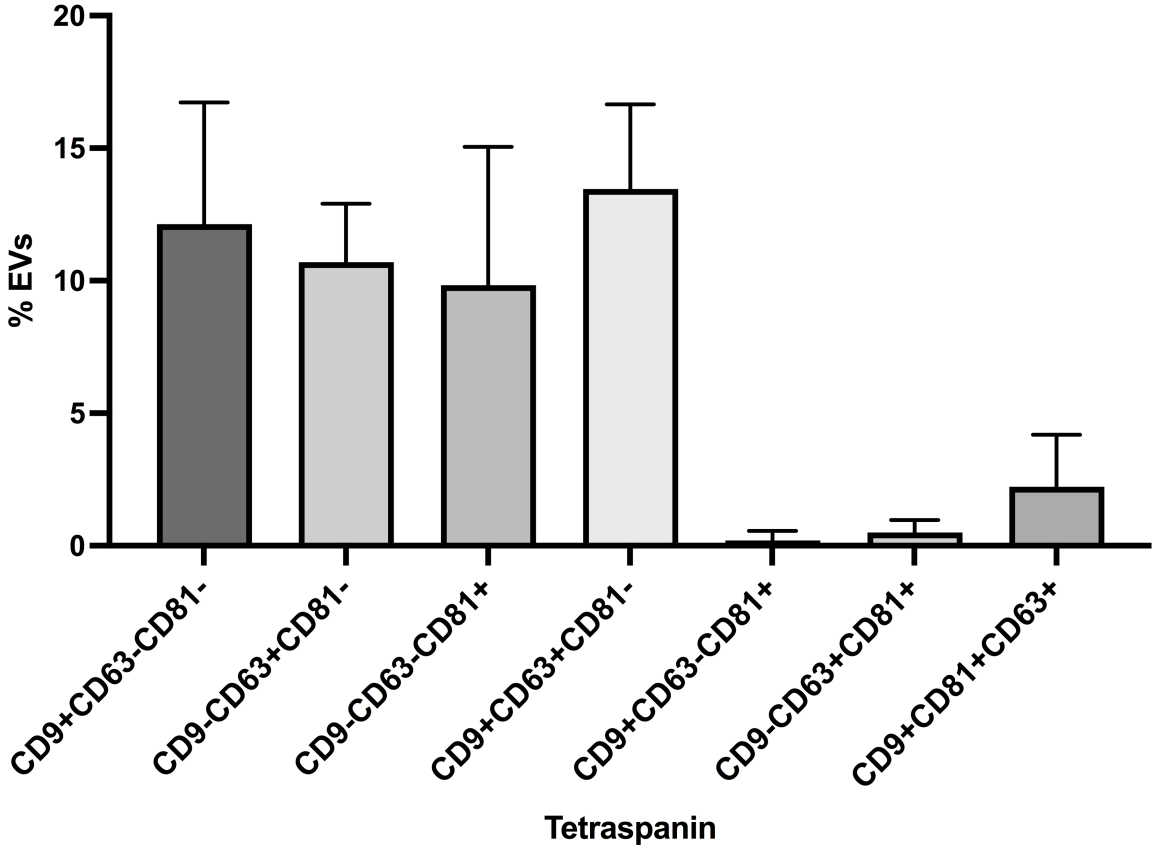

Figure 3.1.17. Subpopulations of small EVs by tetraspanins expression (n=5 biological repeats)**.** Percentage of EVs expressing different combinations of tetraspanins. Percentage was determined from triple-tetraspanin and calcein-stained samples.

3.3.12. Protein measurement of isolated EVs

In order to further profile EVs using MACSPlex Exosome kit, the protein concentration of isolated EVs (fractions 1-5) was first measured using the BCA method. BSA was used as the standard and a graph of protein concentration vs absorbance was plotted. Simple linear regression analysis was done to determine goodness of fit (r^2). Standard curves were consistently near 1, with $r^2 = 0.9952$ as shown in figure 3.1.18. Unknown concentrations were interpolated from the standard curve to identify protein concentration of EVs in each sample.

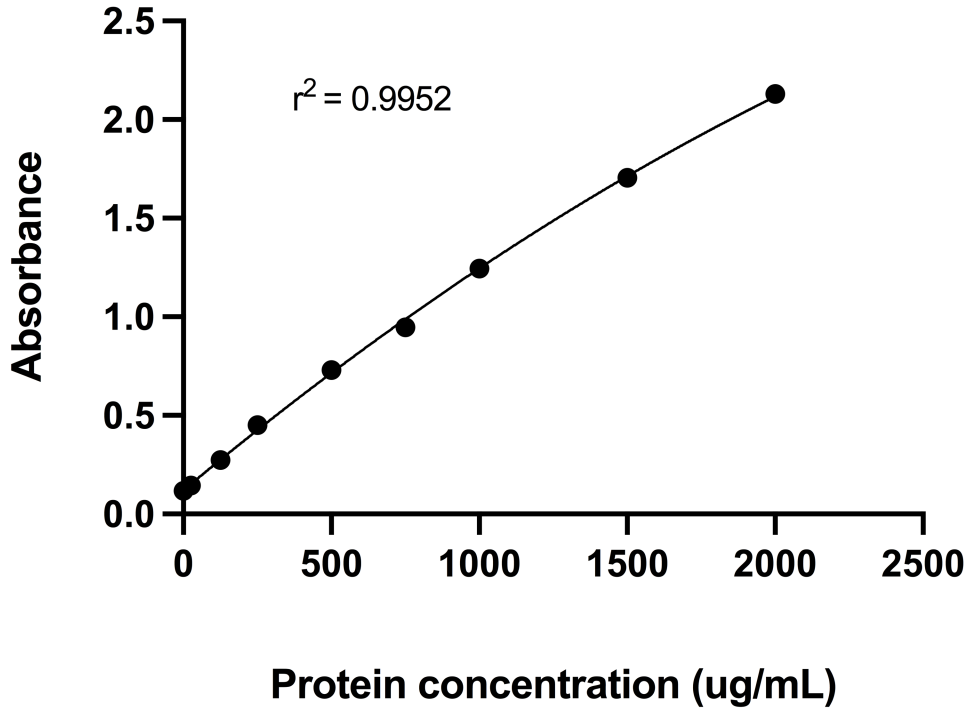

Figure 3.1.18. Protein concentration of EVs. Standard curve of the BCA method for protein quantification.

3.3.13. Surface protein profiling by multiplexed bead assay

To further profile the membrane proteins on the EVs and gain insight into lineage-markers, isolated EVs from unstimulated PMBCs, with more than 70% viability, were phenotyped for 37 surface proteins using the MACSPlex Exosome kit (**Figure 3.1.19.A.**). This was done to study EVs that were produced naturally by cells of the immune system. Initial gates were set to select for all 39 capture bead populations (37 surface markers and 2 isotype controls) by their fluorescence in the FITC vs. PE channels (**Figure 3.1.19.B.i**). EVs were quantified on each protein specific population via staining with APC-conjugated detection antibodies. Buffer control and cell assay and are shown in **Figure 3.1.19.B.ii and iii** respectively, where differences of signal intensities of the single bead populations can be observed between the control and the sample.

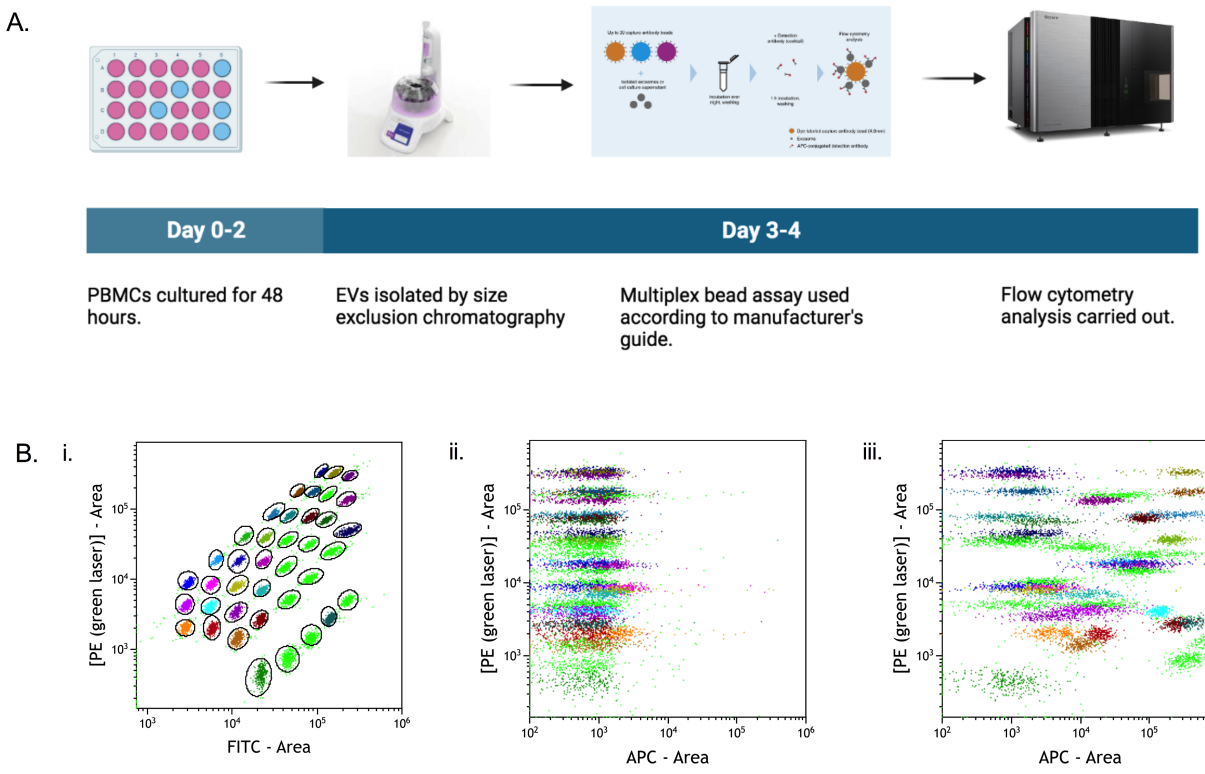

Figure 3.1.19. Multiplex bead-based platform to analyse markers on surface of sEVs. (A) Workflow of methodology. PBMCs were cultured to generate EVs. EVs were isolated by size exclusion chromatography and incubated overnight with 39 different bead populations coupled with capture antibodies. EVs bound to beads were detected with a cocktail of α-CD9-APC, α-CD63-APC and α-CD81-APC antibodies. (B) Representative images of (i) 39 bead populations identified by their fluorescence in the FITC vs PE channel; (ii) APC vs PE signal intensities of single bead populations in buffer control; (iii) APC vs PE signal intensities of single bead populations in stimulated assay.

Samples were normalised relative to CD9, CD63 and CD81 as per manufacturer. For this, the median fluorescence intensity (MFI) for all 39 capture bead subsets was first background corrected by subtracting respective MFI values from matched non-EV buffer or media controls treated like EV-containing samples (buffer/medium + capture beads + antibodies). Data normalization was then directed towards CD9/CD63/CD81 APC signal by using the mean of the median signal intensity of the MACSPlex Exosome Capture Beads CD9, CD63, and CD81 as the normalisation factor for each sample. The signal

intensity of all beads was divided by the normalisation factor of the respective sample. Results showed high levels of CD41b, CD42a, CD62P, CD29 and CD31 (**Figure 3.1.20.)**. Also present in high levels were CD40, HLA-DRDPDQ, HLA-ABC and CD69. Low levels of CD8, CD45, CD44, and CD49e were observed. Some immune cell markers were observed at very low levels, including CD2, CD11c and CD14. Of the tetraspanins, CD9 and CD63 were observed at higher levels than CD81, in agreement with our IFC data.

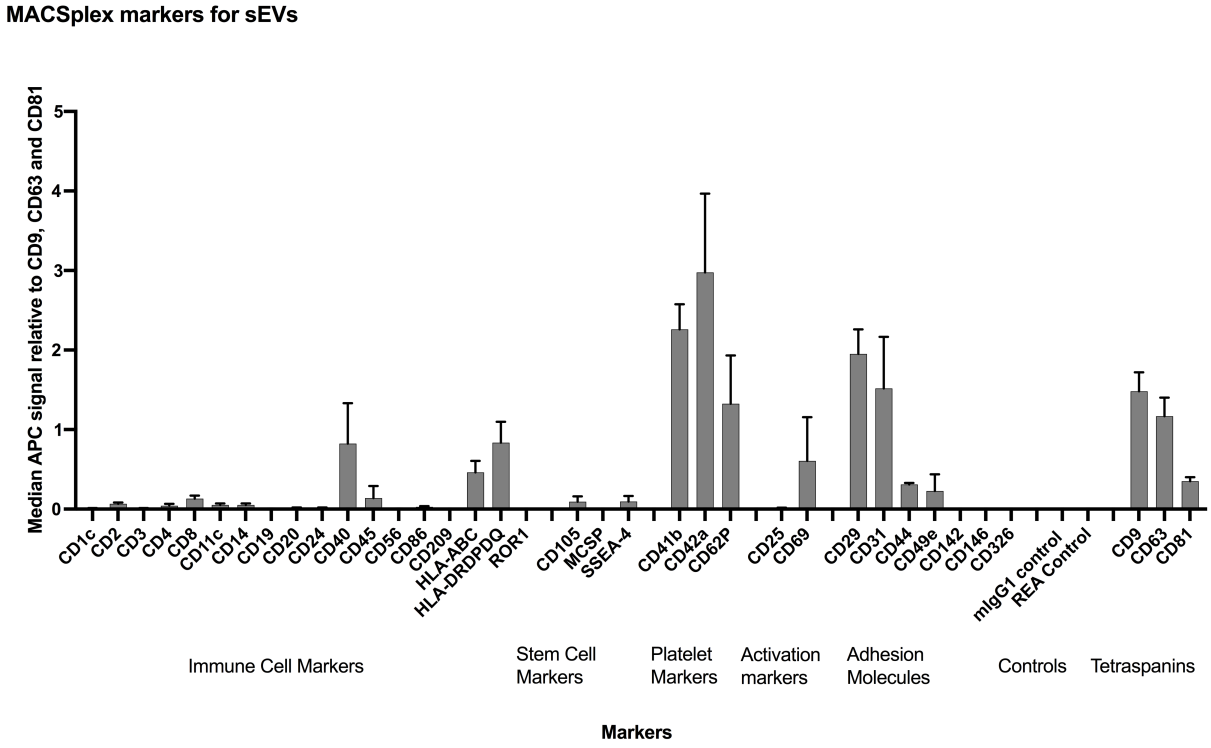

Figure 3.1.20. Markers on surface of sEVs. Quantification of the median APC fluorescence values for all bead populations after background correction and relative to CD9, CD63 and CD81 (n=3 biological repeats).

3.3.14. Internalisation of EVs

To observe if T cells can internalise EVs and thus potentially affect the function of the recipient cell, isolated calcein-stained EVs were introduced to PBMCs labelled with fluorochrome-conjugated antibodies to CD3. Data for two time points, 2 hours and 12 hours, were collected (**Figure 3.1.21.**). T cells with internalised EVs labelled with calcein

were present within the cell cytoplasm following 2-hour incubation (**Figure 3.1.21.A.i.**). In contrast, T cells incubated with EVs for 12 hours showed minimal signal within the cell cytoplasm (**Figure 3.1.21.A.ii.**). Internalisation of EVs was then defined using the internalisation score, which is the ratio of intensity inside the cells to the intensity of the entire cell, on IDEAS software. This was calculated using the CD3 signal (Ch05) and the EV signal (Ch02). Internalisation scores for the 2-hour incubation and 12-hour incubations were 1.5 and 0.5, respectively (**Figure 3.1.21.B.i-ii.**). Higher scores are indicative of a greater concentration of intensity of calcein inside the cell, whereas negative scores indicated that there was little to no internalisation. An internalisation score near 0, as can be seen for the 12-hour incubation, means that cells had equivalent fluorescence on the membrane as inside the cell. A possible reason for the low score at this time point could be due to the breakdown of EVs and therefore loss of calcein after the EVs had been internalised by the cells.

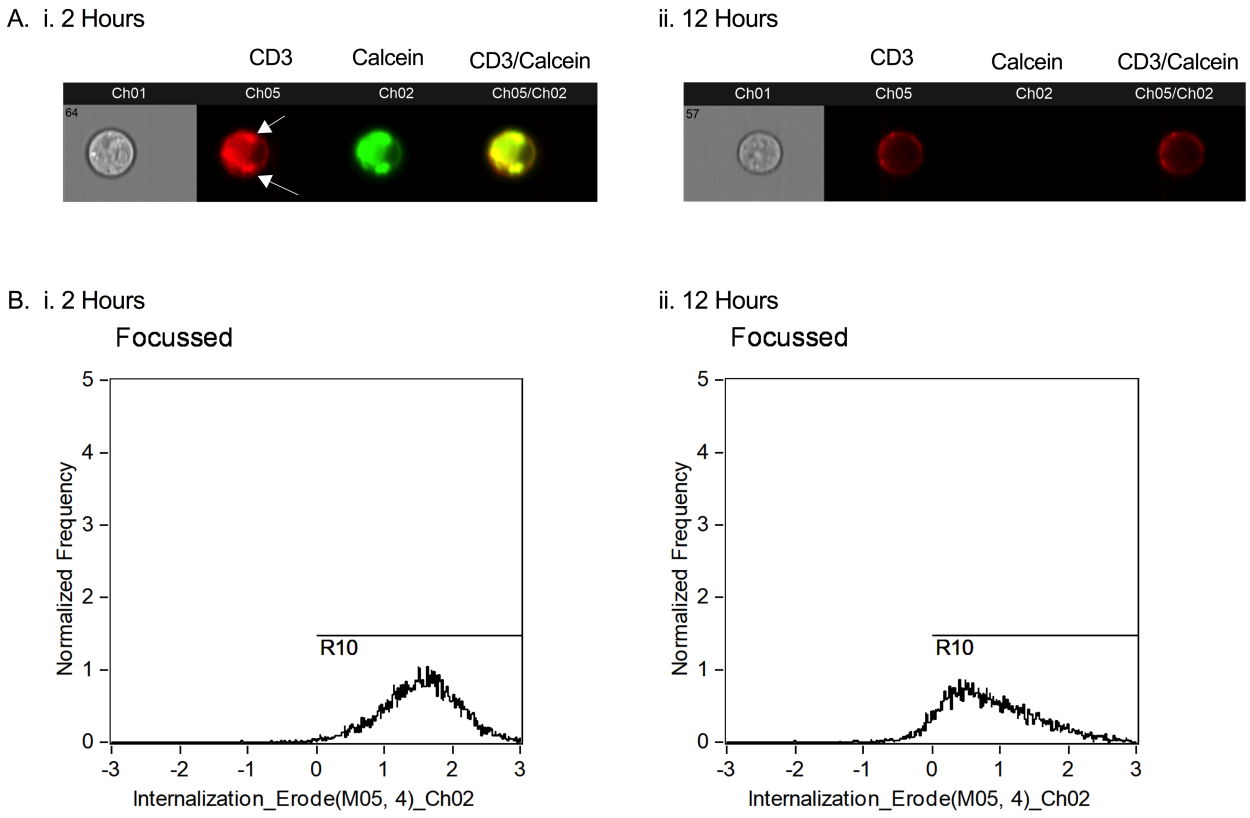

Figure 3.1.21. Internalisation of EVs by T cells. Calcein-stained EVs were isolated and introduced to PBMCs activated with α-CD3 and α-CD28. (A) Representative image of (i) CD3+ T cells that internalised EVs (white arrows) at 2-hour incubation, and (ii) CD3+ T cells at 12-hour incubation with EVs. (B) Internalisation score for CD3 and EVs shown in (A). A higher score of internalisation denotes greater concentration of intensity inside the cell, so cells with internalised signal have positive scores. An internalisation score near 0 indicates a mix of internalisation and membrane intensity.

3.4. Discussion

Healthy individuals between 20-85 years old maintain their circulating EVs with respect to size, particle concentration and total protein per particle [442]. However, even short-term exposure to particulate matter ≤ 10 µm is linked to increased release of EVs [443]. As EVs are considered important mediators of the cross-talk between cells, this PhD aims to observe the effect of CSE and e-cigarette vape exposure on EV production, in particular, quantifying EVs, determining protein composition and observing the effector function of EVs on immune cells. This part of the study aimed to optimise techniques to study extracellular vesicles produced by immune cells. Considering that EVs are small, heterogeneous and difficult to measure, methods that are sensitive and reproducible for EV analysis needed to be optimised.

The first part of this study was determining a method of activation of PBMCs, particularly T cells, as they are a cell population of interest in COPD. EV production by T cells has been shown to be regulated. It is highly increased upon T cell receptor activation, where other mitogenic signals including PMA and ionomycin do not induce release [429]. In humans, the frequency of CD3+ T cells within the lymphocyte population is 70-85 % [444, 445]. Additionally, α-CD3/α-CD28 treatment of PBMCs has been shown to activate all classes of lymphocytes, either directly or indirectly, in contrast to other methods including LPS, which specifically targets monocytes [446]. For the activation of T cells, two signals are required. Signal 1 is generated after the interaction of the T cell receptor (TCR) with its ligand, and signal 2 is generated via an interaction between costimulatory molecules on the antigen presenting cell (APC) and counterreceptors on the T cell, such as CD28 [447]. In vitro, signal 1 is provided by antibodies specific for the TCR-CD3 complex; however, proliferation of T cells is dependent on the co-stimulatory signal (signal 2) which is provided by the CD28 molecule [448]. Thus, stimulation of T cells with α-CD3 and α-CD28 antibodies occurs whereby α-CD3 binds to CD3, thus activating the TCR complex without antigenic peptide/MHC complex engagement, and α-CD28 binds to CD28, stimulating T cells in culture, again without APCs [449]. In this study, the experiments on activation of T-cells

compared immobilised α-CD3 with soluble α-CD3, along with soluble α-CD28 in both instances, to observe which method would provide the highest activation. This was measured by observing early, mid and late activation markers, which are CD69+/CD25-, CD69+/CD25+, and CD69-.CD25+, respectively. The results showed that immobilised α-CD3 at a concentration of 2 μg/mL along with soluble α-CD28 (2 μg/mL) provided higher levels of activation and allowed for selection of CD3+ cells. Soluble α-CD3 resulted in populations of interest unable to be selected, and additionally, resulted in lower activation. These results have also been noted in previous studies where free antibodies, such as soluble α-CD3, provided inadequate cross-linking of the receptor, with rates of proliferation of T cells being inferior for soluble α-CD3 when compared to immobilised α-CD3 [448, 450]. Therefore, immobilised α-CD3 with soluble α-CD28, at 2μg/mL, were selected for continuation as this would allow for efficient activation and expansion of T cells.

Consideration was then given to the culture medium to be used for studies in relation to EVs. This was due to recommendations by MISEV guidelines, as medium components and supplements are known to either contain EVs or affect EV production and/or composition, respectively [399]. As such, experiments investigated five medium conditions, three were serum-free media: AIM-V, Immunocult-XF and ExVivo-15, and two were RPMI media, one with FBS and the other with exosome-depleted FBS. The data from our studies show AIM-V to be an optimum serum-free media for PBMCs as it allowed for optimal conditions of cell growth and viability, demonstrated by the AnnexinV/PI staining results, and efficient EV production, demonstrated by IFC analysis. Comparing the media, there was a higher level of cell viability cultured in AIM-V and this was accompanied by consistent EV production for every experiment, compared to the other mediums used in the study. This is consistent with a previous study comparing a serum-free culture medium and a culture medium with vesicle-depleted serum, where results showed that there were higher levels of viable cells in the serum-free media [451]. In addition, the study raised doubts about the reproducibility of the overall depletion of serum EVs from the EV-depleted serum. Indeed, a previous study has also

demonstrated that commercial EV-depleted FBS (Exo-FBS) still provided high amounts of serum EVs and also resulted in poor primary astrocyte cell growth and viability in culture [411]. Other studies have also noted impaired cell growth in FBS EV-depleted media [452, 453] and that EV-depleted FBS altered the phenotype and activity of cells [453-456]. Therefore, Exo-FBS may contaminate in vitro primary cell-derived EV analysis and may also provide a suboptimal environment for cell growth and viability, while also influencing cell phenotype.

Furthermore, isolated EVs were analysed by nFCM to consider EV fractions that were to be pooled for further EV analysis. Size distribution of EVs in all fractions showed mean and median diameter size of particles were under 100 nm. nFCM analysis also showed that the highest concentrations of particles were in fractions 1-3. This is in agreement with a previous study that has shown that later fractions are enriched in proteins and are low in EVs [414, 457]. SEC utilises porous polymer beads to form a porous stationary phase in a column which allows particles of different sizes to be differentially eluted by gravity-flow, and although low/very low density lipoproteins cannot be completely removed, SEC is able to sufficiently separate EVs from highly abundant protein contaminations [457]. Therefore, due to our results, fractions 1-5 were pooled for future experiments. Pooled fractions (1-5) of isolated EVs were then analysed by TEM and NTA to confirm observed EV population using well-established techniques. Size distribution of isolated EVs observed by NTA showed most EVs were under 200 nm in size with a mode of 128.4 nm, in agreement with previous data generated by TEM. Both NTA and nFCM are single-particle analysis techniques that rely on distinct physical principles. NTA is a method dependent on light scattering that tracks the Brownian motion of each particle individually in order to determine the mean square displacement of individual particles. Here, the 2D Stoke-Einstein equation is used to determine hydrodynamic diameters of particles individually and particle concentration is determined from the number of particles tracked in an estimated illumination volume [458, 459]. nFCM, a subset of flow cytometry, is a method whereby single particles are hydro-dynamically focused in a sheath fluid stream and subsequently exposed to laser excitation [459].

Here, single photon detectors measure scattered light refracted from particles and can also measure fluorescence photons emitted by attached fluorophores [460]. For sizing of EVs, intensity of side scattered light is compared to a standard curve generated by measurement of a four-modal silica nanosphere mixture with a refractive index of approximately 1.45, similar to the refractive index of that reported for EVs (1.37-1.42) [459-462]. Isolated EVs were also analysed by IFC to demonstrate the EV population could still be identified with the gating strategy developed for EVs.

Here we also show the use of Calcein AM to enumerate EVs using flow cytometry. The use of Imaging Flow Cytometry (IFC) for EV analysis allows us to overcome some of the challenges of measuring EVs in the submicron range often encountered with traditional flow cytometry, such as coincidence detection. The IFC has a precision syringe-based sample acquisition which allows for accurate enumeration of EV concentrations without using counting beads [463]. IFC has all the advantages of traditional flow cytometry, including the ability to measure scatter and multiple fluorescent markers in a high throughput manner, along with also being able to see images of the cells/particles being measured. Additionally, image analysis features, such as the automated spot count feature, can be used to demonstrate that coincident events that are swarming do not occur [425]. This avoids the need for laborious serial dilution experiments required for conventional flow cytometry. Furthermore, identification and analysis of EVs using flow cytometry typically involve exploiting the lipid nature of EVs by staining with conjugated antibodies against specific surface markers, including Annexin V or lactadherin against the membrane phospholipid phosphatidylserine (PS), or non-specific membrane dyes [464, 465]. However, lipoproteins have been shown to interfere with flow cytometric analysis of EVs when lipid-based strategies are used, as both Annexin V and lactadherin also label Apolipoprotein B containing lipoproteins [464]. Indeed, conjugated antibodies against cell surface markers also fail to discriminate between intact vesicles and debris [403]. Calcein AM allows for discrimination between intact EVs and debris, as it requires hydrolysis by intravesicular esterase to be converted into a fluorescent analogue that is EV-impermeant and has been used to successfully stain for EVs [403-405, 466]. A study

by Gray et al [403] has shown that Calcein AM was as sensitive at detecting EVs as PKH26 and selectively labelled intact EVs. As the staining was applied to both purified EVs and culture supernatant in this study, it was of particular importance to selectively stain intact EVs as culture supernatants are more likely to contain variable numbers of disrupted EVs and EV fragments. Furthermore, techniques such as NTA and other methods used for EV detection are unable to differentiate heterogeneous EVs from other particles with overlapping sizes, including lipoproteins and aggregated protein particles [467]. A previous study showed that Calcein AM had low sensitivity in EV samples, however, EVs were isolated prior to being stained with Calcein AM [466]. In this study, samples were stained in culture and analysed by IFC, with a gating strategy that allowed the selection of small EVs (i.e. under 200 nm). In terms of analysis of EVs, the results in this study show that EV counts for 1:50 dilution were higher compared to 1:100. However, CalceinAM is solubilised in dimethyl sulfoxide (DMSO), and previous studies have suggested that for cell culture the maximum DMSO concentration should be 0.5% as DMSO can affect viability of cell in a dose-dependent manner [468]. DMSO is ideal for dissolving poorly soluble polar and non-polar substances due to its amphipathic nature but is also able to induce changes in cellular processes in cells [469]. As a result, Calcein 1:100 was considered to be the optimum dilution for future experiments, with a final concentration of 0.005% DMSO.

Another control in the reporting framework of MIFlowCyt-EV following MISEV guidelines set by ISEV is treating samples with a detergent [399, 402]. The rationale for this control was to aid in the determination of whether EV-detected events were membrane-enclosed or any other protein complex. With the detergent treatment, the EVs would be lysed and as a result, the numbers and signals of EVs would be reduced, which would allow the differentiation of EVs from other particulates [402]. In early experiments, Tween20 was the only detergent used and results showed that 10% Tween20 was sufficient to reduce the EV numbers per mL drastically, demonstrating that the events were EVs. Tween20 was compared to an additional detergent, TritonX-100, as there are different subpopulations of EVs and some may require a different detergent. These

detergents were selected based on a study by Osteikoetxea et al [434] which investigated various concentrations of different detergents, including Triton X-100 and Tween 20, to find an optimal detergent concentration for lysing EV subpopulations. The results presented here demonstrated that 10% Tween20 was sufficient to lyse a high percentage of EV subpopulations and was therefore used as a control in further experiments.

To further profile EVs, this study observed the presence of tetraspanins (namely CD9, CD63 and CD81), which have broad tissue expression, and as plasma membrane and endosome membrane proteins, can be used as specific EV markers. The use of tetraspanins is an additional tool to overcome limitations of EV detection [467]. Additionally, tetraspanin characterisation of EVs could indicate the subcellular origin of EVs, allowing for determination of the exosomal or ectosomal nature of EVs [470]. Previous studies have analysed co-expression of two tetraspanins using flow cytometry [471, 472]. Barranco et al [471] assessed co-expression of tetraspanins on EVs isolated from porcine seminal plasma using flow cytometry, observing that CD63 + CD81 + was higher in exosomes than MVs and that the proportion of CD9 + CD81 + in exosomes was higher than in MVs; here they defined exosomes and MVs according to their size, diameter below 120 nm and above 120 nm, respectively. Ibrahim et al [472] observed that EVs from serum and uterine lavage of mares were positive for CD9 and CD63 using flow cytometry. Co-expression of all three tetraspanins, however, has not been assessed using IFC. CD9-CD63-CD81-triple-positive EVs have been previously observed to comprise a substantial portion of EVs using total internal-reflection microscopy [473]. In this study, we detected three different tetraspanins per sample with the use of IFC to analyse subsets of EVs. Here, we show that the presence of all 3 tetraspanins can be simultaneously detected along with calcein without compromising the sensitivity of staining. We also demonstrate higher numbers of EVs expressing both CD9 and CD63 than EVs bearing CD63 and CD81 or CD9 and CD81. These data are in keeping with those previously reported for EVs isolated from blood samples, where $CD81^+$ EVs form the smallest EV subpopulation [474]. Furthermore, CD9 is expressed in all major types of

leukocytes including B and T cells, NK cells, macrophages and DCs, and as such, may be found on EVs derived from immune cells [475]. Kowal et al [476] examined multiplex expression of tetraspanins using bead-based immunocapture and successive western blot, and observed that CD9 and CD81 were found on most dendritic cell-derived EVs, but were not necessarily co-expressed. Additionally, they found that CD63 was a less common marker on DC-derived EVs. Koliha et al [477] observed, using a multiplex platform and stimulated emission depletion (STED) microscopy, that CD63 and CD81 could be detected on NK-cell derived EVs. Furthermore, results show over 90% of EVs expressed 1 tetraspanin on their membrane. Less than 10% of EVs did not have any of the 3 tetraspanins, demonstrating selective labelling with CD9, CD63 and CD81 leaves some EVs uncharacterised. Tetraspanins found in EVs have been shown to function in EV biogenesis, cargo selection, cell targeting and cell uptake under physiological and pathological conditions [307]. CD9 and CD81, along with integrin $\alpha_v\beta_3$ have been suggested to be involved in the targeting and uptake of EVs by dendritic cells [308].

To profile the membrane of EVs for lineage-specific proteins, isolated EVs from PMBCs were phenotyped for 37 surface markers using the MACSPlex Exosome kit. The presence of 9 surface proteins (CD62P, CD41b, CD42a, HLA-DRDPDQ, HLA-ABC, CD40, CD69, CD31 and CD29) at high levels were observed. These EVs carried molecules that are involved in immune regulation (HLA-DR/DP/DQ, HLA-A/B/C and CD40) and cell adhesion (CD31 and CD29). Furthermore, CD62P, CD41b and CD42a are markers expressed on platelets and megakaryocytes [478], suggesting EVs derived from these sources are also present. This reflects the fact that platelet- and megakaryocyte-derived EVs are the most abundant EVs in human blood, accounting for more than half of all EVs in the peripheral blood [479, 480].

In conclusion, we have outlined a protocol to analyse immune cell-derived EVs. This protocol focuses on high-throughput flow-based methods, including imaging flow cytometry (IFC) that incorporates a novel gating strategy (using the spot count feature) and a rapid staining protocol that allows for quantification of EVs in culture and following isolation. Additionally, we have demonstrated the ability to observe three

tetraspanins on calcein-labelled EVs by IFC. Furthermore, we have used multiplexed beads assay to profile the membrane protein composition of EVs for lineage-specific proteins.

4.0. EVs produced by CSE- and ECVE-exposed PBMCs

4.1.1. Introduction

Investigating the impact of environmental factors on human health is essential for understanding disease mechanisms. Cigarette smoke (CS) is one of the many environmental exposures with systemic effects that contributes to the pathogenesis of chronic respiratory diseases, cardiovascular diseases, neurodegenerative disease and various forms of cancer [481]. Although cigarette smoking rates have decreased over the last decade, this has been filled by the use of electronic cigarettes (e-cigarettes, e-cigs or ECs). Indeed, there is an increased global trend in e-cigarette use as a 'less harmful' alternative, however, the lack of longitudinal data on the safety and health effects of e-cigarettes is worrying. E-cigarettes are electronic nicotine delivery systems (ENDS) that deliver vaporised liquid, consisting of mainly nicotine and propylene glycol, through the mouth into the lungs, thus mimicking the effects of conventional cigarettes [482, 483].

Furthermore, EVs are now receiving significant attention in biomedical research due to their role in intercellular communication and their potential as biomarkers for various diseases. A key challenge in EV research, however, is being able to accurately characterise and quantify EVs which are usually in the nanometre to micrometre size range. The use of traditional methods to characterise EVs usually involves a trade-off between throughput and resolution which limits a comprehensive analysis of EVs in terms of heterogeneity and interactions with cells. For example, conventional flow cytometry is efficient in analysing large sample volumes; however, it lacks the ability to observe individual EVs and distinguish subtle differences in their properties. Moreover, microscopy-based approaches allow for superior imaging resolution but are limited by their low throughput and labour-intensive nature [484, 485]. Among the variety of advanced techniques used for analysis of EVs, imaging flow cytometry (IFC) is a powerful tool in this area of research as it combines the high-throughput of conventional flow cytometry with the imaging resolution of microscopy [485], thus addressing these limitations of traditional methods. In the context of this study, IFC presents a novel

avenue for studying EVs as it allows for the simultaneous assessment of the concentration, size distribution, and phenotypic and functional characteristics of EVs at the single-particle level, and allows for observation of the interaction of EVs with cells. Indeed, IFC enables a more comprehensive characterisation of EV populations, allowing for the identification of subpopulation of EVs and possible investigation into their biological significance. IFC together with the use of complementary methodologies and techniques including size exclusion chromatography, protein quantification, and tetraspanin and membrane marker profiling, provides a comprehensive view of EV composition and heterogeneity.

Additionally, we have previously incorporated Calcein AM staining with our IFC assays, thus providing a novel approach that allows us to label and visualise EVs. Calcein AM, a membrane-permeable dye that fluoresces when cleaved by intracellular esterase, produces a green fluorescent signal and is trapped within the vesicle [403-405, 466]. This allows for the specific labelling of EVs without interfering with their structure or function. Using Calcein AM in conjunction with IFC also allows for this staining to be combined with other assays to investigate cargo and biological activity of EVs. This can be noted when EVs are co-stained with antibodies against specific markers or proteins in order to study cell origin or incorporate fluorescent reporters to observe uptake by recipient cells that have been stained or cargo delivery. Thus, integrating Calcein AM staining with IFC demonstrates a novel and innovative approach to studying EVs, where it offers enhanced sensitivity, resolution and flexibility compared to traditional methods and provides potential to advance our understanding of EVs.

In this study, we focus on investigating the effects of cigarette smoke and e-cigarette vapour, on the generation and composition of EVs derived from peripheral blood mononuclear cells (PBMCs). Here, we utilise IFC in conjunction with Calcein AM to enable rapid analysis of large EV populations to observe and quantify EV subpopulations with distinct morphologies and surface markers. By employing established methodologies detailed in the previous chapter (Chapter 3), our aim is to comprehensively profile EVs following exposure to CSE and ECVE.

4.1.2. Aim

The aim of this study was to observe and profile EVs derived from PBMCs after exposure to cigarette smoke extract (CSE) and e-cigarette vape extract (ECVE) using methods developed in the lab (Section 3.0).

4.2. Methods

4.2.1. Processing of blood samples and Peripheral Blood Mononuclear Cell (PBMC) Isolation.

Blood was drawn by venepuncture and collected into heparin tubes for PBMC isolation. Isolation of PBMCs from fresh whole blood was done by histopaque density gradient centrifugation. Full details of the methodology can be found in chapter 2 section 2.1 and details of reagent used are in table 2.1.

4.2.2. Cigarette smoke extract

CSE was made fresh on the day of the experiment to be used as quickly as possible. Details of the method can be found in Chapter 2, section 2.3.

4.2.3. E-cigarette vape extract

E-cigarette solution was made fresh on the day of the experiment and used as quickly as possible. Details of the method can be found in Chapter 2, section 2.4.

4.2.4. Controls set for EV analysis

Following MISEV guidelines and the MIFlowCyt-EV framework for standardized reporting of EV flow cytometry experiments, table 4 shows the controls set to enable accurate analysis of EVs [399, 402]. Details of the assay controls to enable accurate extracellular vesicles analysis and reporting can be found in Chapter 2, section 2.7.

4.2.5. Calcein AM staining of EVs

Calcein AM staining for EVs was done to obtain images of the cells and EVs using imaging flow cytometry (IFC). Details of calcein AM staining of EVs can be found in chapter 2, section 2.8.

4.2.6. Tetraspanin staining of EVs

For staining, α-tetraspanin moAbs for CD9, CD63 and CD81 were added. Detailed methodology for tetraspanin staining of EVs can be found in chapter 2, section 2.9.

4.2.7. EV isolation by Size Exclusion Chromatography

EV isolation by size exclusion chromatography (SEC) was done using qEV original 35 columns (Izon Science) and Automatic Fraction Collector (AFC; Izon Science) and according to manufacturer's instructions. Detailed methodology can be found in chapter 2, section 2.10.

4.2.8. ImageStreamX Small Particles Acquisition and Analysis

Imaging flow cytometry was performed using ImageStreamX (ISX) (Luminex, USA). Details of data acquisition using the ISX can be found in chapter 2, section 2.15. Samples were acquired for a time span of 10 minutes unless the acquisition was complete, using the software INSPIRE, and exported data was analysed using ISX Data Exploration and Analysis Software (IDEAS).

4.2.9. Protein measurements

Protein concentrations in isolated EV fractions were measured using a BCA protein assay kit (ThermoFisher, Loughborough, UK) according to manufacturer's instructions. Details of methods can be found in chapter 2, section 2.16.

4.2.10. Macsplex surface protein profiling

The MACSPlex Exosome Kit (Miltenyi Biotec,) allows for detection of 37 surface markers present on EVs plus two isotypes. The MACSPlex kit was used according to the manufacturer's instructions for the assay using 1.5 mL tubes. Details of methods can be found in chapter 2, section 2.16.

4.2.11. Data analysis

Data analysis was performed using Prism software, version 8.2.1c (GraphPad). Statistically significant differences of cell viability using Annexin V/PI staining between CSE concentration and between 0, 24 and 48 hours (Figure 4.2.) were assessed with ordinary two-way ANOVA, followed by Tukey's multiple comparisons test, with a single-pooled variance. Statistically significant differences of sEV concentration for sample vs controls between 24 hours and 48 hours (Figure 4.4.) were analysed by ordinary two-way ANOVA, followed by Tukey's multiple comparisons test, with a single-pooled variance. Statistical significance of differences in % focussed EVs for tetraspanins for sample vs control at 24 hours (Figure 4.5.) were assessed with ordinary two-way ANOVA, followed by Tukey's multiple comparisons test, with a single-pooled variance, and this was repeated for % focussed EVs for tetraspanins for sample vs control at 48 hours. Statistical significance of differences in tetraspanin+ focussed EVs between 24 and 48 hours (Figure 4.5.) were assessed by RM two-way ANOVA, followed by Sidak's multiple comparisons test, with a single pooled variance (this was done for each CSE concentration).

Statistically significant differences of sEV concentration from control vs CSE-exposed PBMCs and 1% vs 3% CSE exposed PBMCs (Figure 4.6.) were assessed with ordinary one-way ANOVA, followed by Tukey's multiple comparisons test. Statistical significance of differences in tetraspanin expression of % focussed sEVs (Figure 4.7.) was assessed with ordinary two-way ANOVA, followed by Tukey's multiple comparisons test for each tetraspanin at each CSE concentration. Statistically significant differences of % focussed single- vs double- vs triple-stained sEVs for each tetraspanins (CD9, CD63, CD81) (Figure

4.8.) were analysed by two-way ANOVA, followed by Tukey's multiple comparisons test. Statistically significant differences in protein expression on control vs CSE PBMC-derived sEVs detected by the MACSPlex exosome kit (Figure 4.9.) were analysed with two-way ANOVA, followed by Tukey's multiple comparisons test. Significance for tests was defined as $P < 0.05$. Statistical significance of differences in EVs/mL for CSE, ECVE, nicotine samples and control (Figure 4.10.) were assessed by Ordinary one-way ANOVA, followed by Tukey's multiple comparisons test, with a single-pooled variance. Statistically significant differences in single tetraspanin expression on control vs CSE-, ECVE-, and nicotine (Figure 4.11.) were analysed by ordinary two-way ANOVA, followed by Tukey's multiple comparisons test, with a single-pooled variance. Statistically significant differences of EV subpopulation for CSE- and ECVE- samples vs controls (Figure 4.12.) were analysed by ordinary two-way ANOVA, followed by Tukey's multiple comparisons test, with a single-pooled variance.

4.3. Results

4.3.1. Cigarette smoke extract

CSE has previously been used for investigating the effect of cigarette smoke, particularly with *in vitro* models such as oxidative stress and inflammation. Previous experiments have used a concentration range of 1-3% CSE treat cells *in vitro* [129, 486-489]. In this study, CSE was freshly prepared and added to cell culture within 30 minutes of preparation to avoid breakdown of substances in the extract and the evaporation of any volatile components. The brand of Marlboro cigarettes was used in the study to follow from previous research conducted in this lab [129]. In total, twenty-six (n=26) cigarettes were processed during the entire project. The trend of absorbance according to CSE dilution can be seen in **Figure 4.1.**, showing that the pattern of absorbance at 320 nm had very little difference between different preparations of CSE. Absorbance at 320 nm was done to measure tar content in CSE preparations as has been shown in previous studies [129, 400, 401]. Additionally, an absorbance of 0.15 was considered as 100% CSE to standardise the concentration of CSE used for every experiment and follows previous studies carried out in this lab [129].

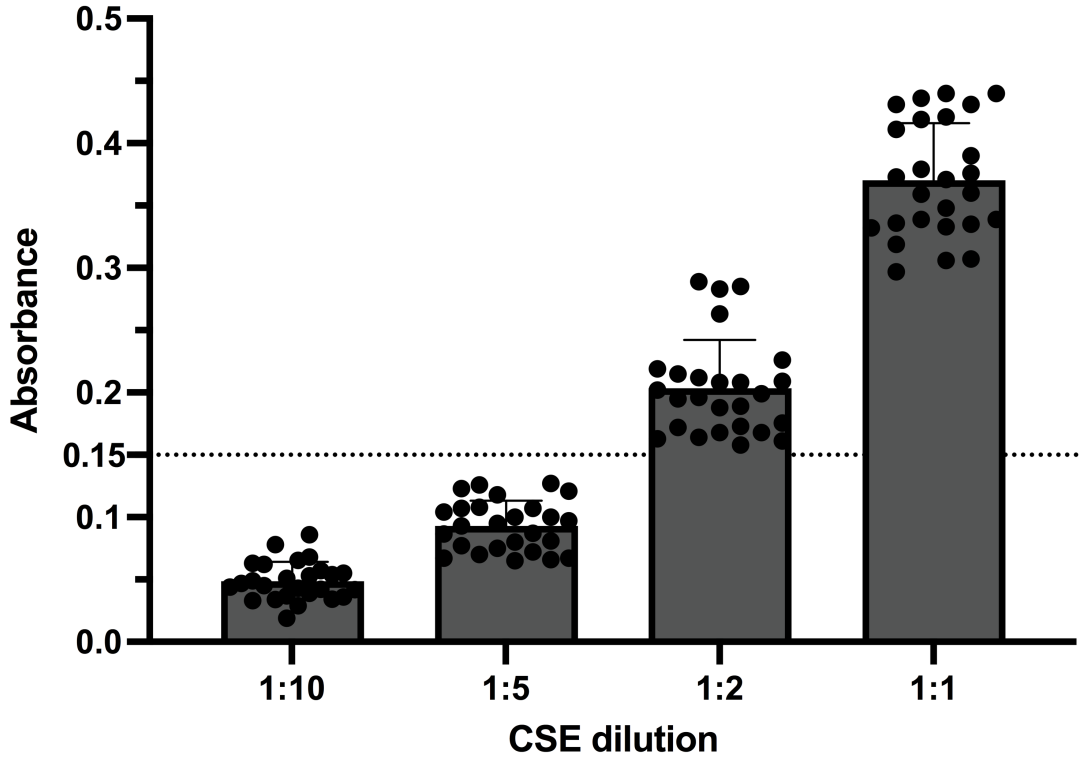

Figure 4.1. Absorbance of CSE at different dilutions (n=26 biological repeats). An absorbance of 0.15 was considered as 100% CSE.

4.3.2. EV production at 24 and 48 hours following CS exposure

After initial observation of EV production from PBMCs, we then wanted to compare production of EVs at 24 hours and 48 hours after exposure to CS (1% and 3% CSE) and no CSE (0% CSE) as a negative control. As cigarette smoke consists of compounds known to be mutagenic, carcinogenic, antigenic, and cytotoxic, the effect of CSE concentrations on cell viability prior to EV analysis was tested using Annexin V/ PI staining at 0 and 48 hours in culture (**Figure 4.2.**). Results show that for each treatment and control there was no significant changes in % of viable cells (**Figure 4.2.A-C.**), also showing viability was consistently over 50%.

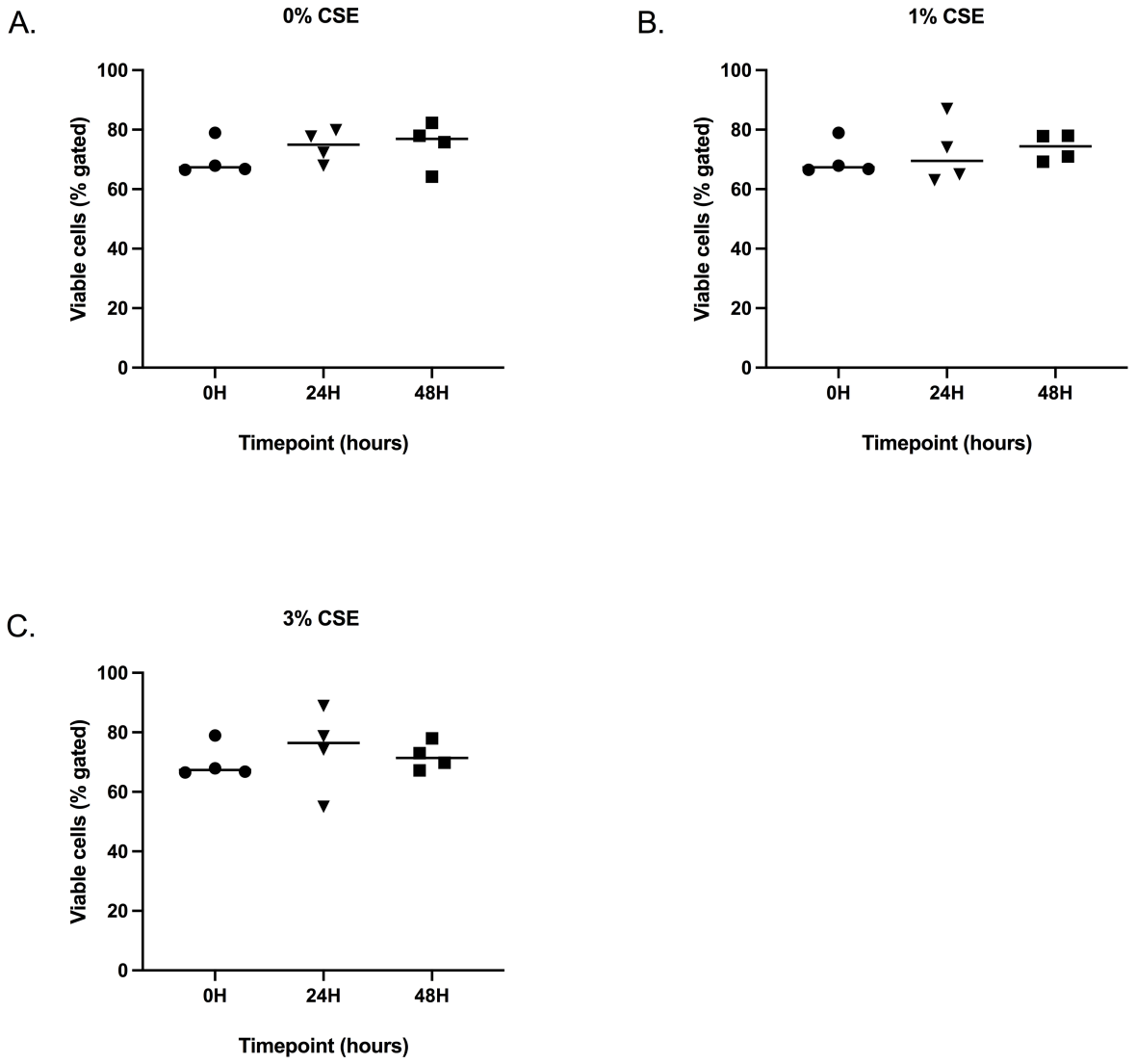

Figure 4.2. Viability of CSE-stimulated PBMCs. (A) Viability of PBMCs from start of culture (0 hours) to 24 and 48 hours. Data are expressed as mean ± SD; Ordinary One-way ANOVA; Tukey's multiple comparisons post-hoc analyses indicated no significant differences observed. (n = 4 biological repeats)

Having shown that viability of cells after 48-hour culture was satisfactory, analysis of smaller EVs produced by PBMCs exposed to CSE was carried out. Controls showed minimal background EVs in media-only controls, Tween20 (10%) control, and no-calcein control (**Figure 4.3.**), therefore EV analysis was then carried out on the supernatants.

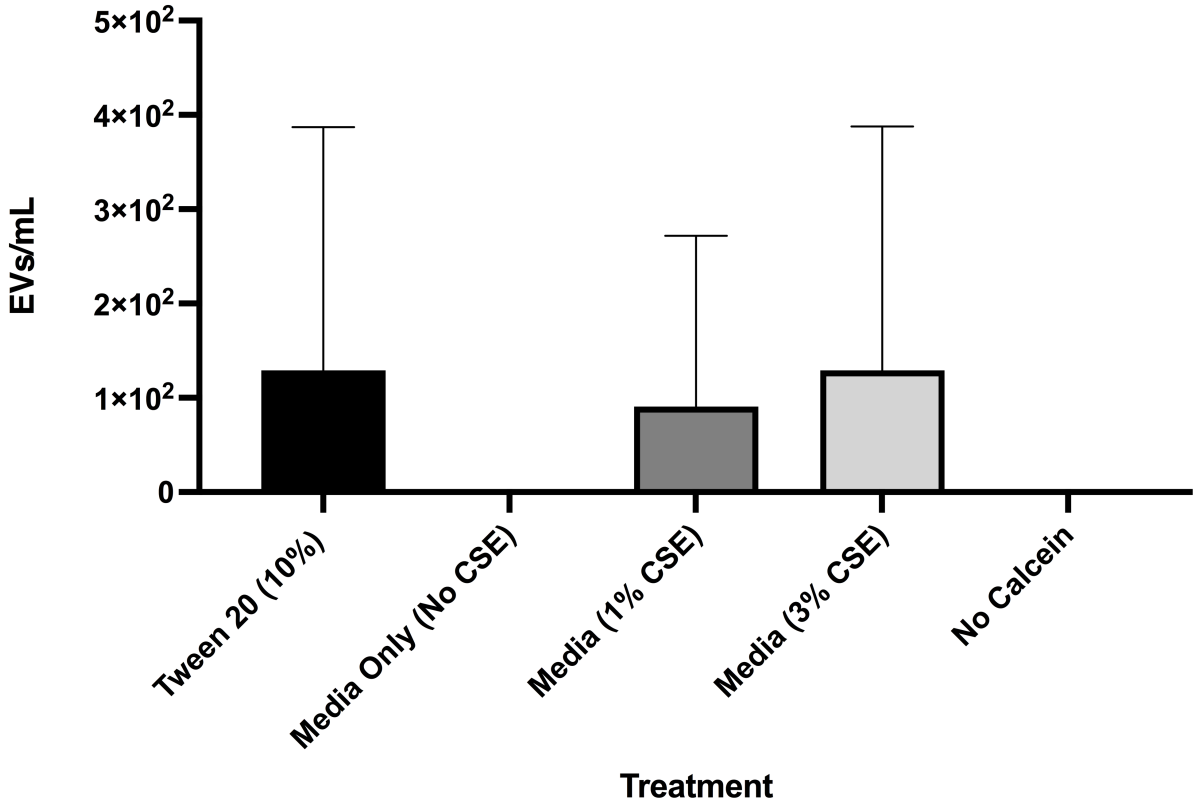

Figure 4.3. Controls in EV experiments. IFC data collected (EVs/mL) for controls and CSE-media samples. Data are expressed as mean ± SD. (n = 4 biological repeats)

Results show that the number of smaller EVs/mL produced were lower at 48 hours, compared to 24 hours (**Figure 4.4.**), however, this difference was not significant. Additionally, in these experiments no additional stimulation was given to cells other than the addition of CSE. Interestingly, there was an increased count in EVs/mL after 48 hours for one particular donor, who was an everyday cigarette smoker, although this was not noted before the experiment. Smoking status was important to note going forward in experiments, as samples from smokers have previously been shown to have increased numbers of circulating EVs compared to non-smokers [341].

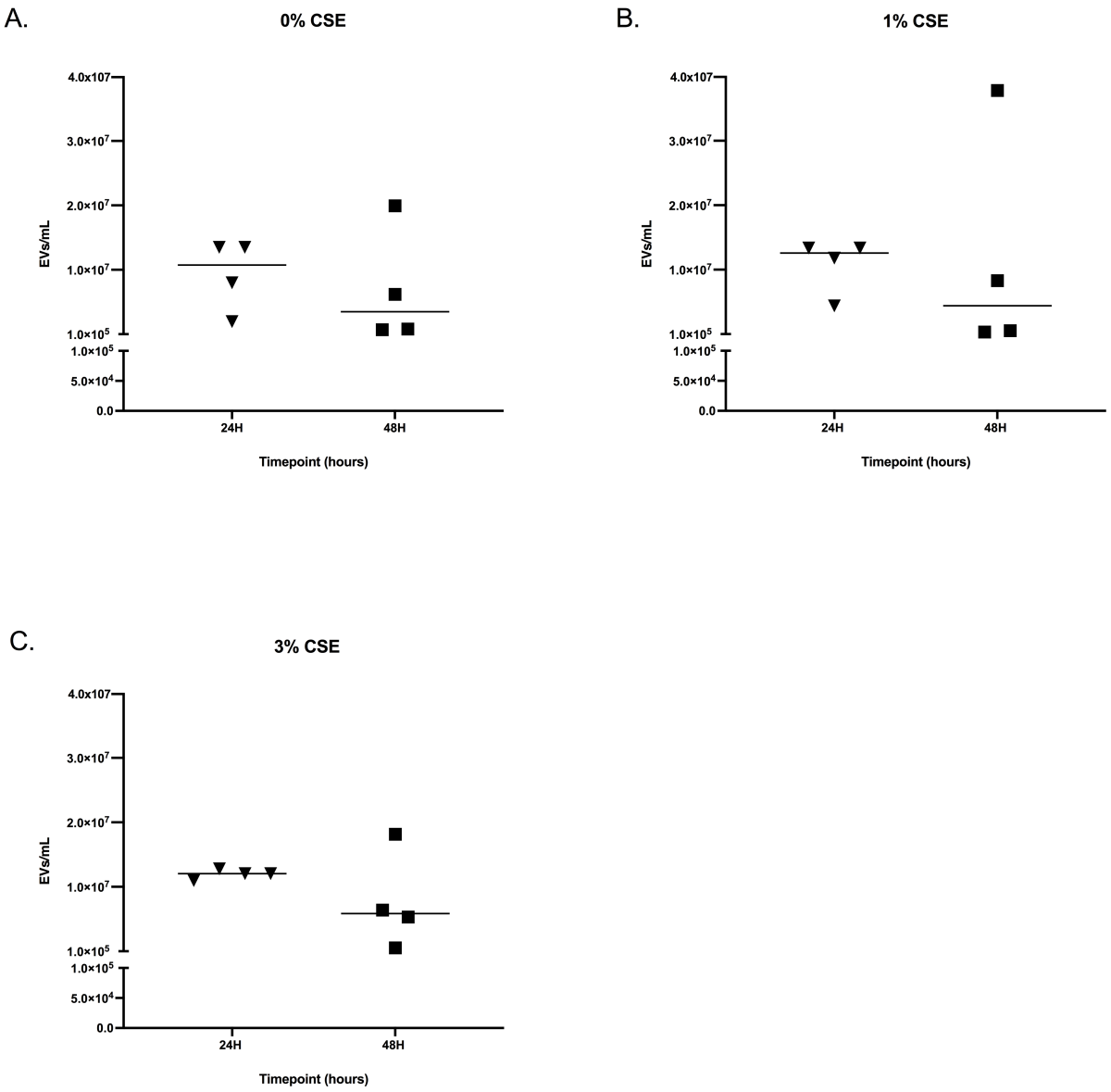

Figure 4.4. EV production by CSE-stimulated PBMCs. IFC data collected (EVs/mL) for control and CSE-stimulated samples at 24 hours and 48 hours. Data are expressed as mean ± SD; Ordinary two-way ANOVA; Tukey's multiple comparisons post-hoc analyses indicated no significant differences observed between each CSE concentration and control and between time points. (n = 4 biological repeats)

Furthermore, we analysed the EVs that were positive for each tetraspanins at 24 hours and 48 hours after exposure to CS (1% and 3% CSE) and the 0% CSE control. Results show that the tetraspanins composition had minor changes at the different time points (**Figure 4.5.**). At 24 hours, higher percentages of EVs were positive for CD9 (>40%) in particular for 1% CSE, and this percentage decreased below 40% at 48 hours (**Figure 4.5.A.**). The pattern of CD63 expression also slightly changed between 24 and 48 hours, as at 24 hours there was slight increase after exposure to 3% CSE, and at 48 hours percent of EV expressing CD63 were lower after exposure to 1% CSE and 3% CSE compared to control (**Figure 4.5.B**.). Expression of CD81 between 24 hours and 48 hours remained relatively constant, with slight increase in % EVs expressing CD81 at 48 hours (**Figure 4.5.C**.). The differences noted here, however, were not significant.

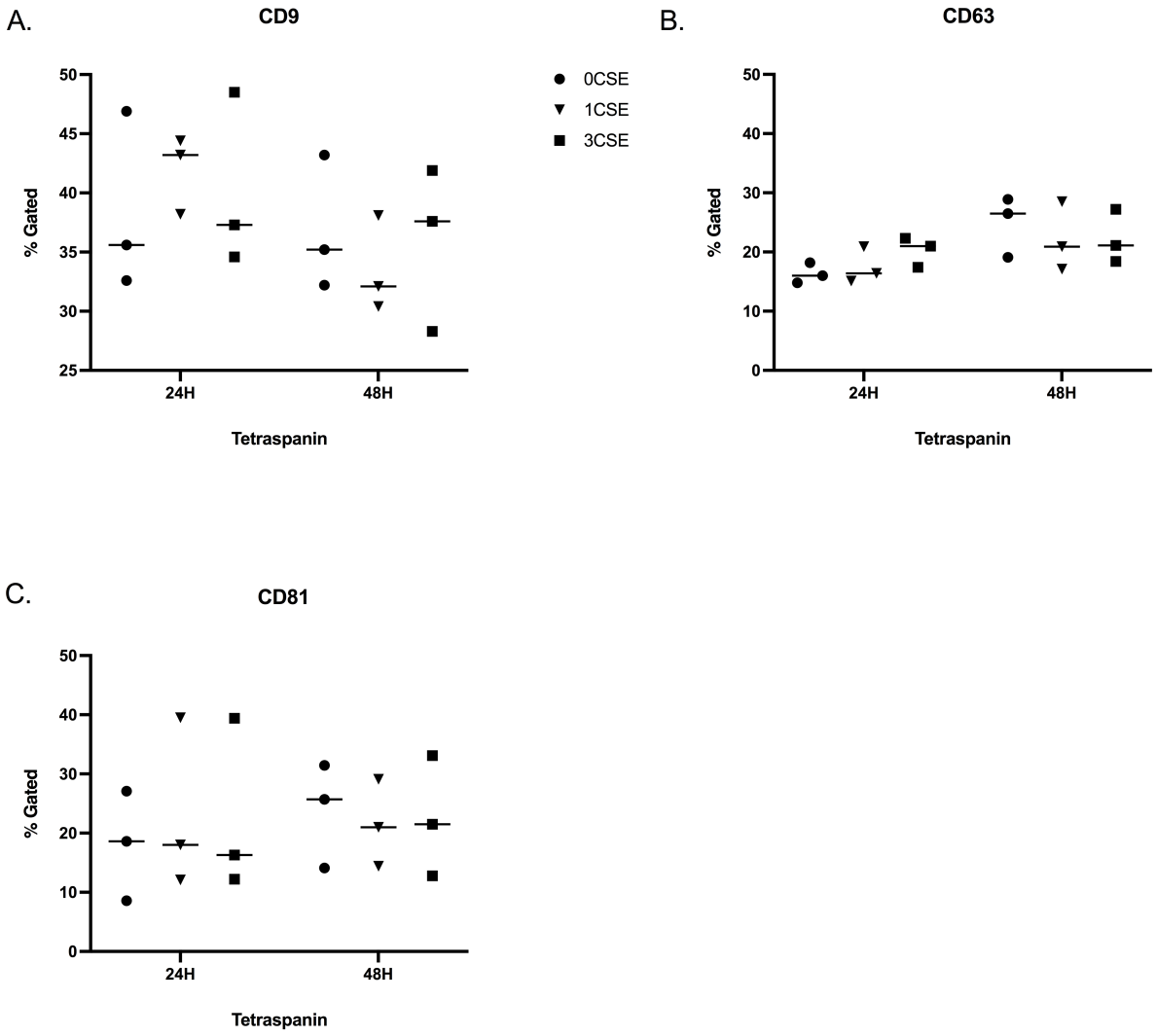

Figure 4.5. Tetraspanins on EVs produced by CSE-stimulated PBMCs. Percent of EVs positive for each CSE concentration and control at 24 hours and 48 hours for: (A) CD9, (B) CD63 and (C) CD81. Data are expressed as mean ± SD; Ordinary Two-way ANOVA; Tukey's multiple comparisons post-hoc analyses indicated no significant differences observed. (n=3 biological repeats)

4.3.3. Cigarette Smoke on EV Production by PBMCs at 32 hours.

After observing count and tetraspanin profile of EVs produced by PBMCs between 24 and 48 hours, we then applied previous techniques from section 3.1 to our current research. This included observing EV count, tetraspanins profile for single-, double- and triple-tetraspanin positive EVs, and membrane profile using the MACSPlex exosome kit,

all for EVs derived from PBMCs exposed to cigarette smoke. PBMC culture were exposed to two concentrations of cigarette smoke (1% and 3% CSE) or were unstimulated (0% CSE) to determine the effects on PBMC-derived EVs with the time point of data collection at 32 hours. This time point was chosen as there was no significant difference in EV count between 24 and 48 hours, as previously demonstrated. Results show that there were small non-significant changes in the number of sEVs produced when exposed to 1% and 3% CSE (**Figure 4.6.**).

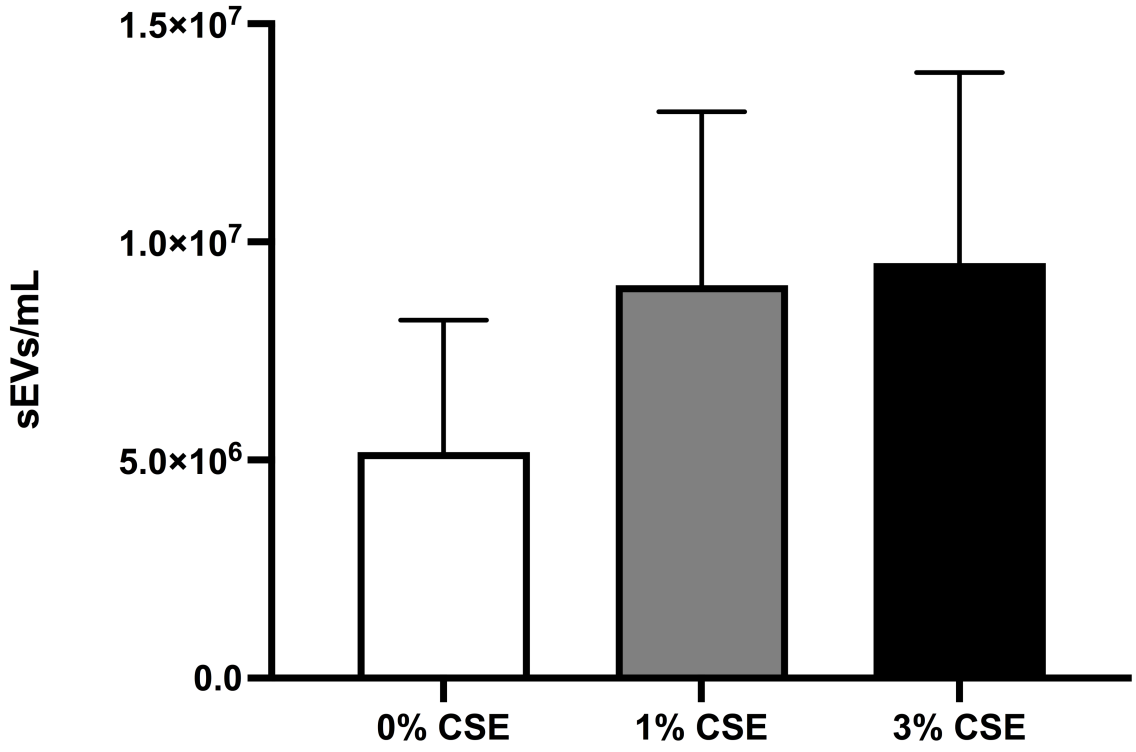

Figure 4.6. Count of small EVs (sEVs) derived from CSE-stimulated PBMCs (3 biological repeats). IFC data collected for control and CSE-stimulated samples: sEVs/mL data of control and CSE samples. Data are expressed as mean ± SD; One-way ANOVA; Tukey's multiple comparisons post-hoc analyses indicated no significant differences observed.

Furthermore, tetraspanin composition remained unchanged (**Figure 4.7.**). Results show that CD9 was most highly expressed tetraspanin, regardless of CSE concentration. Percent of EVs expressing CD63 slightly increased with exposure to CSE (1% and 3%),

however, this change was not significant. CD81+ EVs also increased with exposure to CSE, but this was also not significant.

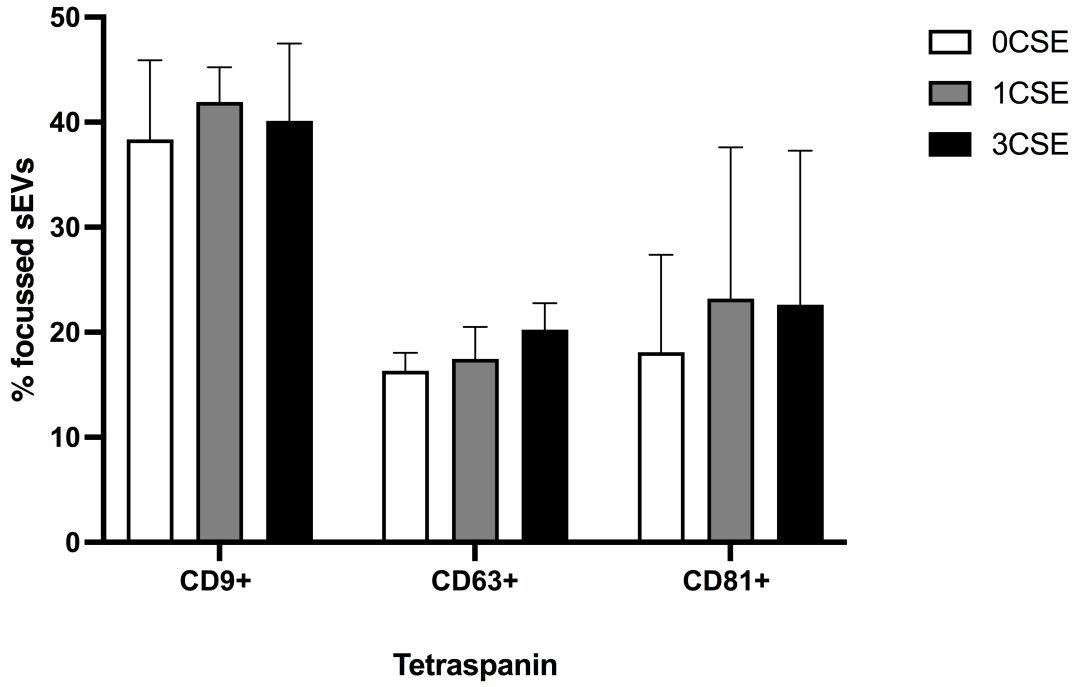

Figure 4.7. Tetraspanin expression of small EVs (sEVs) derived from CSE-stimulated PBMCs (3 biological repeats). Percent focussed sEVs/mL of control and CSE samples. Data are expressed as mean ± SD; Ordinary Two-way ANOVA; Tukey's multiple comparisons post-hoc analyses indicated no significant differences observed.

Furthermore, EVs were also analysed for subpopulations by tetraspanins expression (**Figure 4.8.**). CD9+ only (CD9+CD63-CD81-) EVs were the highest percentage, regardless of CSE concentration, with CD63+ only (CD9-CD63+CD81-) EVs being the lowest single positive tetraspanins EVs. In the double tetraspanin EV population, CD9+CD63+ CD81- and CD9+CD63-CD81+ EVs were observed more than CD9-CD63+CD81+ EVs. Finally, less than 10% of EVs were positive for all 3 tetraspanins (CD9+CD63+CD81+).

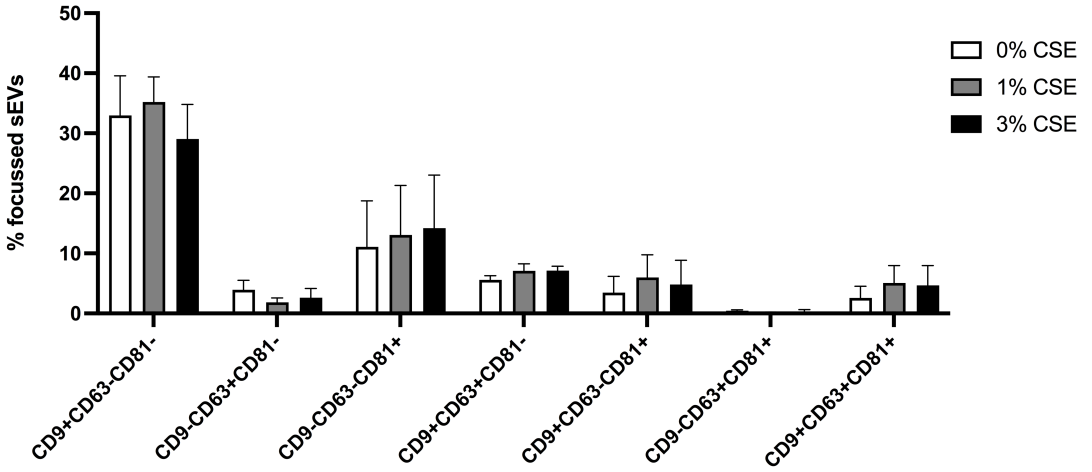

Figure 4.8. Subpopulations of EVs derived from CSE-stimulated PBMCs analysed determined tetraspanin expression (3 biological repeats). Percent focussed sEVs of control and CSE samples. Data are expressed as mean ± SD; Ordinary Two-way ANOVA; Tukey's multiple comparisons post-hoc analyses indicated no significant differences observed.

Isolated EVs from CSE-stimulated PBMCs were then profiled for the surface protein composition using the multiplex bead-based array (**Figure 4.9.**), revealing an altered profile in cigarette exposed PBMC-derived EVs. Few cell lineage markers were observed. Interestingly, CD40 was significantly downregulated at 1% CSE compared to 3% CSE ($p = 0.0371$). Immune cell markers HLA-ABC (HLA-Class I) and HLA-DRDPDQ (HLA-Class II) were present in the EVs isolated, although their levels did not change on exposure to CSE. Platelet markers, including CD62P, CD41b and CD42a, were detected at high levels. CD41b was significantly upregulated at 1% CSE compared to control ($p = 0.0295$) and 3% CSE ($p = 0.0222$), and CD42a was significantly upregulated at 1% CSE compared to 3% CSE ($p = 0.0035$). Interestingly, levels of CD69, a marker that shows activation, significantly decreased at 1% CSE compared to 3% CSE ($p = 0.0488$). Furthermore, the adhesion molecule CD31 was significantly decreased at 1% CSE compared to control ($p<0.0001$) and 3% CSE ($p = 0.0027$). Control and CSE-EVs displayed similar levels of tetraspanins. Due to the results observed here, markers CD29, CD40, CD49e, CD69 and

HLA-DR were selected for the next step of this study, where the phenotype of PBMCs producing EVs after exposure to CSE were analysed (Section 3.3.)

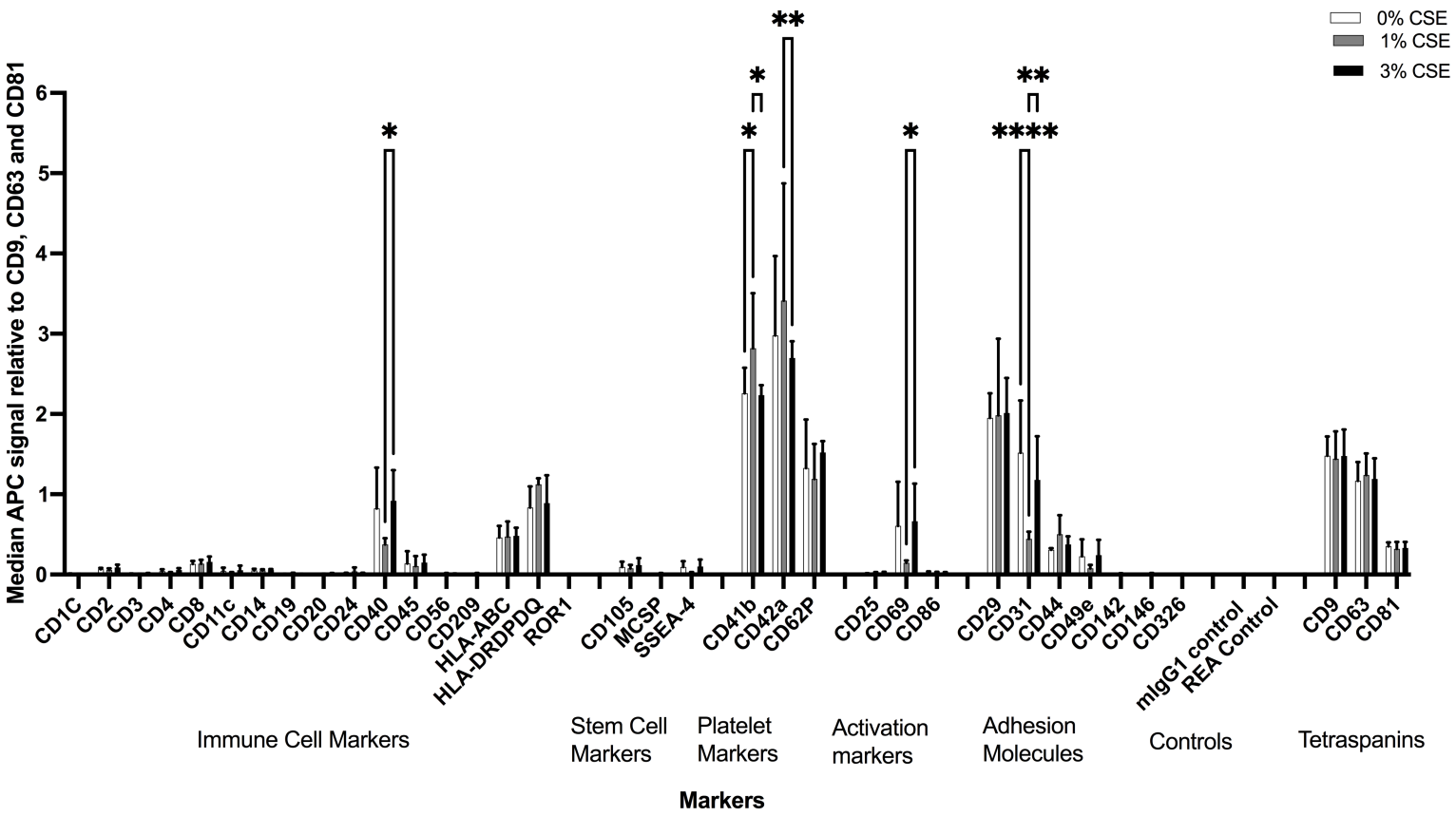

Figure 4.9. Surface marker profile of small EVs derived from CSE-stimulated PBMCs (3 biological repeats). Surface marker profiles of control and CSE-EVs. Expression of CD41b was significantly upregulated for 1% CSE-EVs compared to control ($p = 0.0295$) and 3% CSE-EVs ($p = 0.0222$). Expression level of CD42a was significantly increased between 1%CSE- and 3% CSE-EVs ($p=0.0035$). Expression levels of CD40 ($p = 0.0371$) and CD69 ($p=0.0488$) were significantly lower between 1%CSE and 3% CSE EVs. Expression levels of CD31 was significantly lower at 1% CSE compared to control ($p<0.0001$) and 3% CSE ($p = 0.0027$). Data are expressed as mean $\pm$ SD; Two-way ANOVA; Tukey's multiple comparisons post-hoc analyses.

4.3.4. Production of EVs from PBMCs exposed to CSE and ECVE

After EVs were observed from PBMCs exposed to CSE, we then wanted to compare EV production from both conventional cigarettes and e-cigarettes. To do this, PBMCs were exposed to CSE (1% and 3%), ECVE (1% and 3%). Two nicotine controls (12 μg/mL and 200 μg/mL) were also included, as well as a 0% control. Other controls in these experiments included the media-only control, detergent control and no-Calcein control. EVs for each cell culture condition were then analysed by IFC to obtain EV count and tetraspanin profile. Results show minor non-significant changes observed in EV count when PBMCs were exposed to CSE and ECVE, compared to controls (**Figure 4.10.**). PBMCs exposed to 3% CSE had a slight increase in number of EVs/mL compared to other conditions of cell culture, and this was particularly high for one donor sample. Additionally, exposure to both concentrations of nicotine produced lower count of EVs, compared to other conditions and the 0% control.

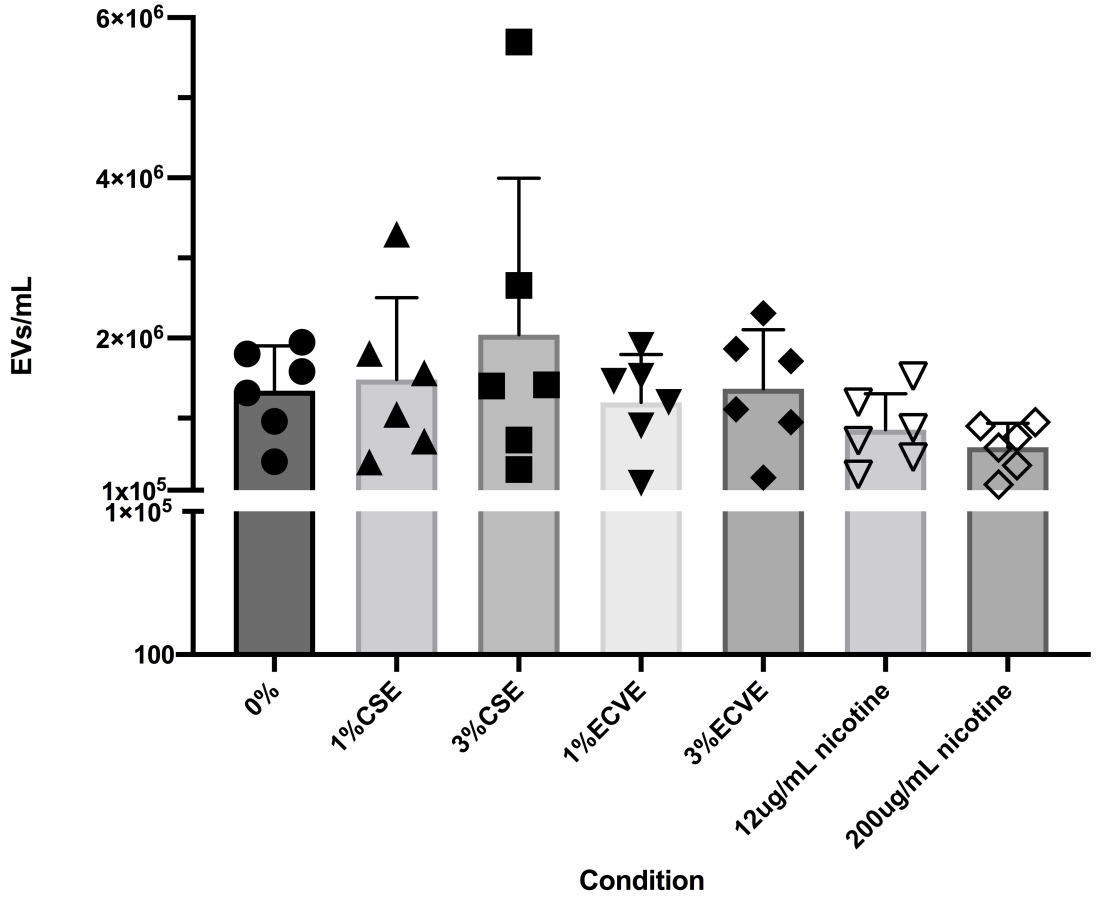

Figure 4.10. IFC analysis of EVs derived from PBMCs exposed to CSE and ECVE (n=6 biological repeats)**.** IFC data collected for controls, CSE- and ECVE-stimulated samples: EVs/mL data of control, CSE and ECVE samples. Data are expressed as mean ± SD; One-way ANOVA; Tukey's multiple comparisons post-hoc analyses indicated no significant differences observed.

4.3.5. Tetraspanin profile of EVs from PBMCs exposed to CSE and ECVE

EVs from PBMCs exposed to CSE and ECVE were also analysed for their tetraspanin profile by using IFC. Once the count was obtained (Calcein+ EVs), tetraspanins gating was added to first observe EVs that were positive for each tetraspanin, CD9, CD63 and CD81. Results show changes in tetraspanins expression for samples vs controls (**Figure 4.11.**). In particular, CD9+ EVs significantly increased for 3% ECVE compared to 0% control ($p = 0.0054$) and 200 μg/mL nicotine control ($p = 0.006$). There were additional

non-significant changes to CD9+ EVs, including increase at both CSE concentrations compared to 0% control and an increase at 1% ECVE compared to 0% control. CD63+ EVs slightly decreased at both CSE and ECVE concentrations and at 12 μg/mL nicotine, compared to 0% control and 200 μg/mL nicotine control; however, these changes were not significant. CD81+ EVs remained relatively constant under all conditions.

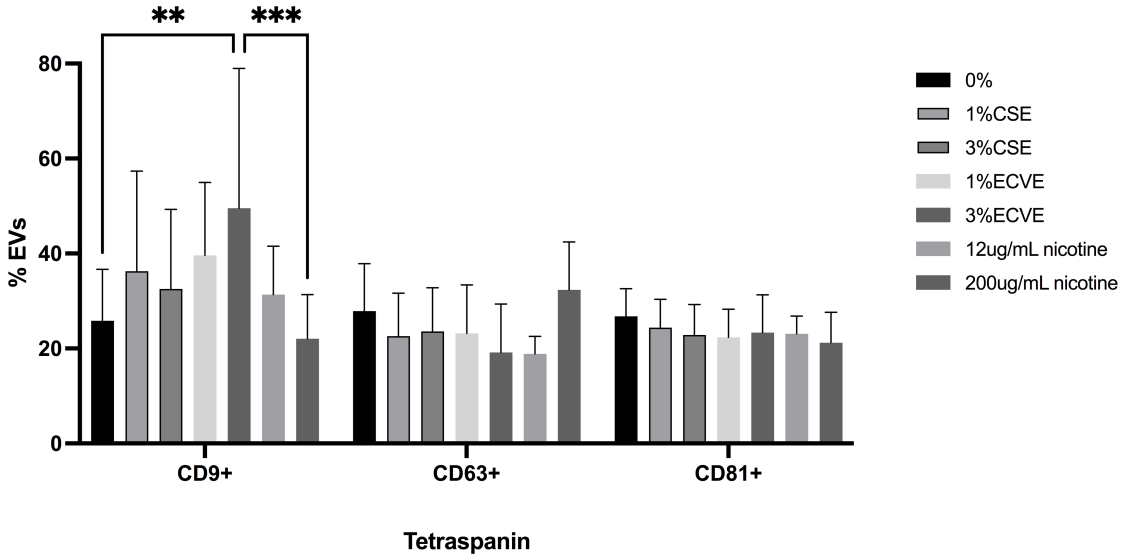

Figure 4.11. Tetraspanin expression of small EVs derived from CSE- and ECVE-stimulated PBMCs (n=6). Percent focussed EVs of controls, CSE and ECVE-samples. Percent of CD9+ EV was significantly increased between 0% and 3% ECVE (p = 0.0054) and increased between 3% ECVE and 200 μg/mL nicotine (p = 0.0006). Data are expressed as mean ± SD; Ordinary Two-way ANOVA; Tukey's multiple comparisons post-hoc analyses.

After initial observation of tetraspanin expression of the EVs, subpopulations of EVs based on their multiple tetraspanins expression were observed. Here, EVs were analysed for subpopulations expressing a single tetraspanins (CD9+ only, CD63+ only, CD81+ only), two tetraspanins simultaneously (CD9+CD63+, CD9+CD81+ or CD63+CD81+), or three tetraspanins simultaneously (CD9+CD63+CD81+). Results show significant changes in EV subpopulations after exposure to CSE and ECVE conditions compared to controls (**Figure 3.2.12.**). Specifically, the subpopulation of CD9+ only EVs

(CD9+) had significant increase after 1% and 3% ECVE ($p = 0.0162$; $p < 0.0001$, respectively) exposure compared to 0% control. There was also significant difference in percent of CD9+ only EVs (CD9+) between 1% CSE and 3% ECVE ($p = 0.0404$), and 1% CSE and 200 μg/mL nicotine ($p = 0.0430$). Interestingly, exposure to 3% ECVE had higher CD9+ EV subpopulation compared to 3% CSE ($p = 0.0046$) and 200 μg/mL nicotine ($p < 0.0001$), which are its matched CSE concentration and nicotine control.

Another subpopulation of EVs that had significant changes was CD63+ EVs (expression CD63 only), with a significant increase at 200 μg/mL nicotine compared to 3% ECVE ($p = 0.0377$). This subpopulation of EVs (CD63+) had other non-significant changes, including decrease at 1% CSE and 1% ECVE compared to 0% control, and a decrease at 3% ECVE with every other condition. The CD81+ EV subpopulation remained relatively unchanged. Furthermore, the highest double tetraspanins positive subpopulation was CD9+CD63+, whereas the lowest double tetraspanins positive subpopulation was CD9+CD81+ EVs, with no significant changes between culture conditions. EVs that were CD63+CD81+ were also relatively low compared to other EV subpopulations. Lastly, approximately 10% of the EVs were positive for all 3 tetraspanins with no significant differences in this subpopulation between cell culture conditions.

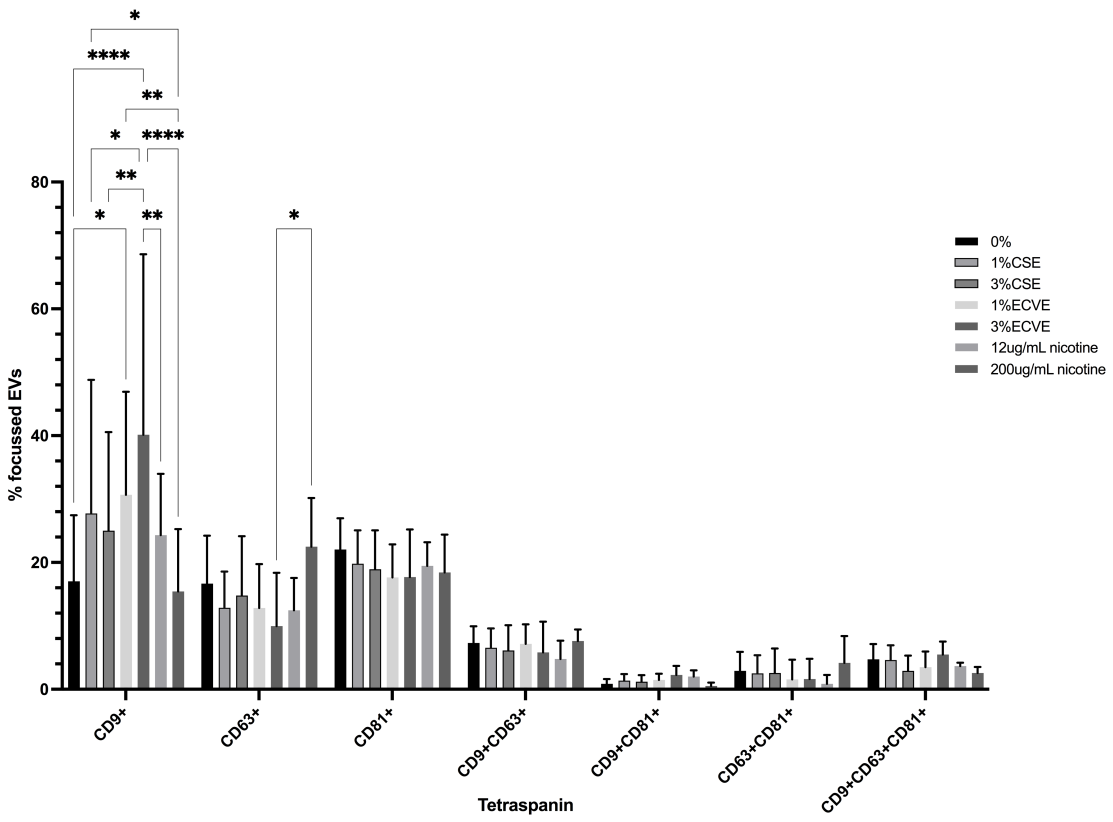

Figure 4.12. Subpopulations of EVs derived from CSE- and ECVE-stimulated PBMCs(n=6). Percent focussed EVs of controls, CSE and ECVE-samples. Compared to 0% control, percent of CD9+ EV subpopulation had significant increase after 1% CSE (p = 0.0162) and 3% ECVE (p <0.0001). Percent of CD9+ only EVs (CD9+) was also significantly increased for 3% ECVE compared to 1% CSE (p = 0404). Percent of CD9+ only EVs (CD9+) was significantly increased for 3% ECVE compared to 3% CSE (p = 0.0046) and 200 μg/mL nicotine (p <0.0001). Percent CD63+ EVs was significantly increased at 200 μg/mL nicotine compared to 3% ECVE (p = 0.0377). Data are expressed as mean ± SD; Ordinary Two-way ANOVA; Tukey's multiple comparisons post-hoc analyses.

4.3.5. Membrane profile of EVs exposed to CSE and ECVE

Due to the previous results observed of the membrane profile of EVs from CSE-stimulated PBMCs in the previous section, the difference between membrane profile of EVs exposed to CSE or ECVE were also compared. Again, PBMC cultures were exposed to two concentrations of cigarette smoke (1% and 3% CSE), two concentrations of e-cigarette vapour (1% and 3% e-cig or ECVE), two concentrations of nicotine (12 ug/mL

and 200 mg/mL) or were unstimulated (0%) to determine whether there were any differences in the expression of the 37 markers included in the MACSPlex exosome kit. Here, the median APC signal for the 0% control was subtracted from the matched median APC signal for each of the CSE, ECVE and nicotine samples to observe if there was an increase or decrease in expression of the markers on EVs derived from PBMCs following cell culture under the conditions mentioned above.

Results show that some markers did not change following exposure to CSE, ECVE or nicotine. For example, some immune cell markers, (CD1c, CD3, CD4, CD14, CD19, CD86, CD209, ROR1) and some adhesion molecules (CD142, CD146, CD326) did not change in levels following any CSE, ECVE or nicotine exposure (**Figure 4.13.**).

Interestingly, some markers did have small non-significant changes when background was subtracted. For example, MHC Class I (HLA-ABC) was down-regulated following exposure to ECVE and nicotine, but up-regulated following exposure to CSE. Here, we have subtracted the MFI of the control from the treated samples, explaining a difference in observation. Other EV markers were up- or down-regulated according to donor. For example, CD2 and CD8 expression was downregulated following exposure to CSE for one donor but not the others. MHC Class II (HLA-DRDPDQ) was downregulated for one donor but not the other two, and was also observed to be downregulated for both concentrations of E-cigarette (E-cig), but was upregulated at 200 μg/mL nicotine. Platelet markers CD41b and CD42a also had donor to donor variation, where markers were downregulated at 3% CSE. On the other hand, CD42a and CD62P were upregulated at 3% ECVE and 200 μg/mL nicotine for 2 of the 3 donors. Finally, some markers, including immune cells markers, were not expressed on EVs under any of the conditions.

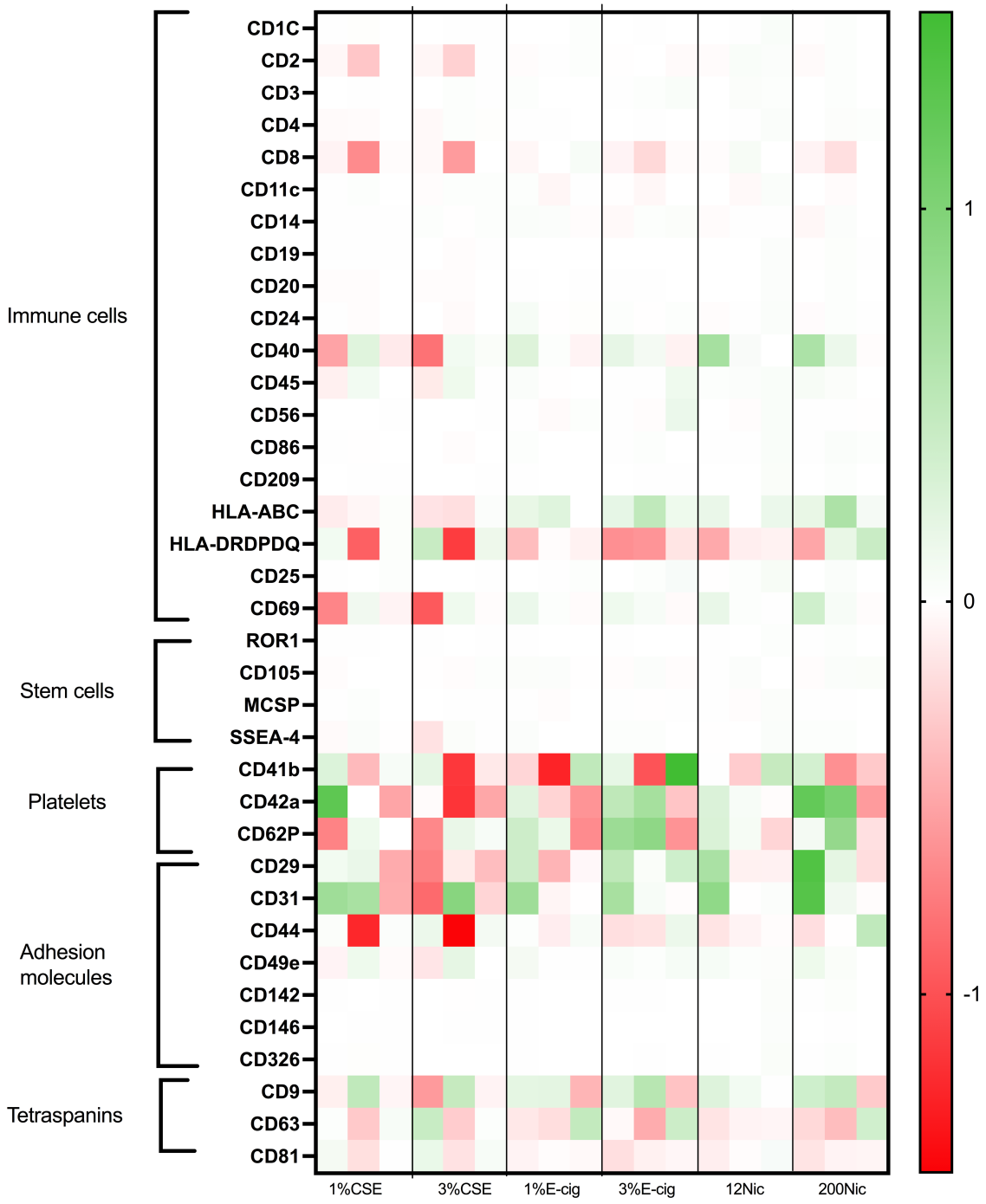

Figure 4.13. Membrane profiling of small EVs derived from CSE-stimulated and ECVE-stimulated PBMCs using the MACSPlex exosome kit. A heat map was generated using the markers included in the MACSPlex exosome kit. The median APC signal for the 0% control was subtracted from the matched median APC signal for each of the CSE, ECVE and nicotine samples. Green indicates upregulation and red indicates downregulation of makers, compared to 0% control. (n=3).

4.4. Discussion

This study focuses on the effects of CSE, ECVE and nicotine on EVs released from PBMCs. The concentrations of CSE (1% and 3%) used in this study were based on those used in previous studies observing the effect of CSE on cells in vitro [129, 486, 487] and based on a previous study of a "physiological" in vitro model to analyse cellular and histological effects of cigarette smoke in culture [490]. Results show that the method used in this study to generate CSE made reproducible samples of CSE. Absorbance at 320 nm was done to measure tar content in CSE preparations as has been shown in previous studies [129, 400, 401]. Additionally, an absorbance of 0.15 was considered as 100% CSE to standardise the concentration of CSE used for every experiment and follows from previous studies carried out in this lab [129]. Indeed, CSE generation across studies has differences in terminology, methodology and approaches. Studies have detailed methods to generate CSE, including using 8-10 puffs in 20 mL media [401, 491] or 1 cigarette in 25 mL RPMI-1640 [492] or as many as 10 cigarettes per 10 mL solvent (1 cigarette per mL), where the CSE was then classified as 100% CSE [493]. Furthermore, there are over four thousand components in cigarettes that contribute to the diversity of cigarette brands. Marlboro Red cigarettes were chosen as this was noted as the brand of cigarettes used most often by 42.4% of smokers [494]. Here, we utilised an approach that led to the consistent generation of CSE that provided reproducibility and had minimal batch-to-batch variation, as we utilised the same brand and type of cigarette (Marlboro Red), culture medium, and measured absorbance to specify final concentration in culture.

Furthermore, the concentrations of ECVE (1% and 3%) used in this study were also based on previous studies that investigated the effects of ECVE *in vitro* [260, 495, 496]. Here, as done in the previously cited studies, vaping 200 mg of e-liquid was considered as 100% e-cigarette vape extract. Additionally, the e-cigarette device was weighed before and during the experiment using a precision scale to ensure that the quantity of liquid consumed did not exceed 200 mg. ECVE generation has differences in methodology and approaches. Previous studies include using a 55mL puff volume with 3

seconds on and 30 seconds off puffing system [234, 497], or 10 x 55mL puffs in 20 mL media [401], or exposing filters to 25 puffs over 5 minutes [498], to be considered as 100% e-liquid aerosol extract. Additionally, the use of nicotine (12 μg/mL and 200 μg/mL) follows from a previous study conducted in this lab [129, 260]. The nicotine concentrations were chosen based on 12 μg representing approximately 1% of the nicotine inhaled per cigarette and 200 μg representing approximately 1% of nicotine inhaled by smoking 15-20 cigarettes per day [499] and were consistent with those used in previous studies [129, 489, 500-502].

The next step of our study was to select a time point to analyse EVs. For this, CSE was used for stimulation. Before carrying out analysis of EVs, we first observed the viability of PBMCs during exposure to CSE. Results showed no significant differences from the start of culture to 24 hours and 48 hours. Indeed, a previous study by Mian et al [487] observed that exposure to varying concentrations of CSE did not affect the viability of PBMCs; however, the study assessed cell viability using trypan blue dye exclusion. Wieczfinska et al, also observed less than 10% difference in cell viability of PBMCs after exposure to cigarette smoke ingredients compared to control, using trypan blue dye exclusion for assessment [503]. Trypan blue exclusion assay is a rapid standard and inexpensive method to distinguish viable cells from dead cells using light microscopy [504]. However, this method is subject to the problem that viability is determined indirectly from cell membrane integrity, where it may be possible that a cell's viability could be compromised while its membrane integrity is maintained [505]. On the other hand, membrane integrity may be abnormal but the cell may have the ability to repair itself and become fully viable. Additionally, dye uptake is assessed subjectively, where some cell injury may go unnoticed. As a result, trypan blue exclusion assay performed using a fluorescence microscope may result in scoring of more nonviable cells with dye uptake. A more sophisticated method used to measure cell viability is using flow cytometric analysis. In this study, AnnexinV/PI staining analysed by flow cytometry was used to assess for viable cells only. This allowed for the exclusion of any apoptotic and necrotic cells, as FITC-labelled Annexin V attaches to the surface of the early membrane-

intact apoptotic cells and to the internal phospholipids once membrane lysis occurs, and PI is used in combination to identify necrotic cells as it induces a fluorescence of the DNA in the membrane damaged cells [506]. Therefore, the flow cytometric approach allowed for more accurate and precise measurements of viable cells, as dye exclusion is more likely to lead to error due to operator subjectivity.

Once viability of cells was confirmed, we then compared EV production at 24 hours and 48 hours after exposure to CSE. There were no significant differences in EV production from PBMCs after exposure to CSE between 24 and 48 hours. A study by Russell et al [367] observed no significant differences in particle number derived from immature dendritic cells in CSE-conditioned media and unconditioned media (control) from day 1 to day 5 of exposure. Currently, there are limited studies that observe EV production between 24 and 48 hours after exposure to CSE or CS components. Additionally, in this experiment, we observed that one donor had a very high count of EVs/mL at 48 hours after exposure to 1% CSE compared to the other donors who had decreased EVs/mL at 48 hours. This donor confirmed that they smoke cigarettes every day. A previous study has shown that the numbers of circulating EVs were increased in smokers compared to non-smokers [341], possibly suggesting that cells of smokers may be more sensitive to cigarette smoke [503, 507]. Tetraspanin profile of the EVs was also analysed at 24 hours and 48 hours, where CD9 tetraspanin was found to be the highest expressed at both time points, followed by similar levels of CD63 and CD81. A study by Pugholm et al [508] detected CD9 on all leukocyte-derived EVs. Additionally, the study also observed CD81 on all EVs but at lower levels, with CD63 only detected on EVs from cultured T cells [508]. Furthermore, no significant differences in tetraspanin expression were observed between EVs from CSE-stimulated PBMCs versus controls and between 24 and 48 hour timepoints in this study. Therefore, with the results of this experiment, it was decided that going forward EV analysis would be carried out at 32 hours to allow for time in setting up experiments that will observe PBMC phenotype and EV count and membrane profile following exposure to both CSE and e-cigarette vape extract (ECVE).

Having optimised and demonstrated novel techniques to study PBMC-derived EVs, including IFC and a rapid staining protocol that allows for quantification of EVs in culture and following isolation as described in section 3.3.1., these methods were then applied to current research in the lab, specifically smoking-related inflammatory conditions. Here, PBMCs were exposed to CSE (1% and 3%) or were unstimulated (0% CSE) and EVs were analysed by IFC for EV count and tetraspanin profile and membrane profile was analysed using the MACSPlex exosome kit. No significant differences were observed in the number of sEVs from control or CSE-exposed PBMCs. A previous study has reported significantly more EVs released from CSE-exposed primary human DCs (iDCs) [367], although CSE concentration for that study was markedly higher at 50%, which is beyond physiological range. In this study, we used CSE concentrations of 1% and 3%, consistent with previous studies of the effects of CSE on cells in vitro [129, 486-489]. Furthermore, observation of tetraspanin expression in this study showed that tetraspanin composition remained unchanged after exposure to CSE. CD9 was the highest expressed tetraspanins, followed by CD81, with CD63 being the tetraspanin least expressed. Previous studies have also noted that some tetraspanins may be observed in lower intensities compared to others, particularly studies have noted lower intensities for CD63 compared to CD9 and CD81 [509-511]. This highlights the importance of using a cocktail of antibodies against tetraspanins to observe EVs, as has been done in this study, as using a single α-tetraspanin antibody may overlook some subsets of EVs. Additionally, EVs expressing both CD9 and CD63 was the highest detected double tetraspanins positive subpopulation followed by CD9 and CD81, although this was relatively low compared to other subpopulations of EVs. EVs bearing both CD63 and CD81 were minimally detected. Cho et al [512] observed that a small percentage of HEK293 EVs were CD81/CD63 double positive (2.3%) compared to other subpopulations, where EVs were labelled with a cocktail of three fluorescent antibodies and measured using NTA. Han et al [473] observed that the proportions of CD63/CD81 double positive HEK293-EVs were negligible (below 3%), where analysis was done using total internal-reflection microscopy. Additionally, in this study about 5% of EVs were shown to bear all

three tetraspanins, with non-significant increases after exposure to CSE. Studies by Cho et al [512] and Han et al [473] observed 21% and 5% of EVs to be positive for all three tetraspanins, respectively. Studies observing triple tetraspanins-positive EVs are limited, with this study being the first to observe this subpopulation of EVs using IFC. Furthermore, studies have shown that immune-cell derived EVs are functionally active as they harbour a range of immune cell-derived surface receptors and effector molecules from parental cells [513-516]. As a result, immune cell-derived EVs can modulate specific mechanisms of the innate and adaptive immune response. Therefore, we examined the expression of 37 exosomal surface markers in sEVs isolated from PBMCs exposed to CSE at different percentages, reflecting membrane proteins of the original cells. Data from the MACSplex assay show significant differences in expression of CD40, CD41b, CD42a, CD69 and CD31 between control and CSE or between CSE concentrations. CD40 is a costimulatory molecule expressed by B cells, professional antigen-presenting cells (including macrophages/monocytes, and dendritic cells), sometimes T cells, as well as non-immune cells and tumours [517-519]. CD40-CD40L coupling is important in various aspects of the immune response, including activation of kinases, expression of genes related to cellular stress, regulation of apoptosis, expression of surface molecules, as well as activation and differentiation of immune cells and autoimmunity [518, 520, 521]. Cigarette smoke has been shown to increase CD40 expression on lung mononuclear cells of mice exposed to cigarette smoke for 4 weeks and on bone marrow derived dendritic cells from healthy mice cultured in vitro with CSE for 24 hours [522]. Another study demonstrated an initial increase in CD40 expression in primary murine DCs cultured in vitro with CSE for 24 hours, however, this expression was significantly downregulated after continuous CSE exposure [119]. Here, exposing human PBMCs to CSE *in vitro* for up to 48 hours, we show significantly decreased levels of CD40 positive EVs at 1% CSE, suggesting that timing of exposure may also affect expression of CD40 observed. Additionally, in this study, we show significantly increased percentages of CD41b and CD42a positive EVs at 1% CSE. CD41b and CD42a are markers of platelets, suggesting these are platelet-derived EVs [480, 523]

however, currently there is no research on platelet derived EVs and cigarette smoking. A previous study, however, has noted that platelet derived EVs were significantly increased after exposure to active inhalation of e-cigarette vapour with nicotine [348]. CD69 is detected on the surface of activated lymphocytes as an early lymphocyte activation marker [478]. CSE has previously been shown to significantly inhibit the expression of CD69 by natural killer cells [137, 524]. However, cell surface expression of CD69 on cytotoxic T cells was enhanced in BALF of patients with COPD and smokers with normal lung function compared to never-smokers [525]. In this study, decrease of CD69 expression on EVs was observed at 1% CSE suggesting reduced activation of cells producing EVs after exposure to 1% CSE. Additionally, EV expression of CD31 decreased at 1% CSE concentration compared to control and 3% CSE concentration. CD31 is an endothelial cell adhesion molecule expressed by vascular endothelial cells platelets and leukocytes [526, 527] and is thought to have a function in downregulating T cell activation [527, 528]. Contradicting studies have shown increased CD31 expression in EVs derived from primary human DCs exposed to 50% CSE [367] and increased CD31+ EMPs in circulation in rats after exposure to cigarette smoke [320, 345]. Here, we also observed expression of HLA-ABC (MHC-I) and HLA-DRDPDQ (MHC-II), although there were no significant differences in level of expression between concentrations of CSE and controls for both markers. A previous study has shown increased expression of HLA-ABC in EVs derived from primary human dendritic cells exposed to 50% CSE [367]. Another study observed significantly lower expression of HLA-ABC and HLA-DRDPDQ in bronchoalveolar lavage-derived macrophages from smokers, however, the study also exposed alveolar macrophages from healthy volunteers to 10% CSE in vitro and observed no significant differences in expression of HLA-ABC or HLA-DRDPDQ [529]. HLA-ABC is fundamental for the activation of cytotoxic CD8+ T lymphocytes and can be found on the surface of almost all nucleated cells [530, 531]. HLA-DRDPDQ molecules are classically found only on B cells and antigen presenting cells, such as dendritic cells and macrophages, thus having the ability to activate CD4+ T cells [530]. Furthermore,

there were no significant differences in the expression of tetraspanins CD9, CD63 and CD81 between control and CSE-stimulated EVs.

Finally, EV production was observed from PBMCs exposed to both CSE and ECVE to compare the effects between cigarette smoking and e-cigarette vaping. It is important to note that e-cigarettes are being promoted as a safe alternative to cigarette smoking. Furthermore, the use of e-cigarettes has increased rapidly, in particular amongst adolescents and young adults [532]. E-cigarette use is higher among young adults aged 18-24 compared to other adult age groups [533]. Hence, in this study we compared the effects of e-cigarette and cigarette smoke on production of EVs by PBMC. To do this, we examined the number of EVs produced under both conditions, in addition to nicotine and a negative control. Subpopulations of EVs based on tetraspanins profile was also observed, and finally membrane profile was characterised under all conditions to observe if there were any changes. Here, no significant differences in number of EVs produced under any of the conditions were observed. Singh et al [392] observed no significant difference in plasma particle concentration between cigarette smokers, e-cigarette users and dual smokers, where particle concentration was obtained using NTA. Research comparing EV number or concentration is limited in both *in vivo* and *in vitro* studies, highlighting the importance of research in this area. Furthermore, this study observed significant differences of tetraspanins between conditions. Particularly, CD9 percentage was significantly different between control and 3% ECVE, with CD9 being significantly increased at 3% ECVE. A previous study by Kumar et al [534] observed levels of CD9 in plasma EVs in rats after “self-administration” of nicotine with menthol through the use of an implant and noted an increase in CD9 levels compared to before self-administration. They observed no differences in expression of CD3 positive EVs.

In our study, when observing subpopulations of EVs based on multiple tetraspanins expression, significant differences were observed under exposure to both CSE and ECVE compared to controls. In particular, single CD9+ tetraspanin was significantly increased after exposure to both concentrations of ECVE compared to control and compared to nicotine. This significant increase was also observed between 3% ECVE and its matched

CSE (3%) and nicotine (200 μg/mL) concentrations. Single CD63+ EVs also had significant changes with 3% ECVE compared to its matched nicotine control. CD9 and CD63 are tetraspanins that function in the formation and cargo recruitment of EVs. Pugholm et al [508] noted that EVs released from cultured PBMCs displayed fewer markers than EVs derived from monocultures and additionally noted that cellular and vesicular presentation of lineage-specific and vesicle-related makers differed.

In addition, membrane marker profile was also compared for each condition (CSE, ECVE, nicotine and control). It is well known that EV content, including protein and surface marker profile, may be dependent on the cell source, its activation status and other factors [535, 536]. Thus, analysis of EV surface signature in biological fluid may have the potential to reveal changes in the parent cell types releasing the EVs, leading to the possible ability of identifying EV surface marker profiles that may correspond to health conditions; and therefore, the use of EVs as biomarkers of disease. Here, we used a multiplex-bead based flow cytometry assay to assess surface proteins on EVs from PBMCs cultured under different treatments (CSE, ECVE, nicotine and control). Other new methods and assays to study surface markers on EVs based on flow cytometry have been described; however, some may be time-consuming and may demand extensive operator expertise for sample preparation, acquisition and data analysis. The multiplex-bead based flow cytometric assay used here is compatible with most standard flow cytometers and allows for robust and simultaneous semi-quantitative detection of up to 37 different EV surface markers in one sample. A study by Wiklander et al [537] showed that the kit facilitates analysis from limited cellular material and low supernatant volumes with high reproducibility. They also indicated that this multiplex bead-based assay is suitable for detection, quantification and comparison of EV surface signatures in different sample types, including unprocessed cell culture supernatants, cell culture-derived EVs isolated by different methods, and biological fluids [537]. The results in our study showed donor-to-donor variation for markers and that EVs did not express some markers included in the MACSPlex exosome kit. Archibald et al previous suggested that markers may not be detected on the MACSPlex kit due to the marker being primarily

carried on medium-large EVs rather than on small EVs or on exosomes [538]. This was further supported by Elkstrom et al [536], who suggested that absence of some markers may be due to the markers being mainly distributed on microvesicles and not on small EVs/exosomes [536].

In conclusion, this study has observed and profiled EVs derived from PBMCs after exposure to cigarette smoke extract (CSE), e-cigarette vape extract (ECVE) and nicotine, compared to control. We showed that number of EVs produced by PBMCs did not significantly change under any of the conditions. We did, however, observe significant differences in tetraspanin profile of EVs, particularly for CD9 and CD63, between conditions. We also observed that the protein and surface marker profile of EVs was affected by CSE treatment. As we have observed the number and surface profile of EVs being produced by PBMCs under the treatments mentions, it is also important to observe the effect of CSE, ECVE and nicotine on PBMC phenotype, which is the next step of this study.

5.0. Effect of CSE and ECVE on PBMCs

5.1. Introduction

Chronic cigarette smoking increases the risk for the development of various conditions including COPD, cardiovascular disease, stroke and cancer. Oxidative stress and chronic inflammation induced by smoking alters innate and adaptive immune responses. The effect of tobacco products on PBMCs have been previously assessed. Previous study has shown that exposure to whole-smoke conditioned medium potently suppressed agonist-stimulated cytokine secretion and target cell killing in PBMCs [539]. Indeed, PBMCs isolated from cigarette smokers have been shown to have attenuated cytotoxic activity [487] and significant decrease in induction of IL-15 by poly I:C [137]. Furthermore, van Leeuwen et al [540] previously observed that cigarette smoke condensate and its constituents caused changes in gene expression in human PBMCs *in vitro*, including expression of SERPINB2, which is activated in response to cell stress. Arimilli et al [541] observed that whole-smoke conditioned media significantly inhibited biological functions in PBMCs, including functions related to cell migration, survival and proliferation, and activation and chemotaxis of blood cells.

The acute and long-term effects of e-cigarettes on PBMCs have not been fully elucidated. Di Biase et al has previously observed that e-cigarette vapour caused an increase in ROS similar to that of cigarette smoke in immune cells from rats [542]. Studies observing whole PBMC populations on exposure to e-cigarettes are limited, however, some studies have observed exposure on individual immune cell populations. Gomez et al [543] observed that e-cigarette vapour extracts impaired phagocytic function and cytokine response in macrophages in response to *Mycobacterium tuberculosis* burden. Scott et al [234] observing decreased viability of AMs, excessive ROS production and increased inflammatory cytokines and chemokines production after exposure to e-cigarette vapour condensate, suggesting that e-cigarette vapour may induce an inflammatory state in AMs within the lungs. Furthermore, Chen et al [260] observed that e-cigarette vapour affected human DCs, as exposure suppressed HLA-DR

and CD86 expression, enhanced IL-6 production, and significantly upregulated signalling molecules and cytoplasmic proteins in DCs. Current research investigating the effect of e-cigarettes on immune cells is limited, highlighting the need to shed light on how exposure to e-cigarette vapour may lead to changes in immune cells.

In this study, we have analysed immune cell-derived EVs from PBMCs after exposure to CSE, ECVE and nicotine. It is, however, also important to observed the effect of CSE, ECVE and nicotine on PBMCs themselves. Previously, we have examined cell viability to meet MISEV guidelines, but we have not shown cell phenotypes. To date, there is limited research looking at immune cell profiles using high throughput high parameter flow cytometry, so the aim of this chapter is to define how CSE, ECVE and nicotine affects the immune cell phenotype and profile. In addition, we aim to observe any changes in markers previously identified on EVs after exposure to treatment. Markers of interest were selected on the results from the MACSPlex exosome kit and included CD29, CD49e, CD40 and HLA-DR. CD29 was selected as it was found to be a highly expressed adhesion molecule on EVs previously collected. Also known as integrin beta-1, CD29 is expressed by various cell lineages [544], including immune cells, such as T cells, B cells, NK cells [545], polymorphonuclear lymphocytes (PMNL) and monocytes [546]. CD40 and CD49e were found to have been downregulated on EVs following 1% CSE exposure, and HLA-DR was selected as it was found to be one of the higher expressed immune cells markers on EVs. CD49e, also known as integrin α5, is an adhesion molecule expressed on monocytes [547], T cells [548], B cells [549, 550] , NK cells [551], and DCs [552]. HLA-DR, or MHC II, is a key cell surface receptor expressed on antigen presenting cells, including dendritic cells, B cells, monocytes and macrophages. CD40 is expressed by B cells and other various cells, including DCs, monocytes, macrophages, mast cells, epithelial cells and endothelial cells [553].

5.2. Methods

5.2.1. Processing of blood samples and Peripheral Blood Mononuclear Cell (PBMC) Isolation.

Blood was drawn by venepuncture and collected into heparin tubes for PBMC isolation. Isolation of PBMCs from fresh whole blood was done by histopaque density gradient centrifugation. Full details of the methodology can be found in chapter 2 section 2.1 and details of reagent used are in table 2.1.

5.2.2. Conditioned smoke extract

CSE was made fresh on the day of the experiment to be used as quickly as possible. Details of the method can be found in Chapter 2, section 2.3.

5.2.3. E-cigarette vape extract

E-cigarette solution was made fresh on the day of the experiment and used as quickly as possible. Details of the method can be found in Chapter 2, section 2.4.

5.2.4. Extracellular Staining

Cells were stained with viability dye and surface markers (Table 3.3.1.), and incubated in the dark for 30 minutes at 4 °C. Cells were then washed with PBA (PBS, 0.5-1% BSA, 0.1% NaN3 sodium azide*) at 500xg (9↑, 9↓) for 10 minutes. Cell were fixed with 4% paraformaldehyde and stored at 4 °C.

Table 5.1. Flow cytometry panel for cell surface markers.

Target	Fluorophore	Clone	Product code	Manufacturer	Volume per 100 μL of cells (μL)
Live/Dead	Zombie Aqua		423101	Biolegend	0.3
CD3	PerCP-Cy5.5	OKT3	317336	Biolegend	1
CD4	APC-Fire750	RPA-T4	300560	Biolegend	2
CD8	Alexa Fluor 700	SK1	344724	Biolegend	2
CD56	Brilliant Violet 785	5.1H11	362550	Biolegend	2
CD14	Brilliant Violet 605	63D3	367126	Biolegend	2
CD19	Brilliant Violet 650	SJ25C1	363026	Biolegend	2
CD16	Alexa Fluor 488	3G8	302019	Biolegend	2
CD11c	PE-Cy7	Bu15	337216	Biolegend	2
CD69	PE/ Fire640	FN50	310960	Biolegend	2
CD29	PE	TS2/16	303004	Biolegend	2
HLA-DR	Brilliant Violet 711	L243	307644	Biolegend	2
CD40	Brilliant Violet 421	5C3	334332	Biolegend	2
CD49e	APC	NKI-SAM-1	328012	Biolegend	2

5.2.5. Flow Cytometry

A minimum of 200,000 lymphocytes were acquired by flow cytometry using an ID7000 spectral cell analyzer (Sony Biotechnology). A spectral matrix was constructed by analyzing single colour controls samples for all fluorophores before data was spectrally unmixed using the weighted-least squares method. Exported data was analysed using Kaluza (v2.1 Beckman Coulter).

5.2.6. High Dimensional Analysis of Flow Cytometry Data

Single viable lymphocytes were gated in FlowJo (V10, Becton Dickinson, Plymouth, UK) before equal sampling of 20,000 events from each donor with DownSample plugin, as reducing the number of events fed intro an algorithm will increase speed of calculation of t-SNE and FlowSOM. The downsampled populations were concatenated in one single file. t-distributed stochastic-neighbour embedding (t-SNE) was performed with opt-SNE learning configuration [408], 1000 iterations, a perplexity of 30, learning rate of 3500, Exact (vantage point tree) KNN and Barnes-Hut gradient algorithm. Next, with FlowSOM and Cluster explorer plugins, FlowSOM clustering [409] was performed using 15 meta-clusters and projected on the t-SNE using Cluster Explorer.

5.2.7. Data analysis

Data analysis was performed using Prism software, version 9.5.0. (GraphPad). Statistically significant differences of cell viability between conditions were assessed with Ordinary one-way ANOVA, followed by Tukey's multiple comparisons test, with a single-pooled variance. Statistically significant differences of CD8+ T cells, CD4+ T cells, NK cells and NK cells between all conditions were analysed by Ordinary two-way ANOVA, followed by Tukey's multiple comparisons test, with a single-pooled variance. Statistically significant differences in activation (CD69+) of CD8+ T cells, CD4+ T cells, NK cells and NK cells between all conditions were analysed by Ordinary two-way ANOVA, followed by Tukey's multiple comparisons test, with a single-pooled variance. Statistical significance of differences in CD14+ monocytes, CD19+ B cells and CD11c+SSCHi DCs between all conditions was determined by applying a two-tailed Student's t test. Statistically significant differences of MFI of CD29 for every population identified between all conditions were assessed by Ordinary one-way ANOVA followed by Tukey's multiple comparisons test, with a single-pooled variance and this was repeated for CD49e. Statistically significant differences of MFI of HLA-DR for every population identified between all conditions were assessed by Ordinary two-way ANOVA followed by Tukey's multiple comparisons test, with a single-pooled variance and this was

repeated for CD40 Finally, statistical significance of differences of population 0 identified during cluster analysis between all conditions were analysed by Ordinary two-way ANOVA followed by Tukey's multiple comparisons test, with a single-pooled variance and this was repeated for populations 1-14. Significance for tests was defined as $P < 0.05$.

5.3. Results

5.3.1. Viability of PBMCs

Prior to analysing the phenotype of PBMCs, viability of cells for each treatment was assessed using Zombie-Aqua viability dye. First, analysis density plots of Forward Scatter (FCS) vs Side Scatter (SSC) were created to exclude debris (**Figure 5.1.A.**). Density plots of SSC-Area vs SSC-Height were then created to gate for single cells (**Figure 5.1.B.**). Viable cells were then gated as shown in representative density plot of Zombie-Aqua vs SSC (**Figure 5.1.C.**).

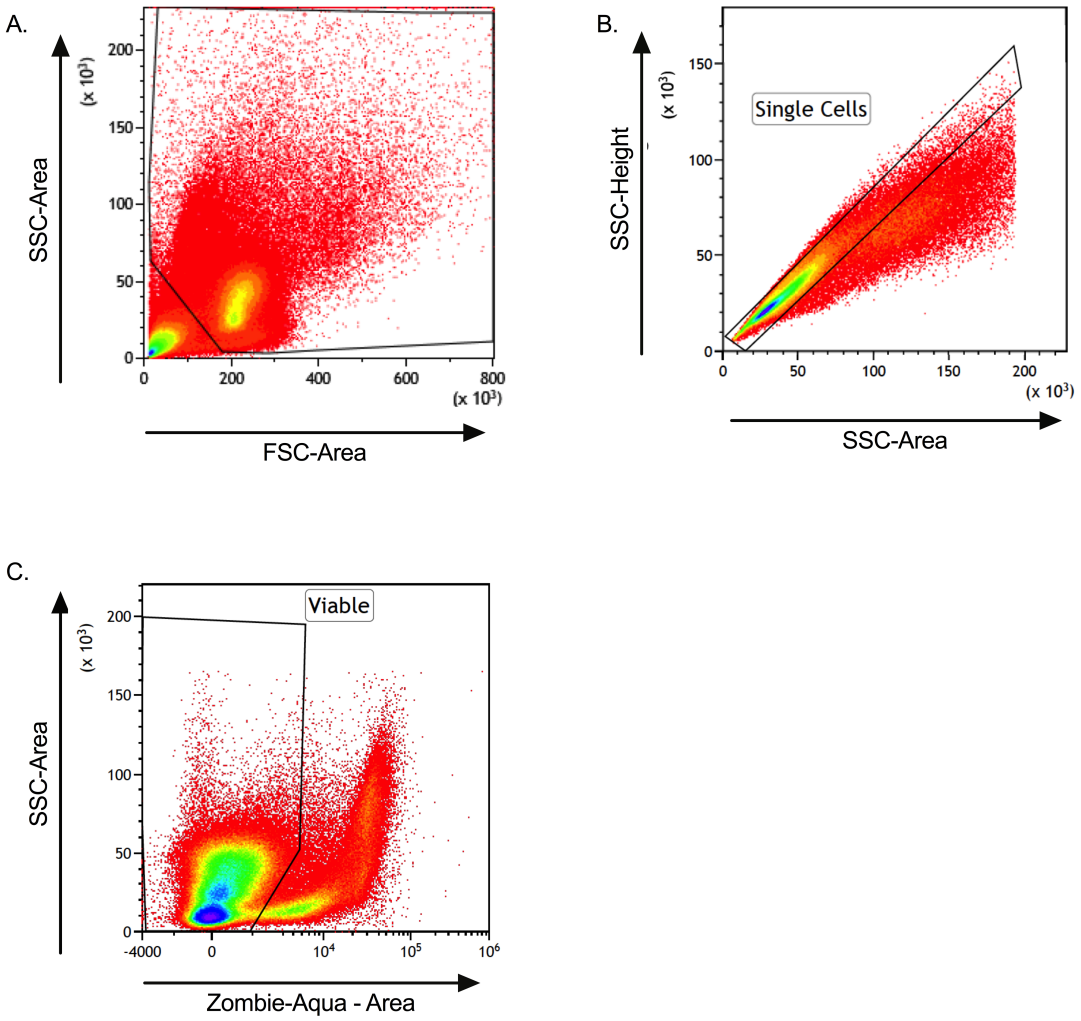

Figure 5.1. Spectral flow cytometry for analysis of PBMCs. Representative density plots of: (A) Forward Scatter (FCS) vs Side Scatter (SSC) to exclude debris; (B) of SSC-Area vs SSC-Height to select single cells; (C) Zombie-Aqua vs SSC to gate for viable cells.

Results show that there were no significant differences in % of total viable cells between the different treatments with either CSE, ECVE or nicotine (**Figure 5.2.**).

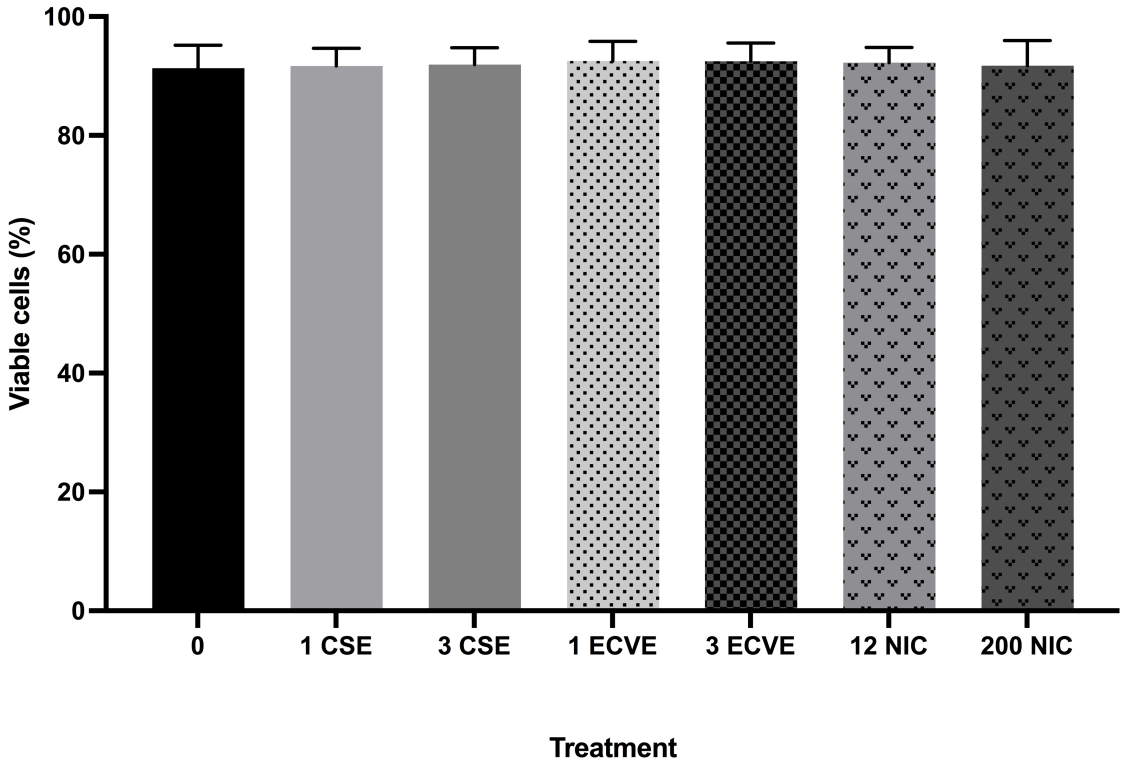

Figure 5.2. Viability of PBMCs (n=6 biological repeats). Viability of PBMCs had no significant changes between treatments. Data are expressed as mean ±SD; Ordinary one-way ANOVA; Tukey's multiple comparisons post-hoc analyses.

5.3.2. PBMC phenotype profiling

PBMCs were then profiled with 13 surface markers (in addition to zombie-aqua viability dye) to observe PBMC populations under each treatment. Gating was carried out based on pattern of expression and using unstained samples. After gating for viable cells, spectral flow analysis density plots of CD3 vs SSC were created for identification of CD3+ cells **(Figure 5.3.A.i.).** Density plots of CD8 vs CD4 for CD3+ cells were then created to gate for CD8+ T cells (CD3+CD8+) and for CD4+ T cells (CD3+CD4+) (**Figure 5.3.A.ii.**). A density plot of CD3 vs CD56 with a Boolean operator [CD14 NOT CD19] was created to select for CD3+CD56+ NKT cells (**Figure 5.3.B.i.**). Here, Boolean gating allows for

combination of previously defined gates using logical operators (AND, NOT and OR) to determine whether events in the gate are to be included or excluded. A density plot of CD16 vs CD56 with a Boolean operator [NOT CD3 NOT CD14 NOT CD19] was then created to select for NK cells (**Figure 5.3.B.ii.**), as NK cells are known to lack expression of CD3, CD14 and CD19 but express CD16 and CD56 [554, 555].

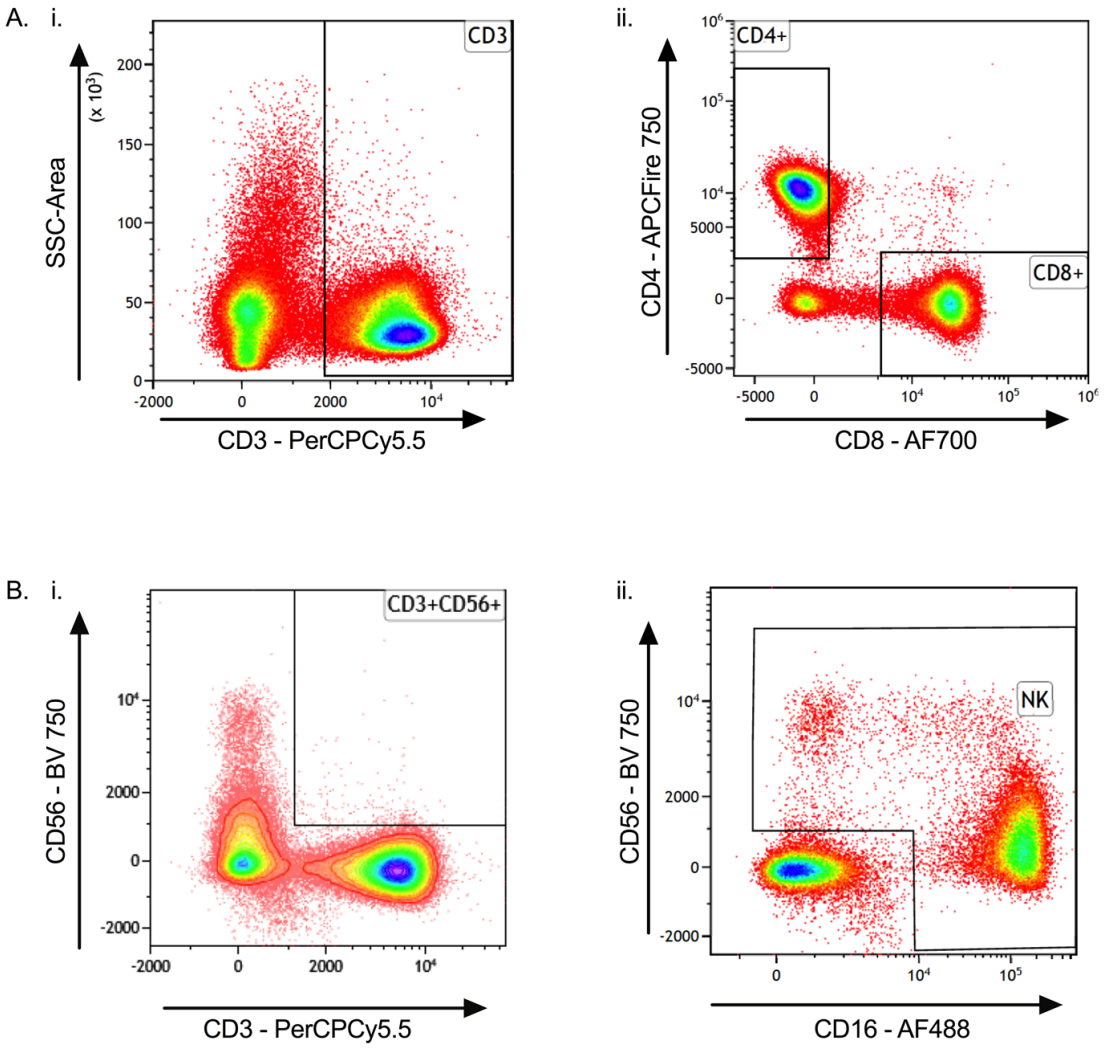

Figure 5.3. Spectral flow cytometry analysis of PBMC populations. Representative spectral flow analysis density plots of: (A) (i) CD3 vs SSC to select CD3+ cells; (ii) CD8 vs CD4 for CD3+ cells to gate for CD3+CD8+ and CD3+CD4+ T cells; (B) (i) CD3 vs CD56 with Boolean operator [CD14 NOT CD19] to select for CD3+CD56+ cells; (ii) CD16 vs CD56 with a Boolean operator [NOT CD3 NOT CD14 NOT CD19] to gate for NK cells that were CD56+.

Results showed cell populations as % of total viable cells (**Figure 5.4.**). Here, after viable cells were selected, the % of each cell population was calculated within the total viable cells. Results show that there were no significant differences in % of total viable cells between conditions for each cell population (**Figure 5.4.**). Additionally, CD4+ T cells was the cell population present in the highest percentage of viable PBMCs, making up over 40% of the cell population. CD8+ T cells were the second highest population, making up between 20-30% of the cell population. CD56+ NK cells made up the third highest population, making up between 10-15% of viable cells. NKT cells that were CD3+CD56+ made up about 2% of the viable cells.

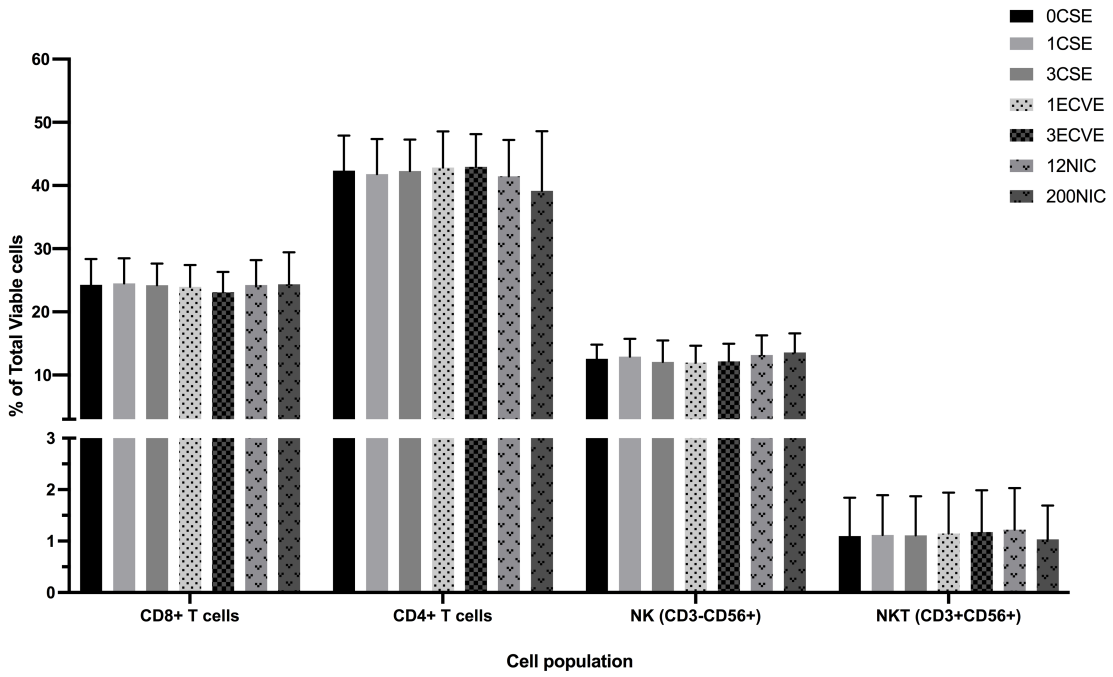

Figure 5.4. PBMC populations (n=6)**.** CD8 and CD4 T cells, NK cells (CD56+) and NK T cells (CD3+CD56+) present in PBMCs in control versus treatment groups. There were no significant differences in populations after treatment compared to control. Data are expressed as mean ± SD; Ordinary Two-way ANOVA; Tukey's multiple comparisons post-hoc analyses indicated no significant differences observed.

Activation of cells identified was then analysed with the use of CD69, an early marker of activation for T cells, NK cells and NKT cells. Spectral flow analysis density plots of CD69 vs CD4 was done for identification of CD3+CD4+ T cells (that were CD69+ (**Figure 5.5.A.i.**). Density plots of CD69 vs CD8 was then created for identification of CD3+CD8+ T cells that were CD69+ (**Figure 5.5.A.ii**.). Density plots of CD69 vs SSC was then created for CD3+CD56+ cells to identify NKT cells that were CD69+ (**Figure 5.5.B.i.**). Density plots of CD69 vs SSC was then created for NK cells to identify cells that were CD69+ (**Figure 5.5.B.ii.**).

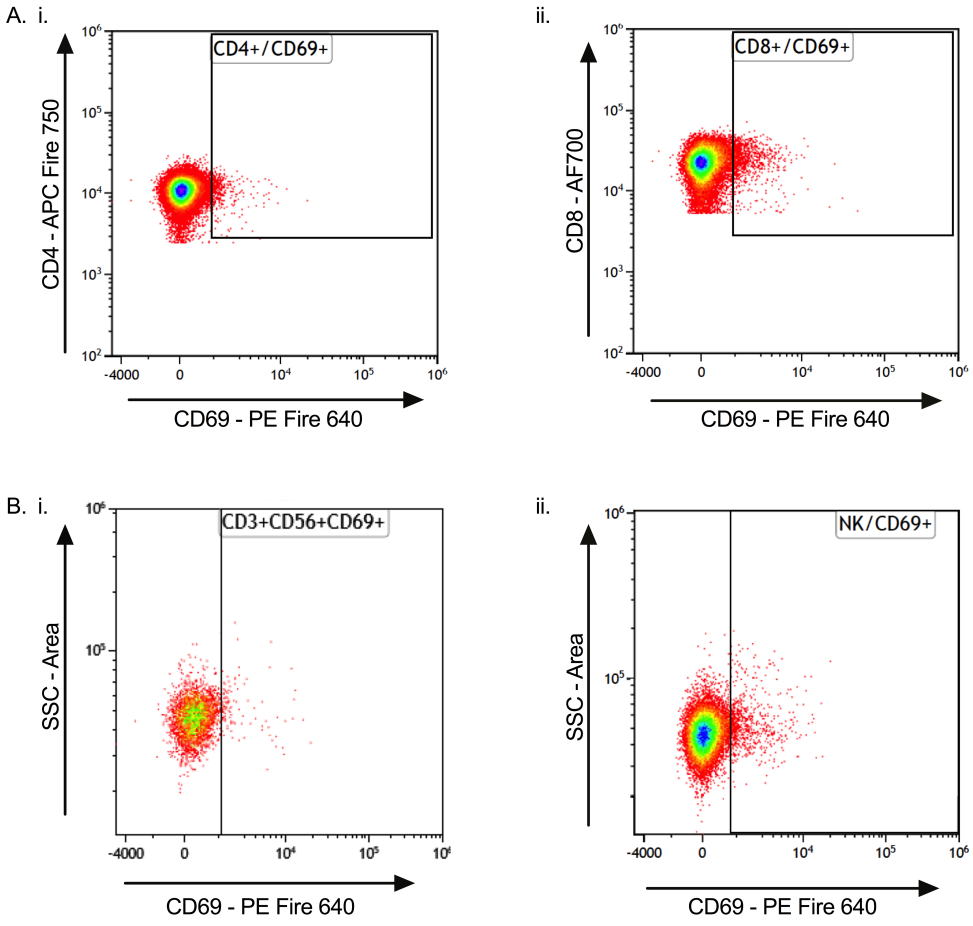

Figure 5.5. Spectral flow cytometry analysis of activation of PBMC populations. Representative spectral flow analysis density plots of: (A) (i) CD69 vs CD4 to identify CD4 T (CD3+CD4+) cells that were CD69+; (ii) CD69 vs CD8 to identify CD8 T (CD3+CD8+) cells that were CD69+; (B) CD69 vs SSC of (i) CD3+CD56+ cells to identify CD69+ population; (ii) NK cells to identify CD69+ population.

Results show that there were no significant differences in early activation (CD69+) between conditions for each cell population (**Figure 5.6.**). Nicotine at 200 μg/mL decreased activation of CD4+ T cells, although this was not significant. Additionally, CD8+ T cells had a slight nonsignificant decrease in activation after 1% and 3% CSE and 200 μg/mL nicotine exposure compared to control, but this was not significant. For NKT cells (CD3+CD56+), the results were variable.

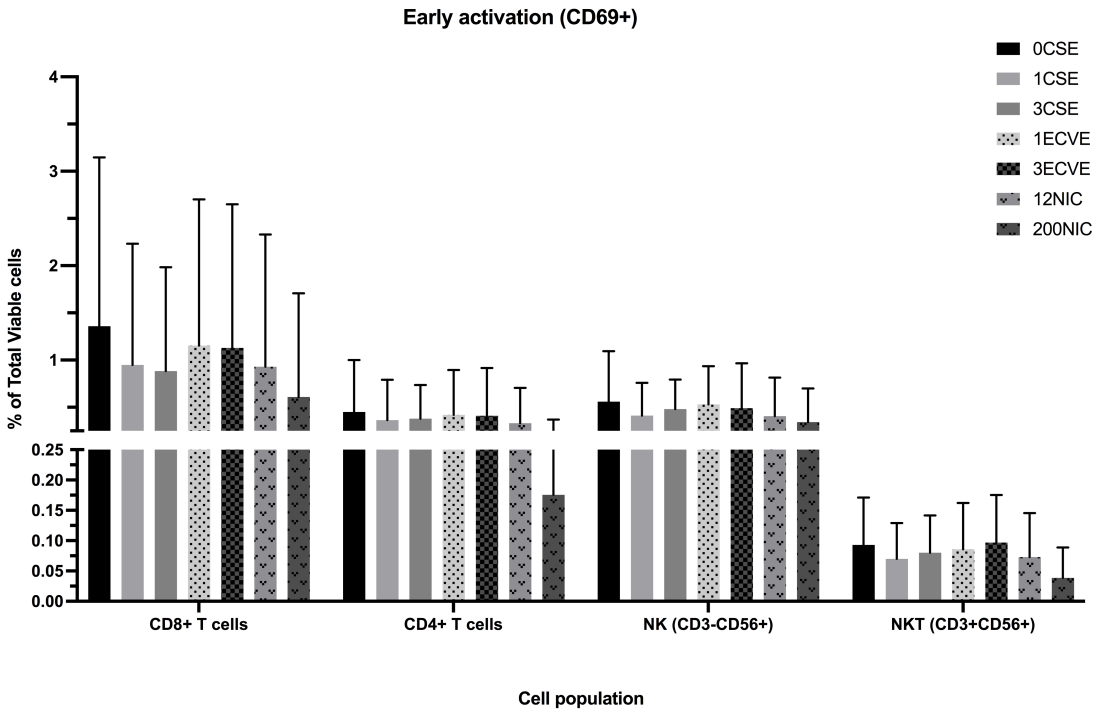

Figure 5.6. Early activation of cell populations (n=6). CD69 expression of PBMC populations in control and treatment. Results showed no significant differences in early activation of cell populations after exposure to treatment versus control. Data are expressed as mean ± SD; Ordinary Two-way ANOVA; Tukey's multiple comparisons post-hoc analyses indicated no significant differences observed.

Spectral flow analysis density plots of CD19 vs CD14 with a Boolean operator [NOT CD3] was done for identification of B cells (CD19+) and monocytes (CD14+) (**Figure 5.7.A.**). Density plots of CD11c vs SSC with Boolean operator [NOT CD3 NOT CD14 NOT CD19] were then created to gate for DCs that were CD11c+ and SSC high (CD11c+SSCHi) (**Figure 5.7.B.**). Results showed a significant increase in % of CD14+ monocytes for 3% CSE compared to control (p=0.0110) and 200 nicotine (p=0.0045) (**Figure 5.7.C.i.**). There were no significant differences in B cells present between each condition for every cell population (**Figure 5.7.C.ii.**). CD11c+SSCHi DCs were significantly increased at 1% CSE (p=0.0025) and 3% CSE (p=0.0299), compared to control (**Figure 5.7.C.iii.**). This population was also significantly decreased at 1% ECVE compared to 1% CSE (p=0.0026). Furthermore, percent of monocytes were very low. Monocytes make up about 10-20% of PBMCs; however, cells were cultured in plates for over 24 hours and so would have adhered to the plate, resulting in their low percentage.

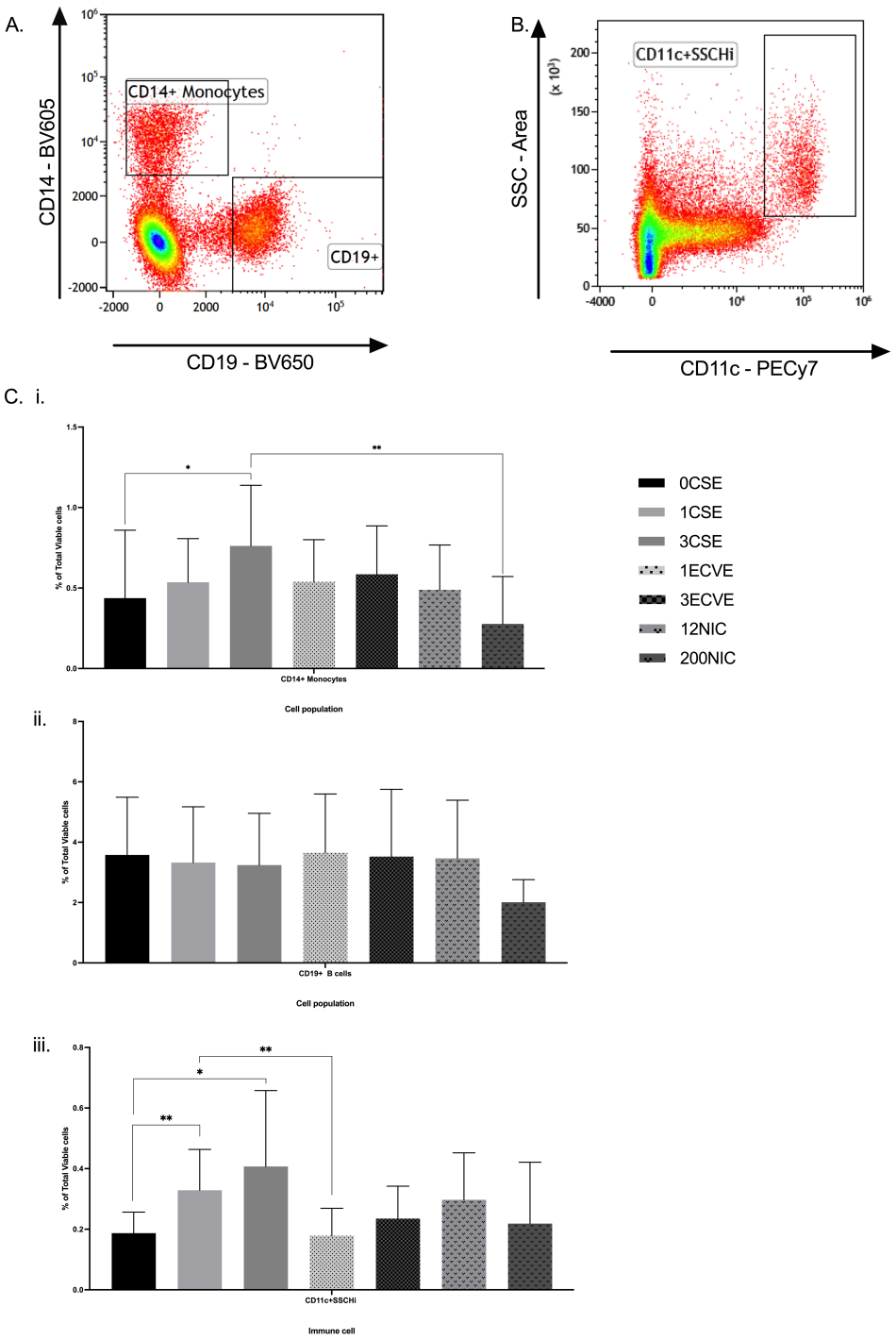

Figure 5.7. Spectral flow cytometry analysis of monocytes, B cells and dendritic cell populations. Representative spectral flow analysis density plots of: (A) CD19 vs CD14 to gate for B cells (CD19+) and monocytes (CD14+); and (B) CD11c vs SSC-Area to gate for DCs (CD11c+SSCHi). (C) Cell population percentage of total viable cells for (i) CD14+ monocytes, (ii) CD19+ B cells and DCs (n=6). Data are expressed as mean ± SD; Two-tailed t test; $P < 0.05$.

After identifying specific immune cell populations (CD4+ and CD8+ T cells, NKT cells, NK cells, B cells, CD14+ monocytes and CD11c+/SSCHi DCs), markers previously identified in EVs using the MACSPlex exosome kit were then analysed on each cell population (**Figure 5.8.**). The markers selected were CD29, CD49e, CD40 and HLA-DR. CD40 was found to have been significantly downregulated on EVs following 1% CSE exposure when analysed using the MACSPlex exosome kit. HLA-DR was selected as it was found to be one of the higher expressed immune cells markers on EVs. CD29 was selected as it was found to be a highly expressed adhesion molecule on EVs previously collected. Histogram plots were created to visualise CD29, CD49e, HLA-DR and CD40 expression. Here, the divider gate was set using unstained samples to mark the cut-off between positive and negative events (**Figure 5.8.**). CD29 had two peaks as subsets of the population could be dim or bright for CD29, as previous studies have shown lymphocytes to express CD29 in this manner [556, 557].

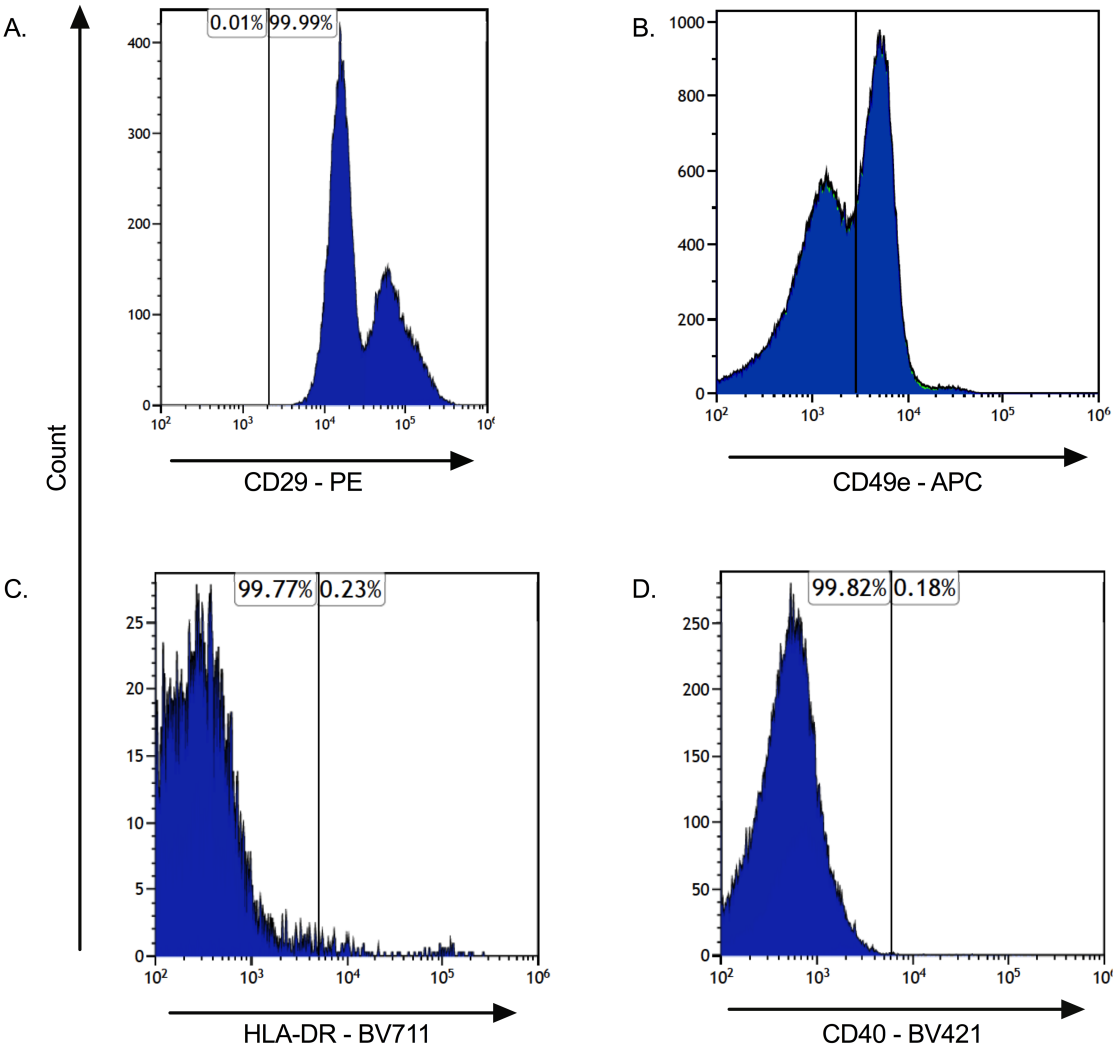

Figure 5.8. Identification of marker expression on PBMCs. Representative histograms with gates to mark the cut-off between positive and negative events for (A) CD29, (B) CD49e, (C) HLA-DR, and (D) CD40.

The unstained signal was subtracted from the signal of each marker to obtain the mean fluorescence intensity (MFI) of each marker. This was done for each marker for every cell population previously identified. CD29, also known as integrin beta-1, is expressed by various cell lineages [544] and include immune cells, such as T cells, B cells, NK cells [545], polymorphonuclear lymphocytes (PMNL) and monocytes [546]. Results for CD29 show no significant differences in expression of CD29 in any of the cell populations under any of the conditions (**Figure 5.9.A-G**). Furthermore, CD19+ cell population

showed the lowest MFI of CD29 compared with other cell populations. CD14+ monocytes and NKT (CD3+CD56+) cells had the highest MFI of CD29.

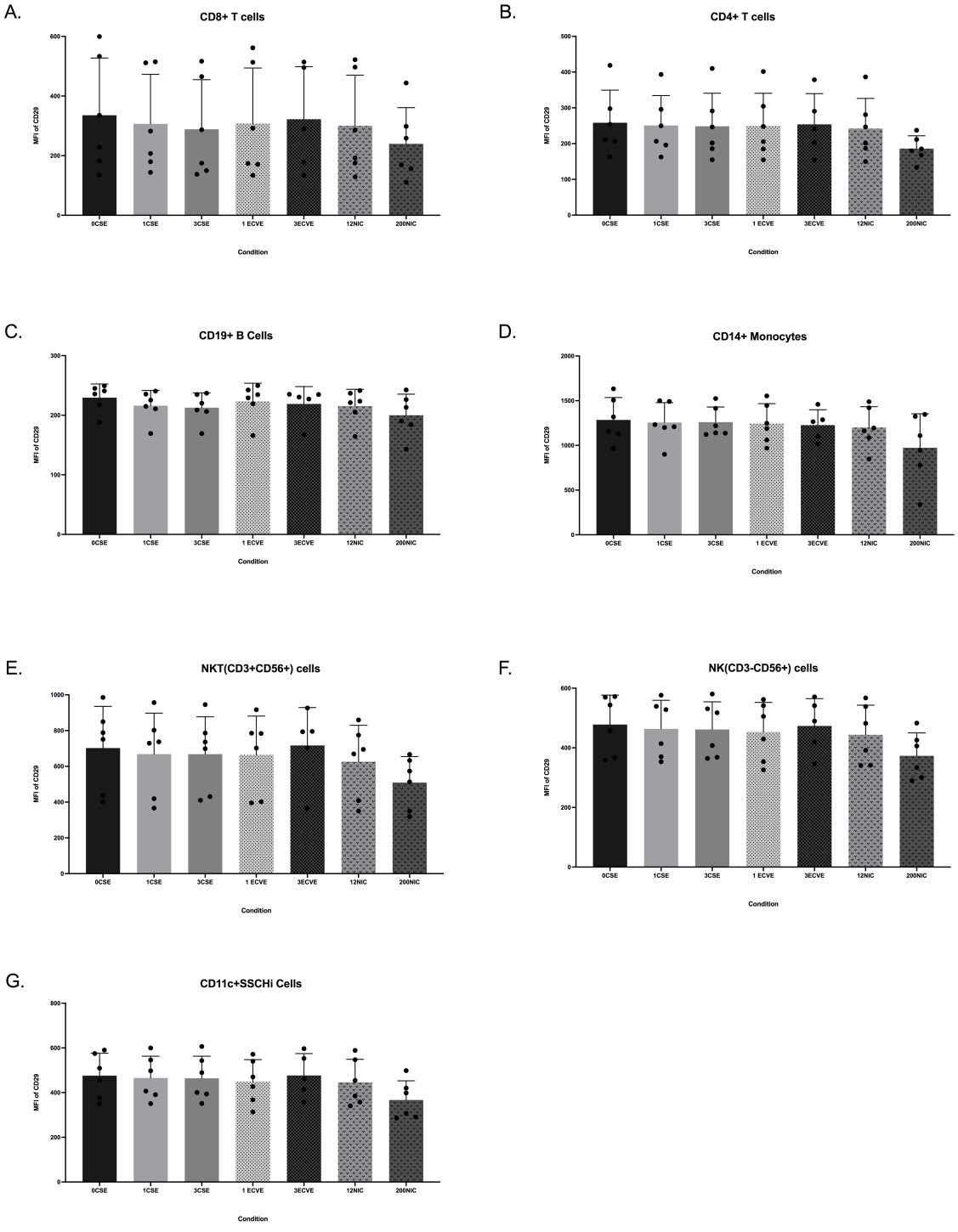

Figure 5.9. CD29 MFI in PBMC cell populations (n=6 biological repeats)**.** There were no significant differences in MFI of CD29 for the cell populations under any of the conditions. Data are expressed as mean ±SD; One-way ANOVA; Tukey's multiple comparisons post-hoc analyses.

CD49e, also known as integrin α5, is an adhesion molecule expressed on monocytes [547], T cells [548], B cells [549, 550] , NK cells [551], and DCs [552]. Results for MFI of CD49e show no significant differences in expression of CD49e in any of the cell populations under any of the conditions (**Figure 5.10.A-G**). Furthermore, CD14+ monocytes showed the highest expression of CD49e. CD8+ and CD4+ T cells had low MFI of CD49e, and CD19+ B cells had the lowest MFI of CD49e.

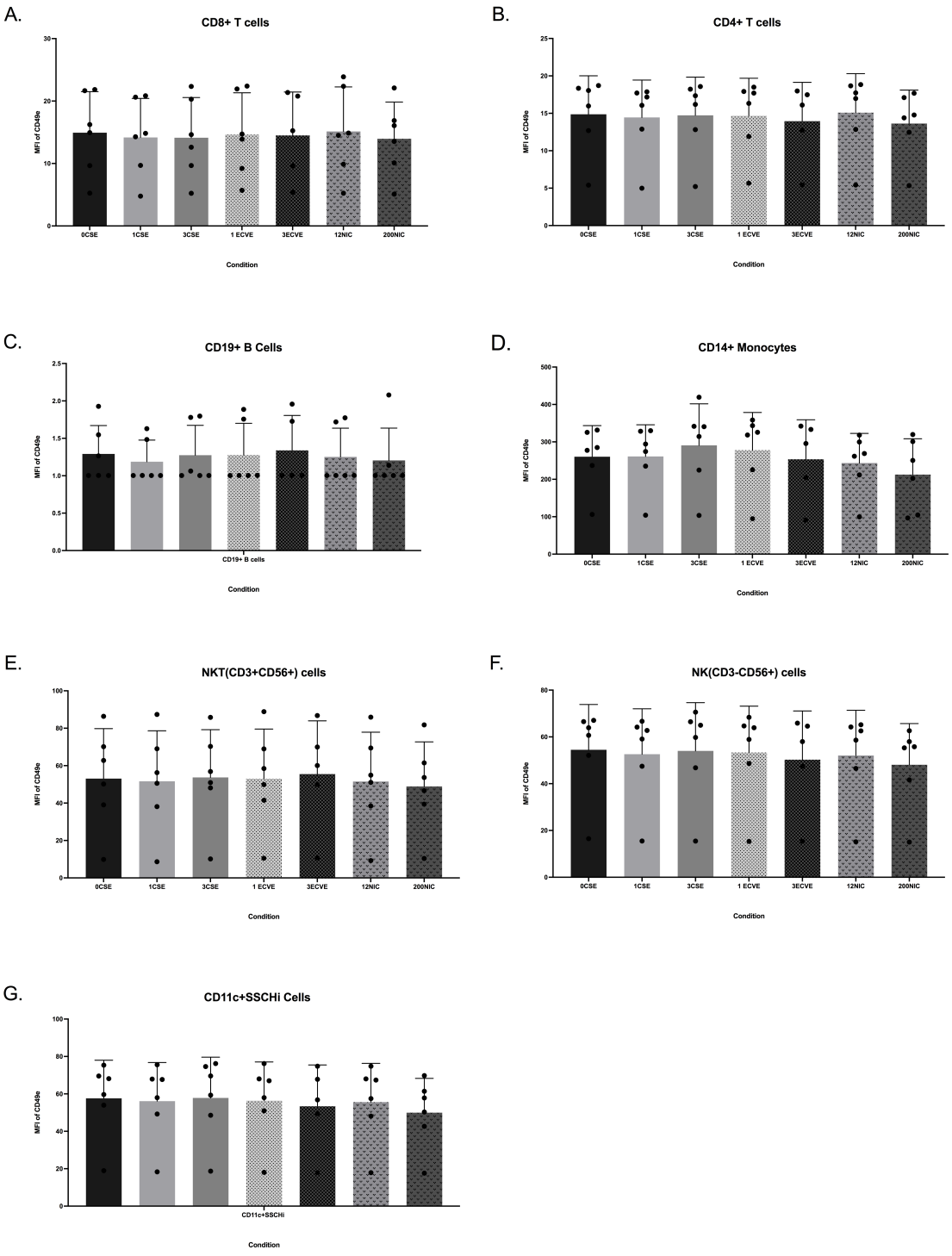

Figure 5.10. MFI of CD49e in PBMC cell populations (n=6 biological repeats)**.** There were no significant differences in MFI of CD49e for the cell populations under any of the conditions. Data are expressed as mean ±SD; One-way ANOVA; Tukey's multiple comparisons post-hoc analyses

HLA-DR, or MHC II, is a key cell surface receptor expressed on antigen presenting cells, including dendritic cells, B cells, monocytes and macrophages. Results for MFI of HLA-DR shows no significant differences in expression of HLA-DR in any of the cell populations under any of the conditions (**Figure 5.11.**). Furthermore, only CD19+ B cells and CD14+ monocytes showed high expression of HLA-DR.

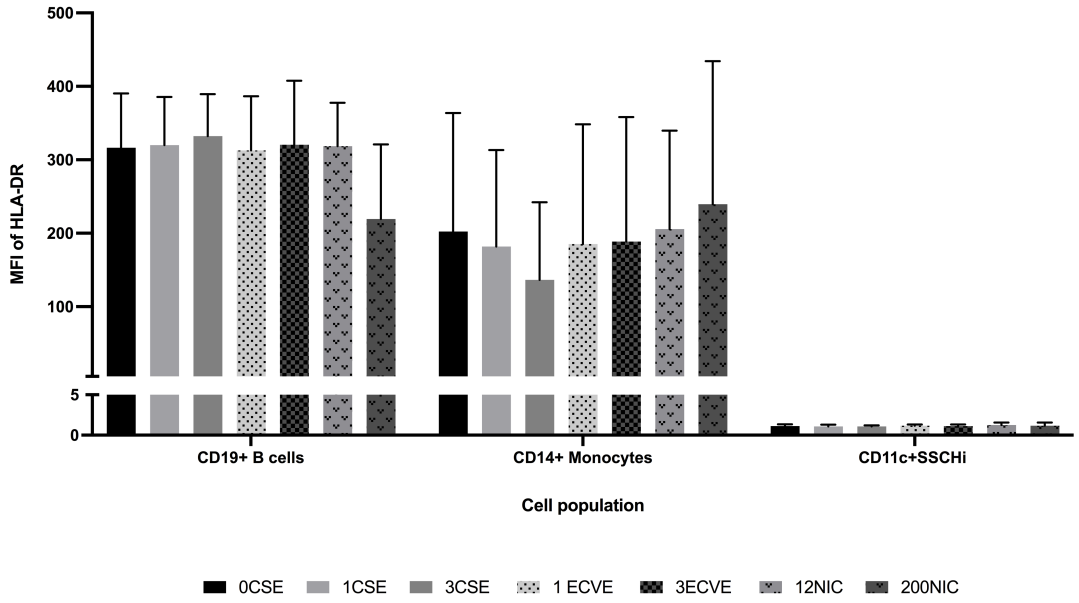

Figure 5.11. MFI of HLA-DR in PBMC cell populations (n=6 biological repeats)**.** There were no significant differences in MFI of HLA-DR for the cell populations under any of the conditions. Data are expressed as mean ±SD; Two-way ANOVA; Tukey's multiple comparisons post-hoc analyses.

CD40 is expressed by B cells and other various cells, including DCs, monocytes, macrophages, mast cells, epithelial cells and endothelial cells [553]. Results of MFI of CD40 show significant decrease in CD19+ B cells at 200 μg/mL nicotine compared to control ($p = 0.0033$), 1% ($p = 0.0118$) and 3% ($p = 0.0084$) CSE and 1% ($p = 0.0065$) ECVE and 12 μg/mL nicotine ($p = 0.0425$) (**Figure 5.12.**). Other cell populations showed no significant differences in expression of CD40 under any conditions. Furthermore, CD19+ B cells had the highest MFI of CD40. CD14+ monocytes had low MFI of CD40 under all

conditions, with non-significant increases following 1% ECVE and 200 μg/mL nicotine treatments. CD11c+SSCHi cells had low MFI of CD40 and no significant differences between treatment. Additionally, we note here that the data has low MFI, so it can be questioned whether the data is true representation of cells.

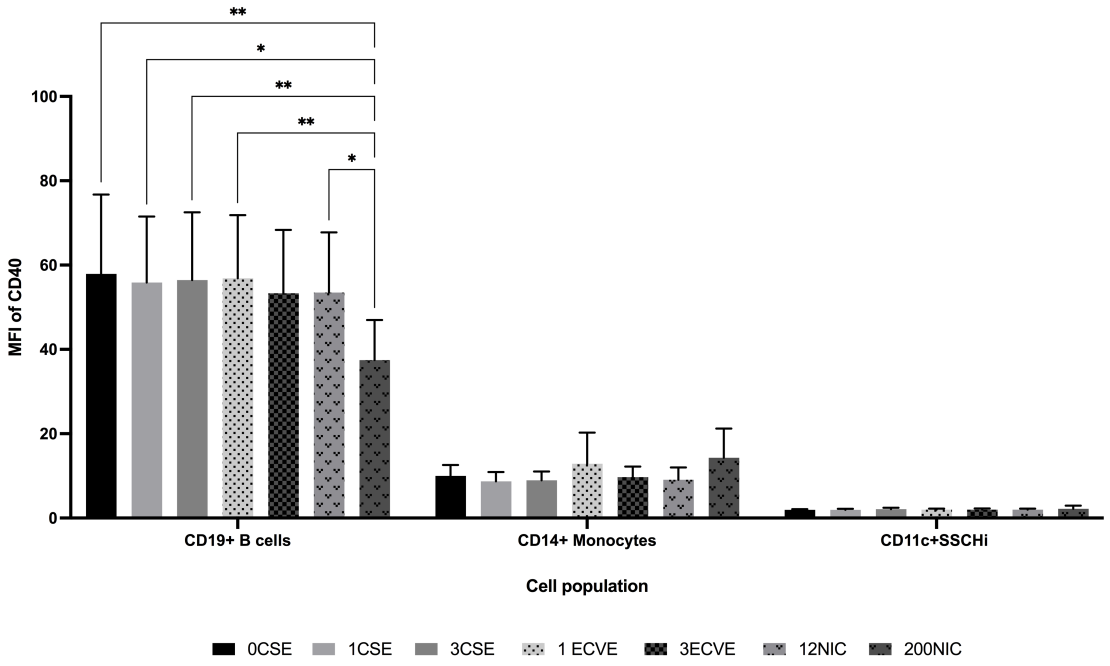

Figure 5.12. MFI of CD40 in PBMC cell populations (n=6 biological repeats)**.** MFI was significantly decreased for CD19+ B cell population exposed to 200 μg/mL nicotine compared to control (p = 0.0033), 1% (p = 0.0118) and 3% (p = 0.0084) CSE and 1% (p = 0.0065) ECVE and 12 μg/mL nicotine (p = 0.0425). Data are expressed as mean ±SD; Two-way ANOVA; Tukey's multiple comparisons post-hoc analyses.

5.3.2. Clustering analysis

In addition to conventional flow cytometry, to do an unbiased analysis of the flow data generated, clustering analysis using FlowJo was undertaken. So far, we have selected the cell populations we wanted to observe, however, clustering analysis would allow for unbiased analysis of the same markers to observe if there were any unique populations upregulated as a consequence to CSE, ECVE or nicotine exposure. Single viable cells were first gated in FlowJo before equal sampling of 5,000 events from 6 subjects. Clustering analysis was then performed on PBMCs for each treatment (1% and 3% CSE, 1% and 3% ECVE, and 12 and 200 μg/mL nicotine) and control samples to observe any differences in the identified metaclusters. The analysis found 15 metaclusters present, which was presented in a tSNE plot (**Figure 5.13.A.i.**), where population 7 had the highest % of events at almost 45%, followed by population 0 at about 22%, then population at about 12.5% (**Figure 5.13.A.ii.**). Many of the populations were very small, being 5% and below. After analysing PBMCs with the following parameters: CD3, CD8, CD11c, CD14, CD16, CD19, CD29, CD40, CD49e, CD56, CD69, and HLA-DR, expression of these markers was observed across the clusters (**Figure 5.13.B.**).

Interestingly, CD4+ T cells, CD8+ T cells were clustered largely together, with CD3 and CD4 or CD8 being highly expressed in their particular clusters. CD16 was highly expressed in one of the clusters. CD29 was expressed in all but one cluster. HLA-DR was observed to be expressed in a cluster that also expressed CD19.

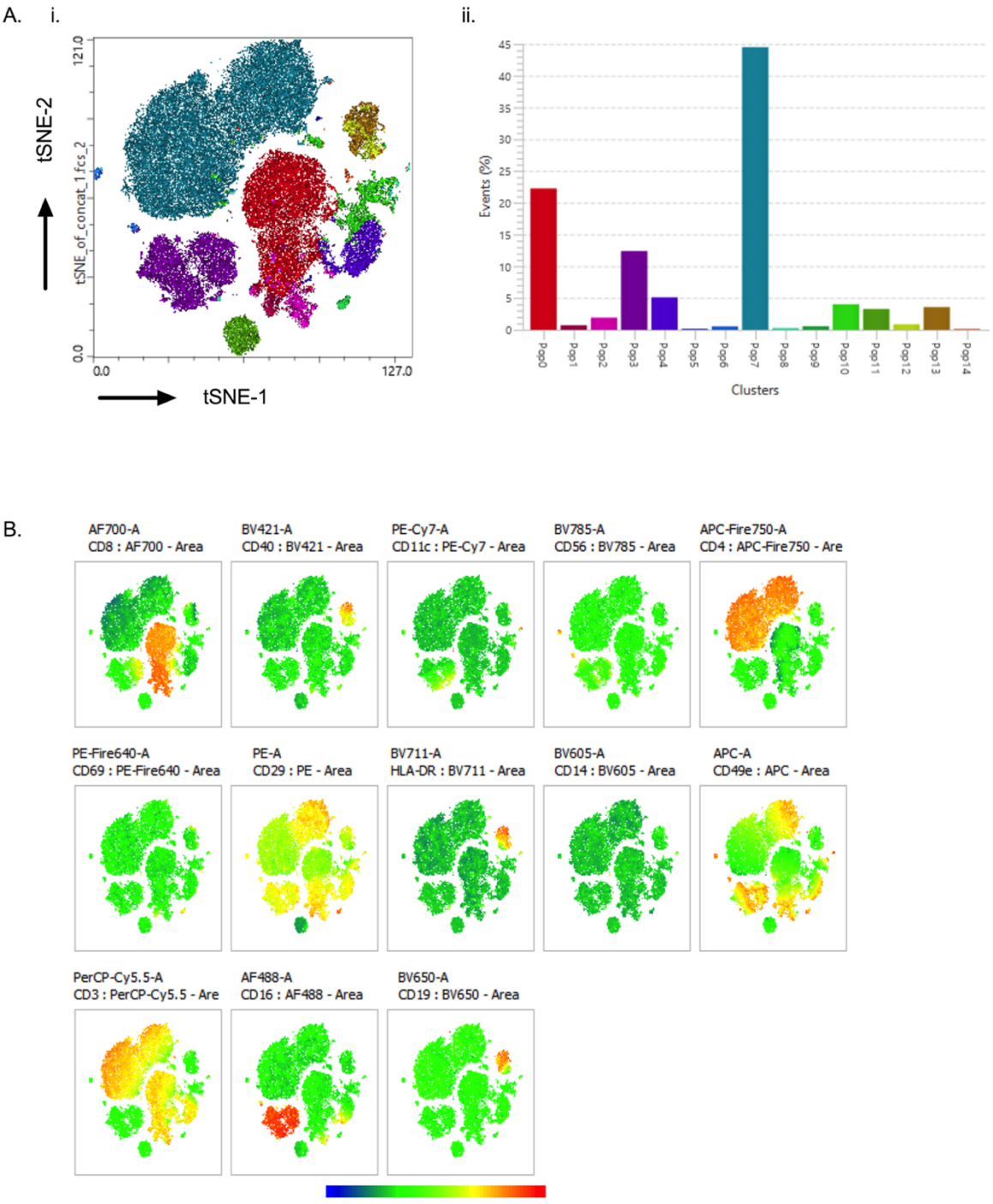

Figure 5.13. PBMCs clustering analysis (n=6 biological repeats). (A) (i) FlowSOM clusters from PBMCs presented as a tSNE plot; (ii) FlowSOM clusters by events (%). (B) Heat maps of clusters by marker expression.

Marker expression for each population was then examined. Population 0 (pop0) was the second highest population at approximately 22% of the events (**Figure 5.14.A.**). Additionally, population 0 had high relative expression of markers CD3 and CD8 (**Figure 5.14.B.**), indicative of CD8 T cell population. This CD8 T cell population also expressed CD29 and had a mixture of CD49e expression (+/-). As previously mentioned, CD29 is expressed by immune cells, including T cells, B cells, NK cells, PMNL, and monocytes, and CD49e, an adhesion molecule, is expressed on monocytes, T cells, B cells, NK cells, and DCs.

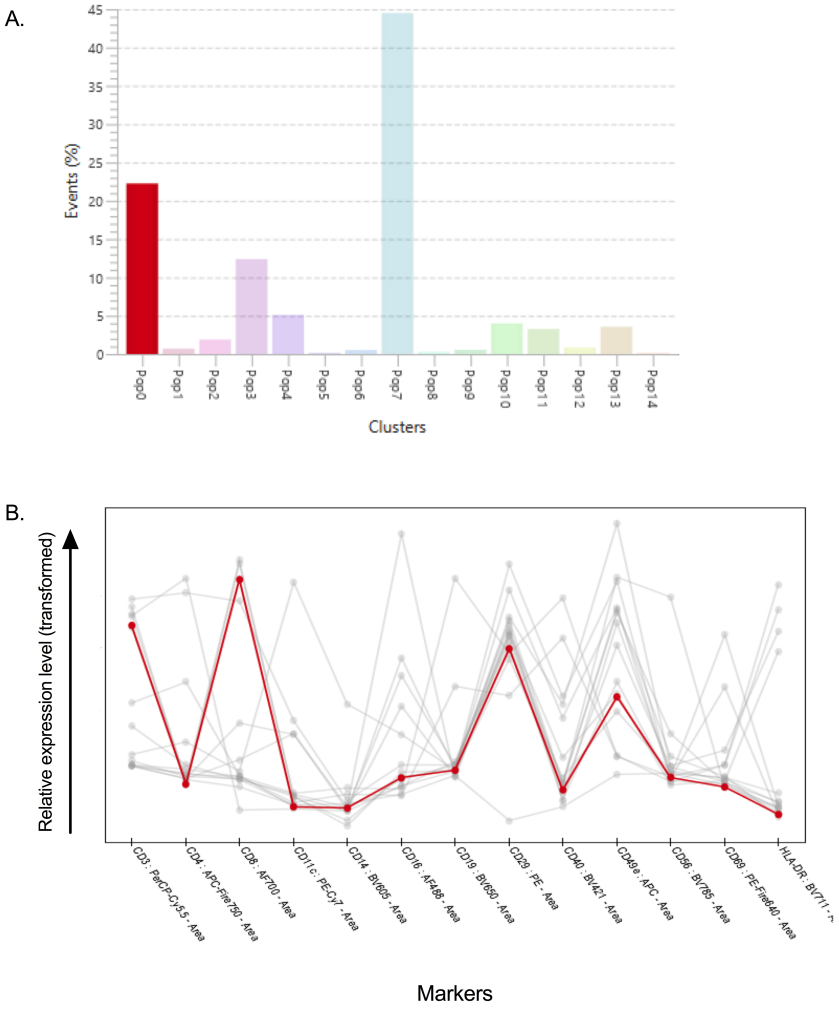

Figure 5.14. Phenotype profile of population 0. (A) Events (%) of population 0 (Pop0) highlighted in red. (B) Marker expression profile of population 0 showing expression of CD3, CD8, CD29 and CD49e.

Population 1 (Pop1) was one of the lowest populations in percent of events (**Figure 5.15.A.**). Population 1 had high relative expression of markers CD3 and CD8 (**Figure 5.15.B.**), indicative of CD8 T cell population. This CD8 T cell population also expressed CD29 and CD49e and differed from Pop0 by the expression of CD40 and CD69 and higher expression of CD49e (++). Increased expression of CD69 indicates CD8 T cells in early activation state. Furthermore, CD40 is upregulated when T cells are activated [558], further indicating this population was activated CD8 T cell population.

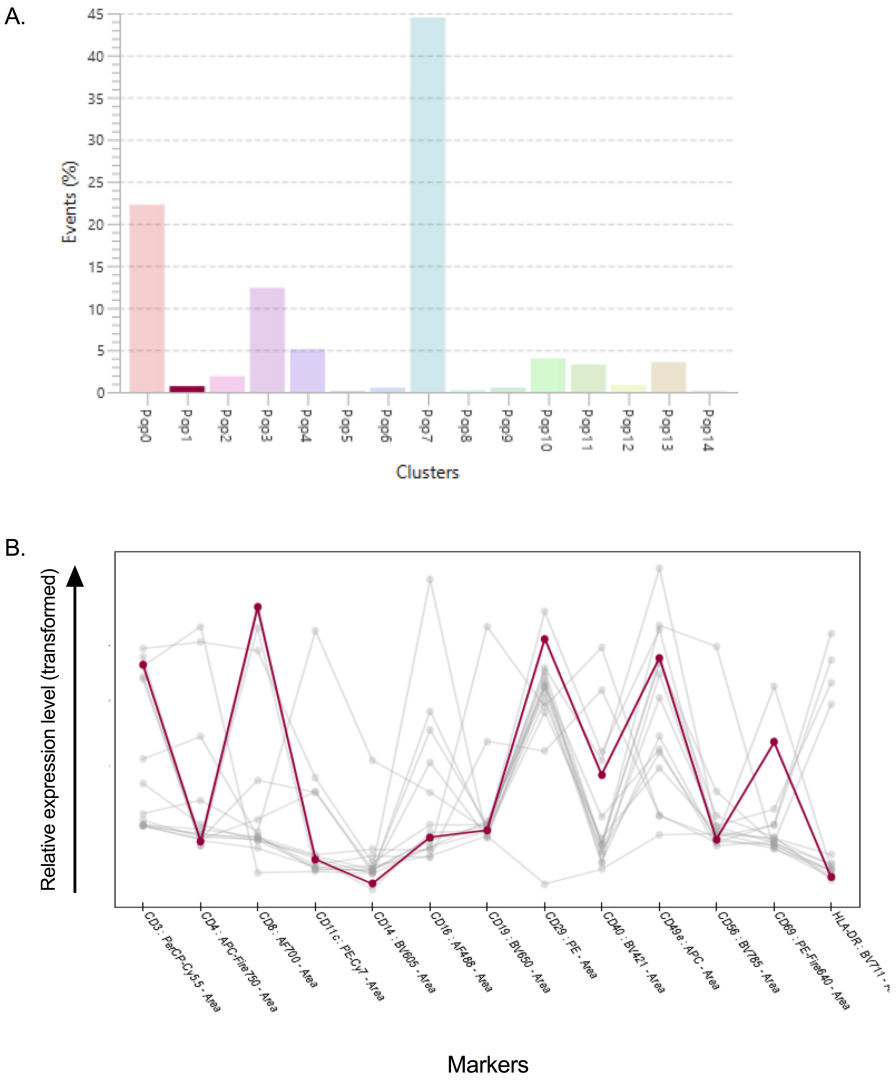

Figure 5.15. Phenotype profile of population 1. (A) Events (%) of population 1 (Pop1) highlighted in crimson. (B) Marker expression profile of population 1 shows expression of CD3, CD8, CD29, CD49e, and CD69 in this population.

Population 2 (Pop2) was another low population, making up approximately 2% of events (**Figure 5.16.A.**). Population 2 had high relative expression of markers CD3 and CD8 (**Figure 5.16.B.**). Other markers that were also expressed were CD16, CD29 and CD49e. Therefore, this was a CD8 T cell population expressing CD16, CD29 and CD49e. Previous study has shown that a small percentage of lymphocytes in peripheral blood co-expresses CD3 and CD16 [559].

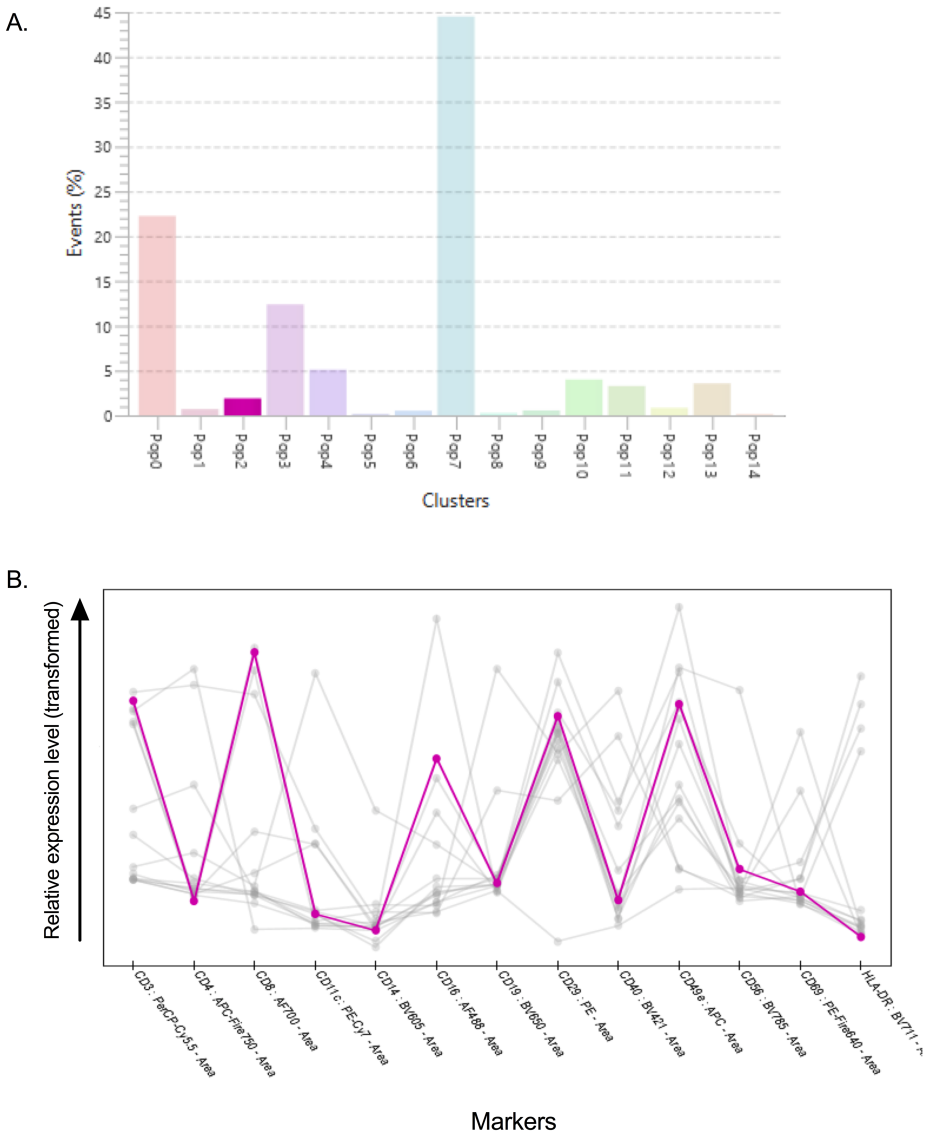

Figure 5.16. Phenotype profile of population 2. (A) Events (%) of population 2 (Pop2) highlighted in pink. (B) Marker expression profile of population 2 shows expression of CD3, CD8, CD16 CD29, and CD49e in this population.

Population 3 (Pop3) was the third highest populations observed in the clustering analysis at about 12% of events (**Figure 5.17.A.**). Population 3 had high relative expression of markers CD16, CD29 and CD49e (**Figure 5.17.B.**). Other markers that were also expressed were CD8, CD11c, and CD56, although expression was not as high as the previously mentioned markers. NK cells from peripheral blood consists of two distinct populations, $CD56^{Dim}CD16+$, which makes up 90% of the cells, and $CD56^{Bright}CD16-$ [560, 561]. Therefore, this suggests that Pop3 consisted of NK ($CD56^{Dim}$) cells, expressing CD16, CD29, CD49e, CD8 and CD11c.

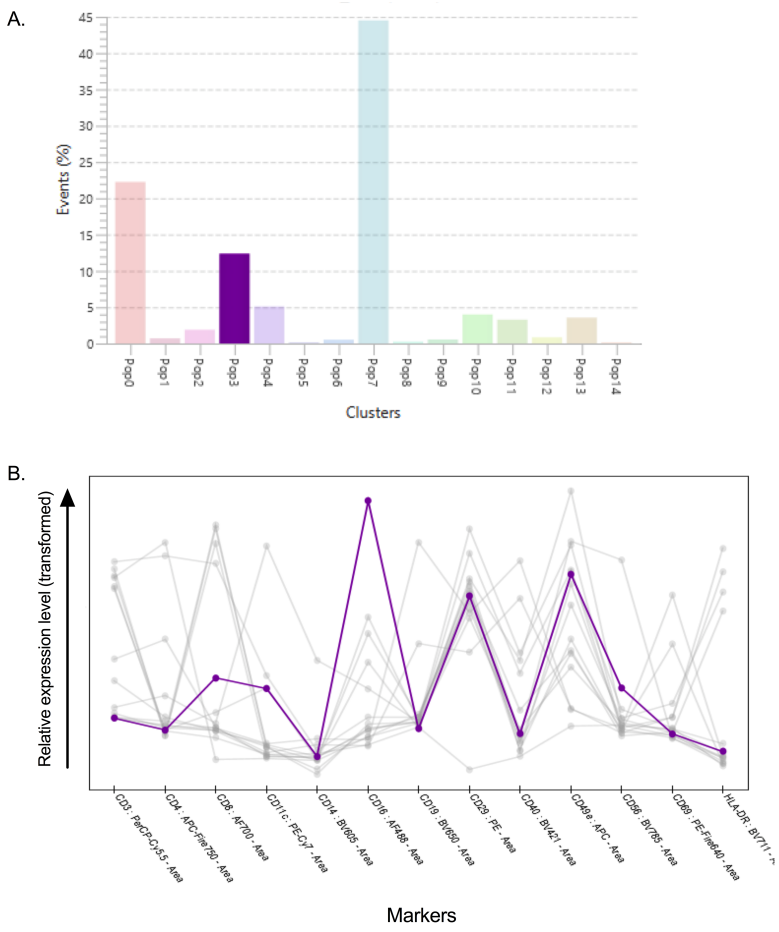

Figure 5.17. Phenotype profile of population 3. (A) Events (%) of population 3 (Pop3) highlighted in purple. (B) Marker expression profile of population 3 shows high expression of CD16, CD29 and CD49e, with lower expression of CD8, CD11c and CD56 in this population.

Population 4 (Pop4) was the fourth highest populations observed in the clustering analysis at about 5% (**Figure 5.18.A.**). Population 4 had high relative expression of markers CD3, CD16, CD29 and CD49e (**Figure 5.18.B.**). Due to expression of these markers, this population consisted of double negative (CD4-/CD8-) T cells (CD3+), expressing CD16, CD29 and CD49e.

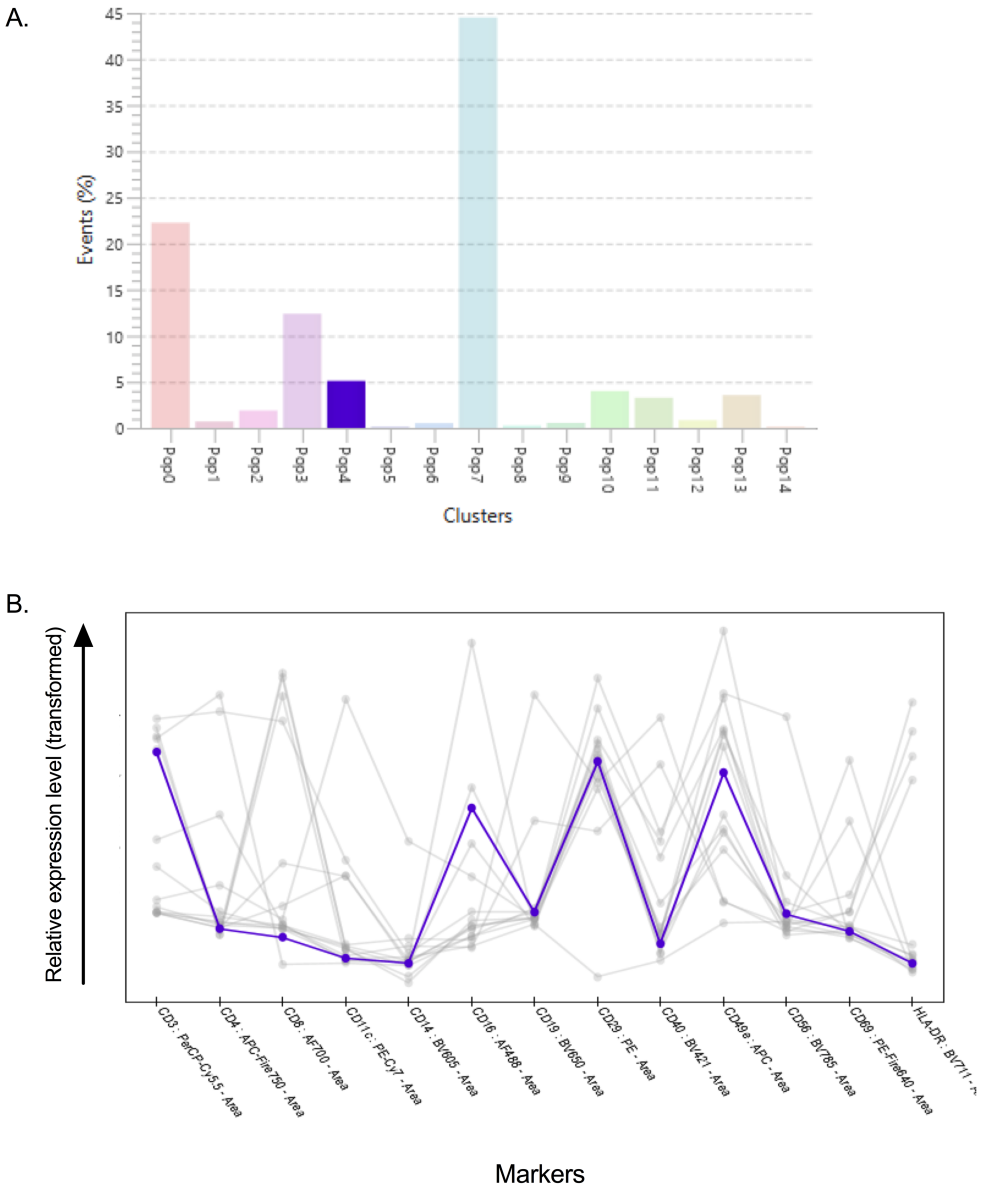

Figure 5.18. Phenotype profile of population 4. (A) Events (%) of population 4 (Pop4) highlighted in blue-purple. (B) Marker expression profile of population 4 shows high expression of CD3, CD16, CD29 and CD49e.

Population 5 (Pop5) was one of the lowest populations observed in the clustering analysis, representing below 1% of events (**Figure 5.19.A.**). Population 5 had high relative expression of markers CD3, CD4, CD8, CD29 and CD49e (**Figure 5.19.B.**). As a result, Pop5 consisted of double positive (CD4+/CD8+) T cells (CD3+), expressing CD29 and CD49e.

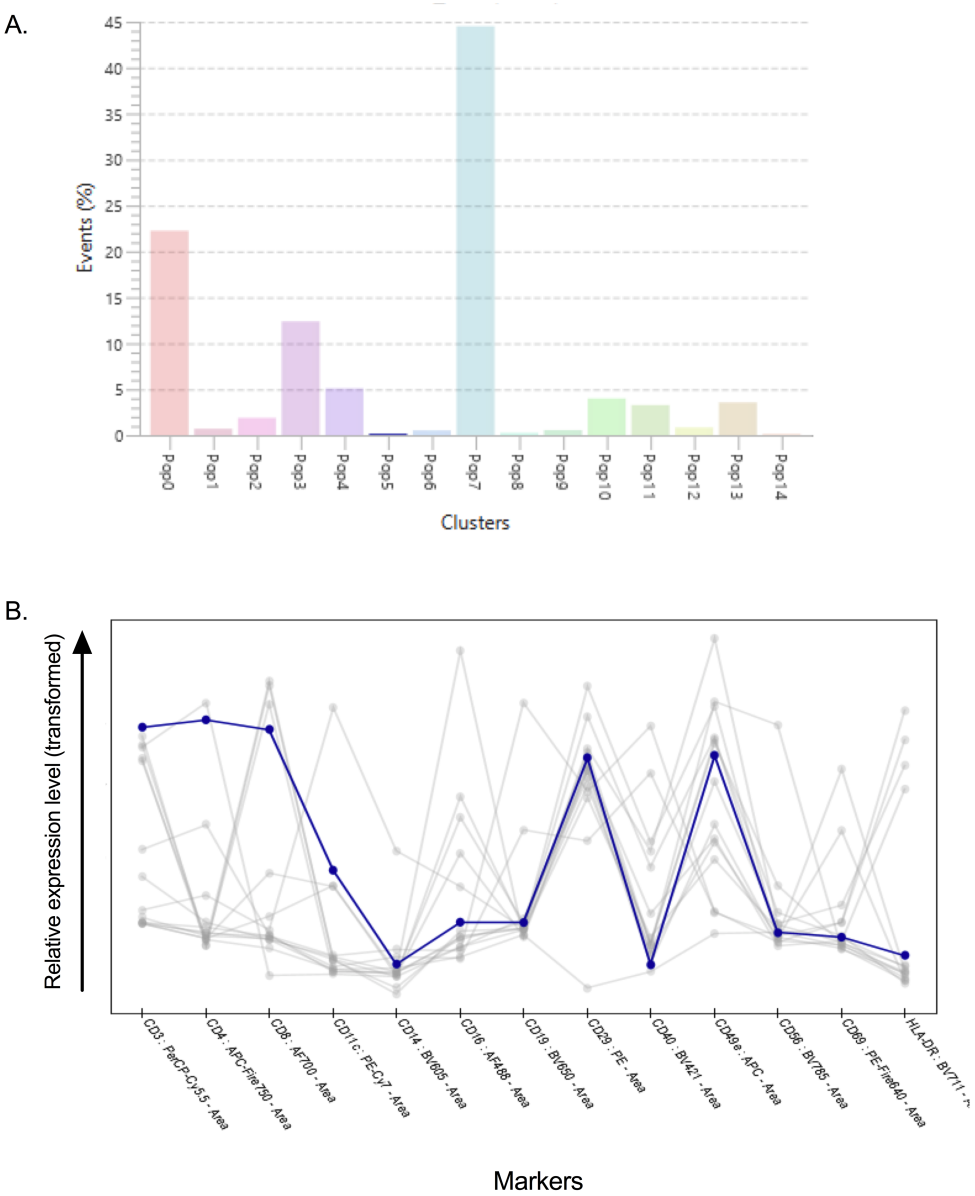

Figure 5.19. Phenotype profile of population 5. (A) Events (%) of population 5 (Pop5) highlighted in dark blue. (B) Marker expression profile of population 5 shows expression of CD3, CD4, CD8, CD11c, CD29 and CD49e.

Population 6 (Pop6) was a low population observed in the clustering analysis, representing about 1% of events (**Figure 5.20.A.**). CD29, CD49e, and CD56 were markers that were highly expressed (**Figure 5.20.B.**). In this population, cells also expressed CD11c (+/-) and CD16 (+/-), where further observation indicated a mixture of positive and negative populations for these markers (+/-). This population consisted of CD56^{Bright} NK cells, that express CD29, CD49e, with some cells expressing CD11c and CD16.

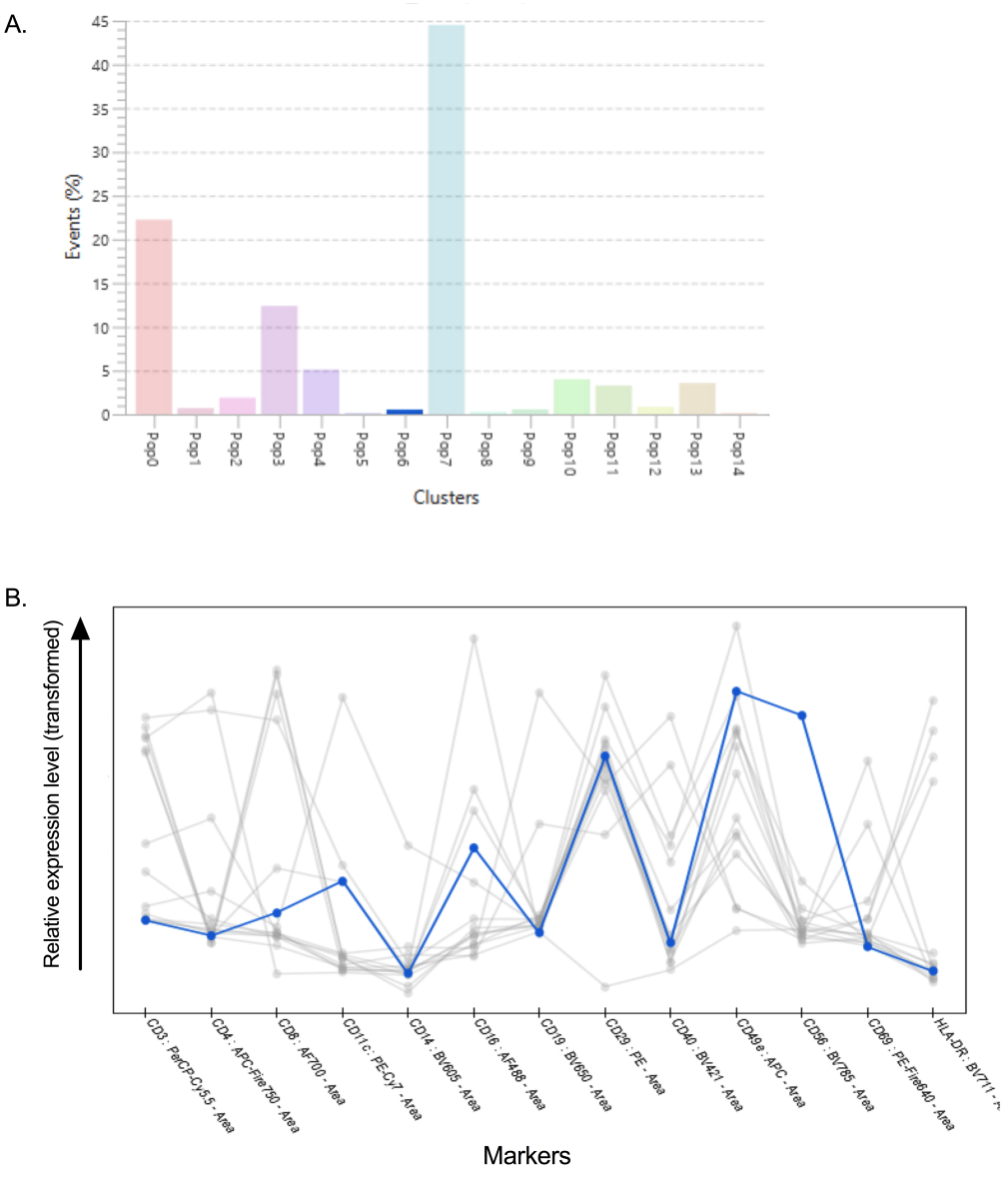

Figure 5.20. Phenotype profile of population 6. (A) Events (%) of population 6 (Pop6) highlighted in blue. (B) Marker expression profile of population 6 shows expression of CD11c, CD16, CD29, CD49e and CD56.

Population 7 (Pop7) was the highest population observed in the clustering analysis, representing almost 45% of events (**Figure 5.21.A.**). This population had high relative expression of markers CD3 and CD4 (**Figure 5.21.B.**), indicative of CD4 T cell population. This CD4 T cell population also had high CD29 expression with some CD49e expression (+/-).

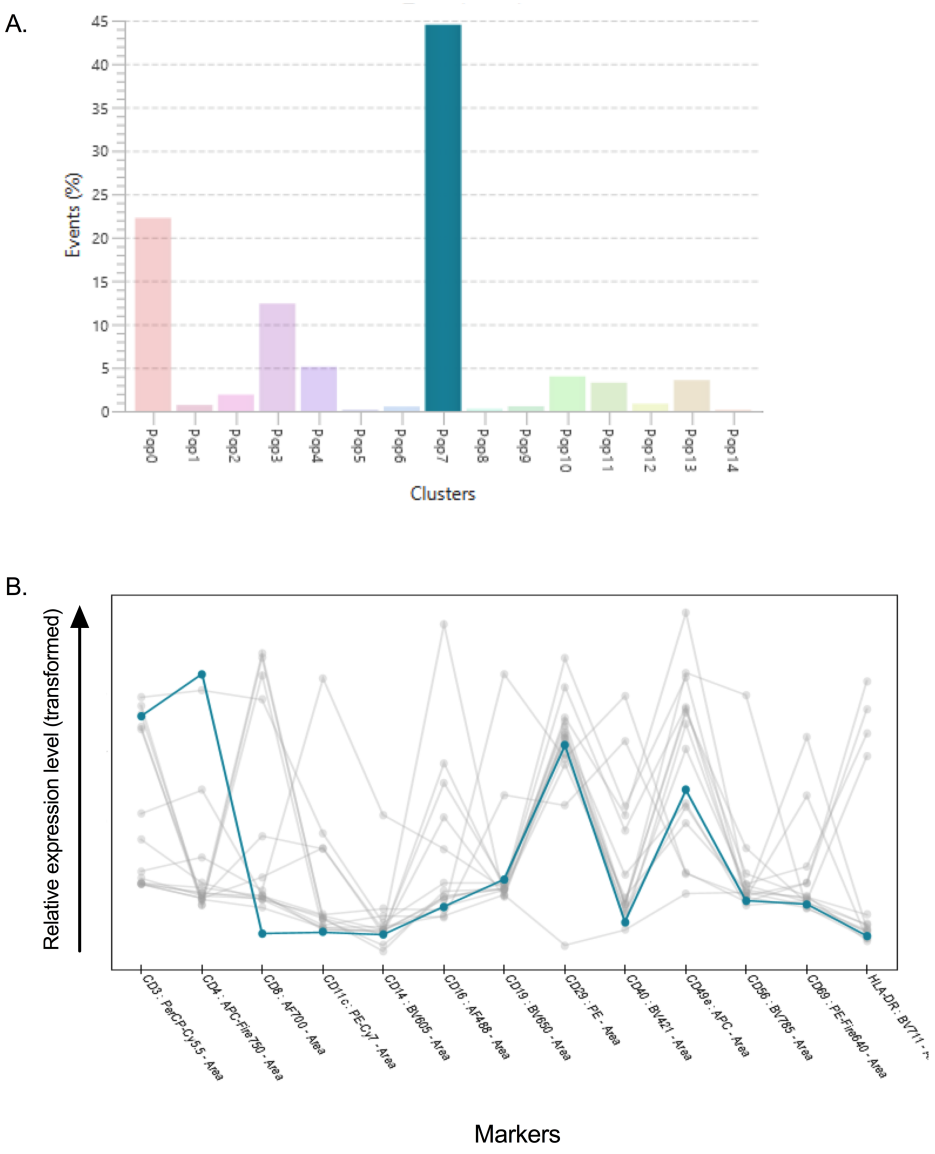

Figure 5.21. Phenotype profile of population 7. (A) Events (%) of population 7 (Pop7) highlighted in blue-green. (B) Marker expression profile of population 7 shows expression of CD3, CD4, CD29 and CD49e.

Population 8 (Pop8) represented below 1% of events in the clustering analysis (**Figure 5.22.A.**). This population expressed markers CD11c, CD29, and CD49e (**Figure 5.22.B.**). Other markers expressed in population 8 included CD14 (+/-), CD16 (+/-), CD40 (+/-), CD69 (+/-) and HLA-DR (+/-). As a result, population 8 may consist of monocytes, as monocytes can express CD14, CD16, HLA-DR, CD11c, CD49e and CD40 [562-565].

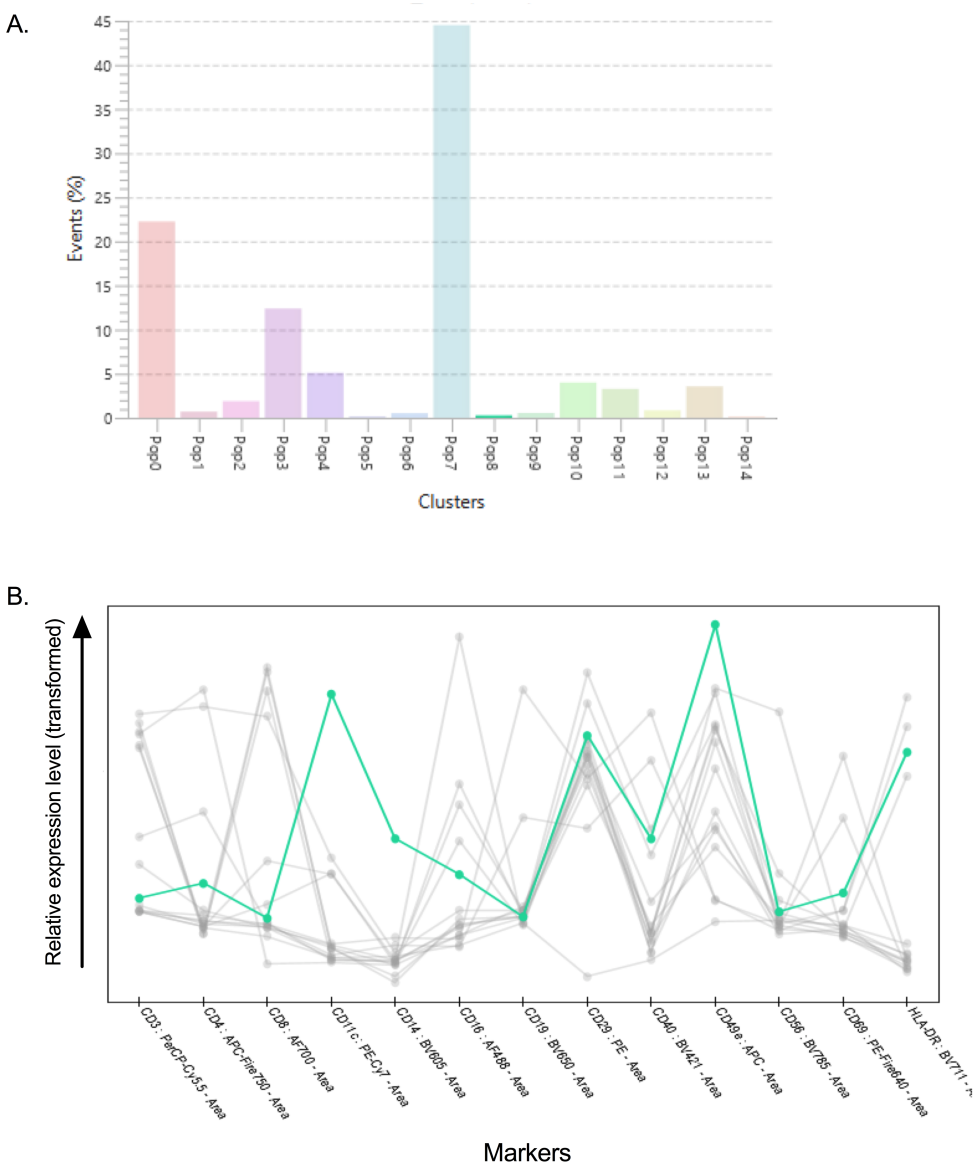

Figure 5.22. Phenotype profile of population 8. (A) Events (%) of population 8 (Pop8) highlighted in green. (B) Marker expression profile of population 8 shows expression of CD11c, CD14, CD16, CD29, CD49e and HLA-DR.

Population 9 (Pop9) represented below 1% of events in the clustering analysis (**Figure 5.23.A.**). Population 9 had high relative expression of markers CD29, CD49e and CD69 (**Figure 5.23.B.**). There was also expression of CD40 in this population but not as highly expressed as other markers. As a result, this population may consist of a mix population of cells with no single phenotype.

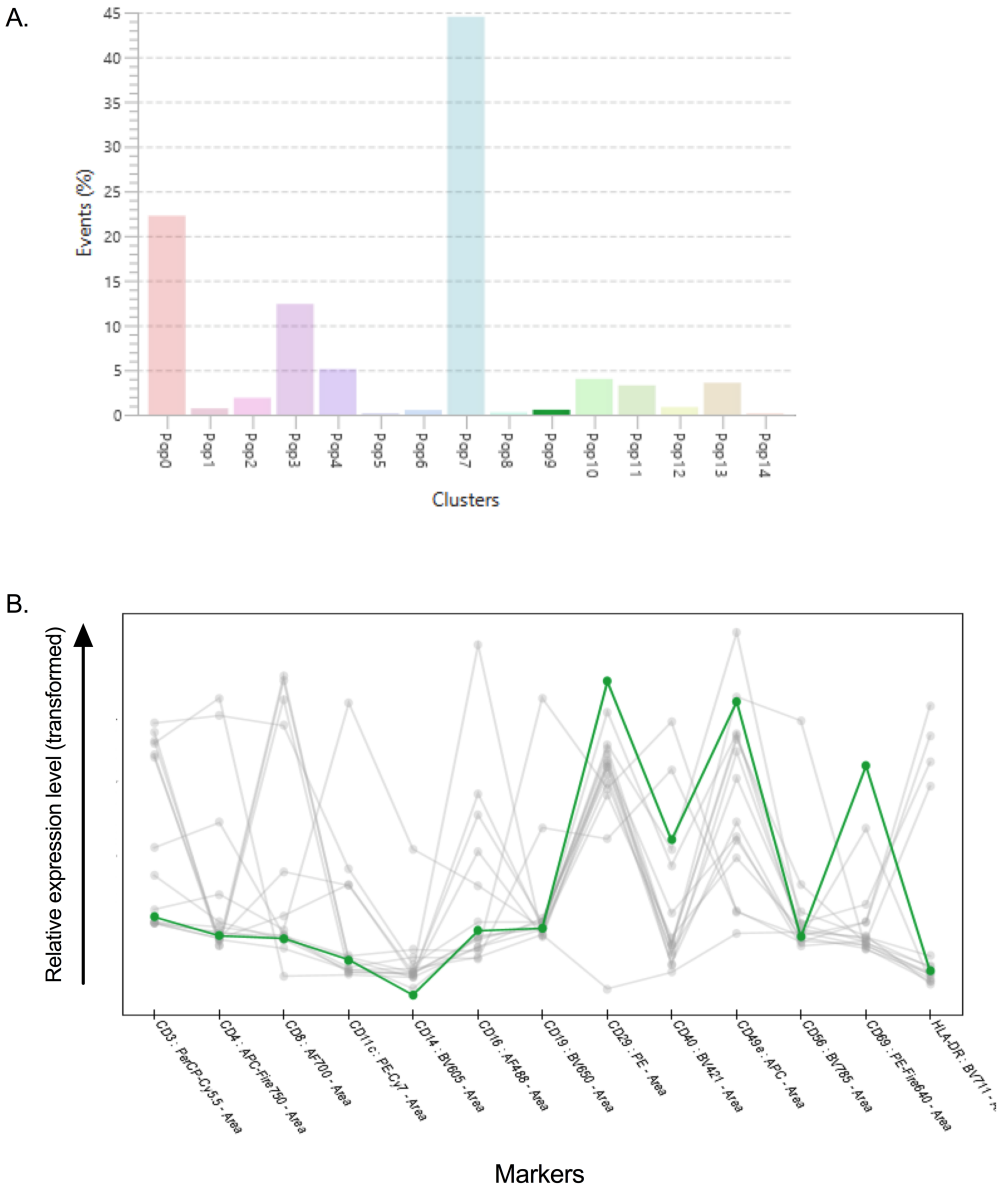

Figure 5.23. Phenotype profile of population 9. (A) Events (%) of population 9 (Pop9) highlighted in green. (B) Marker expression profile of population 9 shows expression of CD29, CD40, CD49e and CD69.

Population 10 (Pop10) represented about 4% of events in the clustering analysis (**Figure 5.24.A.**). Here there was expression of markers CD29 and CD49e, with lower expression of CD3 and CD4 (**Figure 5.24.B.**). Therefore, this population consisted of CD4+ T cells expressing CD29 and CD49e.

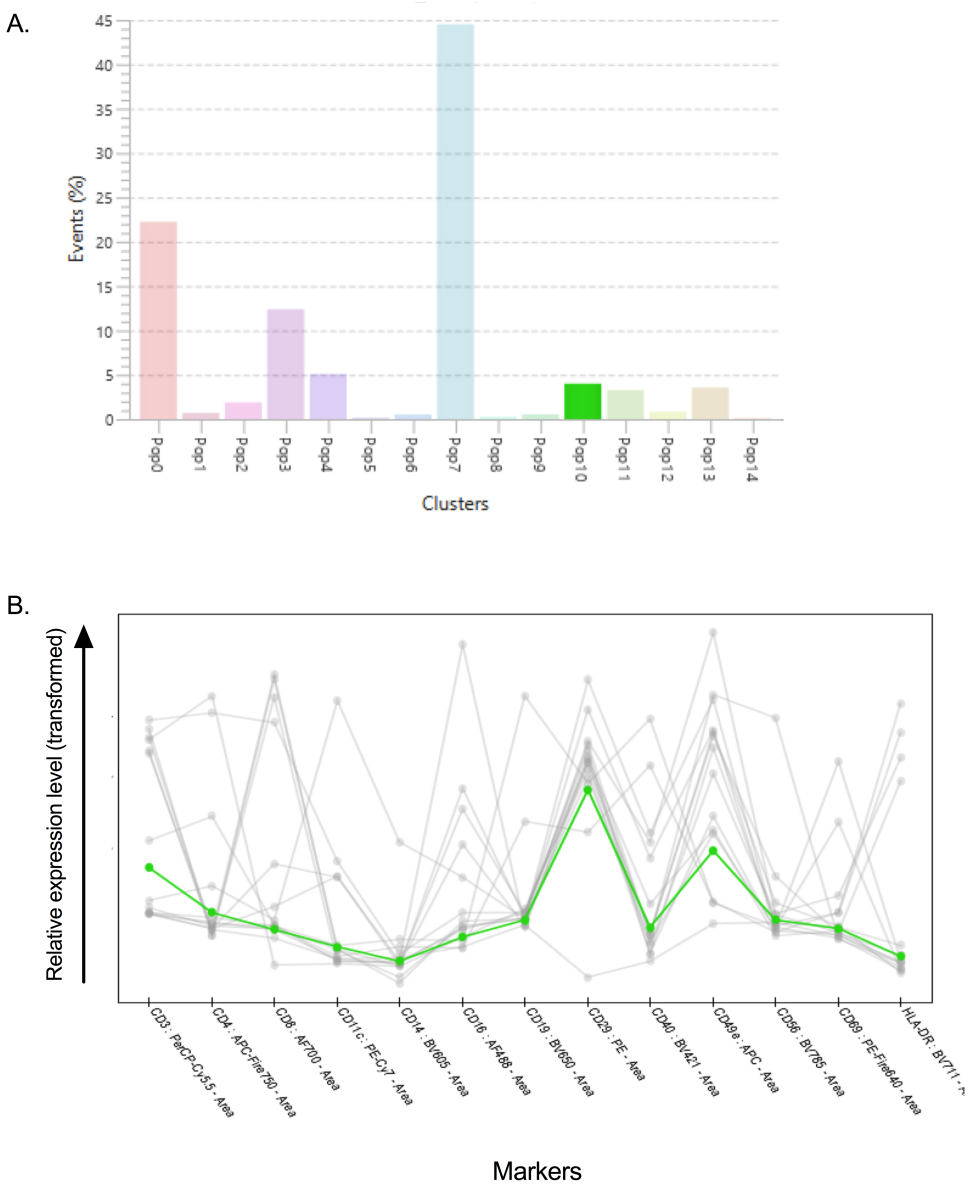

Figure 5.24. Phenotype profile of population 10. (A) Events (%) of population 10 (Pop10) highlighted in green. (B) Marker expression profile of population 9 shows expression of CD29, and CD49e, with lower expression of CD3.

Population 11 (Pop11) represented about 4% of events in the clustering analysis (**Figure 5.25.A.**). This population had no expression of any markers included in this analysis (**Figure 5.25.B.**). As a result, population 11 may consist of a mix of cells that do not express the markers included and/or cell fragments.

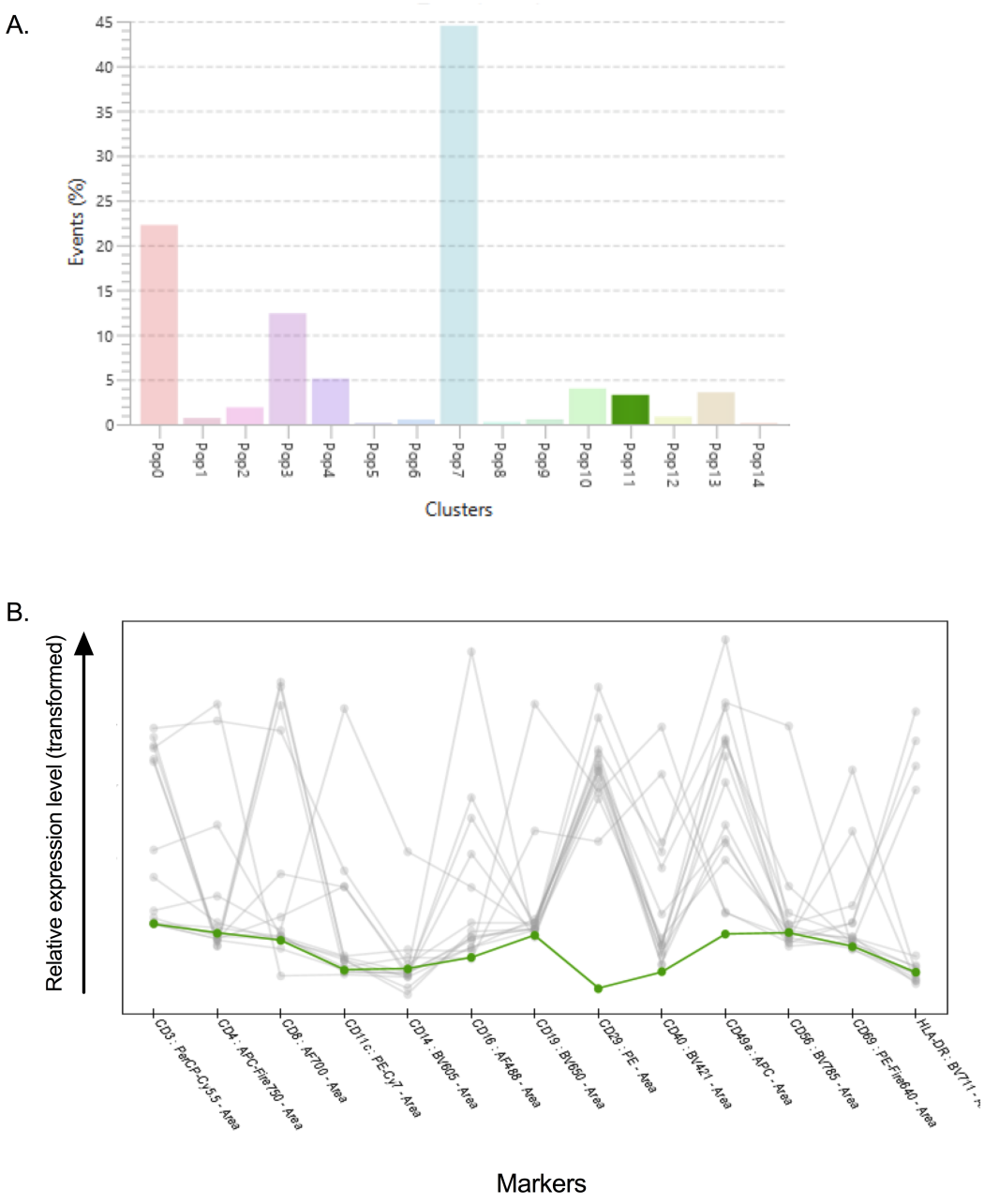

Figure 5.25. Phenotype profile of population 11. (A) Events (%) of population 11 (Pop11) highlighted in green. (B) Marker expression profile of population 11 shows low expression of all markers included in the analysis.

Population 12 (Pop12) represented about 1% of events in the clustering analysis (**Figure 5.26.A.**). Population 12 expressed CD19, CD29, CD40 and HLA-DR (**Figure 5.26.B.**), which suggests that this population consists of B cells.

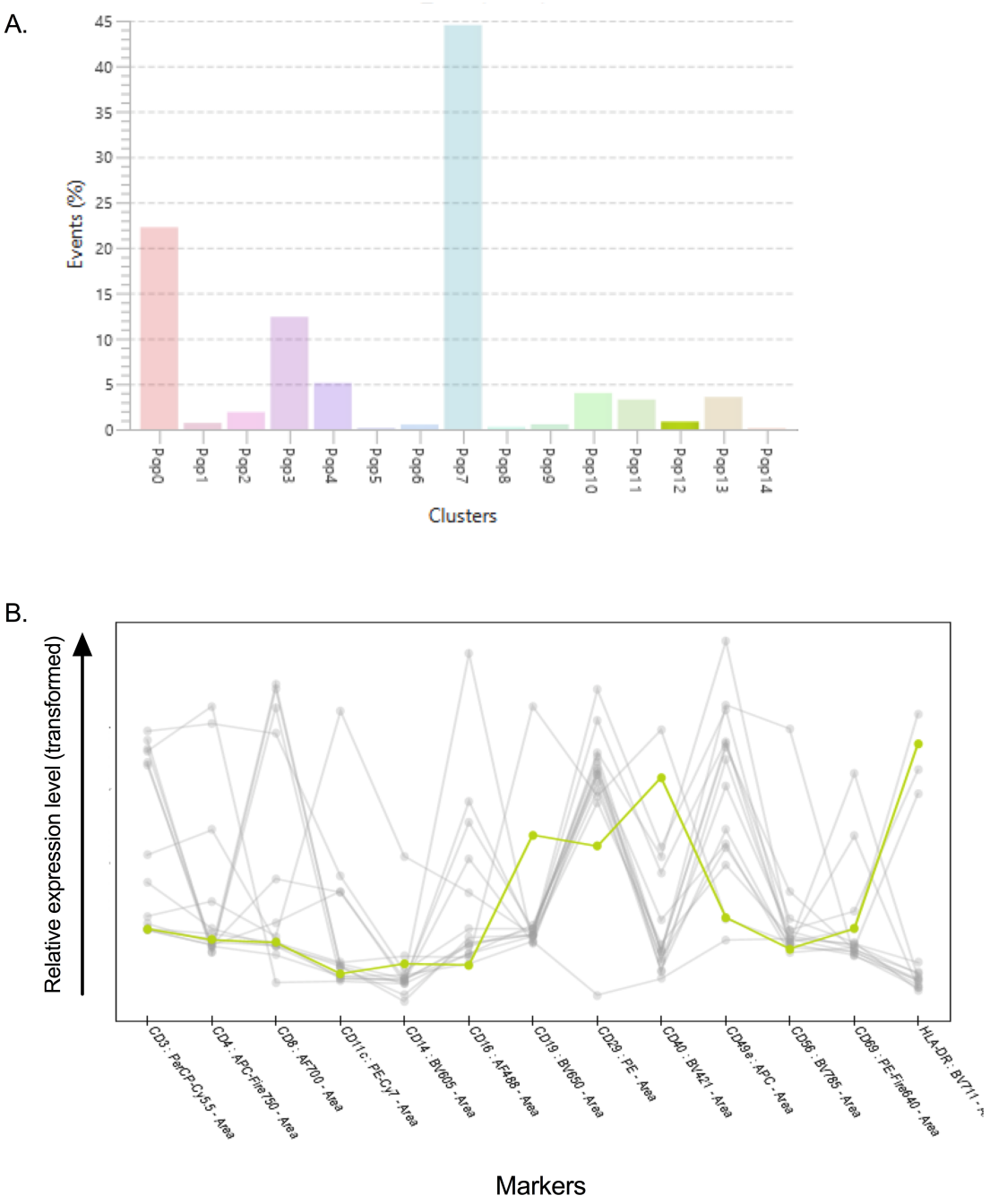

Figure 5.26. Phenotype profile of population 12. (A) Events (%) of population 12 (Pop12) highlighted in green. (B) Marker expression profile of population 12 shows expression of CD19, CD29, CD40 and HLA-DR.

Population 13 (Pop13) represented about 4% of events in the clustering analysis (**Figure 5.27.A.**). Population 13 had high relative expression of markers CD19, CD29, CD40 and HLA-DR (**Figure 5.27.B.**). In this B cell population, expression of CD19 and CD40 was higher compared to expression in population 12 B cells.

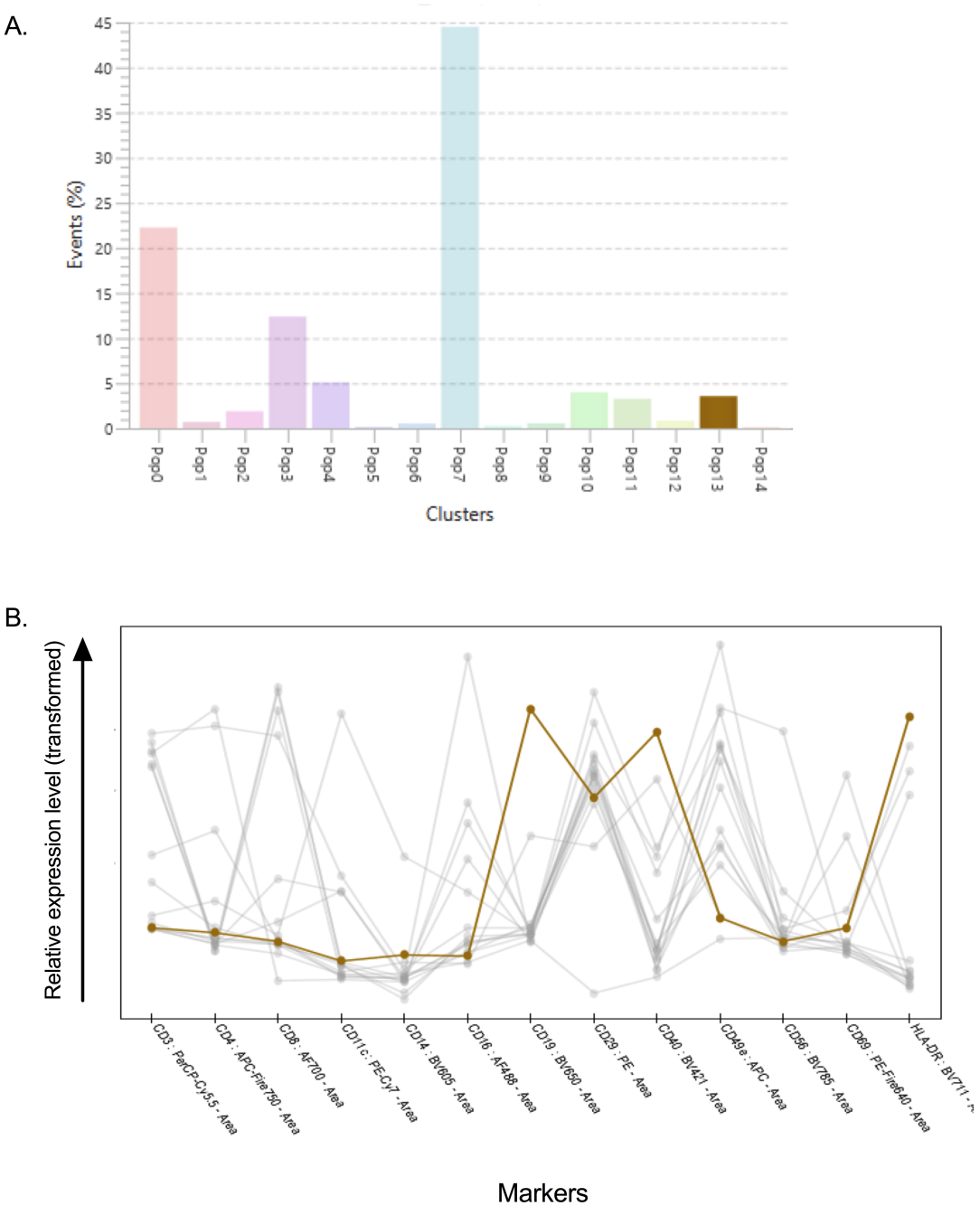

Figure 5.27. Phenotype profile of population 13. (A) Events (%) of population 13 (Pop13). (B) Marker expression profile of population 13 shows expression of CD19, CD29, CD40 and HLA-DR.

Population 14 (Pop14) was one of the lowest populations, representing less than 1% of events in the clustering analysis (**Figure 5.28.A.**). Population 14 expressed markers CD3, CD4, CD29, CD49e and HLA-DR (**Figure 5.28.B.**). Therefore, this population consists of CD4+ T cells, that differed from other CD4+ T cells (Pop7 and Pop10) by their expression of HLA-DR.

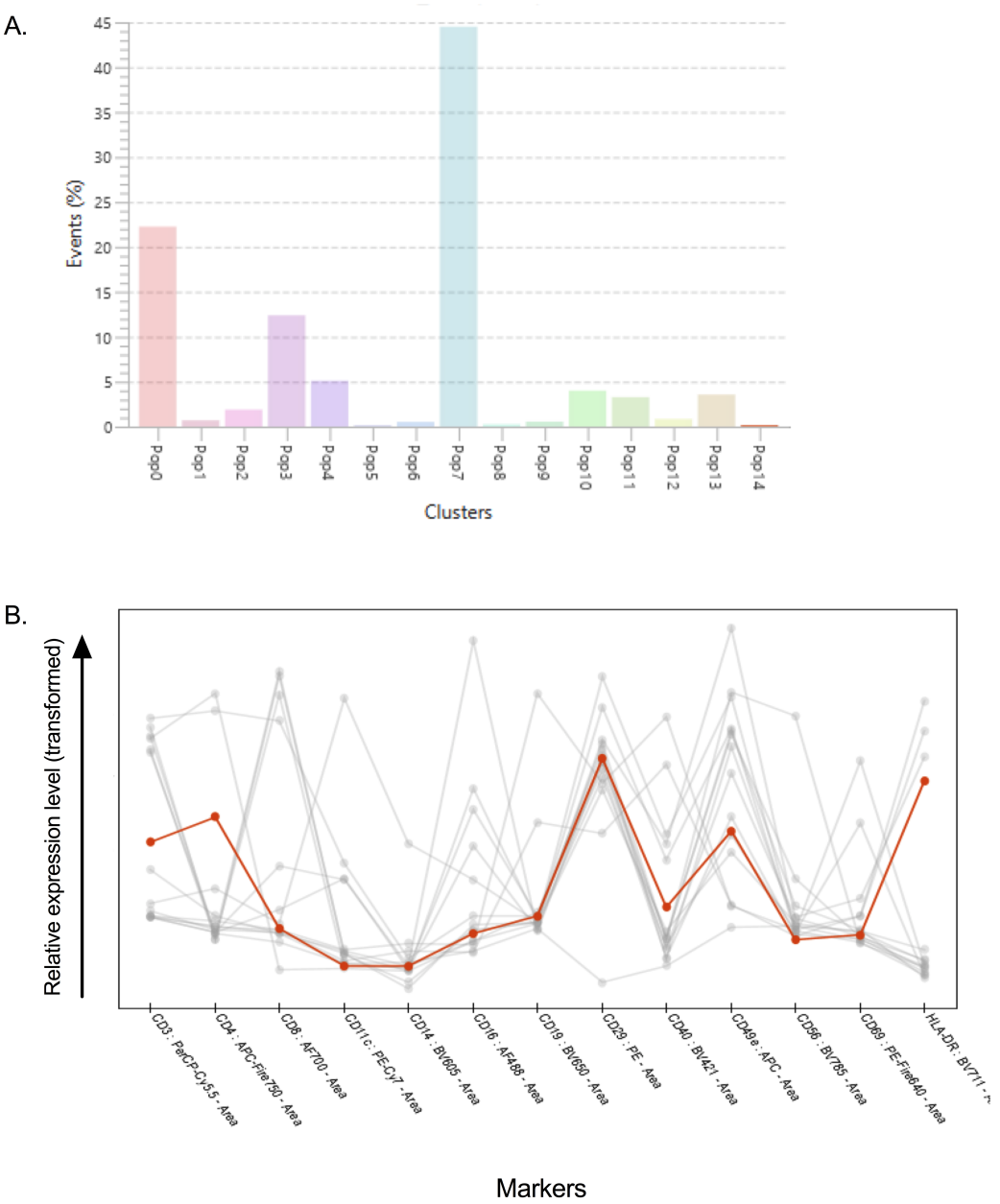

Figure 5.28. Phenotype profile of population 14. (A) Events (%) of population 14 (Pop14), highlighted in orange. (B) Marker expression profile of population 14 shows expression of CD3, CD4, CD29, CD49e and HLA-DR.

A summary of the PBMCs phenotype profiles for the 15 populations according to the 13 differentially expressed immune cell markers was then created (**Figure 5.29.**), with red boxes showing highest expression of a marker and blue showing low expression of the marker.

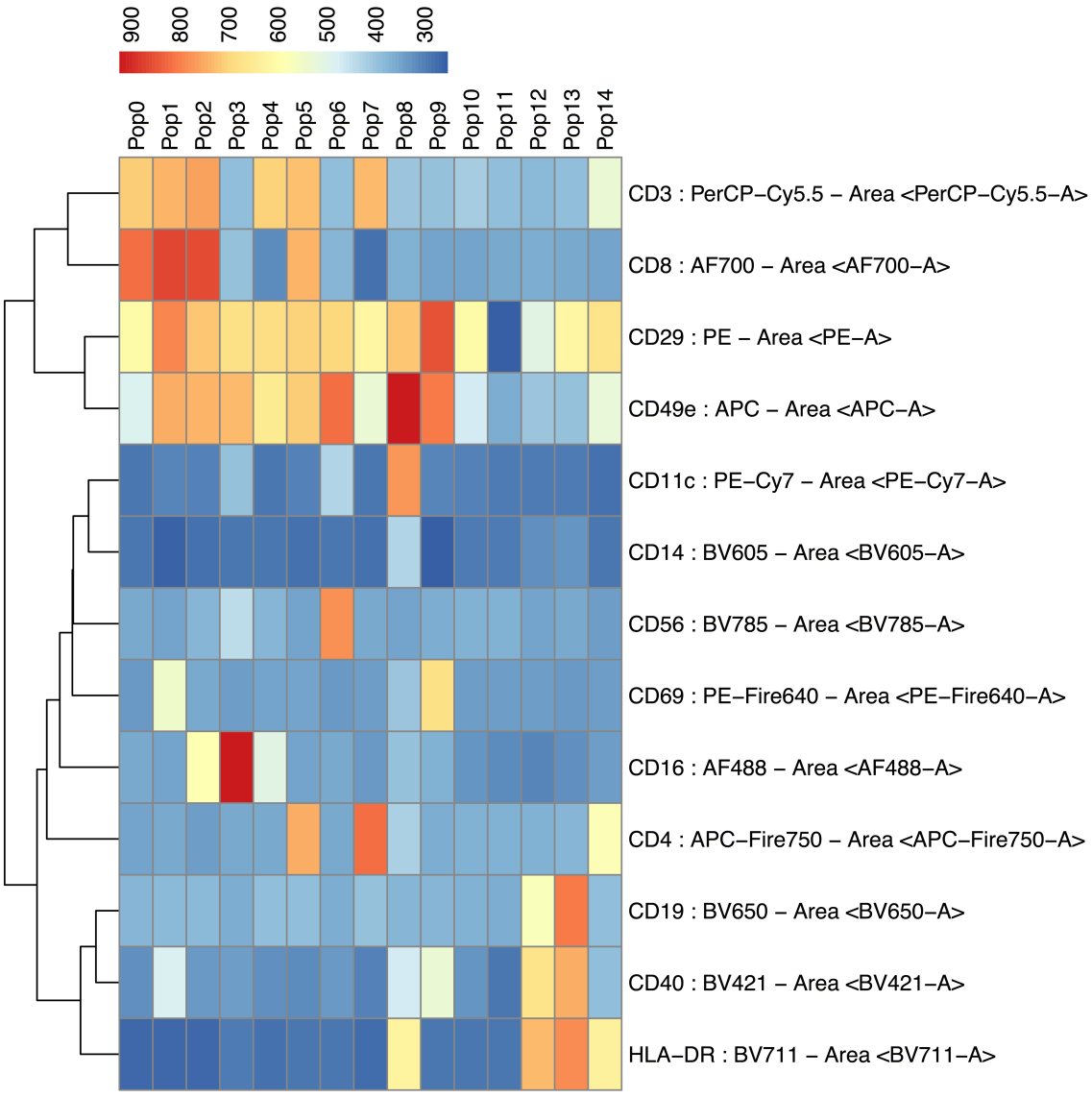

Figure 5.29. PBMCs phenotype profile. Hierarchal clustering and heat map of the 13 differentially expressed immune cell markers in 15 populations identified in the clustering analysis. From the right, clusters progressively join until a single cluster is formed at the left. (n=6 biological repeats)

Furthermore, the percentage of subjects (for each treatment) present in each cluster was measured in order to determine if there were any differences in patterns between treatments (**Figure 5.30.A.**). Results showed that there were no significant differences between treatments (**Figure 5.30.B.**).

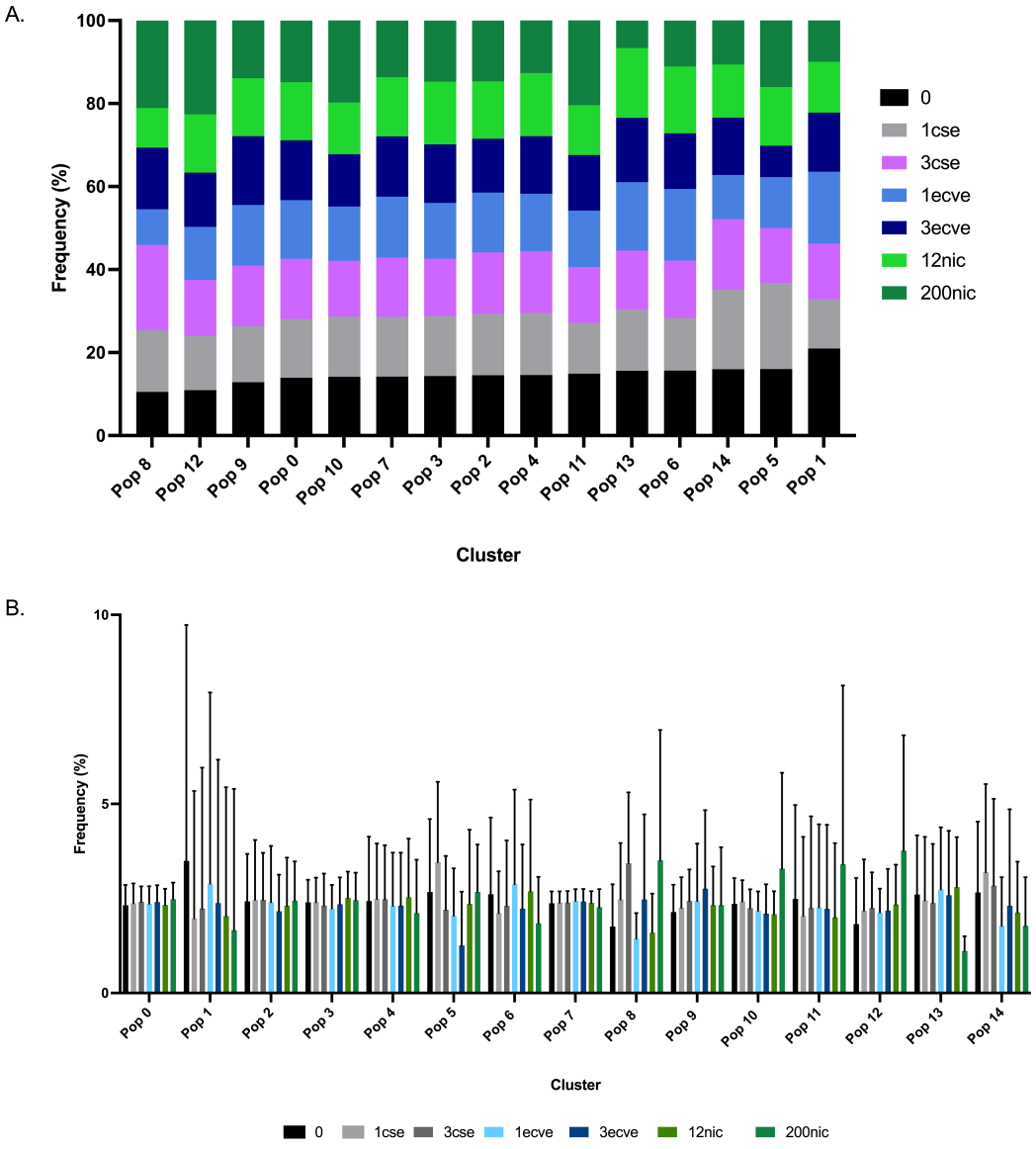

Figure 5.30. Cluster analysis of PBMCs. Percent of cluster occupied by each treatment. Statistical analysis showed no significant difference between treatments for each population. Data are expressed as mean ±SD; Ordinary Two-way ANOVA; Tukey's multiple comparisons post-hoc analyses.

5.4. Discussion

In this chapter the effect of CSE, ECVE and nicotine on the phenotype of immune cells is examined to determine which cell types were present and in what proportions. PBMCs were isolated and cultured for up to 32 hours with no stimulation (control) or with CSE, ECVE or nicotine and then analysed by spectral flow cytometry using a 14-colour panel. High-dimensional flow cytometry allows for the assessment of expression of various surface markers simultaneously at the single-cell level and delineation of the human immune system, during both the steady-state and in context of diseases [566-568]. Recently, the capabilities of flow cytometers have increased due to the introduction of additional lasers and detectors that allow for detection of even greater numbers of markers per cells [569]. Indeed, additional fluorophores have also been introduced to meet the demands of this field. Conventional flow cytometry primarily measures the peak emission of each fluorophore [569]. Contrastingly, full spectrum flow cytometry measures the entire emission spectra for every fluorophore across all laser lines, which allows for collection of substantially more information about each cell [569]. In this study, we utilised full spectrum flow cytometry that would allow us to observe PBMC phenotype using a 14-colour panel.

Results showed that there were no differences in viability of cells under any of the conditions (CSE, ECVE, nicotine) compared to control. CSE results here are in keeping with previous results of this study (Chapter 3.2.), where CSE did not significantly affect PBMC viability even at the 48-hour time point, and with previous studies that observed that exposure to varying concentrations of CSE did not affect viability of PBMCs [128, 487, 503]. Limited studies have compared the effect of CSE and ECVE on cell viability of PBMCs. Rigg et al [570] observed that adenocarcinoma human alveolar basal epithelial (A549) cells treated with 5% ECVE, 5% nicotine-free ECVE and 5% nicotine had a significant decrease in cell number and viability compared to control, whereas treatment with CSE (5%) did not have a significant effect. Here, cells were treated with higher percentages of CSE, ECVE and nicotine than what we have used in our study, which may explain differences in results.

Furthermore, results showed that most of the cell populations did not significantly change after exposure to CSE, ECVE or nicotine compared to control. Two cell populations that did increase, however, were CD14+ monocytes after exposure to 3% CSE and 200 μg/mL nicotine and DCs (CD11c+SSCHi) after exposure to 1% CSE and 3% CSE, compared to control. DCs also significantly decreased at 1% ECVE compared to 1% CSE. A previous study by Di Biase et al [542] reported no significant differences of CD3+CD4+ and CD3+CD8+ cells in PBMCs grown in medium containing tobacco cigarette smoke or e-cigarette vapour, although CD3+ percentage in PBMCs were increased after e-cigarette vapour exposure with or without nicotine. Di Biase et al did not observe changes in other cell populations and did not include a pure nicotine exposure. Jubri et al [571] observed that white blood cell counts and CD3+ cells and B cell percentages were significantly higher in smokers compared to nonsmokers. The study also observed that NK cells percentages were lower in smokers compared to nonsmokers, and that CD4+ T cells were increased in smokers according to number of cigarettes per day [571]. In this study, we also wanted to observe whether there were any changes to CD29, CD49e, CD40 and HLA-DR in the cell populations identified. These markers were selected based on previous results of this study. The results here showed that the markers changed for some populations. Particularly, B cells had decrease in expression of CD40 at 200 nicotine μg/mL compared to other conditions. There are limited studies on the effect of nicotine on expression of these markers in PBMCs. However, nicotine is a constituent of tobacco smoke and many e-cigarette products that acts on nicotinic acetylcholine receptors (nAChRs) [572] and has profound immunological effects, altering a range of immunological functions, including innate and adaptive immune responses [127]. Nicotine modifies immune responses by affecting inflammation, decreasing PBMC proliferation, regulating lymphocytes, macrophages and DCs, and affecting secretion of cytokines by lymphocytes [572].

Finally, clustering analysis was done using FlowJo software to analyse phenotypes of PBMC populations between treatments. High-dimensional single-cell analysis described here provided a landscape of PBMCs under varying conditions, with tSNE allowing for

dimensionality reduction to distinguish cellular subsets. The advantage of this approach is the unbiased nature of the analysis, as with an unbiased peak detection algorithm, it enables objective determination of the number of clusters and may discover unexpected changes in marker expression and identify a new phenotype [573]. Additionally, automated clustering is carried out on data reduced to two t-SNE dimensions allowing for visual verification of sensible cluster boundaries [573]. Furthermore, FlowSOM analysis of the PBMC panel resolved populations identified by manual gating strategy and several populations that we may not have visualised. Here, we identified 15 clusters present, and results showed no significant differences between these clusters. Additionally, the cell populations (CD4+ T cells, CD8+ T cells, B cells, NK cells) were clustered largely together, with minor cell populations (cell with no identifiable markers) being more distant.

In conclusion, here we have shown high dimensional flow cytometry analysis of PBMC population following exposure to CSE, ECVE and nicotine. We show that CSE, ECVE and nicotine do influence some cell populations, as shown in the manually selected population analysis. Clustering analysis identified 15 clusters present but showed no significant differences between the clusters, which may be due to the number of samples analysed. Therefore, further research will focus on higher number of samples to be included in analysis.

Discussion

6.0 Discussion

Chronic Obstructive Pulmonary Disease (COPD) is an inflammatory disease of the airway, affecting the airways, lung parenchyma, and vasculature, and is characterized by irreversible airflow limitation. Over 70% of COPD cases in high-income countries and 30-40% of COPD cases in low- and middle-income countries can be linked to tobacco smoking [1]. Indeed, cigarette smoking is a significant risk factor associated with various diseases, including COPD, cardiovascular disease and cancers. E-cigarettes are promoted as a safer alternative to cigarettes and are being used as substitutes to quit cigarette smoking to reduce risk to health. The acute and long-term effects of e-cigarettes have not been fully elucidated, but an increasing amount of evidence suggests that e-cigarettes are a source of toxic chemical exposure with carcinogenic properties and may contribute to pulmonary and systemic inflammatory processes and increase the risk of respiratory and cardiovascular diseases [206, 207]. Furthermore, extracellular vesicles (EVs) are important intercellular communication mediators released by cells into the extracellular environment, with the capacity to transfer biological signals and information between cells and as such, influence the recipient cell function [276-278]. EVs have significant cell-to-cell communication roles in cellular responses and are involved in physiological roles and pathology of various diseases, including pulmonary diseases [33]. Both cigarette smoke and e-cigarettes have been linked to increased release of EVs from a number of cellular sources. To date, however, there are limited studies on EVs derived from immune cells exposed to cigarette smoke or e-cigarette vapour.

This research aimed to explore the effects of cigarette smoke and e-cigarette vapour on the production of extracellular vesicles by immune cells. The research also aimed to optimise and develop techniques to study EVs and investigate the effect of cigarette smoke extract and e-cigarette vapour extract on the production of extracellular vesicles by cells of the immune system. We also aimed to investigate the effect of CSE and ECVE on the phenotype of immune cells when producing EVs. This research was conducted with the hypothesis that cigarette smoke extract and e-cigarette vapour extract may

modify the production of EVs by immune cells and may modify the phenotype of immune cells. The first aim of this study was to optimise methods that are sensitive and reproducible for EV analysis. In this study, using serum-free AIM-V cell culture medium for culture of PBMCs, we have optimised novel techniques to study PBMC-derived EVs, focusing on high-throughput flow-based methods, including imaging flow cytometry (IFC) and a rapid staining protocol that allows for quantification of EVs in culture and following isolation. Using the methods developed in this study, we showed that neither CSE nor ECVE significantly altered the number of EVs produced by PBMC. Previous studies have shown that CSE exposure results in increased numbers of EVs produced by DCs [367] and PBMCs [334], however, cells were exposed to higher concentrations of CSE, and particle numbers were analysed by NTA and conventional flow cytometry, limiting the comparability of measurements with our study. We have observed expression of tetraspanins CD9, CD63 and CD81 simultaneously. This is the first study, to our knowledge, showing that all three tetraspanins can be simultaneously detected along with calcein on EVs using IFC. Results in this study demonstrated that the tetraspanin profile of EVs did change between conditions, particularly for tetraspanins CD9 and CD63. Tetraspanins have widely been used as markers of EVs, however, recently they have been described to play vital roles in EV physiology [574]. Indeed, cigarette smoke has been shown to modify EV profiles in humans [575], and it may be possible that exposure to CSE modifies intracellular signalling pathways that in turn affect EV formation and consequently their release [576]. We also showed in this study that membrane profile, in terms of marker expression, of EVs was altered by CSE. Spectral flow cytometry was then used to analyse the phenotype of CSE- and ECVE-stimulated PBMCs producing EVs, with manual gating analysis and unsupervised cluster analysis. This study shows that although there were no significant differences in the viability of cells after exposure to CSE and ECVE, there were changes in cell populations following exposure. Finally, clustering analysis identified 15 clusters present in the data but showed no significant differences in clusters between treatments.

Furthermore, MISEV guidelines [399] published by ISEV provide a number of recommendations regarding how to characterise and confirm the identity, yield and purity of EVs. The guidelines highlight that multiple, complementary techniques are to be used when characterising EVs [399]. In this study, we utilised nanoparticle flow cytometry (nFCM), transmission electron microscopy (TEM), nanoparticle tracking analysis (NTA), conventional flow cytometry and imaging flow cytometry (IFC) to observe and analyse EVs in culture and following isolation by SEC. The main focus of this study was the use of imaging flow cytometry with calcein AM to develop a novel gating strategy that allows for quantification of EVs in culture and following isolation and that allows for the ability to observe three tetraspanins on calcein-labelled EVs. Moreover, due to the unique challenges of EV flow cytometry, we followed MISEV guidelines [399] and the MIFlowCyt-EV framework [402], to include a number of controls that are not typically included when analysing cells and other micron-size particles. In this study, we included: buffer-only controls to measure the instrument's background event rate at the same settings used to analyse EV samples; buffer with reagents to demonstrate whether the background signal is altered; unstained controls to provide estimates of the background event or signals that may be expected with stained samples or isotypes; isotypes controls; and single-stained controls for assessment of whether a fluorescent reagent's spectrum affects the detection parameter of another fluorescent agent [402]. We also included detergent controls, using Tween 20, which help to determine whether detected events are membrane-enclosed vesicles or other protein complexes, as detergent treatment lyses membrane-enclosed vesicles, thus reducing their number and signal. Protein complexes and other particulates are detergent-resistant and as such, will persist following treatment, allowing for differentiation from EVs [402].

There are a few limitations to this study. Firstly, there were individual differences in our data, possibly due to a lack of information about the health status of our donors. Recent infections or the use of medications, which donors may have been taking but not required to disclose, may impact the functionality of the immune cells isolated. As a result, future experiments will be required to assess variables including age, sex, recent

infections or last known date of infection, diagnosis of any chronic conditions and any medications taken prior to blood donations. Another limitation in our study was the presence of platelets in our PBMC samples, as platelets are known to produce EVs in culture. Future experiments will focus on the magnetic isolation of PBMCs using CD45 magnetic beads to decrease the presence of platelets, as CD45 is found on all PBMCs but not on platelets and megakaryocytes. A third limitation in our study is the diversity of current methodologies used to analyse EVs, as the comparability of measurements is restricted by the lack of standardisation. However, we have used MISEV 2018 guidelines in our study to ensure that the criteria for EV studies were met within our protocols and methods. The MISEV guidelines have been published to provide recommendations on the nomenclature, preparation, characterisation and reporting criteria for EV studies. Additionally, MIFlowCyt-EV also provides a framework for reporting of extracellular vesicle flow cytometry experiments; which over time, its adoption may improve the ability to quantitatively compare results between studies and may support the development of new instruments and assays for measurements of EVs.

The next phase of this study would involve the recruitment of individuals with COPD. Blood samples would be obtained from them, and PBMCs would be isolated and exposed to CSE and ECVE. The concentration of EVs produced after exposure would be measured to detected any changes and these would be compared to healthy controls. EVs derived from PBMCs exposed to CSE and ECVE would then be isolated and characterised using techniques, including those used in this study, such as NTA, TEM, and IFC. Proteomic analysis and transcriptomic analysis of EV cargo would also be carried out to identify changes in molecular composition of EVs in response to CSE and ECVE exposure. These analyses would be useful in elucidating any changes in the molecular composition of EVs in response to CSE and ECVE exposure. Proteomic analysis of EVs by mass spectrometry is known to provide the most comprehensive analysis of EV protein cargo, allowing for identification of biomarkers of diseases. Additionally, transcriptomic analysis of EVs may reveal information on the nucleic acid components, also allowing for the potential discovery of biomarkers related to disease. This would be

done through RNAseq to identify both the coding and non-coding RNA cargo of EVs. *In vitro* studies could be done using epithelial cell lines and immune cells to investigate if EVs affect epithelial cell and immune cell function following exposure to cigarette smoke and e-cigarette vapour. Another approach would be the use of organ-on-chip systems (OCMS), which have been used to model and decode inter-organ communication that may occur via EVs [577]. These techniques can be used to study the effects of CSE and ECVE on lung biology and to investigate cellular responses to EVs derived from cells and tissues exposed to CSE and ECVE. Furthermore, isolated EVs derived from exposed cells in the study would be introduced to recipient cells or tissues using *in vitro* assays. This would be useful in investigating the functional effects of EVs and any potential impacts of EVs on inflammatory signalling pathways, oxidative stress and cell proliferation in cells involved in the pathogenesis of COPD. Additionally, with the recruitment of individuals with COPD, associations between EV concentration and/or characteristics and clinical outcomes, such as lung function decline or frequency of exacerbation episodes, would be explored.

Finally, ISEV has recently published the MISEV 2023 [282] guidelines to include advanced techniques and approaches that are currently widening the field of EV research. This overview includes *in vivo* approaches to study EVs. Here, the recommendation is for larger mammalian models to recapitulate aspects of human physiology and disease processes, allowing for the assessment of EVs and their interaction with target cells. For example, mouse models have been used to observe EVs produced from epithelial cells [578], red blood cells[579], mouse tumour cells [580, 581] to observe cell-specific EVs in plasma, ischaemic heart, and metastasis, respectively. Thus, future study in this field could be done using *in vivo* approaches including the use of mouse models. Here, endogenous EVs could be traced and examined using fluorescent or bioluminescent tags to investigate their functional role and their uptake by recipient cells. Another approach would include introducing exogenous EVs into an organism. Here, exogenous EVs may be unlabelled to observe disease or physiologic outcome. In case of imaging, EVs would be fluorescently or bioluminescently labelled

and observed using magnetic resonance imaging (MRI), X-ray computed tomopgraphy (CT) imaging, magnetic particle imaging (MPI or positron emission tomography (PET), as has been carried out in recent studies [582, 583]. Overall, *in vivo* models would provide the opportunity to assess the release of physiological levels of EVs and investigate their interaction with target cells, further elucidating mechanisms involved in disease development.

In conclusion, this study has outlined a method to study extracellular vesicles derived from immune cells in an inflammatory disease model. We have shown that, whilst the number of EVs produced was not affected, the membrane profile of EVs was modified after exposure to CSE and ECVE. Spectral flow cytometry was used to analyse the phenotype of CSE- and ECVE-stimulated PBMCs producing EVs, with manual gating analysis and cluster analysis. Our results suggest that CSE and ECVE may modify EV profiles in humans, and exposure to these components can result in changes within the cells producing EVs and consequently, affect EV formation. These EVs may carry signalling molecules that contribute to the development and progression of COPD. Therefore, it is important to understand the interplay between CSE, ECVE, and EVs to elucidate the underlying mechanisms of COPD pathogenesis, which may lead to identifying novel therapeutic targets.

References:

1. WHO, *Chronic obstructive pulmonary disease (COPD)*, Newsroom, Editor. 2023, World Health Organization.
2. BLF, *Chronic obstructive pulmonary disease (COPD) statistics.* British Lung Foundation.
3. Syamlal, G., *Chronic Obstructive Pulmonary Disease Prevalence Among Adults Who Have Never Smoked, by Industry and Occupation — United States, 2013–2017*, C.f.D.C.a. Prevention, Editor. 2019, Centers for Disease Control and Prevention.
4. Kc, R., Shukla, S.D., Gautam, S.S., Hansbro, P.M., and O'Toole, R.F., *The role of environmental exposure to non-cigarette smoke in lung disease.* Clin Transl Med, 2018. **7**(1): p. 39.
5. Cho, M.H., Hobbs, B.D., and Silverman, E.K., *Genetics of chronic obstructive pulmonary disease: understanding the pathobiology and heterogeneity of a complex disorder.* Lancet Respir Med, 2022. **10**(5): p. 485-496.
6. Silverman, E.K., *Genetics of COPD.* Annu Rev Physiol, 2020. **82**: p. 413-431.
7. Barnes, P.J., *Targeting cytokines to treat asthma and chronic obstructive pulmonary disease.* Nat Rev Immunol, 2018. **18**(7): p. 454-466.
8. Barnes, P.J., Burney, P.G., Silverman, E.K., Celli, B.R., Vestbo, J., Wedzicha, J.A., and Wouters, E.F., *Chronic obstructive pulmonary disease.* Nat Rev Dis Primers, 2015. **1**: p. 15076.
9. Barnes, P.J., *Chronic obstructive pulmonary disease: effects beyond the lungs.* PLoS Med, 2010. **7**(3): p. e1000220.
10. Vogelmeier, C.F., Criner, G.J., Martinez, F.J., Anzueto, A., Barnes, P.J., Bourbeau, J., Celli, B.R., Chen, R., Decramer, M., Fabbri, L.M., Frith, P., Halpin, D.M., Lopez Varela, M.V., Nishimura, M., Roche, N., Rodriguez-Roisin, R., Sin, D.D., Singh, D., Stockley, R., Vestbo, J., Wedzicha, J.A., and Agusti, A., *Global Strategy for the Diagnosis, Management, and Prevention of Chronic Obstructive Lung Disease 2017 Report: GOLD Executive Summary.* Arch Bronconeumol, 2017. **53**(3): p. 128-149.
11. Mannino, D.M. and Buist, A.S., *Global burden of COPD: risk factors, prevalence, and future trends.* Lancet, 2007. **370**(9589): p. 765-73.
12. Wedzicha, J.A. and Seemungal, T.A., *COPD exacerbations: defining their cause and prevention.* Lancet, 2007. **370**(9589): p. 786-96.
13. Mirza, S., Clay, R.D., Koslow, M.A., and Scanlon, P.D., *COPD Guidelines: A Review of the 2018 GOLD Report.* Mayo Clin Proc, 2018. **93**(10): p. 1488-1502.
14. Wouters, E.F.M., Breyer, M.K., Breyer-Kohansal, R., and Hartl, S., *COPD Diagnosis: Time for Disruption.* J Clin Med, 2021. **10**(20).
15. Fazleen, A. and Wilkinson, T., *Early COPD: current evidence for diagnosis and management.* Ther Adv Respir Dis, 2020. **14**: p. 1753466620942128.
16. Celli, B.R., *Update on the management of COPD.* Chest, 2008. **133**(6): p. 1451-1462.

17. Vogelmeier, C.F., Criner, G.J., Martinez, F.J., Anzueto, A., Barnes, P.J., Bourbeau, J., Celli, B.R., Chen, R., Decramer, M., Fabbri, L.M., Frith, P., Halpin, D.M., Lopez Varela, M.V., Nishimura, M., Roche, N., Rodriguez-Roisin, R., Sin, D.D., Singh, D., Stockley, R., Vestbo, J., Wedzicha, J.A., and Agusti, A., *Global Strategy for the Diagnosis, Management, and Prevention of Chronic Obstructive Lung Disease 2017 Report. GOLD Executive Summary.* Am J Respir Crit Care Med, 2017. **195**(5): p. 557-582.
18. Matera, M.G., Cazzola, M., and Page, C., *Prospects for COPD treatment.* Curr Opin Pharmacol, 2021. **56**: p. 74-84.
19. Zhang, Y., Wang, L., Mutlu, G.M., and Cai, H., *More to Explore: Further Definition of Risk Factors for COPD - Differential Gender Difference, Modest Elevation in PM2.5, and e-Cigarette Use.* Front Physiol, 2021. **12**: p. 669152.
20. Song, Q., Chen, P., and Liu, X.M., *The role of cigarette smoke-induced pulmonary vascular endothelial cell apoptosis in COPD.* Respir Res, 2021. **22**(1): p. 39.
21. Bhatt, S.P., Kim, Y.I., Harrington, K.F., Hokanson, J.E., Lutz, S.M., Cho, M.H., DeMeo, D.L., Wells, J.M., Make, B.J., Rennard, S.I., Washko, G.R., Foreman, M.G., Tashkin, D.P., Wise, R.A., Dransfield, M.T., Bailey, W.C., and Investigators, C.O., *Smoking duration alone provides stronger risk estimates of chronic obstructive pulmonary disease than pack-years.* Thorax, 2018. **73**(5): p. 414-421.
22. Blair, K.A. and Evelo, A.J., *Risk factors for COPD: what do NPs know?* J Am Assoc Nurse Pract, 2014. **26**(3): p. 123-30.
23. Raad, D., Gaddam, S., Schunemann, H.J., Irani, J., Abou Jaoude, P., Honeine, R., and Akl, E.A., *Effects of water-pipe smoking on lung function: a systematic review and meta-analysis.* Chest, 2011. **139**(4): p. 764-774.
24. Safiri, S., Carson-Chahhoud, K., Noori, M., Nejadghaderi, S.A., Sullman, M.J.M., Ahmadian Heris, J., Ansarin, K., Mansournia, M.A., Collins, G.S., Kolahi, A.A., and Kaufman, J.S., *Burden of chronic obstructive pulmonary disease and its attributable risk factors in 204 countries and territories, 1990-2019: results from the Global Burden of Disease Study 2019.* BMJ, 2022. **378**: p. e069679.
25. Stoller, J.K. and Aboussouan, L.S., *Alpha1-antitrypsin deficiency.* Lancet, 2005. **365**(9478): p. 2225-36.
26. Lee, Y.J., Choi, S., Kwon, S.Y., Lee, Y., Lee, J.K., Heo, E.Y., Chung, H.S., and Kim, D.K., *A Genome-Wide Association Study in Early COPD: Identification of One Major Susceptibility Loci.* Int J Chron Obstruct Pulmon Dis, 2020. **15**: p. 2967-2975.
27. Bowler, R.P., Hansel, N.N., Jacobson, S., Graham Barr, R., Make, B.J., Han, M.K., O'Neal, W.K., Oelsner, E.C., Casaburi, R., Barjaktarevic, I., Cooper, C., Foreman, M., Wise, R.A., DeMeo, D.L., Silverman, E.K., Bailey, W., Harrington, K.F., Woodruff, P.G., Drummond, M.B., for, C., and Investigators, S., *Electronic Cigarette Use in US Adults at Risk for or with COPD: Analysis from Two Observational Cohorts.* J Gen Intern Med, 2017. **32**(12): p. 1315-1322.

28. Kosmider, L., Sobczak, A., Prokopowicz, A., Kurek, J., Zaciera, M., Knysak, J., Smith, D., and Goniewicz, M.L., *Cherry-flavoured electronic cigarettes expose users to the inhalation irritant, benzaldehyde.* Thorax, 2016. **71**(4): p. 376-7.
29. Hill, A.T., Haworth, C.S., Aliberti, S., Barker, A., Blasi, F., Boersma, W., Chalmers, J.D., De Soyza, A., Dimakou, K., Elborn, J.S., Feldman, C., Flume, P., Goeminne, P.C., Loebinger, M.R., Menendez, R., Morgan, L., Murris, M., Polverino, E., Quittner, A., Ringshausen, F.C., Tino, G., Torres, A., Vendrell, M., Welte, T., Wilson, R., Wong, C., O'Donnell, A., Aksamit, T., and group, E.B.d.w., *Pulmonary exacerbation in adults with bronchiectasis: a consensus definition for clinical research.* Eur Respir J, 2017. **49**(6).
30. Chen, Y.W., Leung, J.M., and Sin, D.D., *A Systematic Review of Diagnostic Biomarkers of COPD Exacerbation.* PLoS One, 2016. **11**(7): p. e0158843.
31. Celli, B.R. and Barnes, P.J., *Exacerbations of chronic obstructive pulmonary disease.* Eur Respir J, 2007. **29**(6): p. 1224-38.
32. Rodriguez-Roisin, R., *Toward a consensus definition for COPD exacerbations.* Chest, 2000. **117**(5 Suppl 2): p. 398S-401S.
33. Kadota, T., Fujita, Y., Yoshioka, Y., Araya, J., Kuwano, K., and Ochiya, T., *Extracellular Vesicles in Chronic Obstructive Pulmonary Disease.* Int J Mol Sci, 2016. **17**(11).
34. MacNee, W., *Pathogenesis of chronic obstructive pulmonary disease.* Proc Am Thorac Soc, 2005. **2**(4): p. 258-66; discussion 290-1.
35. Chung, K.F. and Adcock, I.M., *Multifaceted mechanisms in COPD: inflammation, immunity, and tissue repair and destruction.* Eur Respir J, 2008. **31**(6): p. 1334-56.
36. Arezina, R., Chen, T., and Wang, D., *Conventional, Complementary and Alternative Medicines: Mechanistic Insights into Therapeutic Landscape of Chronic Obstructive Pulmonary Disease.* Int J Chron Obstruct Pulmon Dis, 2023. **18**: p. 447-457.
37. Bagdonas, E., Raudoniute, J., Bruzauskaite, I., and Aldonyte, R., *Novel aspects of pathogenesis and regeneration mechanisms in COPD.* Int J Chron Obstruct Pulmon Dis, 2015. **10**: p. 995-1013.
38. Wang, C., Zhou, J., Wang, J., Li, S., Fukunaga, A., Yodoi, J., and Tian, H., *Progress in the mechanism and targeted drug therapy for COPD.* Signal Transduct Target Ther, 2020. **5**(1): p. 248.
39. Gadek, J.E., Fells, G.A., and Crystal, R.G., *Cigarette smoking induces functional antiprotease deficiency in the lower respiratory tract of humans.* Science, 1979. **206**(4424): p. 1315-6.
40. Ramos, F.L., Krahnke, J.S., and Kim, V., *Clinical issues of mucus accumulation in COPD.* Int J Chron Obstruct Pulmon Dis, 2014. **9**: p. 139-50.
41. Rab, A., Rowe, S.M., Raju, S.V., Bebok, Z., Matalon, S., and Collawn, J.F., *Cigarette smoke and CFTR: implications in the pathogenesis of COPD.* Am J Physiol Lung Cell Mol Physiol, 2013. **305**(8): p. L530-41.

42. Kim, V. and Criner, G.J., *The chronic bronchitis phenotype in chronic obstructive pulmonary disease: features and implications.* Curr Opin Pulm Med, 2015. **21**(2): p. 133-41.
43. Dotan, Y., So, J.Y., and Kim, V., *Chronic Bronchitis: Where Are We Now?* Chronic Obstr Pulm Dis, 2019. **6**(2): p. 178-192.
44. Kim, V. and Criner, G.J., *Chronic bronchitis and chronic obstructive pulmonary disease.* Am J Respir Crit Care Med, 2013. **187**(3): p. 228-37.
45. Spurzem, J.R. and Rennard, S.I., *Pathogenesis of COPD.* Semin Respir Crit Care Med, 2005. **26**(2): p. 142-53.
46. Singh, D., *Small Airway Disease in Patients with Chronic Obstructive Pulmonary Disease.* Tuberc Respir Dis (Seoul), 2017. **80**(4): p. 317-324.
47. Higham, A., Quinn, A.M., Cancado, J.E.D., and Singh, D., *The pathology of small airways disease in COPD: historical aspects and future directions.* Respir Res, 2019. **20**(1): p. 49.
48. Hogg, J.C., Pare, P.D., and Hackett, T.L., *The Contribution of Small Airway Obstruction to the Pathogenesis of Chronic Obstructive Pulmonary Disease.* Physiol Rev, 2017. **97**(2): p. 529-552.
49. Bonini, M. and Usmani, O.S., *The role of the small airways in the pathophysiology of asthma and chronic obstructive pulmonary disease.* Ther Adv Respir Dis, 2015. **9**(6): p. 281-93.
50. Stewart, J.I. and Criner, G.J., *The small airways in chronic obstructive pulmonary disease: pathology and effects on disease progression and survival.* Curr Opin Pulm Med, 2013. **19**(2): p. 109-15.
51. Barnes, P.J. and Celli, B.R., *Systemic manifestations and comorbidities of COPD.* Eur Respir J, 2009. **33**(5): p. 1165-85.
52. Gan, W.Q., Man, S.F., Senthilselvan, A., and Sin, D.D., *Association between chronic obstructive pulmonary disease and systemic inflammation: a systematic review and a meta-analysis.* Thorax, 2004. **59**(7): p. 574-80.
53. Nussbaumer-Ochsner, Y. and Rabe, K.F., *Systemic manifestations of COPD.* Chest, 2011. **139**(1): p. 165-73.
54. Hopkinson, N.S., Tennant, R.C., Dayer, M.J., Swallow, E.B., Hansel, T.T., Moxham, J., and Polkey, M.I., *A prospective study of decline in fat free mass and skeletal muscle strength in chronic obstructive pulmonary disease.* Respir Res, 2007. **8**: p. 25.
55. Gosker, H.R., Kubat, B., Schaart, G., van der Vusse, G.J., Wouters, E.F., and Schols, A.M., *Myopathological features in skeletal muscle of patients with chronic obstructive pulmonary disease.* Eur Respir J, 2003. **22**(2): p. 280-5.
56. Zuo, L., He, F., Sergakis, G.G., Koozehchian, M.S., Stimpfl, J.N., Rong, Y., Diaz, P.T., and Best, T.M., *Interrelated role of cigarette smoking, oxidative stress, and immune response in COPD and corresponding treatments.* Am J Physiol Lung Cell Mol Physiol, 2014. **307**(3): p. L205-18.
57. Lu, Q., Gottlieb, E., and Rounds, S., *Effects of cigarette smoke on pulmonary endothelial cells.* Am J Physiol Lung Cell Mol Physiol, 2018. **314**(5): p. L743-L756.

58. Cai, B., Li, Z., Wang, R., Geng, Z., Shi, Y., Xie, S., Wang, Z., Yang, Z., and Ren, X., *Emission level of seven mainstream smoke toxicants from cigarette with variable tobacco leaf constituents.* Regul Toxicol Pharmacol, 2019. **103**: p. 181-188.
59. Lugg, S.T., Scott, A., Parekh, D., Naidu, B., and Thickett, D.R., *Cigarette smoke exposure and alveolar macrophages: mechanisms for lung disease.* Thorax, 2022. **77**(1): p. 94-101.
60. Afridi, H.I., Kazi, T.G., Talpur, F.N., and Brabazon, D., *Evaluation of trace and toxic elements in the samples of different cigarettes and their impact on human health of Irish diabetes mellitus patients.* Clin Lab, 2015. **61**(1-2): p. 123-40.
61. Fresquez, M.R., Pappas, R.S., and Watson, C.H., *Establishment of toxic metal reference range in tobacco from US cigarettes.* J Anal Toxicol, 2013. **37**(5): p. 298-304.
62. Li, X., *In vitro toxicity testing of cigarette smoke based on the air-liquid interface exposure: A review.* Toxicol In Vitro, 2016. **36**: p. 105-113.
63. Lee, J., Taneja, V., and Vassallo, R., *Cigarette smoking and inflammation: cellular and molecular mechanisms.* J Dent Res, 2012. **91**(2): p. 142-9.
64. McGrath, J.J.C. and Stampfli, M.R., *The immune system as a victim and aggressor in chronic obstructive pulmonary disease.* J Thorac Dis, 2018. **10**(Suppl 17): p. S2011-S2017.
65. Bhat, T.A., Panzica, L., Kalathil, S.G., and Thanavala, Y., *Immune Dysfunction in Patients with Chronic Obstructive Pulmonary Disease.* Ann Am Thorac Soc, 2015. **12 Suppl 2**: p. S169-75.
66. Caramori, G., Casolari, P., Barczyk, A., Durham, A.L., Di Stefano, A., and Adcock, I., *COPD immunopathology.* Semin Immunopathol, 2016. **38**(4): p. 497-515.
67. Barnes, P.J., *Inflammatory mechanisms in patients with chronic obstructive pulmonary disease.* J Allergy Clin Immunol, 2016. **138**(1): p. 16-27.
68. Brusselle, G.G., Joos, G.F., and Bracke, K.R., *New insights into the immunology of chronic obstructive pulmonary disease.* Lancet, 2011. **378**(9795): p. 1015-26.
69. Gamble, E., Grootendorst, D.C., Hattotuwa, K., O'Shaughnessy, T., Ram, F.S., Qiu, Y., Zhu, J., Vignola, A.M., Kroegel, C., and Morell, F., *Airway mucosal inflammation in COPD is similar in smokers and ex-smokers: a pooled analysis.* European Respiratory Journal, 2007. **30**(3): p. 467-471.
70. Strzelak, A., Ratajczak, A., Adamiec, A., and Feleszko, W., *Tobacco Smoke Induces and Alters Immune Responses in the Lung Triggering Inflammation, Allergy, Asthma and Other Lung Diseases: A Mechanistic Review.* Int J Environ Res Public Health, 2018. **15**(5).
71. Bhalla, D.K., Hirata, F., Rishi, A.K., and Gairola, C.G., *Cigarette smoke, inflammation, and lung injury: a mechanistic perspective.* J Toxicol Environ Health B Crit Rev, 2009. **12**(1): p. 45-64.
72. Traves, S.L., Culpitt, S.V., Russell, R.E., Barnes, P.J., and Donnelly, L.E., *Increased levels of the chemokines GROalpha and MCP-1 in sputum samples from patients with COPD.* Thorax, 2002. **57**(7): p. 590-5.

73. Perez-Rial, S., del Puerto-Nevado, L., Terron-Exposito, R., Giron-Martinez, A., Gonzalez-Mangado, N., and Peces-Barba, G., *Role of recently migrated monocytes in cigarette smoke-induced lung inflammation in different strain of mice.* PLoS One, 2013. **8**(9): p. e72975.
74. John, G., Kohse, K., Orasche, J., Reda, A., Schnelle-Kreis, J., Zimmermann, R., Schmid, O., Eickelberg, O., and Yildirim, A.O., *The composition of cigarette smoke determines inflammatory cell recruitment to the lung in COPD mouse models.* Clin Sci (Lond), 2014. **126**(3): p. 207-21.
75. Kark, J.D., Lebiush, M., and Rannon, L., *Cigarette smoking as a risk factor for epidemic a (h1n1) influenza in young men.* New England Journal of Medicine, 1982. **307**(17): p. 1042-1046.
76. Chavez, J. and Hai, R., *Effects of Cigarette Smoking on Influenza Virus/Host Interplay.* Pathogens, 2021. **10**(12).
77. Mallia, P., Message, S.D., Gielen, V., Contoli, M., Gray, K., Kebadze, T., Aniscenko, J., Laza-Stanca, V., Edwards, M.R., Slater, L., Papi, A., Stanciu, L.A., Kon, O.M., Johnson, M., and Johnston, S.L., *Experimental Rhinovirus Infection as a Human Model of Chronic Obstructive Pulmonary Disease Exacerbation.* American Journal of Respiratory and Critical Care Medicine, 2011. **183**(6): p. 734-742.
78. Linden, D., Guo-Parke, H., Coyle, P.V., Fairley, D., McAuley, Danny F., Taggart, C.C., and Kidney, J., *Respiratory viral infection: a potential "missing link" in the pathogenesis of COPD.* European Respiratory Review, 2019. **28**(151).
79. Rahman, I., *Oxidative stress and redox regulation of lung inflammation in COPD.* European Respiratory Journal, 2006. **28**(1): p. 219-242.
80. Tam, A., Wadsworth, S., Dorscheid, D., Man, S.F., and Sin, D.D., *The airway epithelium: more than just a structural barrier.* Ther Adv Respir Dis, 2011. **5**(4): p. 255-73.
81. Dye, J.A. and Adler, K.B., *Effects of cigarette smoke on epithelial cells of the respiratory tract.* Thorax, 1994. **49**(8): p. 825-34.
82. Amatngalim, G.D., Broekman, W., Daniel, N.M., van der Vlugt, L.E., van Schadewijk, A., Taube, C., and Hiemstra, P.S., *Cigarette Smoke Modulates Repair and Innate Immunity following Injury to Airway Epithelial Cells.* PLoS One, 2016. **11**(11): p. e0166255.
83. Aghapour, M., Raee, P., Moghaddam, S.J., Hiemstra, P.S., and Heijink, I.H., *Airway Epithelial Barrier Dysfunction in Chronic Obstructive Pulmonary Disease: Role of Cigarette Smoke Exposure.* Am J Respir Cell Mol Biol, 2018. **58**(2): p. 157-169.
84. Rahman, I., Li, X.Y., Donaldson, K., Harrison, D.J., and MacNee, W., *Glutathione homeostasis in alveolar epithelial cells in vitro and lung in vivo under oxidative stress.* Am J Physiol, 1995. **269**(3 Pt 1): p. L285-92.
85. Lannan, S., Donaldson, K., Brown, D., and MacNee, W., *Effect of cigarette smoke and its condensates on alveolar epithelial cell injury in vitro.* Am J Physiol, 1994. **266**(1 Pt 1): p. L92-100.

86. Li, X.Y., Rahman, I., Donaldson, K., and MacNee, W., *Mechanisms of cigarette smoke induced increased airspace permeability.* Thorax, 1996. **51**(5): p. 465-71.
87. Aoshiba, K. and Nagai, A., *Oxidative stress, cell death, and other damage to alveolar epithelial cells induced by cigarette smoke.* Tob Induc Dis, 2003. **1**(3): p. 219-26.
88. Herr, C., Tsitouras, K., Niederstrasser, J., Backes, C., Beisswenger, C., Dong, L., Guillot, L., Keller, A., and Bals, R., *Cigarette smoke and electronic cigarettes differentially activate bronchial epithelial cells.* Respir Res, 2020. **21**(1): p. 67.
89. Hoshino, Y., Mio, T., Nagai, S., Miki, H., Ito, I., and Izumi, T., *Cytotoxic effects of cigarette smoke extract on an alveolar type II cell-derived cell line.* Am J Physiol Lung Cell Mol Physiol, 2001. **281**(2): p. L509-16.
90. Wang, H., Liu, X., Umino, T., Skold, C.M., Zhu, Y., Kohyama, T., Spurzem, J.R., Romberger, D.J., and Rennard, S.I., *Cigarette smoke inhibits human bronchial epithelial cell repair processes.* Am J Respir Cell Mol Biol, 2001. **25**(6): p. 772-9.
91. Kasahara, Y., Tuder, R.M., Cool, C.D., Lynch, D.A., Flores, S.C., and Voelkel, N.F., *Endothelial cell death and decreased expression of vascular endothelial growth factor and vascular endothelial growth factor receptor 2 in emphysema.* Am J Respir Crit Care Med, 2001. **163**(3 Pt 1): p. 737-44.
92. Segura-Valdez, L., Pardo, A., Gaxiola, M., Uhal, B.D., Becerril, C., and Selman, M., *Upregulation of gelatinases A and B, collagenases 1 and 2, and increased parenchymal cell death in COPD.* Chest, 2000. **117**(3): p. 684-94.
93. Mio, T., Romberger, D.J., Thompson, A.B., Robbins, R.A., Heires, A., and Rennard, S.I., *Cigarette smoke induces interleukin-8 release from human bronchial epithelial cells.* Am J Respir Crit Care Med, 1997. **155**(5): p. 1770-6.
94. Kode, A., Yang, S.R., and Rahman, I., *Differential effects of cigarette smoke on oxidative stress and proinflammatory cytokine release in primary human airway epithelial cells and in a variety of transformed alveolar epithelial cells.* Respir Res, 2006. **7**(1): p. 132.
95. Antherieu, S., Garat, A., Beauval, N., Soyez, M., Allorge, D., Garcon, G., and Lo-Guidice, J.M., *Comparison of cellular and transcriptomic effects between electronic cigarette vapor and cigarette smoke in human bronchial epithelial cells.* Toxicol In Vitro, 2017. **45**(Pt 3): p. 417-425.
96. Herr, C., Beisswenger, C., Hess, C., Kandler, K., Suttorp, N., Welte, T., Schroeder, J.M., Vogelmeier, C., and Group, R.B.f.t.C.S., *Suppression of pulmonary innate host defence in smokers.* Thorax, 2009. **64**(2): p. 144-9.
97. Bals, R., Wang, X., Wu, Z., Freeman, T., Bafna, V., Zasloff, M., and Wilson, J.M., *Human beta-defensin 2 is a salt-sensitive peptide antibiotic expressed in human lung.* J Clin Invest, 1998. **102**(5): p. 874-80.
98. Pace, E., Ferraro, M., Minervini, M.I., Vitulo, P., Pipitone, L., Chiappara, G., Siena, L., Montalbano, A.M., Johnson, M., and Gjomarkaj, M., *Beta defensin-2 is reduced in central but not in distal airways of smoker COPD patients.* PLoS One, 2012. **7**(3): p. e33601.

99. Lee, J.W., Chun, W., Lee, H.J., Min, J.H., Kim, S.M., Seo, J.Y., Ahn, K.S., and Oh, S.R., *The Role of Macrophages in the Development of Acute and Chronic Inflammatory Lung Diseases.* Cells, 2021. **10**(4).
100. Zhang, L. and Wang, C.C., *Inflammatory response of macrophages in infection.* Hepatobiliary Pancreat Dis Int, 2014. **13**(2): p. 138-52.
101. Kroger, M., Scheffel, J., Shirshin, E.A., Schleusener, J., Meinke, M.C., Lademann, J., Maurer, M., and Darvin, M.E., *Label-free imaging of M1 and M2 macrophage phenotypes in the human dermis in vivo using two-photon excited FLIM.* Elife, 2022. **11**.
102. Smith, T.D., Tse, M.J., Read, E.L., and Liu, W.F., *Regulation of macrophage polarization and plasticity by complex activation signals.* Integr Biol (Camb), 2016. **8**(9): p. 946-55.
103. Desch, A.N., Gibbings, S.L., Goyal, R., Kolde, R., Bednarek, J., Bruno, T., Slansky, J.E., Jacobelli, J., Mason, R., Ito, Y., Messier, E., Randolph, G.J., Prabagar, M., Atif, S.M., Segura, E., Xavier, R.J., Bratton, D.L., Janssen, W.J., Henson, P.M., and Jakubzick, C.V., *Flow Cytometric Analysis of Mononuclear Phagocytes in Nondiseased Human Lung and Lung-Draining Lymph Nodes.* Am J Respir Crit Care Med, 2016. **193**(6): p. 614-26.
104. Akata, K., Yamasaki, K., Leitao Filho, F.S., Yang, C.X., Takiguchi, H., Sahin, B., Whalen, B.A., Yang, C.W.T., Leung, J.M., Sin, D.D., and van Eeden, S.F., *Abundance of Non-Polarized Lung Macrophages with Poor Phagocytic Function in Chronic Obstructive Pulmonary Disease (COPD).* Biomedicines, 2020. **8**(10).
105. Mehta, H., Nazzal, K., and Sadikot, R.T., *Cigarette smoking and innate immunity.* Inflamm Res, 2008. **57**(11): p. 497-503.
106. Tetley, T.D., *Macrophages and the pathogenesis of COPD.* Chest, 2002. **121**(5 Suppl): p. 156S-159S.
107. Profita, M., Sala, A., Bonanno, A., Riccobono, L., Ferraro, M., La Grutta, S., Albano, G.D., Montalbano, A.M., and Gjomarkaj, M., *Chronic obstructive pulmonary disease and neutrophil infiltration: role of cigarette smoke and cyclooxygenase products.* Am J Physiol Lung Cell Mol Physiol, 2010. **298**(2): p. L261-9.
108. Quint, J.K. and Wedzicha, J.A., *The neutrophil in chronic obstructive pulmonary disease.* J Allergy Clin Immunol, 2007. **119**(5): p. 1065-71.
109. Bazzan, E., Turato, G., Tine, M., Radu, C.M., Balestro, E., Rigobello, C., Biondini, D., Schiavon, M., Lunardi, F., Baraldo, S., Rea, F., Simioni, P., Calabrese, F., Saetta, M., and Cosio, M.G., *Dual polarization of human alveolar macrophages progressively increases with smoking and COPD severity.* Respir Res, 2017. **18**(1): p. 40.
110. Kirkham, P.A., Spooner, G., Rahman, I., and Rossi, A.G., *Macrophage phagocytosis of apoptotic neutrophils is compromised by matrix proteins modified by cigarette smoke and lipid peroxidation products.* Biochem Biophys Res Commun, 2004. **318**(1): p. 32-7.

111. Droemann, D., Goldmann, T., Tiedje, T., Zabel, P., Dalhoff, K., and Schaaf, B., *Toll-like receptor 2 expression is decreased on alveolar macrophages in cigarette smokers and COPD patients.* Respir Res, 2005. **6**(1): p. 68.
112. Sarir, H., Mortaz, E., Karimi, K., Kraneveld, A.D., Rahman, I., Caldenhoven, E., Nijkamp, F.P., and Folkerts, G., *Cigarette smoke regulates the expression of TLR4 and IL-8 production by human macrophages.* J Inflamm (Lond), 2009. **6**: p. 12.
113. Woodruff, P.G., Koth, L.L., Yang, Y.H., Rodriguez, M.W., Favoreto, S., Dolganov, G.M., Paquet, A.C., and Erle, D.J., *A distinctive alveolar macrophage activation state induced by cigarette smoking.* Am J Respir Crit Care Med, 2005. **172**(11): p. 1383-92.
114. Hou, H.H., Wang, H.C., Cheng, S.L., Chen, Y.F., Lu, K.Z., and Yu, C.J., *MMP-12 activates protease-activated receptor-1, upregulates placenta growth factor, and leads to pulmonary emphysema.* Am J Physiol Lung Cell Mol Physiol, 2018. **315**(3): p. L432-L442.
115. Hou, H.-H., Wang, H.-C., Cheng, S.-L., Chen, Y.-F., Lu, K.-Z., and Yu, C.-J., *MMP-12 activates protease-activated receptor-1, upregulates placenta growth factor, and leads to pulmonary emphysema.* American Journal of Physiology-Lung Cellular and Molecular Physiology, 2018. **315**(3): p. L432-L442.
116. Mortaz, E., Kraneveld, A.D., Smit, J.J., Kool, M., Lambrecht, B.N., Kunkel, S.L., Lukacs, N.W., Nijkamp, F.P., and Folkerts, G., *Effect of cigarette smoke extract on dendritic cells and their impact on T-cell proliferation.* PLoS One, 2009. **4**(3): p. e4946.
117. Palucka, K. and Banchereau, J., *Dendritic cells: a link between innate and adaptive immunity.* J Clin Immunol, 1999. **19**(1): p. 12-25.
118. Tsoumakidou, M., Demedts, I.K., Brusselle, G.G., and Jeffery, P.K., *Dendritic cells in chronic obstructive pulmonary disease: new players in an old game.* Am J Respir Crit Care Med, 2008. **177**(11): p. 1180-6.
119. Givi, M.E., Folkerts, G., Wagenaar, G.T., Redegeld, F.A., and Mortaz, E., *Cigarette smoke differentially modulates dendritic cell maturation and function in time.* Respir Res, 2015. **16**: p. 131.
120. Freeman, C.M. and Curtis, J.L., *Lung Dendritic Cells: Shaping Immune Responses throughout Chronic Obstructive Pulmonary Disease Progression.* Am J Respir Cell Mol Biol, 2017. **56**(2): p. 152-159.
121. Freeman, C.M. and Curtis, J.L., *It's Complicated: Lung Dendritic Cells in Chronic Obstructive Pulmonary Disease.* Am J Respir Crit Care Med, 2020. **202**(4): p. 479-481.
122. Soler, P., Moreau, A., Basset, F., and Hance, A.J., *Cigarette smoking-induced changes in the number and differentiated state of pulmonary dendritic cells/Langerhans cells.* Am Rev Respir Dis, 1989. **139**(5): p. 1112-7.
123. Rogers, A.V., Adelroth, E., Hattotuwa, K., Dewar, A., and Jeffery, P.K., *Bronchial mucosal dendritic cells in smokers and ex-smokers with COPD: an electron microscopic study.* Thorax, 2008. **63**(2): p. 108-14.

124. Tsoumakidou, M., Elston, W., Zhu, J., Wang, Z., Gamble, E., Siafakas, N.M., Barnes, N.C., and Jeffery, P.K., *Cigarette smoking alters bronchial mucosal immunity in asthma.* Am J Respir Crit Care Med, 2007. **175**(9): p. 919-25.
125. Le Rouzic, O., Kone, B., Kluza, J., Marchetti, P., Hennegrave, F., Olivier, C., Kervoaze, G., Vilain, E., Mordacq, C., Just, N., Perez, T., Bautin, N., Pichavant, M., and Gosset, P., *Cigarette smoke alters the ability of human dendritic cells to promote anti-Streptococcus pneumoniae Th17 response.* Respir Res, 2016. **17**(1): p. 94.
126. Givi, M.E., Redegeld, F.A., Folkerts, G., and Mortaz, E., *Dendritic cells in pathogenesis of COPD.* Curr Pharm Des, 2012. **18**(16): p. 2329-35.
127. Nouri-Shirazi, M. and Guinet, E., *Evidence for the immunosuppressive role of nicotine on human dendritic cell functions.* Immunology, 2003. **109**(3): p. 365-73.
128. Vassallo, R., Tamada, K., Lau, J.S., Kroening, P.R., and Chen, L., *Cigarette smoke extract suppresses human dendritic cell function leading to preferential induction of Th-2 priming.* J Immunol, 2005. **175**(4): p. 2684-91.
129. Alkhattabi, N., Todd, I., Negm, O., Tighe, P.J., and Fairclough, L.C., *Tobacco smoke and nicotine suppress expression of activating signaling molecules in human dendritic cells.* Toxicol Lett, 2018. **299**: p. 40-46.
130. Caligiuri, M.A., *Human natural killer cells.* Blood, 2008. **112**(3): p. 461-9.
131. Tollerud, D.J., Clark, J.W., Brown, L.M., Neuland, C.Y., Mann, D.L., Pankiw-Trost, L.K., Blattner, W.A., and Hoover, R.N., *Association of cigarette smoking with decreased numbers of circulating natural killer cells.* Am Rev Respir Dis, 1989. **139**(1): p. 194-8.
132. Jung, Y.S., Park, J.H., Park, D.I., Sohn, C.I., Lee, J.M., and Kim, T.I., *Impact of Smoking on Human Natural Killer Cell Activity: A Large Cohort Study.* J Cancer Prev, 2020. **25**(1): p. 13-20.
133. Ferson, M., Edwards, A., Lind, A., Milton, G.W., and Hersey, P., *Low natural killer-cell activity and immunoglobulin levels associated with smoking in human subjects.* Int J Cancer, 1979. **23**(5): p. 603-9.
134. Lu, L.M., Zavitz, C.C., Chen, B., Kianpour, S., Wan, Y., and Stampfli, M.R., *Cigarette smoke impairs NK cell-dependent tumor immune surveillance.* J Immunol, 2007. **178**(2): p. 936-43.
135. Andersson, A., Malmhall, C., Houltz, B., Tengvall, S., Sjostrand, M., Qvarfordt, I., Linden, A., and Bossios, A., *Interleukin-16-producing NK cells and T-cells in the blood of tobacco smokers with and without COPD.* Int J Chron Obstruct Pulmon Dis, 2016. **11**: p. 2245-2258.
136. Aktas, O.N., Ozturk, A.B., Erman, B., Erus, S., Tanju, S., and Dilege, S., *Role of natural killer cells in lung cancer.* J Cancer Res Clin Oncol, 2018. **144**(6): p. 997-1003.
137. Mian, M.F., Pek, E.A., Mossman, K.L., Stampfli, M.R., and Ashkar, A.A., *Exposure to cigarette smoke suppresses IL-15 generation and its regulatory NK cell functions in poly I:C-augmented human PBMCs.* Mol Immunol, 2009. **46**(15): p. 3108-16.

138. Stolberg, V.R., Martin, B., Mancuso, P., Olszewski, M.A., Freeman, C.M., Curtis, J.L., and Chensue, S.W., *Role of CC chemokine receptor 4 in natural killer cell activation during acute cigarette smoke exposure.* Am J Pathol, 2014. **184**(2): p. 454-63.
139. Kearley, J., Silver, J.S., Sanden, C., Liu, Z., Berlin, A.A., White, N., Mori, M., Pham, T.H., Ward, C.K., Criner, G.J., Marchetti, N., Mustelin, T., Erjefalt, J.S., Kolbeck, R., and Humbles, A.A., *Cigarette smoke silences innate lymphoid cell function and facilitates an exacerbated type I interleukin-33-dependent response to infection.* Immunity, 2015. **42**(3): p. 566-79.
140. Wang, J., Urbanowicz, R.A., Tighe, P.J., Todd, I., Corne, J.M., and Fairclough, L.C., *Differential activation of killer cells in the circulation and the lung: a study of current smoking status and chronic obstructive pulmonary disease (COPD).* PLoS One, 2013. **8**(3): p. e58556.
141. Urbanowicz, R.A., Lamb, J.R., Todd, I., Corne, J.M., and Fairclough, L.C., *Enhanced effector function of cytotoxic cells in the induced sputum of COPD patients.* Respir Res, 2010. **11**: p. 76.
142. Fairclough, L., Urbanowicz, R.A., Corne, J., and Lamb, J.R., *Killer cells in chronic obstructive pulmonary disease.* Clin Sci (Lond), 2008. **114**(8): p. 533-41.
143. Godfrey, D.I., MacDonald, H.R., Kronenberg, M., Smyth, M.J., and Van Kaer, L., *NKT cells: what's in a name?* Nat Rev Immunol, 2004. **4**(3): p. 231-7.
144. Liu, X., Li, L., Si, F., Huang, L., Zhao, Y., Zhang, C., Hoft, D.F., and Peng, G., *NK and NKT cells have distinct properties and functions in cancer.* Oncogene, 2021. **40**(27): p. 4521-4537.
145. Urbanowicz, R.A., Lamb, J.R., Todd, I., Corne, J.M., and Fairclough, L.C., *Altered effector function of peripheral cytotoxic cells in COPD.* Respir Res, 2009. **10**: p. 53.
146. Urbanowicz, R.A., Lamb, J.R., Todd, I., Corne, J.M., and Fairclough, L.C., *Enhanced effector function of cytotoxic cells in the induced sputum of COPD patients.* Respir Res, 2010. **11**(1): p. 76.
147. Hogan, A.E., Corrigan, M.A., O'Reilly, V., Gaoatswe, G., O'Connell, J., Doherty, D.G., Lynch, L., and O'Shea, D., *Cigarette smoke alters the invariant natural killer T cell function and may inhibit anti-tumor responses.* Clin Immunol, 2011. **140**(3): p. 229-35.
148. Pichavant, M., Remy, G., Bekaert, S., Le Rouzic, O., Kervoaze, G., Vilain, E., Just, N., Tillie-Leblond, I., Trottein, F., Cataldo, D., and Gosset, P., *Oxidative stress-mediated iNKT-cell activation is involved in COPD pathogenesis.* Mucosal Immunol, 2014. **7**(3): p. 568-78.
149. Eriksson Strom, J., Pourazar, J., Linder, R., Blomberg, A., Lindberg, A., Bucht, A., and Behndig, A.F., *Cytotoxic lymphocytes in COPD airways: increased NK cells associated with disease, iNKT and NKT-like cells with current smoking.* Respir Res, 2018. **19**(1): p. 244.
150. O'Donnell, R., Breen, D., Wilson, S., and Djukanovic, R., *Inflammatory cells in the airways in COPD.* Thorax, 2006. **61**(5): p. 448-54.

151. Butler, A., Walton, G.M., and Sapey, E., *Neutrophilic Inflammation in the Pathogenesis of Chronic Obstructive Pulmonary Disease.* COPD, 2018. **15**(4): p. 392-404.
152. Aloe, C., Wang, H., Vlahos, R., Irving, L., Steinfort, D., and Bozinovski, S., *Emerging and multifaceted role of neutrophils in lung cancer.* Transl Lung Cancer Res, 2021. **10**(6): p. 2806-2818.
153. Rungelrath, V., Kobayashi, S.D., and DeLeo, F.R., *Neutrophils in innate immunity and systems biology-level approaches.* Wiley Interdiscip Rev Syst Biol Med, 2020. **12**(1): p. e1458.
154. Jasper, A.E., McIver, W.J., Sapey, E., and Walton, G.M., *Understanding the role of neutrophils in chronic inflammatory airway disease.* F1000Res, 2019. **8**.
155. Mincham, K.T., Bruno, N., Singanayagam, A., and Snelgrove, R.J., *Our evolving view of neutrophils in defining the pathology of chronic lung disease.* Immunology, 2021. **164**(4): p. 701-721.
156. Keatings, V.M. and Barnes, P.J., *Granulocyte activation markers in induced sputum: comparison between chronic obstructive pulmonary disease, asthma, and normal subjects.* American Journal of Respiratory and Critical Care Medicine, 1997. **155**(2): p. 449-453.
157. Vernooy, J.H.J., Lindeman, J.H.N., Jacobs, J.A., Hanemaaijer, R., and Wouters, E.F.M., *Increased Activity of Matrix Metalloproteinase-8 and Matrix Metalloproteinase-9 in Induced Sputum From Patients With COPD.* Chest, 2004. **126**(6): p. 1802-1810.
158. Gaggar, A., Jackson, P.L., Noerager, B.D., O'Reilly, P.J., McQuaid, D.B., Rowe, S.M., Clancy, J.P., and Blalock, J.E., *A novel proteolytic cascade generates an extracellular matrix-derived chemoattractant in chronic neutrophilic inflammation.* J Immunol, 2008. **180**(8): p. 5662-9.
159. Pilette, C., Colinet, B., Kiss, R., Andre, S., Kaltner, H., Gabius, H.J., Delos, M., Vaerman, J.P., Decramer, M., and Sibille, Y., *Increased galectin-3 expression and intra-epithelial neutrophils in small airways in severe COPD.* Eur Respir J, 2007. **29**(5): p. 914-22.
160. Donaldson, G.C., Seemungal, T.A., Patel, I.S., Bhowmik, A., Wilkinson, T.M., Hurst, J.R., Maccallum, P.K., and Wedzicha, J.A., *Airway and systemic inflammation and decline in lung function in patients with COPD.* Chest, 2005. **128**(4): p. 1995-2004.
161. Sapey, E., Stockley, J.A., Greenwood, H., Ahmad, A., Bayley, D., Lord, J.M., Insall, R.H., and Stockley, R.A., *Behavioral and structural differences in migrating peripheral neutrophils from patients with chronic obstructive pulmonary disease.* Am J Respir Crit Care Med, 2011. **183**(9): p. 1176-86.
162. Stanescu, D., Sanna, A., Veriter, C., Kostianev, S., Calcagni, P.G., Fabbri, L.M., and Maestrelli, P., *Airways obstruction, chronic expectoration, and rapid decline of FEV1 in smokers are associated with increased levels of sputum neutrophils.* Thorax, 1996. **51**(3): p. 267-71.

163. Lonergan, M., Dicker, A.J., Crichton, M.L., Keir, H.R., Van Dyke, M.K., Mullerova, H., Miller, B.E., Tal-Singer, R., and Chalmers, J.D., *Blood neutrophil counts are associated with exacerbation frequency and mortality in COPD.* Respir Res, 2020. **21**(1): p. 166.
164. Pouwels, S.D., Zijlstra, G.J., van der Toorn, M., Hesse, L., Gras, R., Ten Hacken, N.H., Krysko, D.V., Vandenabeele, P., de Vries, M., van Oosterhout, A.J., Heijink, I.H., and Nawijn, M.C., *Cigarette smoke-induced necroptosis and DAMP release trigger neutrophilic airway inflammation in mice.* Am J Physiol Lung Cell Mol Physiol, 2016. **310**(4): p. L377-86.
165. Moazed, F., Burnham, E.L., Vandivier, R.W., O'Kane, C.M., Shyamsundar, M., Hamid, U., Abbott, J., Thickett, D.R., Matthay, M.A., McAuley, D.F., and Calfee, C.S., *Cigarette smokers have exaggerated alveolar barrier disruption in response to lipopolysaccharide inhalation.* Thorax, 2016. **71**(12): p. 1130-1136.
166. Qiu, S.L., Zhang, H., Tang, Q.Y., Bai, J., He, Z.Y., Zhang, J.Q., Li, M.H., Deng, J.M., Liu, G.N., and Zhong, X.N., *Neutrophil extracellular traps induced by cigarette smoke activate plasmacytoid dendritic cells.* Thorax, 2017. **72**(12): p. 1084-1093.
167. David, B., Bafadhel, M., Koenderman, L., and De Soyza, A., *Eosinophilic inflammation in COPD: from an inflammatory marker to a treatable trait.* Thorax, 2021. **76**(2): p. 188-195.
168. Tashkin, D.P. and Wechsler, M.E., *Role of eosinophils in airway inflammation of chronic obstructive pulmonary disease.* Int J Chron Obstruct Pulmon Dis, 2018. **13**: p. 335-349.
169. Martinez, C.H., Li, S.X., Hirzel, A.J., Stolberg, V.R., Alexis, N.E., Barr, R.G., Bleecker, E.R., Carretta, E.E., Christenson, S.A., Cooper, C.B., Couper, D.J., Doerschuk, C.M., Han, M.K., Hansel, N.N., Hastie, A.T., Hoffman, E.A., Kaner, R.J., Martinez, F.J., Meyers, D.A., O'Neal, W.K., Paine, R., 3rd, Putcha, N., Rennard, S.I., Woodruff, P.G., Zeidler, M., Curtis, J.L., Freeman, C.M., and Investigators, S., *Alveolar eosinophilia in current smokers with chronic obstructive pulmonary disease in the SPIROMICS cohort.* J Allergy Clin Immunol, 2018. **141**(1): p. 429-432.
170. Balzano, G., Stefanelli, F., Iorio, C., De Felice, A., Melillo, E.M., Martucci, M., and Melillo, G., *Eosinophilic inflammation in stable chronic obstructive pulmonary disease. Relationship with neutrophils and airway function.* Am J Respir Crit Care Med, 1999. **160**(5 Pt 1): p. 1486-92.
171. Obling, N., Backer, V., Hurst, J.R., and Bodtger, U., *Upper airway symptoms associate with the eosinophilic phenotype of COPD.* ERJ Open Res, 2021. **7**(3).
172. George, L. and Brightling, C.E., *Eosinophilic airway inflammation: role in asthma and chronic obstructive pulmonary disease.* Ther Adv Chronic Dis, 2016. **7**(1): p. 34-51.
173. Vedel-Krogh, S., Nielsen, S.F., Lange, P., Vestbo, J., and Nordestgaard, B.G., *Blood Eosinophils and Exacerbations in Chronic Obstructive Pulmonary Disease. The Copenhagen General Population Study.* Am J Respir Crit Care Med, 2016. **193**(9): p. 965-74.

174. Siddiqui, S.H., Guasconi, A., Vestbo, J., Jones, P., Agusti, A., Paggiaro, P., Wedzicha, J.A., and Singh, D., *Blood Eosinophils: A Biomarker of Response to Extrafine Beclomethasone/Formoterol in Chronic Obstructive Pulmonary Disease.* Am J Respir Crit Care Med, 2015. **192**(4): p. 523-5.
175. Saha, S. and Brightling, C.E., *Eosinophilic airway inflammation in COPD.* Int J Chron Obstruct Pulmon Dis, 2006. **1**(1): p. 39-47.
176. Bafadhel, M., McKenna, S., Terry, S., Mistry, V., Reid, C., Haldar, P., McCormick, M., Haldar, K., Kebadze, T., Duvoix, A., Lindblad, K., Patel, H., Rugman, P., Dodson, P., Jenkins, M., Saunders, M., Newbold, P., Green, R.H., Venge, P., Lomas, D.A., Barer, M.R., Johnston, S.L., Pavord, I.D., and Brightling, C.E., *Acute exacerbations of chronic obstructive pulmonary disease: identification of biologic clusters and their biomarkers.* Am J Respir Crit Care Med, 2011. **184**(6): p. 662-71.
177. Qiu, F., Liang, C.L., Liu, H., Zeng, Y.Q., Hou, S., Huang, S., Lai, X., and Dai, Z., *Impacts of cigarette smoking on immune responsiveness: Up and down or upside down?* Oncotarget, 2017. **8**(1): p. 268-284.
178. Maeno, T., Houghton, A.M., Quintero, P.A., Grumelli, S., Owen, C.A., and Shapiro, S.D., *CD8+ T Cells are required for inflammation and destruction in cigarette smoke-induced emphysema in mice.* J Immunol, 2007. **178**(12): p. 8090-6.
179. Forsslund, H., Mikko, M., Karimi, R., Grunewald, J., Wheelock, A.M., Wahlstrom, J., and Skold, C.M., *Distribution of T-cell subsets in BAL fluid of patients with mild to moderate COPD depends on current smoking status and not airway obstruction.* Chest, 2014. **145**(4): p. 711-722.
180. Wasen, C., Turkkila, M., Bossios, A., Erlandsson, M., Andersson, K.M., Ekerljung, L., Malmhall, C., Brisslert, M., Toyra Silfversward, S., Lundback, B., and Bokarewa, M.I., *Smoking activates cytotoxic CD8(+) T cells and causes survivin release in rheumatoid arthritis.* J Autoimmun, 2017. **78**: p. 101-110.
181. Cosio, M.G., Majo, J., and Cosio, M.G., *Inflammation of the airways and lung parenchyma in COPD: role of T cells.* Chest, 2002. **121**(5 Suppl): p. 160S-165S.
182. Hoffman, W., Lakkis, F.G., and Chalasani, G., *B Cells, Antibodies, and More.* Clin J Am Soc Nephrol, 2016. **11**(1): p. 137-54.
183. Hogg, J.C., Chu, F., Utokaparch, S., Woods, R., Elliott, W.M., Buzatu, L., Cherniack, R.M., Rogers, R.M., Sciurba, F.C., Coxson, H.O., and Pare, P.D., *The nature of small-airway obstruction in chronic obstructive pulmonary disease.* N Engl J Med, 2004. **350**(26): p. 2645-53.
184. Gosman, M.M., Willemse, B.W., Jansen, D.F., Lapperre, T.S., van Schadewijk, A., Hiemstra, P.S., Postma, D.S., Timens, W., Kerstjens, H.A., Groningen, and Leiden Universities Corticosteroids in Obstructive Lung Disease Study, G., *Increased number of B-cells in bronchial biopsies in COPD.* Eur Respir J, 2006. **27**(1): p. 60-4.
185. Burchiel, S.W., Lauer, F.T., Factor-Litvak, P., Liu, X., Santella, R.M., Islam, T., Eunus, M., Alam, N., Islam, T., Rahman, M., Ahmed, A., Ahsan, H., Graziano, J., and Parvez, F., *An increase in circulating B cells and B cell activation markers in*

peripheral blood is associated with cigarette smoking in a male cohort in Bangladesh. Toxicol Appl Pharmacol, 2019. **384**: p. 114783.
186. Brandsma, C.A., Hylkema, M.N., Geerlings, M., van Geffen, W.H., Postma, D.S., Timens, W., and Kerstjens, H.A., *Increased levels of (class switched) memory B cells in peripheral blood of current smokers.* Respir Res, 2009. **10**(1): p. 108.
187. Brandsma, C.A., Kerstjens, H.A., van Geffen, W.H., Geerlings, M., Postma, D.S., Hylkema, M.N., and Timens, W., *Differential switching to IgG and IgA in active smoking COPD patients and healthy controls.* Eur Respir J, 2012. **40**(2): p. 313-21.
188. Andersen, P., Pedersen, O.F., Bach, B., and Bonde, G.J., *Serum antibodies and immunoglobulins in smokers and nonsmokers.* Clin Exp Immunol, 1982. **47**(2): p. 467-73.
189. Gerrard, J.W., Heiner, D.C., Ko, C.G., Mink, J., Meyers, A., and Dosman, J.A., *Immunoglobulin levels in smokers and non-smokers.* Ann Allergy, 1980. **44**(5): p. 261-2.
190. Calapai, G., Caputi, A.P., Mannucci, C., Gregg, E.O., Pieratti, A., Aurora Russo, G., Chaudhary, N., Puntoni, R., Lowe, F., McEwan, M., Bassi, A., Morandi, S., and Nunziata, A., *A cross-sectional investigation of biomarkers of risk after a decade of smoking.* Inhal Toxicol, 2009. **21**(13): p. 1138-43.
191. Giuca, M.R., Pasini, M., Tecco, S., Giuca, G., and Marzo, G., *Levels of salivary immunoglobulins and periodontal evaluation in smoking patients.* BMC Immunol, 2014. **15**: p. 5.
192. Golpasand Hagh, L., Zakavi, F., Ansarifar, S., Ghasemzadeh, O., and Solgi, G., *Association of dental caries and salivary sIgA with tobacco smoking.* Aust Dent J, 2013. **58**(2): p. 219-23.
193. Jensen, E.J., Pedersen, B., Schmidt, E., and Dahl, R., *Serum IgE in nonatopic smokers, nonsmokers, and recent exsmokers: relation to lung function, airway symptoms, and atopic predisposition.* J Allergy Clin Immunol, 1992. **90**(2): p. 224-9.
194. Burrows, B., Halonen, M., Lebowitz, M.D., Knudson, R.J., and Barbee, R.A., *The relationship of serum immunoglobulin E, allergy skin tests, and smoking to respiratory disorders.* J Allergy Clin Immunol, 1982. **70**(3): p. 199-204.
195. Arnson, Y., Shoenfeld, Y., and Amital, H., *Effects of tobacco smoke on immunity, inflammation and autoimmunity.* J Autoimmun, 2010. **34**(3): p. J258-65.
196. Mathews, J.D., Whittingham, S., Hooper, B.M., Mackay, I.R., and Stenhouse, N.S., *Association of autoantibodies with smoking, cardiovascular morbidity, and death in the Busselton population.* Lancet, 1973. **2**(7832): p. 754-8.
197. Masdottir, B., Jonsson, T., Manfredsdottir, V., Vikingsson, A., Brekkan, A., and Valdimarsson, H., *Smoking, rheumatoid factor isotypes and severity of rheumatoid arthritis.* Rheumatology (Oxford), 2000. **39**(11): p. 1202-5.
198. van Wesemael, T.J., Ajeganova, S., Humphreys, J., Terao, C., Muhammad, A., Symmons, D.P., MacGregor, A.J., Hafstrom, I., Trouw, L.A., van der Helm-van Mil, A.H., Huizinga, T.W., Mimori, T., Toes, R.E., Matsuda, F., Svensson, B., Verstappen, S.M., and van der Woude, D., *Smoking is associated with the*

concurrent presence of multiple autoantibodies in rheumatoid arthritis rather than with anti-citrullinated protein antibodies per se: a multicenter cohort study. Arthritis Res Ther, 2016. **18**(1): p. 285.
199. Lee, S.H., Goswami, S., Grudo, A., Song, L.Z., Bandi, V., Goodnight-White, S., Green, L., Hacken-Bitar, J., Huh, J., Bakaeen, F., Coxson, H.O., Cogswell, S., Storness-Bliss, C., Corry, D.B., and Kheradmand, F., *Antielastin autoimmunity in tobacco smoking-induced emphysema.* Nat Med, 2007. **13**(5): p. 567-9.
200. Feghali-Bostwick, C.A., Gadgil, A.S., Otterbein, L.E., Pilewski, J.M., Stoner, M.W., Csizmadia, E., Zhang, Y., Sciurba, F.C., and Duncan, S.R., *Autoantibodies in patients with chronic obstructive pulmonary disease.* Am J Respir Crit Care Med, 2008. **177**(2): p. 156-63.
201. Taraseviciene-Stewart, L., Scerbavicius, R., Choe, K.H., Moore, M., Sullivan, A., Nicolls, M.R., Fontenot, A.P., Tuder, R.M., and Voelkel, N.F., *An animal model of autoimmune emphysema.* Am J Respir Crit Care Med, 2005. **171**(7): p. 734-42.
202. Riker, C.A., Lee, K., Darville, A., and Hahn, E.J., *E-cigarettes: promise or peril?* Nurs Clin North Am, 2012. **47**(1): p. 159-71.
203. Chen, I.L., Todd, I., and Fairclough, L.C., *Immunological and pathological effects of electronic cigarettes.* Basic Clin Pharmacol Toxicol, 2019. **125**(3): p. 237-252.
204. Hajek, P., Phillips-Waller, A., Przulj, D., Pesola, F., Myers Smith, K., Bisal, N., Li, J., Parrott, S., Sasieni, P., Dawkins, L., Ross, L., Goniewicz, M., Wu, Q., and McRobbie, H.J., *A Randomized Trial of E-Cigarettes versus Nicotine-Replacement Therapy.* N Engl J Med, 2019. **380**(7): p. 629-637.
205. Chun, L.F., Moazed, F., Calfee, C.S., Matthay, M.A., and Gotts, J.E., *Pulmonary toxicity of e-cigarettes.* Am J Physiol Lung Cell Mol Physiol, 2017. **313**(2): p. L193-L206.
206. Grana, R., Benowitz, N., and Glantz, S.A., *E-cigarettes: a scientific review.* Circulation, 2014. **129**(19): p. 1972-86.
207. Hess, C.A., Olmedo, P., Navas-Acien, A., Goessler, W., Cohen, J.E., and Rule, A.M., *E-cigarettes as a source of toxic and potentially carcinogenic metals.* Environ Res, 2017. **152**: p. 221-225.
208. Hickman, E., Payton, A., Duffney, P., Wells, H., Ceppe, A.S., Brocke, S., Bailey, A., Rebuli, M.E., Robinette, C., Ring, B., Rager, J.E., Alexis, N.E., and Jaspers, I., *Biomarkers of Airway Immune Homeostasis Differ Significantly with Generation of E-Cigarettes.* Am J Respir Crit Care Med, 2022. **206**(10): p. 1248-1258.
209. Williams, M. and Talbot, P., *Design Features in Multiple Generations of Electronic Cigarette Atomizers.* Int J Environ Res Public Health, 2019. **16**(16).
210. Bar-Zeev, Y., *Unclear role for e-cigarettes during pregnancy.* Nat Med, 2022. **28**(5): p. 900-901.
211. Gordon, T., Karey, E., Rebuli, M.E., Escobar, Y.H., Jaspers, I., and Chen, L.C., *E-Cigarette Toxicology.* Annu Rev Pharmacol Toxicol, 2022. **62**: p. 301-322.
212. Marques, P., Piqueras, L., and Sanz, M.J., *An updated overview of e-cigarette impact on human health.* Respir Res, 2021. **22**(1): p. 151.

213. Phillips, B., Titz, B., Kogel, U., Sharma, D., Leroy, P., Xiang, Y., Vuillaume, G., Lebrun, S., Sciuscio, D., Ho, J., Nury, C., Guedj, E., Elamin, A., Esposito, M., Krishnan, S., Schlage, W.K., Veljkovic, E., Ivanov, N.V., Martin, F., Peitsch, M.C., Hoeng, J., and Vanscheeuwijck, P., *Toxicity of the main electronic cigarette components, propylene glycol, glycerin, and nicotine, in Sprague-Dawley rats in a 90-day OECD inhalation study complemented by molecular endpoints.* Food Chem Toxicol, 2017. **109**(Pt 1): p. 315-332.
214. Woodall, M., Jacob, J., Kalsi, K.K., Schroeder, V., Davis, E., Kenyon, B., Khan, I., Garnett, J.P., Tarran, R., and Baines, D.L., *E-cigarette constituents propylene glycol and vegetable glycerin decrease glucose uptake and its metabolism in airway epithelial cells in vitro.* Am J Physiol Lung Cell Mol Physiol, 2020. **319**(6): p. L957-L967.
215. Zar, T., Graeber, C., and Perazella, M.A., *Recognition, treatment, and prevention of propylene glycol toxicity.* Semin Dial, 2007. **20**(3): p. 217-9.
216. McGowan, M.A., Scheman, A., and Jacob, S.E., *Propylene Glycol in Contact Dermatitis: A Systematic Review.* Dermatitis, 2018. **29**(1): p. 6-12.
217. Ogunwale, M.A., Li, M., Ramakrishnam Raju, M.V., Chen, Y., Nantz, M.H., Conklin, D.J., and Fu, X.A., *Aldehyde Detection in Electronic Cigarette Aerosols.* ACS Omega, 2017. **2**(3): p. 1207-1214.
218. Goniewicz, M.L., Knysak, J., Gawron, M., Kosmider, L., Sobczak, A., Kurek, J., Prokopowicz, A., Jablonska-Czapla, M., Rosik-Dulewska, C., Havel, C., Jacob, P., 3rd, and Benowitz, N., *Levels of selected carcinogens and toxicants in vapour from electronic cigarettes.* Tob Control, 2014. **23**(2): p. 133-9.
219. Zhu, S.H., Sun, J.Y., Bonnevie, E., Cummins, S.E., Gamst, A., Yin, L., and Lee, M., *Four hundred and sixty brands of e-cigarettes and counting: implications for product regulation.* Tob Control, 2014. **23 Suppl 3**(Suppl 3): p. iii3-9.
220. Hutzler, C., Paschke, M., Kruschinski, S., Henkler, F., Hahn, J., and Luch, A., *Chemical hazards present in liquids and vapors of electronic cigarettes.* Arch Toxicol, 2014. **88**(7): p. 1295-308.
221. Omaiye, E.E., McWhirter, K.J., Luo, W., Tierney, P.A., Pankow, J.F., and Talbot, P., *High concentrations of flavor chemicals are present in electronic cigarette refill fluids.* Sci Rep, 2019. **9**(1): p. 2468.
222. Rickard, B.P., Ho, H., Tiley, J.B., Jaspers, I., and Brouwer, K.L.R., *E-Cigarette Flavoring Chemicals Induce Cytotoxicity in HepG2 Cells.* ACS Omega, 2021. **6**(10): p. 6708-6713.
223. Gerloff, J., Sundar, I.K., Freter, R., Sekera, E.R., Friedman, A.E., Robinson, R., Pagano, T., and Rahman, I., *Inflammatory Response and Barrier Dysfunction by Different e-Cigarette Flavoring Chemicals Identified by Gas Chromatography-Mass Spectrometry in e-Liquids and e-Vapors on Human Lung Epithelial Cells and Fibroblasts.* Appl In Vitro Toxicol, 2017. **3**(1): p. 28-40.
224. Bahl, V., Lin, S., Xu, N., Davis, B., Wang, Y.H., and Talbot, P., *Comparison of electronic cigarette refill fluid cytotoxicity using embryonic and adult models.* Reprod Toxicol, 2012. **34**(4): p. 529-37.

225. Behar, R.Z., Davis, B., Wang, Y., Bahl, V., Lin, S., and Talbot, P., *Identification of toxicants in cinnamon-flavored electronic cigarette refill fluids.* Toxicol In Vitro, 2014. **28**(2): p. 198-208.
226. Wavreil, F.D.M. and Heggland, S.J., *Cinnamon-flavored electronic cigarette liquids and aerosols induce oxidative stress in human osteoblast-like MG-63 cells.* Toxicol Rep, 2020. **7**: p. 23-29.
227. Michon, M., Mercier, C., Petit, C., Leclerc, L., Bertoletti, L., Pourchez, J., and Forest, V., *In Vitro Biological Effects of E-Cigarette on the Cardiovascular System-Pro-Inflammatory Response Enhanced by the Presence of the Cinnamon Flavor.* Toxics, 2022. **10**(12).
228. Lerner, C.A., Sundar, I.K., Yao, H., Gerloff, J., Ossip, D.J., McIntosh, S., Robinson, R., and Rahman, I., *Vapors produced by electronic cigarettes and e-juices with flavorings induce toxicity, oxidative stress, and inflammatory response in lung epithelial cells and in mouse lung.* PLoS One, 2015. **10**(2): p. e0116732.
229. Omaiye, E.E., Williams, M., Bozhilov, K.N., and Talbot, P., *Design features and elemental/metal analysis of the atomizers in pod-style electronic cigarettes.* PLoS One, 2021. **16**(3): p. e0248127.
230. Williams, M., Bozhilov, K.N., and Talbot, P., *Analysis of the elements and metals in multiple generations of electronic cigarette atomizers.* Environ Res, 2019. **175**: p. 156-166.
231. Williams, M., Ventura, J., Loza, A., Wang, Y., and Talbot, P., *Chemical Elements in Electronic Cigarette Solvents and Aerosols Inhibit Mitochondrial Reductases and Induce Oxidative Stress.* Nicotine Tob Res, 2020. **22**(Suppl 1): p. S14-S24.
232. Keith, R. and Bhatnagar, A., *Cardiorespiratory and Immunologic Effects of Electronic Cigarettes.* Curr Addict Rep, 2021. **8**(2): p. 336-346.
233. Park, J.A., Crotty Alexander, L.E., and Christiani, D.C., *Vaping and Lung Inflammation and Injury.* Annu Rev Physiol, 2022. **84**: p. 611-629.
234. Scott, A., Lugg, S.T., Aldridge, K., Lewis, K.E., Bowden, A., Mahida, R.Y., Grudzinska, F.S., Dosanjh, D., Parekh, D., Foronjy, R., Sapey, E., Naidu, B., and Thickett, D.R., *Pro-inflammatory effects of e-cigarette vapour condensate on human alveolar macrophages.* Thorax, 2018. **73**(12): p. 1161-1169.
235. Garcia-Arcos, I., Geraghty, P., Baumlin, N., Campos, M., Dabo, A.J., Jundi, B., Cummins, N., Eden, E., Grosche, A., Salathe, M., and Foronjy, R., *Chronic electronic cigarette exposure in mice induces features of COPD in a nicotine-dependent manner.* Thorax, 2016. **71**(12): p. 1119-1129.
236. Crotty Alexander, L.E., Drummond, C.A., Hepokoski, M., Mathew, D., Moshensky, A., Willeford, A., Das, S., Singh, P., Yong, Z., Lee, J.H., Vega, K., Du, A., Shin, J., Javier, C., Tian, J., Brown, J.H., and Breen, E.C., *Chronic inhalation of e-cigarette vapor containing nicotine disrupts airway barrier function and induces systemic inflammation and multiorgan fibrosis in mice.* Am J Physiol Regul Integr Comp Physiol, 2018. **314**(6): p. R834-R847.
237. Reidel, B., Radicioni, G., Clapp, P.W., Ford, A.A., Abdelwahab, S., Rebuli, M.E., Haridass, P., Alexis, N.E., Jaspers, I., and Kesimer, M., *E-Cigarette Use Causes a*

Unique Innate Immune Response in the Lung, Involving Increased Neutrophilic Activation and Altered Mucin Secretion. Am J Respir Crit Care Med, 2018. **197**(4): p. 492-501.

238. Glynos, C., Bibli, S.I., Katsaounou, P., Pavlidou, A., Magkou, C., Karavana, V., Topouzis, S., Kalomenidis, I., Zakynthinos, S., and Papapetropoulos, A., *Comparison of the effects of e-cigarette vapor with cigarette smoke on lung function and inflammation in mice.* Am J Physiol Lung Cell Mol Physiol, 2018. **315**(5): p. L662-L672.
239. Wang, Q., Sundar, I., Li, D., Lucas, J., Muthumalage, T., McDonough, S., and Rahman, I., *E-cigarette-Induced Pulmonary Inflammation and Dysregulated Repair are Mediated by nAChR alpha7 Receptor: Role of nAChR alpha7 in ACE2 Covid-19 receptor regulation.* Res Sq, 2020.
240. Kleinman, M.T., Arechavala, R.J., Herman, D., Shi, J., Hasen, I., Ting, A., Dai, W., Carreno, J., Chavez, J., Zhao, L., and Kloner, R.A., *E-cigarette or Vaping Product Use-Associated Lung Injury Produced in an Animal Model From Electronic Cigarette Vapor Exposure Without Tetrahydrocannabinol or Vitamin E Oil.* J Am Heart Assoc, 2020. **9**(18): p. e017368.
241. Lerner, C.A., Sundar, I.K., Watson, R.M., Elder, A., Jones, R., Done, D., Kurtzman, R., Ossip, D.J., Robinson, R., McIntosh, S., and Rahman, I., *Environmental health hazards of e-cigarettes and their components: Oxidants and copper in e-cigarette aerosols.* Environ Pollut, 2015. **198**: p. 100-7.
242. Azimi, P., Keshavarz, Z., Lahaie Luna, M., Cedeno Laurent, J.G., Vallarino, J., Christiani, D.C., and Allen, J.G., *An Unrecognized Hazard in E-Cigarette Vapor: Preliminary Quantification of Methylglyoxal Formation from Propylene Glycol in E-Cigarettes.* Int J Environ Res Public Health, 2021. **18**(2).
243. Yu, V., Rahimy, M., Korrapati, A., Xuan, Y., Zou, A.E., Krishnan, A.R., Tsui, T., Aguilera, J.A., Advani, S., Crotty Alexander, L.E., Brumund, K.T., Wang-Rodriguez, J., and Ongkeko, W.M., *Electronic cigarettes induce DNA strand breaks and cell death independently of nicotine in cell lines.* Oral Oncol, 2016. **52**: p. 58-65.
244. Son, Y., Mishin, V., Laskin, J.D., Mainelis, G., Wackowski, O.A., Delnevo, C., Schwander, S., Khlystov, A., Samburova, V., and Meng, Q., *Hydroxyl Radicals in E-Cigarette Vapor and E-Vapor Oxidative Potentials under Different Vaping Patterns.* Chem Res Toxicol, 2019. **32**(6): p. 1087-1095.
245. Carson, J.L., Zhou, L., Brighton, L., Mills, K.H., Zhou, H., Jaspers, I., and Hazucha, M., *Temporal structure/function variation in cultured differentiated human nasal epithelium associated with acute single exposure to tobacco smoke or E-cigarette vapor.* Inhal Toxicol, 2017. **29**(3): p. 137-144.
246. Chung, S., Baumlin, N., Dennis, J.S., Moore, R., Salathe, S.F., Whitney, P.L., Sabater, J., Abraham, W.M., Kim, M.D., and Salathe, M., *Electronic Cigarette Vapor with Nicotine Causes Airway Mucociliary Dysfunction Preferentially via TRPA1 Receptors.* Am J Respir Crit Care Med, 2019. **200**(9): p. 1134-1145.
247. Hwang, J.H., Lyes, M., Sladewski, K., Enany, S., McEachern, E., Mathew, D.P., Das, S., Moshensky, A., Bapat, S., Pride, D.T., Ongkeko, W.M., and Crotty Alexander,

L.E., *Electronic cigarette inhalation alters innate immunity and airway cytokines while increasing the virulence of colonizing bacteria.* J Mol Med (Berl), 2016. **94**(6): p. 667-79.
248. Corriden, R., Moshensky, A., Bojanowski, C.M., Meier, A., Chien, J., Nelson, R.K., and Crotty Alexander, L.E., *E-cigarette use increases susceptibility to bacterial infection by impairment of human neutrophil chemotaxis, phagocytosis, and NET formation.* Am J Physiol Cell Physiol, 2020. **318**(1): p. C205-C214.
249. Ghosh, A., Coakley, R.C., Mascenik, T., Rowell, T.R., Davis, E.S., Rogers, K., Webster, M.J., Dang, H., Herring, L.E., Sassano, M.F., Livraghi-Butrico, A., Van Buren, S.K., Graves, L.M., Herman, M.A., Randell, S.H., Alexis, N.E., and Tarran, R., *Chronic E-Cigarette Exposure Alters the Human Bronchial Epithelial Proteome.* Am J Respir Crit Care Med, 2018. **198**(1): p. 67-76.
250. Sussan, T.E., Gajghate, S., Thimmulappa, R.K., Ma, J., Kim, J.H., Sudini, K., Consolini, N., Cormier, S.A., Lomnicki, S., Hasan, F., Pekosz, A., and Biswal, S., *Exposure to electronic cigarettes impairs pulmonary anti-bacterial and anti-viral defenses in a mouse model.* PLoS One, 2015. **10**(2): p. e0116861.
251. Kumral, T.L., Salturk, Z., Yildirim, G., Uyar, Y., Berkiten, G., Atar, Y., and Inan, M., *How does electronic cigarette smoking affect sinonasal symptoms and nasal mucociliary clearance?* B-ENT, 2016. **12**(1): p. 17-21.
252. Scheffler, S., Dieken, H., Krischenowski, O., Forster, C., Branscheid, D., and Aufderheide, M., *Evaluation of E-cigarette liquid vapor and mainstream cigarette smoke after direct exposure of primary human bronchial epithelial cells.* Int J Environ Res Public Health, 2015. **12**(4): p. 3915-25.
253. Moses, E., Wang, T., Corbett, S., Jackson, G.R., Drizik, E., Perdomo, C., Perdomo, C., Kleerup, E., Brooks, D., O'Connor, G., Dubinett, S., Hayden, P., Lenburg, M.E., and Spira, A., *Molecular Impact of Electronic Cigarette Aerosol Exposure in Human Bronchial Epithelium.* Toxicol Sci, 2017. **155**(1): p. 248-257.
254. Cervellati, F., Muresan, X.M., Sticozzi, C., Gambari, R., Montagner, G., Forman, H.J., Torricelli, C., Maioli, E., and Valacchi, G., *Comparative effects between electronic and cigarette smoke in human keratinocytes and epithelial lung cells.* Toxicol In Vitro, 2014. **28**(5): p. 999-1005.
255. Higham, A., Bostock, D., Booth, G., Dungwa, J.V., and Singh, D., *The effect of electronic cigarette and tobacco smoke exposure on COPD bronchial epithelial cell inflammatory responses.* Int J Chron Obstruct Pulmon Dis, 2018. **13**: p. 989-1000.
256. Miyashita, L. and Foley, G., *E-cigarettes and respiratory health: the latest evidence.* J Physiol, 2020. **598**(22): p. 5027-5038.
257. Bozier, J., Zakarya, R., Chapman, D.G., and Oliver, B.G.G., *How harmless are E-cigarettes? Effects in the pulmonary system.* Curr Opin Pulm Med, 2020. **26**(1): p. 97-102.
258. Ween, M.P., Whittall, J.J., Hamon, R., Reynolds, P.N., and Hodge, S.J., *Phagocytosis and Inflammation: Exploring the effects of the components of E-cigarette vapor on macrophages.* Physiol Rep, 2017. **5**(16).

259. Staudt, M.R., Salit, J., Kaner, R.J., Hollmann, C., and Crystal, R.G., *Altered lung biology of healthy never smokers following acute inhalation of E-cigarettes.* Respir Res, 2018. **19**(1): p. 78.
260. Chen, I.L., Todd, I., Tighe, P.J., and Fairclough, L.C., *Electronic cigarette vapour moderately stimulates pro-inflammatory signalling pathways and interleukin-6 production by human monocyte-derived dendritic cells.* Arch Toxicol, 2020. **94**(6): p. 2097-2112.
261. Szafran, B.N., Pinkston, R., Perveen, Z., Ross, M.K., Morgan, T., Paulsen, D.B., Penn, A.L., Kaplan, B.L.F., and Noel, A., *Electronic-Cigarette Vehicles and Flavoring Affect Lung Function and Immune Responses in a Murine Model.* Int J Mol Sci, 2020. **21**(17).
262. Clapp, P.W., Pawlak, E.A., Lackey, J.T., Keating, J.E., Reeber, S.L., Glish, G.L., and Jaspers, I., *Flavored e-cigarette liquids and cinnamaldehyde impair respiratory innate immune cell function.* Am J Physiol Lung Cell Mol Physiol, 2017. **313**(2): p. L278-L292.
263. Guo-Parke, H., Linden, D., Weldon, S., Kidney, J.C., and Taggart, C.C., *Mechanisms of Virus-Induced Airway Immunity Dysfunction in the Pathogenesis of COPD Disease, Progression, and Exacerbation.* Front Immunol, 2020. **11**: p. 1205.
264. Higham, A., Rattray, N.J., Dewhurst, J.A., Trivedi, D.K., Fowler, S.J., Goodacre, R., and Singh, D., *Electronic cigarette exposure triggers neutrophil inflammatory responses.* Respir Res, 2016. **17**(1): p. 56.
265. Chaaban, T., *Acute eosinophilic pneumonia associated with non-cigarette smoking products: a systematic review.* Adv Respir Med, 2020. **88**(2): p. 142-146.
266. Arter, Z.L., Wiggins, A., Hudspath, C., Kisling, A., Hostler, D.C., and Hostler, J.M., *Acute eosinophilic pneumonia following electronic cigarette use.* Respir Med Case Rep, 2019. **27**: p. 100825.
267. Wu, Q., Jiang, D., Minor, M., and Chu, H.W., *Electronic cigarette liquid increases inflammation and virus infection in primary human airway epithelial cells.* PLoS One, 2014. **9**(9): p. e108342.
268. Thota, D. and Latham, E., *Case report of electronic cigarettes possibly associated with eosinophilic pneumonitis in a previously healthy active-duty sailor.* J Emerg Med, 2014. **47**(1): p. 15-7.
269. Suhling, H., Welte, T., and Fuehner, T., *Three Patients With Acute Pulmonary Damage Following the Use of E-Cigarettes-A Case Series.* Dtsch Arztebl Int, 2020. **117**(11): p. 177-182.
270. Menicagli, R., Marotta, O., and Serra, R., *Free Radical Production in the Smoking of E-Cigarettes and their Possible Effects in Human Health.* Int J Prev Med, 2020. **11**: p. 53.
271. Suryadinata, R.V. and Wirjatmadi, B., *The Molecular Pathways of Lung Damage by E-Cigarettes in Male Wistar Rats.* Sultan Qaboos Univ Med J, 2021. **21**(3): p. 436-441.

272. Han, H., Peng, G., Meister, M., Yao, H., Yang, J.J., Zou, M.H., Liu, Z.R., and Ji, X., *Electronic Cigarette Exposure Enhances Lung Inflammatory and Fibrotic Responses in COPD Mice.* Front Pharmacol, 2021. **12**: p. 726586.
273. Chatterjee, S., Tao, J.Q., Johncola, A., Guo, W., Caporale, A., Langham, M.C., and Wehrli, F.W., *Acute exposure to e-cigarettes causes inflammation and pulmonary endothelial oxidative stress in nonsmoking, healthy young subjects.* Am J Physiol Lung Cell Mol Physiol, 2019. **317**(2): p. L155-L166.
274. Jackson, M., Singh, K.P., Lamb, T., McIntosh, S., and Rahman, I., *Flavor Preference and Systemic Immunoglobulin Responses in E-Cigarette Users and Waterpipe and Tobacco Smokers: A Pilot Study.* Int J Environ Res Public Health, 2020. **17**(2).
275. Singh, K.P., Lawyer, G., Muthumalage, T., Maremanda, K.P., Khan, N.A., McDonough, S.R., Ye, D., McIntosh, S., and Rahman, I., *Systemic biomarkers in electronic cigarette users: implications for noninvasive assessment of vaping-associated pulmonary injuries.* ERJ Open Res, 2019. **5**(4).
276. EL Andaloussi, S., Mager, I., Breakefield, X.O., and Wood, M.J., *Extracellular vesicles: biology and emerging therapeutic opportunities.* Nat Rev Drug Discov, 2013. **12**(5): p. 347-57.
277. Raposo, G. and Stoorvogel, W., *Extracellular vesicles: exosomes, microvesicles, and friends.* J Cell Biol, 2013. **200**(4): p. 373-83.
278. Yanez-Mo, M., Siljander, P.R., Andreu, Z., Zavec, A.B., Borras, F.E., Buzas, E.I., Buzas, K., Casal, E., Cappello, F., Carvalho, J., Colas, E., Cordeiro-da Silva, A., Fais, S., Falcon-Perez, J.M., Ghobrial, I.M., Giebel, B., Gimona, M., Graner, M., Gursel, I., Gursel, M., Heegaard, N.H., Hendrix, A., Kierulf, P., Kokubun, K., Kosanovic, M., Kralj-Iglic, V., Kramer-Albers, E.M., Laitinen, S., Lasser, C., Lener, T., Ligeti, E., Line, A., Lipps, G., Llorente, A., Lotvall, J., Mancek-Keber, M., Marcilla, A., Mittelbrunn, M., Nazarenko, I., Nolte-'t Hoen, E.N., Nyman, T.A., O'Driscoll, L., Olivan, M., Oliveira, C., Pallinger, E., Del Portillo, H.A., Reventos, J., Rigau, M., Rohde, E., Sammar, M., Sanchez-Madrid, F., Santarem, N., Schallmoser, K., Ostenfeld, M.S., Stoorvogel, W., Stukelj, R., Van der Grein, S.G., Vasconcelos, M.H., Wauben, M.H., and De Wever, O., *Biological properties of extracellular vesicles and their physiological functions.* J Extracell Vesicles, 2015. **4**: p. 27066.
279. van der Pol, E., Boing, A.N., Harrison, P., Sturk, A., and Nieuwland, R., *Classification, functions, and clinical relevance of extracellular vesicles.* Pharmacol Rev, 2012. **64**(3): p. 676-705.
280. Javeed, N. and Mukhopadhyay, D., *Exosomes and their role in the micro-/macro-environment: a comprehensive review.* J Biomed Res, 2017. **31**(5): p. 386-394.
281. Buzas, E.I., *The roles of extracellular vesicles in the immune system.* Nat Rev Immunol, 2022.
282. Welsh, J.A., Goberdhan, D.C.I., O'Driscoll, L., Buzas, E.I., Blenkiron, C., Bussolati, B., Cai, H., Di Vizio, D., Driedonks, T.A.P., Erdbrugger, U., Falcon-Perez, J.M., Fu, Q.L., Hill, A.F., Lenassi, M., Lim, S.K., Mahoney, M.G., Mohanty, S., Moller, A., Nieuwland, R., Ochiya, T., Sahoo, S., Torrecilhas, A.C., Zheng, L., Zijlstra, A., Abuelreich, S., Bagabas, R., Bergese, P., Bridges, E.M., Brucale, M., Burger, D.,

Carney, R.P., Cocucci, E., Colombo, F., Crescitelli, R., Hanser, E., Harris, A.L., Haughey, N.J., Hendrix, A., Ivanov, A.R., Jovanovic-Talisman, T., Kruh-Garcia, N.A., Ku'ulei-Lyn Faustino, V., Kyburz, D., Lasser, C., Lennon, K.M., Lotvall, J., Maddox, A.L., Martens-Uzunova, E.S., Mizenko, R.R., Newman, L.A., Ridolfi, A., Rohde, E., Rojalin, T., Rowland, A., Saftics, A., Sandau, U.S., Saugstad, J.A., Shekari, F., Swift, S., Ter-Ovanesyan, D., Tosar, J.P., Useckaite, Z., Valle, F., Varga, Z., van der Pol, E., van Herwijnen, M.J.C., Wauben, M.H.M., Wehman, A.M., Williams, S., Zendrini, A., Zimmerman, A.J., Misev, C., Thery, C., and Witwer, K.W., *Minimal information for studies of extracellular vesicles (MISEV2023): From basic to advanced approaches.* J Extracell Vesicles, 2024. **13**(2): p. e12404.

283. Turchinovich, A., Drapkina, O., and Tonevitsky, A., *Transcriptome of Extracellular Vesicles: State-of-the-Art.* Front Immunol, 2019. **10**: p. 202.
284. Kaur, A., Leishangthem, G. D., Bhat, P., V. Mahajan, N. Dev Singh, and H. S. Banga, *Role of Exosomes in Pathology.* Journal of Environmental Pathology, Toxicology and Oncology, 2014.
285. Alipoor, S.D., Mortaz, E., Garssen, J., Movassaghi, M., Mirsaeidi, M., and Adcock, I.M., *Exosomes and Exosomal miRNA in Respiratory Diseases.* Mediators Inflamm, 2016. **2016**: p. 5628404.
286. Konoshenko, M.Y., Lekchnov, E.A., Vlassov, A.V., and Laktionov, P.P., *Isolation of Extracellular Vesicles: General Methodologies and Latest Trends.* Biomed Res Int, 2018. **2018**: p. 8545347.
287. Verweij, F.J., Balaj, L., Boulanger, C.M., Carter, D.R.F., Compeer, E.B., D'Angelo, G., El Andaloussi, S., Goetz, J.G., Gross, J.C., Hyenne, V., Kramer-Albers, E.M., Lai, C.P., Loyer, X., Marki, A., Momma, S., Nolte-'t Hoen, E.N.M., Pegtel, D.M., Peinado, H., Raposo, G., Rilla, K., Tahara, H., Thery, C., van Royen, M.E., Vandenbroucke, R.E., Wehman, A.M., Witwer, K., Wu, Z., Wubbolts, R., and van Niel, G., *The power of imaging to understand extracellular vesicle biology in vivo.* Nat Methods, 2021. **18**(9): p. 1013-1026.
288. Ratajczak, J., Wysoczynski, M., Hayek, F., Janowska-Wieczorek, A., and Ratajczak, M.Z., *Membrane-derived microvesicles: important and underappreciated mediators of cell-to-cell communication.* Leukemia, 2006. **20**(9): p. 1487-95.
289. Letsiou, E. and Bauer, N., *Endothelial Extracellular Vesicles in Pulmonary Function and Disease.* Curr Top Membr, 2018. **82**: p. 197-256.
290. Atkin-Smith, G.K., Paone, S., Zanker, D.J., Duan, M., Phan, T.K., Chen, W., Hulett, M.D., and Poon, I.K., *Isolation of cell type-specific apoptotic bodies by fluorescence-activated cell sorting.* Sci Rep, 2017. **7**: p. 39846.
291. Jiang, L., Paone, S., Caruso, S., Atkin-Smith, G.K., Phan, T.K., Hulett, M.D., and Poon, I.K.H., *Determining the contents and cell origins of apoptotic bodies by flow cytometry.* Sci Rep, 2017. **7**(1): p. 14444.
292. Zhang, H., Freitas, D., Kim, H.S., Fabijanic, K., Li, Z., Chen, H., Mark, M.T., Molina, H., Martin, A.B., Bojmar, L., Fang, J., Rampersaud, S., Hoshino, A., Matei, I., Kenific, C.M., Nakajima, M., Mutvei, A.P., Sansone, P., Buehring, W., Wang, H., Jimenez, J.P., Cohen-Gould, L., Paknejad, N., Brendel, M., Manova-Todorova, K.,

Magalhaes, A., Ferreira, J.A., Osorio, H., Silva, A.M., Massey, A., Cubillos-Ruiz, J.R., Galletti, G., Giannakakou, P., Cuervo, A.M., Blenis, J., Schwartz, R., Brady, M.S., Peinado, H., Bromberg, J., Matsui, H., Reis, C.A., and Lyden, D., *Identification of distinct nanoparticles and subsets of extracellular vesicles by asymmetric flow field-flow fractionation.* Nat Cell Biol, 2018. **20**(3): p. 332-343.

293. Marki, A., Buscher, K., Lorenzini, C., Meyer, M., Saigusa, R., Fan, Z., Yeh, Y.T., Hartmann, N., Dan, J.M., Kiosses, W.B., Golden, G.J., Ganesan, R., Winkels, H., Orecchioni, M., McArdle, S., Mikulski, Z., Altman, Y., Bui, J., Kronenberg, M., Chien, S., Esko, J.D., Nizet, V., Smalley, D., Roth, J., and Ley, K., *Elongated neutrophil-derived structures are blood-borne microparticles formed by rolling neutrophils during sepsis.* J Exp Med, 2021. **218**(3).
294. Teng, F. and Fussenegger, M., *Shedding Light on Extracellular Vesicle Biogenesis and Bioengineering.* Adv Sci (Weinh), 2020. **8**(1): p. 2003505.
295. Abels, E.R. and Breakefield, X.O., *Introduction to Extracellular Vesicles: Biogenesis, RNA Cargo Selection, Content, Release, and Uptake.* Cell Mol Neurobiol, 2016. **36**(3): p. 301-12.
296. Gurung, S., Perocheau, D., Touramanidou, L., and Baruteau, J., *The exosome journey: from biogenesis to uptake and intracellular signalling.* Cell Commun Signal, 2021. **19**(1): p. 47.
297. Fang, Y., Wang, Z., Liu, X., and Tyler, B.M., *Biogenesis and Biological Functions of Extracellular Vesicles in Cellular and Organismal Communication With Microbes.* Front Microbiol, 2022. **13**: p. 817844.
298. Xie, S., Zhang, Q., and Jiang, L., *Current Knowledge on Exosome Biogenesis, Cargo-Sorting Mechanism and Therapeutic Implications.* Membranes (Basel), 2022. **12**(5).
299. Akers, J.C., Gonda, D., Kim, R., Carter, B.S., and Chen, C.C., *Biogenesis of extracellular vesicles (EV): exosomes, microvesicles, retrovirus-like vesicles, and apoptotic bodies.* J Neurooncol, 2013. **113**(1): p. 1-11.
300. Muralidharan-Chari, V., Clancy, J., Plou, C., Romao, M., Chavrier, P., Raposo, G., and D'Souza-Schorey, C., *ARF6-regulated shedding of tumor cell-derived plasma membrane microvesicles.* Curr Biol, 2009. **19**(22): p. 1875-85.
301. Nabhan, J.F., Hu, R., Oh, R.S., Cohen, S.N., and Lu, Q., *Formation and release of arrestin domain-containing protein 1-mediated microvesicles (ARMMs) at plasma membrane by recruitment of TSG101 protein.* Proc Natl Acad Sci U S A, 2012. **109**(11): p. 4146-51.
302. Tauro, B.J., Greening, D.W., Mathias, R.A., Ji, H., Mathivanan, S., Scott, A.M., and Simpson, R.J., *Comparison of ultracentrifugation, density gradient separation, and immunoaffinity capture methods for isolating human colon cancer cell line LIM1863-derived exosomes.* Methods, 2012. **56**(2): p. 293-304.
303. Bucki, R., Bachelot-Loza, C., Zachowski, A., Giraud, F., and Sulpice, J.C., *Calcium induces phospholipid redistribution and microvesicle release in human erythrocyte membranes by independent pathways.* Biochemistry, 1998. **37**(44): p. 15383-91.

304. Pasquet, J.M., Dachary-Prigent, J., and Nurden, A.T., *Calcium influx is a determining factor of calpain activation and microparticle formation in platelets.* Eur J Biochem, 1996. **239**(3): p. 647-54.
305. Wang, T., Gilkes, D.M., Takano, N., Xiang, L., Luo, W., Bishop, C.J., Chaturvedi, P., Green, J.J., and Semenza, G.L., *Hypoxia-inducible factors and RAB22A mediate formation of microvesicles that stimulate breast cancer invasion and metastasis.* Proc Natl Acad Sci U S A, 2014. **111**(31): p. E3234-42.
306. Mazurov, D., Barbashova, L., and Filatov, A., *Tetraspanin protein CD9 interacts with metalloprotease CD10 and enhances its release via exosomes.* FEBS J, 2013. **280**(5): p. 1200-13.
307. Andreu, Z. and Yanez-Mo, M., *Tetraspanins in extracellular vesicle formation and function.* Front Immunol, 2014. **5**: p. 442.
308. Jankovicova, J., Secova, P., Michalkova, K., and Antalikova, J., *Tetraspanins, More than Markers of Extracellular Vesicles in Reproduction.* Int J Mol Sci, 2020. **21**(20).
309. van Niel, G., Charrin, S., Simoes, S., Romao, M., Rochin, L., Saftig, P., Marks, M.S., Rubinstein, E., and Raposo, G., *The tetraspanin CD63 regulates ESCRT-independent and -dependent endosomal sorting during melanogenesis.* Dev Cell, 2011. **21**(4): p. 708-21.
310. Umeda, R., Satouh, Y., Takemoto, M., Nakada-Nakura, Y., Liu, K., Yokoyama, T., Shirouzu, M., Iwata, S., Nomura, N., Sato, K., Ikawa, M., Nishizawa, T., and Nureki, O., *Structural insights into tetraspanin CD9 function.* Nat Commun, 2020. **11**(1): p. 1606.
311. Chairoungdua, A., Smith, D.L., Pochard, P., Hull, M., and Caplan, M.J., *Exosome release of beta-catenin: a novel mechanism that antagonizes Wnt signaling.* J Cell Biol, 2010. **190**(6): p. 1079-91.
312. Buschow, S.I., Nolte-'t Hoen, E.N., van Niel, G., Pols, M.S., ten Broeke, T., Lauwen, M., Ossendorp, F., Melief, C.J., Raposo, G., Wubbolts, R., Wauben, M.H., and Stoorvogel, W., *MHC II in dendritic cells is targeted to lysosomes or T cell-induced exosomes via distinct multivesicular body pathways.* Traffic, 2009. **10**(10): p. 1528-42.
313. Rana, S., Yue, S., Stadel, D., and Zoller, M., *Toward tailored exosomes: the exosomal tetraspanin web contributes to target cell selection.* Int J Biochem Cell Biol, 2012. **44**(9): p. 1574-84.
314. Fanaei, M., Monk, P.N., and Partridge, L.J., *The role of tetraspanins in fusion.* Biochem Soc Trans, 2011. **39**(2): p. 524-8.
315. Anand, S., Samuel, M., Kumar, S., and Mathivanan, S., *Ticket to a bubble ride: Cargo sorting into exosomes and extracellular vesicles.* Biochim Biophys Acta Proteins Proteom, 2019. **1867**(12): p. 140203.
316. O'Brien, K., Breyne, K., Ughetto, S., Laurent, L.C., and Breakefield, X.O., *RNA delivery by extracellular vesicles in mammalian cells and its applications.* Nat Rev Mol Cell Biol, 2020. **21**(10): p. 585-606.

317. Kwok, Z.H., Ni, K., and Jin, Y., *Extracellular Vesicle Associated Non-Coding RNAs in Lung Infections and Injury.* Cells, 2021. **10**(5).
318. Abramowicz, A. and Story, M.D., *The Long and Short of It: The Emerging Roles of Non-Coding RNA in Small Extracellular Vesicles.* Cancers (Basel), 2020. **12**(6).
319. de Rie, D., Abugessaisa, I., Alam, T., Arner, E., Arner, P., Ashoor, H., Astrom, G., Babina, M., Bertin, N., Burroughs, A.M., Carlisle, A.J., Daub, C.O., Detmar, M., Deviatiiarov, R., Fort, A., Gebhard, C., Goldowitz, D., Guhl, S., Ha, T.J., Harshbarger, J., Hasegawa, A., Hashimoto, K., Herlyn, M., Heutink, P., Hitchens, K.J., Hon, C.C., Huang, E., Ishizu, Y., Kai, C., Kasukawa, T., Klinken, P., Lassmann, T., Lecellier, C.H., Lee, W., Lizio, M., Makeev, V., Mathelier, A., Medvedeva, Y.A., Mejhert, N., Mungall, C.J., Noma, S., Ohshima, M., Okada-Hatakeyama, M., Persson, H., Rizzu, P., Roudnicky, F., Saetrom, P., Sato, H., Severin, J., Shin, J.W., Swoboda, R.K., Tarui, H., Toyoda, H., Vitting-Seerup, K., Winteringham, L., Yamaguchi, Y., Yasuzawa, K., Yoneda, M., Yumoto, N., Zabierowski, S., Zhang, P.G., Wells, C.A., Summers, K.M., Kawaji, H., Sandelin, A., Rehli, M., Consortium, F., Hayashizaki, Y., Carninci, P., Forrest, A.R.R., and de Hoon, M.J.L., *An integrated expression atlas of miRNAs and their promoters in human and mouse.* Nat Biotechnol, 2017. **35**(9): p. 872-878.
320. Gomez, N., James, V., Onion, D., and Fairclough, L.C., *Extracellular vesicles and chronic obstructive pulmonary disease (COPD): a systematic review.* Respir Res, 2022. **23**(1): p. 82.
321. He, S., Chen, D., Hu, M., Zhang, L., Liu, C., Traini, D., Grau, G.E., Zeng, Z., Lu, J., Zhou, G., Xie, L., and Sun, S., *Bronchial epithelial cell extracellular vesicles ameliorate epithelial-mesenchymal transition in COPD pathogenesis by alleviating M2 macrophage polarization.* Nanomedicine, 2019. **18**: p. 259-271.
322. Xu, H., Ling, M., Xue, J., Dai, X., Sun, Q., Chen, C., Liu, Y., Zhou, L., Liu, J., Luo, F., Bian, Q., and Liu, Q., *Exosomal microRNA-21 derived from bronchial epithelial cells is involved in aberrant epithelium-fibroblast cross-talk in COPD induced by cigarette smoking.* Theranostics, 2018. **8**(19): p. 5419-5433.
323. Zeng, Z., He, S., Lu, J., Liu, C., Lin, H., Xu, C., Xie, L., and Sun, S., *MicroRNA-21 aggravates chronic obstructive pulmonary disease by promoting autophagy.* Exp Lung Res, 2018. **44**(2): p. 89-97.
324. He, S., Chen, D., Hu, M., Zhang, L., Liu, C., Traini, D., Grau, G.E., Zeng, Z., Lu, J., Zhou, G., Xie, L., and Sun, S., *Bronchial epithelial cell extracellular vesicles ameliorate epithelial-mesenchymal transition in COPD pathogenesis by alleviating M2 macrophage polarization.* Nanomedicine : nanotechnology, biology, and medicine, 2019. **18**: p. 259-271.
325. Cufaro, M.C., Pieragostino, D., Lanuti, P., Rossi, C., Cicalini, I., Federici, L., De Laurenzi, V., and Del Boccio, P., *Extracellular Vesicles and Their Potential Use in Monitoring Cancer Progression and Therapy: The Contribution of Proteomics.* J Oncol, 2019. **2019**: p. 1639854.

326. Raimondo, F., Morosi, L., Chinello, C., Magni, F., and Pitto, M., *Advances in membranous vesicle and exosome proteomics improving biological understanding and biomarker discovery.* Proteomics, 2011. **11**(4): p. 709-20.
327. Rosa-Fernandes, L., Rocha, V.B., Carregari, V.C., Urbani, A., and Palmisano, G., *A Perspective on Extracellular Vesicles Proteomics.* Front Chem, 2017. **5**: p. 102.
328. Mathivanan, S., Ji, H., and Simpson, R.J., *Exosomes: extracellular organelles important in intercellular communication.* J Proteomics, 2010. **73**(10): p. 1907-20.
329. van Niel, G., D'Angelo, G., and Raposo, G., *Shedding light on the cell biology of extracellular vesicles.* Nat Rev Mol Cell Biol, 2018. **19**(4): p. 213-228.
330. Skotland, T., Sagini, K., Sandvig, K., and Llorente, A., *An emerging focus on lipids in extracellular vesicles.* Adv Drug Deliv Rev, 2020. **159**: p. 308-321.
331. Laulagnier, K., Motta, C., Hamdi, S., Roy, S., Fauvelle, F., Pageaux, J.F., Kobayashi, T., Salles, J.P., Perret, B., Bonnerot, C., and Record, M., *Mast cell- and dendritic cell-derived exosomes display a specific lipid composition and an unusual membrane organization.* Biochem J, 2004. **380**(Pt 1): p. 161-71.
332. Llorente, A., Skotland, T., Sylvanne, T., Kauhanen, D., Rog, T., Orlowski, A., Vattulainen, I., Ekroos, K., and Sandvig, K., *Molecular lipidomics of exosomes released by PC-3 prostate cancer cells.* Biochim Biophys Acta, 2013. **1831**(7): p. 1302-9.
333. Li, C., Donninger, H., Eaton, J., and Yaddanapudi, K., *Regulatory Role of Immune Cell-Derived Extracellular Vesicles in Cancer: The Message Is in the Envelope.* Front Immunol, 2020. **11**: p. 1525.
334. Cordazzo, C., Petrini, S., Neri, T., Lombardi, S., Carmazzi, Y., Pedrinelli, R., Paggiaro, P., and Celi, A., *Rapid shedding of proinflammatory microparticles by human mononuclear cells exposed to cigarette smoke is dependent on Ca2+ mobilization.* Inflamm Res, 2014. **63**(7): p. 539-47.
335. Benedikter, B.J., Volgers, C., van Eijck, P.H., Wouters, E.F.M., Savelkoul, P.H.M., Reynaert, N.L., Haenen, G., Rohde, G.G.U., Weseler, A.R., and Stassen, F.R.M., *Cigarette smoke extract induced exosome release is mediated by depletion of exofacial thiols and can be inhibited by thiol-antioxidants.* Free Radic Biol Med, 2017. **108**: p. 334-344.
336. Moon, H.-G., Kim, S.-H., Gao, J., Quan, T., Qin, Z., Osorio, J.C., Rosas, I.O., Wu, M., Tesfaigzi, Y., and Jin, Y., *CCN1 secretion and cleavage regulate the lung epithelial cell functions after cigarette smoke.* American journal of physiology. Lung cellular and molecular physiology, 2014. **307**(4): p. L326-L337.
337. Fujita, Y., Araya, J., Ito, S., Kobayashi, K., Kosaka, N., Yoshioka, Y., Kadota, T., Hara, H., Kuwano, K., and Ochiya, T., *Suppression of autophagy by extracellular vesicles promotes myofibroblast differentiation in COPD pathogenesis.* J Extracell Vesicles, 2015. **4**: p. 28388.
338. Wahlund, C.J.E., Eklund, A., Grunewald, J., and Gabrielsson, S., *Pulmonary Extracellular Vesicles as Mediators of Local and Systemic Inflammation.* Front Cell Dev Biol, 2017. **5**: p. 39.

339. Fujita, Y., Kosaka, N., Araya, J., Kuwano, K., and Ochiya, T., *Extracellular vesicles in lung microenvironment and pathogenesis.* Trends Mol Med, 2015. **21**(9): p. 533-42.
340. Takahashi, T., Kobayashi, S., Fujino, N., Suzuki, T., Ota, C., Tando, Y., He, M., Yamada, M., Kurosawa, S., Yamaya, M., and Kubo, H., *Differences in the released endothelial microparticle subtypes between human pulmonary microvascular endothelial cells and aortic endothelial cells in vitro.* Exp Lung Res, 2013. **39**(4-5): p. 155-61.
341. Strulovici-Barel, Y., Staudt, M.R., Krause, A., Gordon, C., Tilley, A.E., Harvey, B.G., Kaner, R.J., Hollmann, C., Mezey, J.G., Bitter, H., Pillai, S.G., Hilton, H., Wolff, G., Stevenson, C.S., Visvanathan, S., Fine, J.S., and Crystal, R.G., *Persistence of circulating endothelial microparticles in COPD despite smoking cessation.* Thorax, 2016. **71**(12): p. 1137-1144.
342. Thomashow, M.A., Shimbo, D., Parikh, M.A., Hoffman, E.A., Vogel-Claussen, J., Hueper, K., Fu, J., Liu, C.Y., Bluemke, D.A., Ventetuolo, C.E., Doyle, M.F., and Barr, R.G., *Endothelial microparticles in mild chronic obstructive pulmonary disease and emphysema. The Multi-Ethnic Study of Atherosclerosis Chronic Obstructive Pulmonary Disease study.* Am J Respir Crit Care Med, 2013. **188**(1): p. 60-8.
343. Garcia-Lucio, J., Peinado, V.I., de Jover, L., del Pozo, R., Blanco, I., Bonjoch, C., Coll-Bonfill, N., Paul, T., Tura-Ceide, O., and Barbera, J.A., *Imbalance between endothelial damage and repair capacity in chronic obstructive pulmonary disease.* PLoS ONE, 2018. **13**(4): p. e0195724.
344. Barak, O.F., Mladinov, S., Hoiland, R.L., Tremblay, J.C., Thom, S.R., Yang, M., Mijacika, T., and Dujic, Z., *Disturbed blood flow worsens endothelial dysfunction in moderate-severe chronic obstructive pulmonary disease.* Sci Rep, 2017. **7**(1): p. 16929.
345. Liu, H., Ding, L., Zhang, Y., and Ni, S., *Circulating endothelial microparticles involved in lung function decline in a rat exposed in cigarette smoke maybe from apoptotic pulmonary capillary endothelial cells.* J Thorac Dis, 2014. **6**(6): p. 649-55.
346. Nieri, D., Daniele, M., Lombardi, S., Bazzan, E., Santerini, S., De Cusatis, G., Vagaggini, B., Cosio, M.G., Saetta, M., Paggiaro, P., Celi, A., and Neri, T., *Circulating Extracellular Vesicles Are Associated with Disease Severity and Interleukin-6 Levels in COPD: A Pilot Study.* J Clin Med, 2021. **10**(21).
347. Lascano, J., Katz, J., Cearras, M., and Campos, M., *Association of Systemic Endothelial-Derived and Platelet-Derived Microparticles With Clinical Outcomes in Chronic Obstructive Pulmonary Disease.* Chronic Obstr Pulm Dis, 2021. **8**(3): p. 382-395.
348. Mobarrez, F., Antoniewicz, L., Hedman, L., Bosson, J.A., and Lundback, M., *Electronic cigarettes containing nicotine increase endothelial and platelet derived extracellular vesicles in healthy volunteers.* Atherosclerosis, 2020. **301**: p. 93-100.
349. Serban, K.A., Rezania, S., Petrusca, D.N., Poirier, C., Cao, D., Justice, M.J., Patel, M., Tsvetkova, I., Kamocki, K., Mikosz, A., Schweitzer, K.S., Jacobson, S., Cardoso,

A., Carlesso, N., Hubbard, W.C., Kechris, K., Dragnea, B., Berdyshev, E.V., McClintock, J., and Petrache, I., *Structural and functional characterization of endothelial microparticles released by cigarette smoke.* Sci Rep, 2016. **6**: p. 31596.
350. McCubbrey, A.L. and Curtis, J.L., *Efferocytosis and lung disease.* Chest, 2013. **143**(6): p. 1750-1757.
351. Corsello, T., Kudlicki, A.S., Garofalo, R.P., and Casola, A., *Cigarette Smoke Condensate Exposure Changes RNA Content of Extracellular Vesicles Released from Small Airway Epithelial Cells.* Cells, 2019. **8**(12).
352. Feller, D., Kun, J., Ruzsics, I., Rapp, J., Sarosi, V., Kvell, K., Helyes, Z., and Pongracz, J.E., *Cigarette Smoke-Induced Pulmonary Inflammation Becomes Systemic by Circulating Extracellular Vesicles Containing Wnt5a and Inflammatory Cytokines.* Front Immunol, 2018. **9**: p. 1724.
353. Zou, Y., Bhat, O.M., Yuan, X., Li, G., Huang, D., Guo, Y., Zhou, D., and Li, P.L., *Release and Actions of Inflammatory Exosomes in Pulmonary Emphysema: Potential Therapeutic Target of Acupuncture.* J Inflamm Res, 2021. **14**: p. 3501-3521.
354. Wang, L., Chen, Q., Yu, Q., Xiao, J., and Zhao, H., *Cigarette smoke extract-treated airway epithelial cells-derived exosomes promote M1 macrophage polarization in chronic obstructive pulmonary disease.* Int Immunopharmacol, 2021. **96**: p. 107700.
355. Song, L., Peng, J., and Guo, X., *Exosomal lncRNA TCONS_00064356 derived from injured alveolar epithelial type II cells affects the biological characteristics of mesenchymal stem cells.* Life Sci, 2021. **278**: p. 119568.
356. Xia, H., Wu, Y., Zhao, J., Li, W., Lu, L., Ma, H., Cheng, C., Sun, J., Xiang, Q., Bian, T., and Liu, Q., *The aberrant cross-talk of epithelium-macrophages via METTL3-regulated extracellular vesicle miR-93 in smoking-induced emphysema.* Cell Biol Toxicol, 2022. **38**(1): p. 167-183.
357. Chen, Y., Li, G., Liu, Y., Werth, V.P., Williams, K.J., and Liu, M.L., *Translocation of Endogenous Danger Signal HMGB1 From Nucleus to Membrane Microvesicles in Macrophages.* J Cell Physiol, 2016. **231**(11): p. 2319-26.
358. Bourdonnay, E., Zaslona, Z., Penke, L.R., Speth, J.M., Schneider, D.J., Przybranowski, S., Swanson, J.A., Mancuso, P., Freeman, C.M., Curtis, J.L., and Peters-Golden, M., *Transcellular delivery of vesicular SOCS proteins from macrophages to epithelial cells blunts inflammatory signaling.* J Exp Med, 2015. **212**(5): p. 729-42.
359. Schneider, D.J., Speth, J.M., Penke, L.R., Wettlaufer, S.H., Swanson, J.A., and Peters-Golden, M., *Mechanisms and modulation of microvesicle uptake in a model of alveolar cell communication.* J Biol Chem, 2017. **292**(51): p. 20897-20910.
360. Genschmer, K.R., Russell, D.W., Lal, C., Szul, T., Bratcher, P.E., Noerager, B.D., Abdul Roda, M., Xu, X., Rezonzew, G., Viera, L., Dobosh, B.S., Margaroli, C., Abdalla, T.H., King, R.W., McNicholas, C.M., Wells, J.M., Dransfield, M.T.,

Tirouvanziam, R., Gaggar, A., and Blalock, J.E., *Activated PMN Exosomes: Pathogenic Entities Causing Matrix Destruction and Disease in the Lung.* Cell, 2019. **176**(1-2): p. 113-126 e15.
361. Margaroli, C., Madison, M.C., Viera, L., Russell, D.W., Gaggar, A., Genschmer, K.R., and Blalock, J.E., *A novel in vivo model for extracellular vesicle-induced emphysema.* JCI Insight, 2022.
362. Qiu, Q., Dan, X., Yang, C., Hardy, P., Yang, Z., Liu, G., and Xiong, W., *Increased airway T lymphocyte microparticles in chronic obstructive pulmonary disease induces airway epithelial injury.* Life Sci, 2020. **261**: p. 118357.
363. Mause, S.F., von Hundelshausen, P., Zernecke, A., Koenen, R.R., and Weber, C., *Platelet microparticles: a transcellular delivery system for RANTES promoting monocyte recruitment on endothelium.* Arterioscler Thromb Vasc Biol, 2005. **25**(7): p. 1512-8.
364. Vajen, T., Benedikter, B.J., Heinzmann, A.C.A., Vasina, E.M., Henskens, Y., Parsons, M., Maguire, P.B., Stassen, F.R., Heemskerk, J.W.M., Schurgers, L.J., and Koenen, R.R., *Platelet extracellular vesicles induce a pro-inflammatory smooth muscle cell phenotype.* J Extracell Vesicles, 2017. **6**(1): p. 1322454.
365. Vasina, E.M., Cauwenberghs, S., Feijge, M.A., Heemskerk, J.W., Weber, C., and Koenen, R.R., *Microparticles from apoptotic platelets promote resident macrophage differentiation.* Cell Death Dis, 2011. **2**(9): p. e211.
366. Badimon, L., Suades, R., Fuentes, E., Palomo, I., and Padro, T., *Role of Platelet-Derived Microvesicles As Crosstalk Mediators in Atherothrombosis and Future Pharmacology Targets: A Link between Inflammation, Atherosclerosis, and Thrombosis.* Front Pharmacol, 2016. **7**: p. 293.
367. Russell, A.E., Liao, Z., Tkach, M., Tarwater, P.M., Ostrowski, M., Thery, C., and Witwer, K.W., *Cigarette smoke-induced extracellular vesicles from dendritic cells alter T-cell activation and HIV replication.* Toxicol Lett, 2022. **360**: p. 33-43.
368. Giordano, L., Gregory, A.D., Perez Verdaguer, M., Ware, S.A., Harvey, H., DeVallance, E., Brzoska, T., Sundd, P., Zhang, Y., Sciurba, F.C., Shapiro, S.D., and Kaufman, B.A., *Extracellular Release of Mitochondrial DNA: Triggered by Cigarette Smoke and Detected in COPD.* Cells, 2022. **11**(3).
369. Colombo, M., Raposo, G., and Thery, C., *Biogenesis, secretion, and intercellular interactions of exosomes and other extracellular vesicles.* Annu Rev Cell Dev Biol, 2014. **30**: p. 255-89.
370. Sundar, I.K., Li, D., and Rahman, I., *Proteomic Analysis of Plasma-Derived Extracellular Vesicles in Smokers and Patients with Chronic Obstructive Pulmonary Disease.* ACS Omega, 2019. **4**(6): p. 10649-10661.
371. Benedikter, B.J., Bouwman, F.G., Heinzmann, A.C.A., Vajen, T., Mariman, E.C., Wouters, E.F.M., Savelkoul, P.H.M., Koenen, R.R., Rohde, G.G.U., van Oerle, R., Spronk, H.M., and Stassen, F.R.M., *Proteomic analysis reveals procoagulant properties of cigarette smoke-induced extracellular vesicles.* J Extracell Vesicles, 2019. **8**(1): p. 1585163.

372. Wang, W., Zeng, R., Liu, M., Chen, M., Wei, S., Li, B., and Yu, S., *Exosome proteomics study of the effects of traditional cigarettes and electronic cigarettes on human bronchial epithelial cells.* Toxicol In Vitro, 2023. **86**: p. 105516.
373. Lacedonia, D., Carpagnano, G.E., Trotta, T., Palladino, G.P., Panaro, M.A., Zoppo, L.D., Barbaro, M.P.F., and Porro, C., *Microparticles in sputum of COPD patients: A potential biomarker of the disease?* International Journal of COPD, 2016. **11**(1): p. 527-533.
374. Gordon, C., Gudi, K., Krause, A., Sackrowitz, R., Harvey, B.-G., Strulovici-Barel, Y., Mezey, J.G., and Crystal, R.G., *Circulating endothelial microparticles as a measure of early lung destruction in cigarette smokers.* American journal of respiratory and critical care medicine, 2011. **184**(2): p. 224-232.
375. Takahashi, T., Kobayashi, S., Fujino, N., Suzuki, T., Ota, C., Tando, Y., Yamada, M., Yanai, M., Yamaya, M., Kurosawa, S., Yamauchi, M., and Kubo, H., *Annual FEV1 changes and numbers of circulating endothelial microparticles in patients with COPD: a prospective study.* BMJ Open, 2014. **4**(3): p. e004571.
376. Sundar, I.K., Li, D., and Rahman, I., *Small RNA-sequence analysis of plasma-derived extracellular vesicle miRNAs in smokers and patients with chronic obstructive pulmonary disease as circulating biomarkers.* J Extracell Vesicles, 2019. **8**(1): p. 1684816.
377. Jung, A.L., Moller Jorgensen, M., Baek, R., Griss, K., Han, M., Auf Dem Brinke, K., Timmesfeld, N., Bertrams, W., Greulich, T., Koczulla, R., Hippenstiel, S., Suttorp, N., and Schmeck, B., *Surface Proteome of Plasma Extracellular Vesicles as Biomarkers for Pneumonia and Acute Exacerbation of Chronic Obstructive Pulmonary Disease.* J Infect Dis, 2020. **221**(2): p. 325-335.
378. Koba, T., Takeda, Y., Narumi, R., Shiromizu, T., Nojima, Y., Ito, M., Kuroyama, M., Futami, Y., Takimoto, T., Matsuki, T., Edahiro, R., Nojima, S., Hayama, Y., Fukushima, K., Hirata, H., Koyama, S., Iwahori, K., Nagatomo, I., Suzuki, M., Shirai, Y., Murakami, T., Nakanishi, K., Nakatani, T., Suga, Y., Miyake, K., Shiroyama, T., Kida, H., Sasaki, T., Ueda, K., Mizuguchi, K., Adachi, J., Tomonaga, T., and Kumanogoh, A., *Proteomics of serum extracellular vesicles identifies a novel COPD biomarker, fibulin-3 from elastic fibres.* ERJ Open Res, 2021. **7**(1).
379. Soni, S., Garner, J.L., O'Dea, K.P., Koh, M., Finney, L., Tirlapur, N., Srikanthan, K., Tenda, E.D., Aboelhassan, A.M., Singh, S., Wilson, M.R., Wedzicha, J.A., Kemp, S.V., Usmani, O.S., Shah, P.L., and Takata, M., *Intra-alveolar neutrophil-derived microvesicles are associated with disease severity in COPD.* Am J Physiol Lung Cell Mol Physiol, 2021. **320**(1): p. L73-L83.
380. Lucchetti, D., Santini, G., Perelli, L., Ricciardi-Tenore, C., Colella, F., Mores, N., Macis, G., Bush, A., Sgambato, A., and Montuschi, P., *Detection and characterisation of extracellular vesicles in exhaled breath condensate and sputum of COPD and severe asthma patients.* Eur Respir J, 2021. **58**(2).
381. Bazzan, E., Radu, C.M., Tine, M., Neri, T., Biondini, D., Semenzato, U., Casara, A., Balestro, E., Simioni, P., Celi, A., Cosio, M.G., and Saetta, M., *Microvesicles in*

bronchoalveolar lavage as a potential biomarker of COPD. Am J Physiol Lung Cell Mol Physiol, 2021. **320**(2): p. L241-L245.
382. Carpi, S., Polini, B., Nieri, D., Dubbini, N., Celi, A., Nieri, P., and Neri, T., *Expression Analysis of Muscle-Specific miRNAs in Plasma-Derived Extracellular Vesicles from Patients with Chronic Obstructive Pulmonary Disease.* Diagnostics (Basel), 2020. **10**(7).
383. Shen, Y., Wang, L., Wu, Y., Ou, Y., Lu, H., and Yao, X., *A novel diagnostic signature based on three circulating exosomal mircoRNAs for chronic obstructive pulmonary disease.* Exp Ther Med, 2021. **22**(1): p. 717.
384. Kaur, G., Maremanda, K.P., Campos, M., Chand, H.S., Li, F., Hirani, N., Haseeb, M.A., Li, D., and Rahman, I., *Distinct Exosomal miRNA Profiles from BALF and Lung Tissue of COPD and IPF Patients.* Int J Mol Sci, 2021. **22**(21).
385. Sassano, M.F., Davis, E.S., Keating, J.E., Zorn, B.T., Kochar, T.K., Wolfgang, M.C., Glish, G.L., and Tarran, R., *Evaluation of e-liquid toxicity using an open-source high-throughput screening assay.* PLoS Biol, 2018. **16**(3): p. e2003904.
386. Benedikter, B.J. and Koenen, R.R., *Vaping, vapor, vesicles! Electronic cigarettes provoke vascular extracellular vesicle release in healthy volunteers.* Atherosclerosis, 2020. **301**: p. 79-81.
387. Kerr, D.M.I., Brooksbank, K.J.M., Taylor, R.G., Pinel, K., Rios, F.J., Touyz, R.M., and Delles, C., *Acute effects of electronic and tobacco cigarettes on vascular and respiratory function in healthy volunteers: a cross-over study.* J Hypertens, 2019. **37**(1): p. 154-166.
388. Chironi, G.N., Boulanger, C.M., Simon, A., Dignat-George, F., Freyssinet, J.M., and Tedgui, A., *Endothelial microparticles in diseases.* Cell Tissue Res, 2009. **335**(1): p. 143-51.
389. Antoniewicz, L., Bosson, J.A., Kuhl, J., Abdel-Halim, S.M., Kiessling, A., Mobarrez, F., and Lundback, M., *Electronic cigarettes increase endothelial progenitor cells in the blood of healthy volunteers.* Atherosclerosis, 2016. **255**: p. 179-185.
390. Molony, R.D., Wu, C.H., and Lee, Y.F., *E-liquid exposure induces bladder cancer cells to release extracellular vesicles that promote non-malignant urothelial cell transformation.* Sci Rep, 2023. **13**(1): p. 142.
391. Mills, A., Dakhlallah, D., Robinson, M., Kirk, A., Llavina, S., Boyd, J.W., Chantler, P.D., and Olfert, I.M., *Short-term effects of electronic cigarettes on cerebrovascular function: A time course study.* Exp Physiol, 2022. **107**(8): p. 994-1006.
392. Singh, K.P., Maremanda, K.P., Li, D., and Rahman, I., *Exosomal microRNAs are novel circulating biomarkers in cigarette, waterpipe smokers, E-cigarette users and dual smokers.* BMC Med Genomics, 2020. **13**(1): p. 128.
393. Kuang, M., Zheng, D., Tao, X., Peng, Y., Pan, Y., Zheng, S., Zhang, Y., Li, H., Yuan, C., Zhang, Y., Xiang, J., Li, Y., Chen, H., and Sun, Y., *tRNA-based prognostic score in predicting survival outcomes of lung adenocarcinomas.* Int J Cancer, 2019. **145**(7): p. 1982-1990.

394. Kaur, G., Singh, K., Maremanda, K.P., Li, D., Chand, H.S., and Rahman, I., *Differential plasma exosomal long non-coding RNAs expression profiles and their emerging role in E-cigarette users, cigarette, waterpipe, and dual smokers.* PLoS One, 2020. **15**(12): p. e0243065.
395. Zhang, M., Shi, R., Zhang, Y., Shan, H., Zhang, Q., Yang, X., Li, Y., and Zhang, J., *Nix/BNIP3L-dependent mitophagy accounts for airway epithelial cell injury induced by cigarette smoke.* J Cell Physiol, 2019. **234**(8): p. 14210-14220.
396. Leermakers, P.A., Schols, A., Kneppers, A.E.M., Kelders, M., de Theije, C.C., Lainscak, M., and Gosker, H.R., *Molecular signalling towards mitochondrial breakdown is enhanced in skeletal muscle of patients with chronic obstructive pulmonary disease (COPD).* Sci Rep, 2018. **8**(1): p. 15007.
397. Been, T., Alakhtar, B., Traboulsi, H., Tsering, T., Bartolomucci, A., Heimbach, N., Paoli, S., Burnier, J., Mann, K.K., Eidelman, D.H., and Baglole, C.J., *Chronic low-level JUUL aerosol exposure causes pulmonary immunologic, transcriptomic, and proteomic changes.* FASEB J, 2023. **37**(2): p. e22732.
398. Peng, X.C., Gong, F.M., Chen, Y., Qiu, M., Cheng, K., Tang, J., Ge, J., Chen, N., Zeng, H., and Liu, J.Y., *Proteomics identification of PGAM1 as a potential therapeutic target for urothelial bladder cancer.* J Proteomics, 2016. **132**: p. 85-92.
399. Thery, C., Witwer, K.W., Aikawa, E., Alcaraz, M.J., Anderson, J.D., Andriantsitohaina, R., Antoniou, A., Arab, T., Archer, F., Atkin-Smith, G.K., Ayre, D.C., Bach, J.M., Bachurski, D., Baharvand, H., Balaj, L., Baldacchino, S., Bauer, N.N., Baxter, A.A., Bebawy, M., Beckham, C., Bedina Zavec, A., Benmoussa, A., Berardi, A.C., Bergese, P., Bielska, E., Blenkiron, C., Bobis-Wozowicz, S., Boilard, E., Boireau, W., Bongiovanni, A., Borras, F.E., Bosch, S., Boulanger, C.M., Breakefield, X., Breglio, A.M., Brennan, M.A., Brigstock, D.R., Brisson, A., Broekman, M.L., Bromberg, J.F., Bryl-Gorecka, P., Buch, S., Buck, A.H., Burger, D., Busatto, S., Buschmann, D., Bussolati, B., Buzas, E.I., Byrd, J.B., Camussi, G., Carter, D.R., Caruso, S., Chamley, L.W., Chang, Y.T., Chen, C., Chen, S., Cheng, L., Chin, A.R., Clayton, A., Clerici, S.P., Cocks, A., Cocucci, E., Coffey, R.J., Cordeiro-da-Silva, A., Couch, Y., Coumans, F.A., Coyle, B., Crescitelli, R., Criado, M.F., D'Souza-Schorey, C., Das, S., Datta Chaudhuri, A., de Candia, P., De Santana, E.F., De Wever, O., Del Portillo, H.A., Demaret, T., Deville, S., Devitt, A., Dhondt, B., Di Vizio, D., Dieterich, L.C., Dolo, V., Dominguez Rubio, A.P., Dominici, M., Dourado, M.R., Driedonks, T.A., Duarte, F.V., Duncan, H.M., Eichenberger, R.M., Ekstrom, K., El Andaloussi, S., Elie-Caille, C., Erdbrugger, U., Falcon-Perez, J.M., Fatima, F., Fish, J.E., Flores-Bellver, M., Forsonits, A., Frelet-Barrand, A., Fricke, F., Fuhrmann, G., Gabrielsson, S., Gamez-Valero, A., Gardiner, C., Gartner, K., Gaudin, R., Gho, Y.S., Giebel, B., Gilbert, C., Gimona, M., Giusti, I., Goberdhan, D.C., Gorgens, A., Gorski, S.M., Greening, D.W., Gross, J.C., Gualerzi, A., Gupta, G.N., Gustafson, D., Handberg, A., Haraszti, R.A., Harrison, P., Hegyesi, H., Hendrix, A., Hill, A.F., Hochberg, F.H., Hoffmann, K.F., Holder, B., Holthofer, H., Hosseinkhani, B., Hu, G., Huang, Y., Huber, V., Hunt, S., Ibrahim, A.G., Ikezu, T.,

Inal, J.M., Isin, M., Ivanova, A., Jackson, H.K., Jacobsen, S., Jay, S.M., Jayachandran, M., Jenster, G., Jiang, L., Johnson, S.M., Jones, J.C., Jong, A., Jovanovic-Talisman, T., Jung, S., Kalluri, R., Kano, S.I., Kaur, S., Kawamura, Y., Keller, E.T., Khamari, D., Khomyakova, E., Khvorova, A., Kierulf, P., Kim, K.P., Kislinger, T., Klingeborn, M., Klinke, D.J., 2nd, Kornek, M., Kosanovic, M.M., Kovacs, A.F., Kramer-Albers, E.M., Krasemann, S., Krause, M., Kurochkin, I.V., Kusuma, G.D., Kuypers, S., Laitinen, S., Langevin, S.M., Languino, L.R., Lannigan, J., Lasser, C., Laurent, L.C., Lavieu, G., Lazaro-Ibanez, E., Le Lay, S., Lee, M.S., Lee, Y.X.F., Lemos, D.S., Lenassi, M., Leszczynska, A., Li, I.T., Liao, K., Libregts, S.F., Ligeti, E., Lim, R., Lim, S.K., Line, A., Linnemannstons, K., Llorente, A., Lombard, C.A., Lorenowicz, M.J., Lorincz, A.M., Lotvall, J., Lovett, J., Lowry, M.C., Loyer, X., Lu, Q., Lukomska, B., Lunavat, T.R., Maas, S.L., Malhi, H., Marcilla, A., Mariani, J., Mariscal, J., Martens-Uzunova, E.S., Martin-Jaular, L., Martinez, M.C., Martins, V.R., Mathieu, M., Mathivanan, S., Maugeri, M., McGinnis, L.K., McVey, M.J., Meckes, D.G., Jr., Meehan, K.L., Mertens, I., Minciacchi, V.R., Moller, A., Moller Jorgensen, M., Morales-Kastresana, A., Morhayim, J., Mullier, F., Muraca, M., Musante, L., Mussack, V., Muth, D.C., Myburgh, K.H., Najrana, T., Nawaz, M., Nazarenko, I., Nejsum, P., Neri, C., Neri, T., Nieuwland, R., Nimrichter, L., Nolan, J.P., Nolte-'t Hoen, E.N., Noren Hooten, N., O'Driscoll, L., O'Grady, T., O'Loghlen, A., Ochiya, T., Olivier, M., Ortiz, A., Ortiz, L.A., Osteikoetxea, X., Ostergaard, O., Ostrowski, M., Park, J., Pegtel, D.M., Peinado, H., Perut, F., Pfaffl, M.W., Phinney, D.G., Pieters, B.C., Pink, R.C., Pisetsky, D.S., Pogge von Strandmann, E., Polakovicova, I., Poon, I.K., Powell, B.H., Prada, I., Pulliam, L., Quesenberry, P., Radeghieri, A., Raffai, R.L., Raimondo, S., Rak, J., Ramirez, M.I., Raposo, G., Rayyan, M.S., Regev-Rudzki, N., Ricklefs, F.L., Robbins, P.D., Roberts, D.D., Rodrigues, S.C., Rohde, E., Rome, S., Rouschop, K.M., Rughetti, A., Russell, A.E., Saa, P., Sahoo, S., Salas-Huenuleo, E., Sanchez, C., Saugstad, J.A., Saul, M.J., Schiffelers, R.M., Schneider, R., Schoyen, T.H., Scott, A., Shahaj, E., Sharma, S., Shatnyeva, O., Shekari, F., Shelke, G.V., Shetty, A.K., Shiba, K., Siljander, P.R., Silva, A.M., Skowronek, A., Snyder, O.L., 2nd, Soares, R.P., Sodar, B.W., Soekmadji, C., Sotillo, J., Stahl, P.D., Stoorvogel, W., Stott, S.L., Strasser, E.F., Swift, S., Tahara, H., Tewari, M., Timms, K., Tiwari, S., Tixeira, R., Tkach, M., Toh, W.S., Tomasini, R., Torrecilhas, A.C., Tosar, J.P., Toxavidis, V., Urbanelli, L., Vader, P., van Balkom, B.W., van der Grein, S.G., Van Deun, J., van Herwijnen, M.J., Van Keuren-Jensen, K., van Niel, G., van Royen, M.E., van Wijnen, A.J., Vasconcelos, M.H., Vechetti, I.J., Jr., Veit, T.D., Vella, L.J., Velot, E., Verweij, F.J., Vestad, B., Vinas, J.L., Visnovitz, T., Vukman, K.V., Wahlgren, J., Watson, D.C., Wauben, M.H., Weaver, A., Webber, J.P., Weber, V., Wehman, A.M., Weiss, D.J., Welsh, J.A., Wendt, S., Wheelock, A.M., Wiener, Z., Witte, L., Wolfram, J., Xagorari, A., Xander, P., Xu, J., Yan, X., Yanez-Mo, M., Yin, H., Yuana, Y., Zappulli, V., Zarubova, J., Zekas, V., Zhang, J.Y., Zhao, Z., Zheng, L., Zheutlin, A.R., Zickler, A.M., Zimmermann, P., Zivkovic, A.M., Zocco, D. and Zuba-Surma, E.K., *Minimal information for studies of extracellular vesicles 2018 (MISEV2018): a position*

statement of the International Society for Extracellular Vesicles and update of the MISEV2014 guidelines. J Extracell Vesicles, 2018. **7**(1): p. 1535750.
400. Taylor, M., Santopietro, S., Baxter, A., East, N., Breheny, D., Thorne, D., and Gaca, M., *In vitro biological assessment of the stability of cigarette smoke aqueous aerosol extracts.* BMC Res Notes, 2020. **13**(1): p. 492.
401. Taylor, M., Carr, T., Oke, O., Jaunky, T., Breheny, D., Lowe, F., and Gaca, M., *E-cigarette aerosols induce lower oxidative stress in vitro when compared to tobacco smoke.* Toxicol Mech Methods, 2016. **26**(6): p. 465-476.
402. Welsh, J.A., Van Der Pol, E., Arkesteijn, G.J.A., Bremer, M., Brisson, A., Coumans, F., Dignat-George, F., Duggan, E., Ghiran, I., Giebel, B., Gorgens, A., Hendrix, A., Lacroix, R., Lannigan, J., Libregts, S., Lozano-Andres, E., Morales-Kastresana, A., Robert, S., De Rond, L., Tertel, T., Tigges, J., De Wever, O., Yan, X., Nieuwland, R., Wauben, M.H.M., Nolan, J.P., and Jones, J.C., *MIFlowCyt-EV: a framework for standardized reporting of extracellular vesicle flow cytometry experiments.* J Extracell Vesicles, 2020. **9**(1): p. 1713526.
403. Gray, W.D., Mitchell, A.J., and Searles, C.D., *An accurate, precise method for general labeling of extracellular vesicles.* MethodsX, 2015. **2**: p. 360-7.
404. Luo, T., Chen, S.Y., Qiu, Z.X., Miao, Y.R., Ding, Y., Pan, X.Y., Li, Y., Lei, Q., and Guo, A.Y., *Transcriptomic Features in a Single Extracellular Vesicle via Single-Cell RNA Sequencing.* Small Methods, 2022: p. e2200881.
405. Cismasiu, V.B. and Popescu, L.M., *Telocytes transfer extracellular vesicles loaded with microRNAs to stem cells.* J Cell Mol Med, 2015. **19**(2): p. 351-8.
406. Kwon, Y. and Park, J., *Methods to analyze extracellular vesicles at single particle level.* Micro and Nano Systems Letters, 2022. **10**(1): p. 14.
407. Nizamudeen, Z.A., Xerri, R., Parmenter, C., Suain, K., Markus, R., Chakrabarti, L., and Sottile, V., *Low-Power Sonication Can Alter Extracellular Vesicle Size and Properties.* Cells, 2021. **10**(9).
408. Belkina, A.C., Ciccolella, C.O., Anno, R., Halpert, R., Spidlen, J., and Snyder-Cappione, J.E., *Automated optimized parameters for T-distributed stochastic neighbor embedding improve visualization and analysis of large datasets.* Nat Commun, 2019. **10**(1): p. 5415.
409. Van Gassen, S., Callebaut, B., Van Helden, M.J., Lambrecht, B.N., Demeester, P., Dhaene, T., and Saeys, Y., *FlowSOM: Using self-organizing maps for visualization and interpretation of cytometry data.* Cytometry A, 2015. **87**(7): p. 636-45.
410. Arraud, N., Linares, R., Tan, S., Gounou, C., Pasquet, J.M., Mornet, S., and Brisson, A.R., *Extracellular vesicles from blood plasma: determination of their morphology, size, phenotype and concentration.* J Thromb Haemost, 2014. **12**(5): p. 614-27.
411. Lehrich, B.M., Liang, Y., Khosravi, P., Federoff, H.J., and Fiandaca, M.S., *Fetal Bovine Serum-Derived Extracellular Vesicles Persist within Vesicle-Depleted Culture Media.* Int J Mol Sci, 2018. **19**(11).
412. Visan, K.S., Lobb, R.J., Ham, S., Lima, L.G., Palma, C., Edna, C.P.Z., Wu, L.Y., Gowda, H., Datta, K.K., Hartel, G., Salomon, C., and Moller, A., *Comparative*

analysis of tangential flow filtration and ultracentrifugation, both combined with subsequent size exclusion chromatography, for the isolation of small extracellular vesicles. J Extracell Vesicles, 2022. **11**(9): p. e12266.
413. Beck, S., Hochreiter, B., and Schmid, J.A., *Extracellular Vesicles Linking Inflammation, Cancer and Thrombotic Risks.* Frontiers in Cell and Developmental Biology, 2022. **10**.
414. Benedikter, B.J., Bouwman, F.G., Vajen, T., Heinzmann, A.C.A., Grauls, G., Mariman, E.C., Wouters, E.F.M., Savelkoul, P.H., Lopez-Iglesias, C., Koenen, R.R., Rohde, G.G.U., and Stassen, F.R.M., *Ultrafiltration combined with size exclusion chromatography efficiently isolates extracellular vesicles from cell culture media for compositional and functional studies.* Scientific Reports, 2017. **7**(1): p. 15297.
415. Bagci, C., Sever-Bahcekapili, M., Belder, N., Bennett, A.P.S., Erdener, S.E., and Dalkara, T., *Overview of extracellular vesicle characterization techniques and introduction to combined reflectance and fluorescence confocal microscopy to distinguish extracellular vesicle subpopulations.* Neurophotonics, 2022. **9**(2): p. 021903.
416. Emelyanov, A., Shtam, T., Kamyshinsky, R., Garaeva, L., Verlov, N., Miliukhina, I., Kudrevatykh, A., Gavrilov, G., Zabrodskaya, Y., Pchelina, S., and Konevega, A., *Cryo-electron microscopy of extracellular vesicles from cerebrospinal fluid.* PLoS One, 2020. **15**(1): p. e0227949.
417. Kim, C.J., Kuczler, M.D., Dong, L., Kim, J., Amend, S.R., Cho, Y.K., and Pienta, K.J., *Extracellular Vesicle Uptake Assay via Confocal Microscope Imaging Analysis.* J Vis Exp, 2022(180).
418. Kruse, T., Schneider, S., Reger, L.N., Kampmann, M., and Reif, O.W., *A novel approach for enumeration of extracellular vesicles from crude and purified cell culture samples.* Eng Life Sci, 2022. **22**(3-4): p. 334-343.
419. Nizamudeen, Z., Markus, R., Lodge, R., Parmenter, C., Platt, M., Chakrabarti, L., and Sottile, V., *Rapid and accurate analysis of stem cell-derived extracellular vesicles with super resolution microscopy and live imaging.* Biochim Biophys Acta Mol Cell Res, 2018. **1865**(12): p. 1891-1900.
420. Comfort, N., Cai, K., Bloomquist, T.R., Strait, M.D., Ferrante, A.W., Jr., and Baccarelli, A.A., *Nanoparticle Tracking Analysis for the Quantification and Size Determination of Extracellular Vesicles.* J Vis Exp, 2021(169).
421. Momen-Heravi, F., Balaj, L., Alian, S., Tigges, J., Toxavidis, V., Ericsson, M., Distel, R.J., Ivanov, A.R., Skog, J., and Kuo, W.P., *Alternative methods for characterization of extracellular vesicles.* Front Physiol, 2012. **3**: p. 354.
422. Filipe, V., Hawe, A., and Jiskoot, W., *Critical evaluation of Nanoparticle Tracking Analysis (NTA) by NanoSight for the measurement of nanoparticles and protein aggregates.* Pharm Res, 2010. **27**(5): p. 796-810.
423. Usfoor, Z., Kaufmann, K., Rakib, A.S.H., Hergenroder, R., and Shpacovitch, V., *Features of Sizing and Enumeration of Silica and Polystyrene Nanoparticles by Nanoparticle Tracking Analysis (NTA).* Sensors (Basel), 2020. **20**(22).

424. Tertel, T., Görgens, A., and Giebel, B., *Chapter Four - Analysis of individual extracellular vesicles by imaging flow cytometry*, in *Methods in Enzymology*, S. Spada and L. Galluzzi, Editors. 2020, Academic Press. p. 55-78.
425. Woud, W.W., van der Pol, E., Mul, E., Hoogduijn, M.J., Baan, C.C., Boer, K., and Merino, A., *An imaging flow cytometry-based methodology for the analysis of single extracellular vesicles in unprocessed human plasma.* Commun Biol, 2022. **5**(1): p. 633.
426. Gorgens, A., Bremer, M., Ferrer-Tur, R., Murke, F., Tertel, T., Horn, P.A., Thalmann, S., Welsh, J.A., Probst, C., Guerin, C., Boulanger, C.M., Jones, J.C., Hanenberg, H., Erdbrugger, U., Lannigan, J., Ricklefs, F.L., El-Andaloussi, S., and Giebel, B., *Optimisation of imaging flow cytometry for the analysis of single extracellular vesicles by using fluorescence-tagged vesicles as biological reference material.* J Extracell Vesicles, 2019. **8**(1): p. 1587567.
427. Ricklefs, F.L., Maire, C.L., Reimer, R., Duhrsen, L., Kolbe, K., Holz, M., Schneider, E., Rissiek, A., Babayan, A., Hille, C., Pantel, K., Krasemann, S., Glatzel, M., Heiland, D.H., Flitsch, J., Martens, T., Schmidt, N.O., Peine, S., Breakefield, X.O., Lawler, S., Chiocca, E.A., Fehse, B., Giebel, B., Gorgens, A., Westphal, M., and Lamszus, K., *Imaging flow cytometry facilitates multiparametric characterization of extracellular vesicles in malignant brain tumours.* J Extracell Vesicles, 2019. **8**(1): p. 1588555.
428. Armitage, J.D., Tan, D.B.A., Cha, L., Clark, M., Gray, E.S., Fuller, K.A., and Moodley, Y.P., *A standardised protocol for the evaluation of small extracellular vesicles in plasma by imaging flow cytometry.* J Immunol Methods, 2019. **468**: p. 61-66.
429. Blanchard, N., Lankar, D., Faure, F., Regnault, A., Dumont, C., Raposo, G., and Hivroz, C., *TCR activation of human T cells induces the production of exosomes bearing the TCR/CD3/zeta complex.* J Immunol, 2002. **168**(7): p. 3235-41.
430. van der Vlist, E.J., Arkesteijn, G.J., van de Lest, C.H., Stoorvogel, W., Nolte-'t Hoen, E.N., and Wauben, M.H., *CD4(+) T cell activation promotes the differential release of distinct populations of nanosized vesicles.* J Extracell Vesicles, 2012. **1**.
431. Zanders, E.D., Lamb, J.R., Feldmann, M., Green, N., and Beverley, P.C., *Tolerance of T-cell clones is associated with membrane antigen changes.* Nature, 1983. **303**(5918): p. 625-7.
432. Reinherz, E.L., Acuto, O., Fabbi, M., Bensussan, A., Milanese, C., Royer, H.D., Meuer, S.C., and Schlossman, S.F., *Clonotypic surface structure on human T lymphocytes: functional and biochemical analysis of the antigen receptor complex.* Immunol Rev, 1984. **81**: p. 95-129.
433. Alcover, A. and Alarcon, B., *Internalization and intracellular fate of TCR-CD3 complexes.* Crit Rev Immunol, 2000. **20**(4): p. 325-46.
434. Osteikoetxea, X., Sodar, B., Nemeth, A., Szabo-Taylor, K., Paloczi, K., Vukman, K.V., Tamasi, V., Balogh, A., Kittel, A., Pallinger, E., and Buzas, E.I., *Differential detergent sensitivity of extracellular vesicle subpopulations.* Org Biomol Chem, 2015. **13**(38): p. 9775-82.

435. Matthiesen, R., Gameiro, P., Henriques, A., Bodo, C., Moraes, M.C.S., Costa-Silva, B., Cabecadas, J., Gomes da Silva, M., Beck, H.C., and Carvalho, A.S., *Extracellular Vesicles in Diffuse Large B Cell Lymphoma: Characterization and Diagnostic Potential.* Int J Mol Sci, 2022. **23**(21).
436. Pienimaeki-Roemer, A., Kuhlmann, K., Bottcher, A., Konovalova, T., Black, A., Orso, E., Liebisch, G., Ahrens, M., Eisenacher, M., Meyer, H.E., and Schmitz, G., *Lipidomic and proteomic characterization of platelet extracellular vesicle subfractions from senescent platelets.* Transfusion, 2015. **55**(3): p. 507-21.
437. Lubke, T., Lobel, P., and Sleat, D.E., *Proteomics of the lysosome.* Biochim Biophys Acta, 2009. **1793**(4): p. 625-35.
438. Saleem, R.A., Smith, J.J., and Aitchison, J.D., *Proteomics of the peroxisome.* Biochim Biophys Acta, 2006. **1763**(12): p. 1541-51.
439. Mathivanan, S. and Simpson, R.J., *ExoCarta: A compendium of exosomal proteins and RNA.* Proteomics, 2009. **9**(21): p. 4997-5000.
440. Schluter, A., Fourcade, S., Domenech-Estevez, E., Gabaldon, T., Huerta-Cepas, J., Berthommier, G., Ripp, R., Wanders, R.J., Poch, O., and Pujol, A., *PeroxisomeDB: a database for the peroxisomal proteome, functional genomics and disease.* Nucleic Acids Res, 2007. **35**(Database issue): p. D815-22.
441. Brozzi, A., Urbanelli, L., Germain, P.L., Magini, A., and Emiliani, C., *hLGDB: a database of human lysosomal genes and their regulation.* Database (Oxford), 2013. **2013**: p. bat024.
442. Grenier-Pleau, I., Tyryshkin, K., Le, T.D., Rudan, J., Bonneil, E., Thibault, P., Zeng, K., Lasser, C., Mallinson, D., Lamprou, D., Hui, J., Postovit, L.M., Chan, E.Y.W., and Abraham, S.A., *Blood extracellular vesicles from healthy individuals regulate hematopoietic stem cells as humans age.* Aging Cell, 2020. **19**(11): p. e13245.
443. Rota, F., Ferrari, L., Hoxha, M., Favero, C., Antonioli, R., Pergoli, L., Greco, M.F., Mariani, J., Lazzari, L., and Bollati, V., *Blood-derived extracellular vesicles isolated from healthy donors exposed to air pollution modulate in vitro endothelial cells behavior.* Sci Rep, 2020. **10**(1): p. 20138.
444. Kleiveland, C.R., *Peripheral Blood Mononuclear Cells. In: Verhoeckx K, Cotter P, López-Expósito I, et al., editors. The Impact of Food Bioactives on Health: in vitro and ex vivo models*. Peripheral Blood Mononuclear Cells. 2015, Internet: Cham (CH): Springer.
445. Bisset, L.R., Lung, T.L., Kaelin, M., Ludwig, E., and Dubs, R.W., *Reference values for peripheral blood lymphocyte phenotypes applicable to the healthy adult population in Switzerland.* Eur J Haematol, 2004. **72**(3): p. 203-12.
446. Lawlor, N., Nehar-Belaid, D., Grassmann, J.D.S., Stoeckius, M., Smibert, P., Stitzel, M.L., Pascual, V., Banchereau, J., Williams, A., and Ucar, D., *Single Cell Analysis of Blood Mononuclear Cells Stimulated Through Either LPS or Anti-CD3 and Anti-CD28.* Front Immunol, 2021. **12**: p. 636720.
447. Bretscher, P.A., *A two-step, two-signal model for the primary activation of precursor helper T cells.* Proc Natl Acad Sci U S A, 1999. **96**(1): p. 185-90.

448. Trickett, A. and Kwan, Y.L., *T cell stimulation and expansion using anti-CD3/CD28 beads.* J Immunol Methods, 2003. **275**(1-2): p. 251-5.
449. Smith-Garvin, J.E., Koretzky, G.A., and Jordan, M.S., *T cell activation.* Annu Rev Immunol, 2009. **27**: p. 591-619.
450. Lamers, C.H., van de Griend, R.J., Braakman, E., Ronteltap, C.P., Benard, J., Stoter, G., Gratama, J.W., and Bolhuis, R.L., *Optimization of culture conditions for activation and large-scale expansion of human T lymphocytes for bispecific antibody-directed cellular immunotherapy.* Int J Cancer, 1992. **51**(6): p. 973-9.
451. Li, J., Lee, Y., Johansson, H.J., Mager, I., Vader, P., Nordin, J.Z., Wiklander, O.P., Lehtio, J., Wood, M.J., and Andaloussi, S.E., *Serum-free culture alters the quantity and protein composition of neuroblastoma-derived extracellular vesicles.* J Extracell Vesicles, 2015. **4**: p. 26883.
452. Eitan, E., Zhang, S., Witwer, K.W., and Mattson, M.P., *Extracellular vesicle-depleted fetal bovine and human sera have reduced capacity to support cell growth.* J Extracell Vesicles, 2015. **4**: p. 26373.
453. Aswad, H., Jalabert, A., and Rome, S., *Depleting extracellular vesicles from fetal bovine serum alters proliferation and differentiation of skeletal muscle cells in vitro.* BMC Biotechnol, 2016. **16**: p. 32.
454. Beninson, L.A. and Fleshner, M., *Exosomes in fetal bovine serum dampen primary macrophage IL-1β response to lipopolysaccharide (LPS) challenge.* Immunology Letters, 2015. **163**(2): p. 187-192.
455. Liao, Z., Muth, D.C., Eitan, E., Travers, M., Learman, L.N., Lehrmann, E., and Witwer, K.W., *Serum extracellular vesicle depletion processes affect release and infectivity of HIV-1 in culture.* Sci Rep, 2017. **7**(1): p. 2558.
456. Shelke, G.V., Lasser, C., Gho, Y.S., and Lotvall, J., *Importance of exosome depletion protocols to eliminate functional and RNA-containing extracellular vesicles from fetal bovine serum.* J Extracell Vesicles, 2014. **3**.
457. Guo, J., Wu, C., Lin, X., Zhou, J., Zhang, J., Zheng, W., Wang, T., and Cui, Y., *Establishment of a simplified dichotomic size-exclusion chromatography for isolating extracellular vesicles toward clinical applications.* J Extracell Vesicles, 2021. **10**(11): p. e12145.
458. Gardiner, C., Ferreira, Y.J., Dragovic, R.A., Redman, C.W., and Sargent, I.L., *Extracellular vesicle sizing and enumeration by nanoparticle tracking analysis.* J Extracell Vesicles, 2013. **2**.
459. Vogel, R., Savage, J., Muzard, J., Camera, G.D., Vella, G., Law, A., Marchioni, M., Mehn, D., Geiss, O., Peacock, B., Aubert, D., Calzolai, L., Caputo, F., and Prina-Mello, A., *Measuring particle concentration of multimodal synthetic reference materials and extracellular vesicles with orthogonal techniques: Who is up to the challenge?* J Extracell Vesicles, 2021. **10**(3): p. e12052.
460. Tian, Y., Ma, L., Gong, M., Su, G., Zhu, S., Zhang, W., Wang, S., Li, Z., Chen, C., Li, L., Wu, L., and Yan, X., *Protein Profiling and Sizing of Extracellular Vesicles from Colorectal Cancer Patients via Flow Cytometry.* ACS Nano, 2018. **12**(1): p. 671-680.

461. van der Pol, E., Coumans, F.A., Grootemaat, A.E., Gardiner, C., Sargent, I.L., Harrison, P., Sturk, A., van Leeuwen, T.G., and Nieuwland, R., *Particle size distribution of exosomes and microvesicles determined by transmission electron microscopy, flow cytometry, nanoparticle tracking analysis, and resistive pulse sensing.* J Thromb Haemost, 2014. **12**(7): p. 1182-92.
462. Welsh, J.A., van der Pol, E., Bettin, B.A., Carter, D.R.F., Hendrix, A., Lenassi, M., Langlois, M.A., Llorente, A., van de Nes, A.S., Nieuwland, R., Tang, V., Wang, L., Witwer, K.W., and Jones, J.C., *Towards defining reference materials for measuring extracellular vesicle refractive index, epitope abundance, size and concentration.* J Extracell Vesicles, 2020. **9**(1): p. 1816641.
463. Lannigan, J. and Erdbruegger, U., *Imaging flow cytometry for the characterization of extracellular vesicles.* Methods, 2017. **112**: p. 55-67.
464. Botha, J., Handberg, A., and Simonsen, J.B., *Lipid-based strategies used to identify extracellular vesicles in flow cytometry can be confounded by lipoproteins: Evaluations of annexin V, lactadherin, and detergent lysis.* J Extracell Vesicles, 2022. **11**(4): p. e12200.
465. Simonsen, J.B., *Pitfalls associated with lipophilic fluorophore staining of extracellular vesicles for uptake studies.* J Extracell Vesicles, 2019. **8**(1): p. 1582237.
466. de Rond, L., van der Pol, E., Hau, C.M., Varga, Z., Sturk, A., van Leeuwen, T.G., Nieuwland, R., and Coumans, F.A.W., *Comparison of Generic Fluorescent Markers for Detection of Extracellular Vesicles by Flow Cytometry.* Clin Chem, 2018. **64**(4): p. 680-689.
467. Ter-Ovanesyan, D., Norman, M., Lazarovits, R., Trieu, W., Lee, J.H., Church, G.M., and Walt, D.R., *Framework for rapid comparison of extracellular vesicle isolation methods.* Elife, 2021. **10**.
468. Chen, X. and Thibeault, S., *Effect of DMSO concentration, cell density and needle gauge on the viability of cryopreserved cells in three dimensional hyaluronan hydrogel.* Annu Int Conf IEEE Eng Med Biol Soc, 2013. **2013**: p. 6228-31.
469. Verheijen, M., Lienhard, M., Schrooders, Y., Clayton, O., Nudischer, R., Boerno, S., Timmermann, B., Selevsek, N., Schlapbach, R., Gmuender, H., Gotta, S., Geraedts, J., Herwig, R., Kleinjans, J., and Caiment, F., *DMSO induces drastic changes in human cellular processes and epigenetic landscape in vitro.* Sci Rep, 2019. **9**(1): p. 4641.
470. Mathieu, M., Nevo, N., Jouve, M., Valenzuela, J.I., Maurin, M., Verweij, F.J., Palmulli, R., Lankar, D., Dingli, F., Loew, D., Rubinstein, E., Boncompain, G., Perez, F., and Thery, C., *Specificities of exosome versus small ectosome secretion revealed by live intracellular tracking of CD63 and CD9.* Nat Commun, 2021. **12**(1): p. 4389.
471. Barranco, I., Padilla, L., Parrilla, I., Alvarez-Barrientos, A., Perez-Patino, C., Pena, F.J., Martinez, E.A., Rodriguez-Martinez, H., and Roca, J., *Extracellular vesicles isolated from porcine seminal plasma exhibit different tetraspanin expression profiles.* Sci Rep, 2019. **9**(1): p. 11584.

472. Ibrahim, S., Hedia, M., Taqi, M.O., Derbala, M.K., Mahmoud, K.G.M., Ahmed, Y., Sosa, A.S., Saber, Y.H.A., Hasanain, M.H., Nawito, M.F., and Seidel, G.E., *Extracellular vesicles in low volume uterine lavage and serum: novel and promising biomarker for endometritis in Arabian mares.* BMC Vet Res, 2022. **18**(1): p. 42.
473. Han, C., Kang, H., Yi, J., Kang, M., Lee, H., Kwon, Y., Jung, J., Lee, J., and Park, J., *Single-vesicle imaging and co-localization analysis for tetraspanin profiling of individual extracellular vesicles.* J Extracell Vesicles, 2021. **10**(3): p. e12047.
474. Karimi, N., Dalirfardouei, R., Dias, T., Lotvall, J., and Lasser, C., *Tetraspanins distinguish separate extracellular vesicle subpopulations in human serum and plasma - Contributions of platelet extracellular vesicles in plasma samples.* J Extracell Vesicles, 2022. **11**(5): p. e12213.
475. Lorico, A., Lorico-Rappa, M., Karbanova, J., Corbeil, D., and Pizzorno, G., *CD9, a tetraspanin target for cancer therapy?* Exp Biol Med (Maywood), 2021. **246**(9): p. 1121-1138.
476. Kowal, J., Arras, G., Colombo, M., Jouve, M., Morath, J.P., Primdal-Bengtson, B., Dingli, F., Loew, D., Tkach, M., and Thery, C., *Proteomic comparison defines novel markers to characterize heterogeneous populations of extracellular vesicle subtypes.* Proc Natl Acad Sci U S A, 2016. **113**(8): p. E968-77.
477. Koliha, N., Wiencek, Y., Heider, U., Jungst, C., Kladt, N., Krauthauser, S., Johnston, I.C., Bosio, A., Schauss, A., and Wild, S., *A novel multiplex bead-based platform highlights the diversity of extracellular vesicles.* J Extracell Vesicles, 2016. **5**: p. 29975.
478. d'Alessandro, M., Soccio, P., Bergantini, L., Cameli, P., Scioscia, G., Foschino Barbaro, M.P., Lacedonia, D., and Bargagli, E., *Extracellular Vesicle Surface Signatures in IPF Patients: A Multiplex Bead-Based Flow Cytometry Approach.* Cells, 2021. **10**(5).
479. Puhm, F., Boilard, E., and Machlus, K.R., *Platelet Extracellular Vesicles: Beyond the Blood.* Arterioscler Thromb Vasc Biol, 2021. **41**(1): p. 87-96.
480. Tao, S.C., Guo, S.C., and Zhang, C.Q., *Platelet-derived Extracellular Vesicles: An Emerging Therapeutic Approach.* Int J Biol Sci, 2017. **13**(7): p. 828-834.
481. Eckhardt, C.M., Baccarelli, A.A., and Wu, H., *Environmental Exposures and Extracellular Vesicles: Indicators of Systemic Effects and Human Disease.* Current Environmental Health Reports, 2022. **9**(3): p. 465-476.
482. Zhang, Y.Y., Bu, F.L., Dong, F., Wang, J.H., Zhu, S.J., Zhang, X.W., Robinson, N., and Liu, J.P., *The effect of e-cigarettes on smoking cessation and cigarette smoking initiation: An evidence-based rapid review and meta-analysis.* Tob Induc Dis, 2021. **19**: p. 04.
483. Kennedy, R.D., Awopegba, A., De Leon, E., and Cohen, J.E., *Global approaches to regulating electronic cigarettes.* Tob Control, 2017. **26**(4): p. 440-445.
484. Shao, H., Im, H., Castro, C.M., Breakefield, X., Weissleder, R., and Lee, H., *New Technologies for Analysis of Extracellular Vesicles.* Chemical Reviews, 2018. **118**(4): p. 1917-1950.

485. Headland, S.E., Jones, H.R., D'Sa, A.S.V., Perretti, M., and Norling, L.V., *Cutting-Edge Analysis of Extracellular Microparticles using ImageStreamX Imaging Flow Cytometry.* Scientific Reports, 2014. **4**(1): p. 5237.
486. Aoshiba, K., Tamaoki, J., and Nagai, A., *Acute cigarette smoke exposure induces apoptosis of alveolar macrophages.* Am J Physiol Lung Cell Mol Physiol, 2001. **281**(6): p. L1392-401.
487. Mian, M.F., Lauzon, N.M., Stampfli, M.R., Mossman, K.L., and Ashkar, A.A., *Impairment of human NK cell cytotoxic activity and cytokine release by cigarette smoke.* J Leukoc Biol, 2008. **83**(3): p. 774-84.
488. Su, Y., Cao, W., Han, Z., and Block, E.R., *Cigarette smoke extract inhibits angiogenesis of pulmonary artery endothelial cells: the role of calpain.* Am J Physiol Lung Cell Mol Physiol, 2004. **287**(4): p. L794-800.
489. Wongtrakool, C., Grooms, K., Bijli, K.M., Crothers, K., Fitzpatrick, A.M., and Hart, C.M., *Nicotine stimulates nerve growth factor in lung fibroblasts through an NFkappaB-dependent mechanism.* PLoS One, 2014. **9**(10): p. e109602.
490. Bernhard, D., Huck, C.W., Jakschitz, T., Pfister, G., Henderson, B., Bonn, G.K., and Wick, G., *Development and evaluation of an in vitro model for the analysis of cigarette smoke effects on cultured cells and tissues.* J Pharmacol Toxicol Methods, 2004. **50**(1): p. 45-51.
491. Giebe, S., Hofmann, A., Brux, M., Lowe, F., Breheny, D., Morawietz, H., and Brunssen, C., *Comparative study of the effects of cigarette smoke versus next generation tobacco and nicotine product extracts on endothelial function.* Redox Biol, 2021. **47**: p. 102150.
492. Kim, H.J., Liu, X., Wang, H., Kohyama, T., Kobayashi, T., Wen, F.Q., Romberger, D.J., Abe, S., MacNee, W., Rahman, I., and Rennard, S.I., *Glutathione prevents inhibition of fibroblast-mediated collagen gel contraction by cigarette smoke.* Am J Physiol Lung Cell Mol Physiol, 2002. **283**(2): p. L409-17.
493. Ji, M., Zhang, Y., Li, N., Wang, C., Xia, R., Zhang, Z., and Wang, S.L., *Nicotine Component of Cigarette Smoke Extract (CSE) Decreases the Cytotoxicity of CSE in BEAS-2B Cells Stably Expressing Human Cytochrome P450 2A13.* Int J Environ Res Public Health, 2017. **14**(10).
494. *Cigarette brand preferences. 2003, Web. U.S. Department of Health and Human Services. National Institute of Drug Abuse,*. 2003, Substance Abuse and Mental Health Services Administration.
495. Romagna, G., Allifranchini, E., Bocchietto, E., Todeschi, S., Esposito, M., and Farsalinos, K.E., *Cytotoxicity evaluation of electronic cigarette vapor extract on cultured mammalian fibroblasts (ClearStream-LIFE): comparison with tobacco cigarette smoke extract.* Inhal Toxicol, 2013. **25**(6): p. 354-61.
496. Sinha, I., Goel, R., Bitzer, Z.T., Trushin, N., Liao, J., and Sinha, R., *Evaluating electronic cigarette cytotoxicity and inflammatory responses in vitro.* Tob Induc Dis, 2022. **20**: p. 45.
497. Czekala, L., Simms, L., Stevenson, M., Tschierske, N., Maione, A.G., and Walele, T., *Toxicological comparison of cigarette smoke and e-cigarette aerosol using a*

3D in vitro human respiratory model. Regul Toxicol Pharmacol, 2019. **103**: p. 314-324.
498. Miyashita, L., Suri, R., Dearing, E., Mudway, I., Dove, R.E., Neill, D.R., Van Zyl-Smit, R., Kadioglu, A., and Grigg, J., *E-cigarette vapour enhances pneumococcal adherence to airway epithelial cells.* Eur Respir J, 2018. **51**(2).
499. Jarvis, M.J., Boreham, R., Primatesta, P., Feyerabend, C., and Bryant, A., *Nicotine yield from machine-smoked cigarettes and nicotine intakes in smokers: evidence from a representative population survey.* J Natl Cancer Inst, 2001. **93**(2): p. 134-8.
500. Cheng, S.F., Qin, X.S., Han, Z.L., Sun, X.F., Feng, Y.N., Yang, F., Ge, W., Li, L., Zhao, Y., De Felici, M., Zou, S.H., Zhou, Y., and Shen, W., *Nicotine exposure impairs germ cell development in human fetal ovaries cultured in vitro.* Aging (Albany NY), 2018. **10**(7): p. 1556-1574.
501. Daffner, S.D., Waugh, S., Norman, T.L., Mukherjee, N., and France, J.C., *Nicotine Increases Osteoblast Activity of Induced Bone Marrow Stromal Cells in a Dose-Dependent Manner: An in vitro Cell Culture Experiment.* Global Spine J, 2012. **2**(3): p. 153-8.
502. Tinti, F. and Soory, M., *Mechanisms for redox actions of nicotine and glutathione in cell culture, relevant to periodontitis.* Sci Rep, 2012. **2**: p. 566.
503. Wieczfinska, J., Kowalczyk, T., Sitarek, P., Skala, E., and Pawliczak, R., *Analysis of Short-Term Smoking Effects in PBMC of Healthy Subjects-Preliminary Study.* Int J Environ Res Public Health, 2018. **15**(5).
504. Banfalvi, G., *Methods to detect apoptotic cell death.* Apoptosis, 2017. **22**(2): p. 306-323.
505. Strober, W., *Trypan Blue Exclusion Test of Cell Viability.* Curr Protoc Immunol, 2015. **111**: p. A3 B 1-A3 B 3.
506. Vermes, I., Haanen, C., Steffens-Nakken, H., and Reutelingsperger, C., *A novel assay for apoptosis. Flow cytometric detection of phosphatidylserine expression on early apoptotic cells using fluorescein labelled Annexin V.* J Immunol Methods, 1995. **184**(1): p. 39-51.
507. Chen, L., Ge, Q., Tjin, G., Alkhouri, H., Deng, L., Brandsma, C.A., Adcock, I., Timens, W., Postma, D., Burgess, J.K., Black, J.L., and Oliver, B.G., *Effects of cigarette smoke extract on human airway smooth muscle cells in COPD.* Eur Respir J, 2014. **44**(3): p. 634-46.
508. Pugholm, L.H., Baek, R., Sondergaard, E.K., Revenfeld, A.L., Jorgensen, M.M., and Varming, K., *Phenotyping of Leukocytes and Leukocyte-Derived Extracellular Vesicles.* J Immunol Res, 2016. **2016**: p. 6391264.
509. Jorgensen, M.M., Baek, R., and Varming, K., *Potentials and capabilities of the Extracellular Vesicle (EV) Array.* J Extracell Vesicles, 2015. **4**: p. 26048.
510. Revenfeld, A.L.S., Sondergaard, E.K.L., Stensballe, A., Baek, R., Jorgensen, M.M., and Varming, K., *Characterization of a Cell-Culturing System for the Study of Contact-Independent Extracellular Vesicle Communication.* J Circ Biomark, 2016. **5**: p. 3.

511. He, M., Crow, J., Roth, M., Zeng, Y., and Godwin, A.K., *Integrated immunoisolation and protein analysis of circulating exosomes using microfluidic technology.* Lab Chip, 2014. **14**(19): p. 3773-80.
512. Cho, S., Yi, J., Kwon, Y., Kang, H., Han, C., and Park, J., *Multifluorescence Single Extracellular Vesicle Analysis by Time-Sequential Illumination and Tracking.* ACS Nano, 2021. **15**(7): p. 11753-11761.
513. Veerman, R.E., Gucluler Akpinar, G., Eldh, M., and Gabrielsson, S., *Immune Cell-Derived Extracellular Vesicles - Functions and Therapeutic Applications.* Trends Mol Med, 2019. **25**(5): p. 382-394.
514. Yang, P., Peng, Y., Feng, Y., Xu, Z., Feng, P., Cao, J., Chen, Y., Chen, X., Cao, X., Yang, Y., and Jie, J., *Immune Cell-Derived Extracellular Vesicles - New Strategies in Cancer Immunotherapy.* Front Immunol, 2021. **12**: p. 771551.
515. Segura, E., Amigorena, S., and Thery, C., *Mature dendritic cells secrete exosomes with strong ability to induce antigen-specific effector immune responses.* Blood Cells Mol Dis, 2005. **35**(2): p. 89-93.
516. Naslund, T.I., Gehrmann, U., Qazi, K.R., Karlsson, M.C., and Gabrielsson, S., *Dendritic cell-derived exosomes need to activate both T and B cells to induce antitumor immunity.* J Immunol, 2013. **190**(6): p. 2712-9.
517. Elgueta, R., Benson, M.J., de Vries, V.C., Wasiuk, A., Guo, Y., and Noelle, R.J., *Molecular mechanism and function of CD40/CD40L engagement in the immune system.* Immunol Rev, 2009. **229**(1): p. 152-72.
518. Chatzigeorgiou, A., Lyberi, M., Chatzilymperis, G., Nezos, A., and Kamper, E., *CD40/CD40L signaling and its implication in health and disease.* Biofactors, 2009. **35**(6): p. 474-83.
519. Laman, J.D., Claassen, E., and Noelle, R.J., *Functions of CD40 and Its Ligand, gp39 (CD40L).* Crit Rev Immunol, 2017. **37**(2-6): p. 371-420.
520. Roman-Fernandez, I.V., Garcia-Chagollan, M., Cerpa-Cruz, S., Jave-Suarez, L.F., Palafox-Sanchez, C.A., Garcia-Arellano, S., Sanchez-Zuno, G.A., and Munoz-Valle, J.F., *Assessment of CD40 and CD40L expression in rheumatoid arthritis patients, association with clinical features and DAS28.* Clin Exp Med, 2019. **19**(4): p. 427-437.
521. Jabara, H.H., Fu, S.M., Geha, R.S., and Vercelli, D., *CD40 and IgE: synergism between anti-CD40 monoclonal antibody and interleukin 4 in the induction of IgE synthesis by highly purified human B cells.* J Exp Med, 1990. **172**(6): p. 1861-4.
522. Liang, Y., Shen, Y., Kuang, L., Zhou, G., Zhang, L., Zhong, X., Zhang, J., and Liu, J., *Cigarette smoke exposure promotes differentiation of CD4(+) T cells toward Th17 cells by CD40-CD40L costimulatory pathway in mice.* Int J Chron Obstruct Pulmon Dis, 2018. **13**: p. 959-968.
523. Aatonen, M.T., Ohman, T., Nyman, T.A., Laitinen, S., Gronholm, M., and Siljander, P.R., *Isolation and characterization of platelet-derived extracellular vesicles.* J Extracell Vesicles, 2014. **3**.

524. O'Shea, D., Cawood, T.J., O'Farrelly, C., and Lynch, L., *Natural killer cells in obesity: impaired function and increased susceptibility to the effects of cigarette smoke.* PLoS One, 2010. **5**(1): p. e8660.
525. Roos-Engstrand, E., Pourazar, J., Behndig, A.F., Blomberg, A., and Bucht, A., *Cytotoxic T cells expressing the co-stimulatory receptor NKG2 D are increased in cigarette smoking and COPD.* Respir Res, 2010. **11**: p. 128.
526. Piali, L., Hammel, P., Uherek, C., Bachmann, F., Gisler, R.H., Dunon, D., and Imhof, B.A., *CD31/PECAM-1 is a ligand for alpha v beta 3 integrin involved in adhesion of leukocytes to endothelium.* J Cell Biol, 1995. **130**(2): p. 451-60.
527. Liu, L. and Shi, G.P., *CD31: beyond a marker for endothelial cells.* Cardiovasc Res, 2012. **94**(1): p. 3-5.
528. Marelli-Berg, F.M., Clement, M., Mauro, C., and Caligiuri, G., *An immunologist's guide to CD31 function in T-cells.* J Cell Sci, 2013. **126**(Pt 11): p. 2343-52.
529. Hodge, S., Matthews, G., Mukaro, V., Ahern, J., Shivam, A., Hodge, G., Holmes, M., Jersmann, H., and Reynolds, P.N., *Cigarette smoke-induced changes to alveolar macrophage phenotype and function are improved by treatment with procysteine.* Am J Respir Cell Mol Biol, 2011. **44**(5): p. 673-81.
530. Wieczorek, M., Abualrous, E.T., Sticht, J., Alvaro-Benito, M., Stolzenberg, S., Noe, F., and Freund, C., *Major Histocompatibility Complex (MHC) Class I and MHC Class II Proteins: Conformational Plasticity in Antigen Presentation.* Front Immunol, 2017. **8**: p. 292.
531. Boyne, C., Lennox, D., Beech, O., Powis, S.J., and Kumar, P., *What Is the Role of HLA-I on Cancer Derived Extracellular Vesicles? Defining the Challenges in Characterisation and Potential Uses of This Ligandome.* Int J Mol Sci, 2021. **22**(24).
532. Han, G. and Son, H., *A systematic review of socio-ecological factors influencing current e-cigarette use among adolescents and young adults.* Addict Behav, 2022. **135**: p. 107425.
533. Cornelius, M.E., Loretan, C.G., Wang, T.W., Jamal, A., and Homa, D.M., *Tobacco Product Use Among Adults - United States, 2020.* MMWR Morb Mortal Wkly Rep, 2022. **71**(11): p. 397-405.
534. Kumar, A., Sinha, N., Haque, S., Kodidela, S., Wang, T., Martinez, A.G., Chen, H., and Kumar, S., *Nicotine self-administration with menthol and audiovisual cue facilitates differential packaging of CYP2A6 and cytokines/chemokines in rat plasma extracellular vesicles.* Sci Rep, 2021. **11**(1): p. 17393.
535. Li, L., Gorgens, A., Mussack, V., Pepeldjiyska, E., Hartz, A.S., Rank, A., Schmohl, J., Kramer, D., Andaloussi, S.E., Pfaffl, M.W., and Schmetzer, H., *Description and optimization of a multiplex bead-based flow cytometry method (MBFCM) to characterize extracellular vesicles in serum samples from patients with hematological malignancies.* Cancer Gene Ther, 2022. **29**(11): p. 1600-1615.
536. Ekstrom, K., Crescitelli, R., Petursson, H.I., Johansson, J., Lasser, C., and Olofsson Bagge, R., *Characterization of surface markers on extracellular vesicles isolated*

from lymphatic exudate from patients with breast cancer. BMC Cancer, 2022. **22**(1): p. 50.
537. Wiklander, O.P.B., Bostancioglu, R.B., Welsh, J.A., Zickler, A.M., Murke, F., Corso, G., Felldin, U., Hagey, D.W., Evertsson, B., Liang, X.M., Gustafsson, M.O., Mohammad, D.K., Wiek, C., Hanenberg, H., Bremer, M., Gupta, D., Bjornstedt, M., Giebel, B., Nordin, J.Z., Jones, J.C., El Andaloussi, S., and Gorgens, A., *Systematic Methodological Evaluation of a Multiplex Bead-Based Flow Cytometry Assay for Detection of Extracellular Vesicle Surface Signatures.* Front Immunol, 2018. **9**: p. 1326.
538. Archibald, S.J., Hisada, Y., Bae-Jump, V.L., and Mackman, N., *Evaluation of a new bead-based assay to measure levels of human tissue factor antigen in extracellular vesicles in plasma.* Res Pract Thromb Haemost, 2022. **6**(2): p. e12677.
539. Arimilli, S., Damratoski, B.E., Bombick, B., Borgerding, M.F., and Prasad, G.L., *Evaluation of cytotoxicity of different tobacco product preparations.* Regul Toxicol Pharmacol, 2012. **64**(3): p. 350-60.
540. van Leeuwen, D.M., Gottschalk, R.W., van Herwijnen, M.H., Moonen, E.J., Kleinjans, J.C., and van Delft, J.H., *Differential gene expression in human peripheral blood mononuclear cells induced by cigarette smoke and its constituents.* Toxicol Sci, 2005. **86**(1): p. 200-10.
541. Arimilli, S., Makena, P., Liu, G., and Prasad, G.L., *Distinct gene expression changes in human peripheral blood mononuclear cells treated with different tobacco product preparations.* Toxicol In Vitro, 2019. **57**: p. 117-125.
542. Di Biase, A., Attorri, L., Di Benedetto, R., and Sanchez, M., *Comparative effects between electronic cigarette and tobacco cigarette smoke on oxidative markers in cultured immune cells isolated from rats.* Ann Ist Super Sanita, 2018. **54**(4): p. 300-307.
543. Gomez, A.C., Rodriguez-Fernandez, P., Villar-Hernandez, R., Gibert, I., Muriel-Moreno, B., Lacoma, A., Prat-Aymerich, C., and Dominguez, J., *E-cigarettes: Effects in phagocytosis and cytokines response against Mycobacterium tuberculosis.* PLoS One, 2020. **15**(2): p. e0228919.
544. Togarrati, P.P., Dinglasan, N., Desai, S., Ryan, W.R., and Muench, M.O., *CD29 is highly expressed on epithelial, myoepithelial, and mesenchymal stromal cells of human salivary glands.* Oral Dis, 2018. **24**(4): p. 561-572.
545. Sacanella, E., Estruch, R., Gaya, A., Ferrer, K., Fernandez-Sola, J., Alonso, J.R., Nicolas, J.M., and Urbano-Marquez, A., *Upregulated expression of VLA proteins and CD29 in peripheral blood lymphocytes of chronic alcoholics without ethanol-related diseases.* Alcohol Clin Exp Res, 1999. **23**(2): p. 371-5.
546. Shang, X.Z. and Issekutz, A.C., *Beta 2 (CD18) and beta 1 (CD29) integrin mechanisms in migration of human polymorphonuclear leucocytes and monocytes through lung fibroblast barriers: shared and distinct mechanisms.* Immunology, 1997. **92**(4): p. 527-35.

547. Trial, J., Rubio, J.A., Birdsall, H.H., Rodriguez-Barradas, M., and Rossen, R.D., *Monocyte activation by circulating fibronectin fragments in HIV-1-infected patients.* J Immunol, 2004. **173**(3): p. 2190-8.
548. Pilling, J.E., Galvin, A., Robins, A.M., Sewell, H.F., and Mahida, Y.R., *Expression of alpha5 (CD49e) and alpha6 (CD49f) integrin subunits on T cells in the circulation and the lamina propria of normal and inflammatory bowel disease colonic mucosa.* Scand J Immunol, 1998. **48**(4): p. 425-8.
549. Jensen, C.T., Lang, S., Somasundaram, R., Soneji, S., and Sigvardsson, M., *Identification of Stage-Specific Surface Markers in Early B Cell Development Provides Novel Tools for Identification of Progenitor Populations.* J Immunol, 2016. **197**(5): p. 1937-44.
550. Podstawka, J., Sinha, S., Hiroki, C.H., Sarden, N., Granton, E., Labit, E., Kim, J.H., Andonegui, G., Lou, Y., Snarr, B.D., Sheppard, D.C., Rosin, N.L., Biernaskie, J., and Yipp, B.G., *Marginating transitional B cells modulate neutrophils in the lung during inflammation and pneumonia.* J Exp Med, 2021. **218**(9).
551. Hegewisch-Solloa, E., Seo, S., Mundy-Bosse, B.L., Mishra, A., Waldman, E.H., Maurrasse, S., Grunstein, E., Connors, T.J., Freud, A.G., and Mace, E.M., *Differential Integrin Adhesome Expression Defines Human NK Cell Residency and Developmental Stage.* J Immunol, 2021. **207**(3): p. 950-965.
552. McCarthy, D.A., Macey, M.G., Bedford, P.A., Knight, S.C., Dumonde, D.C., and Brown, K.A., *Adhesion molecules are upregulated on dendritic cells isolated from human blood.* Immunology, 1997. **92**(2): p. 244-51.
553. van Kooten, C. and Banchereau, J., *CD40-CD40 ligand.* J Leukoc Biol, 2000. **67**(1): p. 2-17.
554. Vivier, E., Raulet, D.H., Moretta, A., Caligiuri, M.A., Zitvogel, L., Lanier, L.L., Yokoyama, W.M., and Ugolini, S., *Innate or adaptive immunity? The example of natural killer cells.* Science, 2011. **331**(6013): p. 44-9.
555. Ong, S.M., Teng, K., Newell, E., Chen, H., Chen, J., Loy, T., Yeo, T.W., Fink, K., and Wong, S.C., *A Novel, Five-Marker Alternative to CD16-CD14 Gating to Identify the Three Human Monocyte Subsets.* Front Immunol, 2019. **10**: p. 1761.
556. Kawai, K., Tsuno, N.H., Kitayama, J., Okaji, Y., Yazawa, K., Asakage, M., Hori, N., Watanabe, T., Takahashi, K., and Nagawa, H., *Epigallocatechin gallate attenuates adhesion and migration of CD8+ T cells by binding to CD11b.* J Allergy Clin Immunol, 2004. **113**(6): p. 1211-7.
557. Diagbouga, S., Chiron, J.P., Sanou, O., and Ledru, E., *Alteration in CD29(high) CD4(+) lymphocyte subset is a common feature of early HIV disease and of active tuberculosis.* Scand J Immunol, 2001. **53**(1): p. 79-84.
558. Choi, H., Lee, H.J., Sohn, H.J., and Kim, T.G., *CD40 ligand stimulation affects the number and memory phenotypes of human peripheral CD8(+) T cells.* BMC Immunol, 2023. **24**(1): p. 15.
559. Lanier, L.L., Kipps, T.J., and Phillips, J.H., *Functional properties of a unique subset of cytotoxic CD3+ T lymphocytes that express Fc receptors for IgG (CD16/Leu-11 antigen).* J Exp Med, 1985. **162**(6): p. 2089-106.

560. Tsukerman, P., Stern-Ginossar, N., Yamin, R., Ophir, Y., Stanietsky, A.M., and Mandelboim, O., *Expansion of CD16 positive and negative human NK cells in response to tumor stimulation.* Eur J Immunol, 2014. **44**(5): p. 1517-25.
561. Cooper, M.A., Fehniger, T.A., and Caligiuri, M.A., *The biology of human natural killer-cell subsets.* Trends Immunol, 2001. **22**(11): p. 633-40.
562. Abeles, R.D., McPhail, M.J., Sowter, D., Antoniades, C.G., Vergis, N., Vijay, G.K., Xystrakis, E., Khamri, W., Shawcross, D.L., Ma, Y., Wendon, J.A., and Vergani, D., *CD14, CD16 and HLA-DR reliably identifies human monocytes and their subsets in the context of pathologically reduced HLA-DR expression by CD14(hi) /CD16(neg) monocytes: Expansion of CD14(hi) /CD16(pos) and contraction of CD14(lo) /CD16(pos) monocytes in acute liver failure.* Cytometry A, 2012. **81**(10): p. 823-34.
563. Alderson, M.R., Armitage, R.J., Tough, T.W., Strockbine, L., Fanslow, W.C., and Spriggs, M.K., *CD40 expression by human monocytes: regulation by cytokines and activation of monocytes by the ligand for CD40.* J Exp Med, 1993. **178**(2): p. 669-74.
564. De Maria, R., Cifone, M.G., Trotta, R., Rippo, M.R., Festuccia, C., Santoni, A., and Testi, R., *Triggering of human monocyte activation through CD69, a member of the natural killer cell gene complex family of signal transducing receptors.* J Exp Med, 1994. **180**(5): p. 1999-2004.
565. Kapellos, T.S., Bonaguro, L., Gemund, I., Reusch, N., Saglam, A., Hinkley, E.R., and Schultze, J.L., *Human Monocyte Subsets and Phenotypes in Major Chronic Inflammatory Diseases.* Front Immunol, 2019. **10**: p. 2035.
566. Chattopadhyay, P.K. and Roederer, M., *Good cell, bad cell: flow cytometry reveals T-cell subsets important in HIV disease.* Cytometry A, 2010. **77**(7): p. 614-22.
567. Aghaeepour, N., Chattopadhyay, P.K., Ganesan, A., O'Neill, K., Zare, H., Jalali, A., Hoos, H.H., Roederer, M., and Brinkman, R.R., *Early immunologic correlates of HIV protection can be identified from computational analysis of complex multivariate T-cell flow cytometry assays.* Bioinformatics, 2012. **28**(7): p. 1009-16.
568. Liechti, T. and Roederer, M., *OMIP-060: 30-Parameter Flow Cytometry Panel to Assess T Cell Effector Functions and Regulatory T Cells.* Cytometry A, 2019. **95**(11): p. 1129-1134.
569. Park, L.M., Lannigan, J., and Jaimes, M.C., *OMIP-069: Forty-Color Full Spectrum Flow Cytometry Panel for Deep Immunophenotyping of Major Cell Subsets in Human Peripheral Blood.* Cytometry A, 2020. **97**(10): p. 1044-1051.
570. Rigg, S. and Gielda, L.M., *E-Cigarette Vapor Decreases Cellular Proliferation through Nicotine-Dependent Mechanisms.* Journal of Biosciences and Medicines, 2019. **7**(7).
571. Jubri, Z., Latif, A.A., Top, A.G., and Ngah, W.Z., *Perturbation of cellular immune functions in cigarette smokers and protection by palm oil vitamin E supplementation.* Nutr J, 2013. **12**: p. 2.

572. Piao, W.H., Campagnolo, D., Dayao, C., Lukas, R.J., Wu, J., and Shi, F.D., *Nicotine and inflammatory neurological disorders.* Acta Pharmacol Sin, 2009. **30**(6): p. 715-22.
573. Becher, B., Schlitzer, A., Chen, J., Mair, F., Sumatoh, H.R., Teng, K.W., Low, D., Ruedl, C., Riccardi-Castagnoli, P., Poidinger, M., Greter, M., Ginhoux, F., and Newell, E.W., *High-dimensional analysis of the murine myeloid cell system.* Nat Immunol, 2014. **15**(12): p. 1181-9.
574. Toribio, V. and Yanez-Mo, M., *Tetraspanins interweave EV secretion, endosomal network dynamics and cellular metabolism.* Eur J Cell Biol, 2022. **101**(3): p. 151229.
575. Wu, F., Yin, Z., Yang, L., Fan, J., Xu, J., Jin, Y., Yu, J., Zhang, D., and Yang, G., *Smoking Induced Extracellular Vesicles Release and Their Distinct Properties in Non-Small Cell Lung Cancer.* J Cancer, 2019. **10**(15): p. 3435-3443.
576. Ryu, A.R., Kim, D.H., Kim, E., and Lee, M.Y., *The Potential Roles of Extracellular Vesicles in Cigarette Smoke-Associated Diseases.* Oxidative medicine and cellular longevity, 2018. **2018**: p. 4692081-4692081.
577. Thakur, A., *Organ-on-a-Chip Microfluidic Systems for Tracking Exosomal Dynamic Communication.* OpenNano, 2023. **13**: p. 100179.
578. McCann, J.V., Bischoff, S.R., Zhang, Y., Cowley, D.O., Sanchez-Gonzalez, V., Daaboul, G.D., and Dudley, A.C., *Reporter mice for isolating and auditing cell type-specific extracellular vesicles in vivo.* genesis, 2020. **58**(7).
579. Valkov, N., Das, A., Tucker, N.R., Li, G., Salvador, A.M., Chaffin, M.D., Pereira De Oliveira Junior, G., Kur, I., Gokulnath, P., Ziegler, O., Yeri, A., Lu, S., Khamesra, A., Xiao, C., Rodosthenous, R., Srinivasan, S., Toxavidis, V., Tigges, J., Laurent, L.C., Momma, S., Kitchen, R., Ellinor, P., Ghiran, I., and Das, S., *SnRNA sequencing defines signaling by RBC-derived extracellular vesicles in the murine heart.* Life Science Alliance, 2021. **4**(12).
580. Ge, X., Meng, Q., Wei, L., Liu, J., Li, M., Liang, X., Lin, F., Zhang, Y., Li, Y., Liu, Z., Fan, H., and Zhou, X., *Myocardial ischemia-reperfusion induced cardiac extracellular vesicles harbour proinflammatory features and aggravate heart injury.* Journal of Extracellular Vesicles, 2021. **10**(4).
581. Ghoroghi, S., Mary, B., Larnicol, A., Asokan, N., Klein, A., Osmani, N., Busnelli, I., Delalande, F., Paul, N., Halary, S., Gros, F., Fouillen, L., Haeberle, A.-M., Royer, C., Spiegelhalter, C., André-Grégoire, G., Mittelheisser, V., Detappe, A., Murphy, K., Timpson, P., Carapito, R., Blot-Chabaud, M., Gavard, J., Carapito, C., Vitale, N., Lefebvre, O., Goetz, J.G., and Hyenne, V., *Ral GTPases promote breast cancer metastasis by controlling biogenesis and organ targeting of exosomes.* eLife, 2021. **10**.
582. Arifin, D.R., Witwer, K.W., and Bulte, J.W.M., *Non-Invasive imaging of extracellular vesicles: Quo vaditis in vivo?* Journal of Extracellular Vesicles, 2022. **11**(7).
583. Skotland, T., Iversen, T.G., Llorente, A., and Sandvig, K., *Biodistribution, pharmacokinetics and excretion studies of intravenously injected nanoparticles*

and extracellular vesicles: Possibilities and challenges. Advanced Drug Delivery Reviews, 2022. **186**.